The ZEBRA MOZART Programme.
Part 2. MZC and the Control Rod Studies
ZEBRA ASSEMBLIES 12/4 and 12/5

Evaluator

John ROWLANDS
81 South Court Avenue, Dorchester, Dorset DT1 2DA, UK

Internal Reviewer

Atsushi ZUKERAN
Consultant to the OECD/NEA

Independent Reviewers

Masayuki NAKAGAWA
Consultant to the OECD/NEA

Udo K WEHMANN
Consultant to the OECD/NEA

Acknowledgements

The Evaluator wishes to thank the members of the Mozart Team from PNC Japan and UKAEA Winfrith who carried out the experiments, and the authors of the MTN series of Technical Notes describing them, which are the basis of the present document:

A M Broomfield, B L H Burbidge, M D Carter, C G Campbell, P J Collins, C J Dean, B Franklin, J P Hardiman, T Ichimori, G Ingram, D Jowitt, S Kobayashi, T Konishi, J Marshall, C McCombie, J D MacDougall, H Nakamura, M Nakano, W Paterson, J Redfern, I Rickard, J Samways, J Sanders, Miss P A Smart, Miss M P Smith, R W Smith, J Spanton, J M Stevenson, A Sugawara, D Sweet, S Swoboda, W H Taylor, H Yoshida

The shielding series of experiments in the Mozart Programme is not covered in the present document. The programme was documented in the MTN series by:
A F Avery, J Butler, M J Grimstone, A D Knipe, A K McCracken, P C Miller, A Packwood, I C Rickard, Y Sekiguchi.

Thanks also to those who have kindly reviewed the document, Atsushi Zukeran, Masayuki Nakagawa and Udo Wehmann.

I also wish to express my thanks to the Government of Japan for the contracts I have received in support of my work of evaluation. These were provided by the OECD-Nuclear Energy Agency, paid for from the budget of the Government of Japan.

TABLE OF CONTENTS

UK-JAPAN FAST CRITICAL EXPERIMENTS IN SUPPORT OF MONJU DESIGN. THE ZEBRA MOZART PROGRAMME, PART 2. MZC AND THE CONTROL ROD STUDIES.

IDENTIFICATION NUMBER: ZEBRA-LMFR-EXP-003
REAC-RRATE

KEY WORDS:
fast criticals, LMFR, ZEBRA, MOZART Programme, MONJU design, arrays of control rods, mixed uranium plutonium dioxide, sodium cooled, control rod worths, reaction rate scans with arrays of control rods.

SUMMARY

In the MZC phase of the ZEBRA Mozart Programme the reactivity worths of MONJU mock-up control rods were measured, both singly at different radial positions, and in groups of up to 4 rods. The rods contained arrays of 19 absorber pins. The absorber material was boron at 4 different enrichments (natural, 30%, 80% and 90% enriched) and tantalum. In addition there was a rod (denoted B80/B90) which contained a close packed array of 19 B90 plus 18 B80 pins. Rod followers (the channels corresponding to the withdrawn rods) were also simulated and measurements made for partially inserted rods. The measurements were made in versions of the MZB assembly, with the Zebra control rods repositioned (see ZEBRA-LMFR-EXP-002). These were denoted by MZB Version 4 and 5.

Reaction rate distributions were also measured using both fission chambers and foils, for different arrays of absorber rods.

1. DETAILED DESCRIPTION

1.0 Overview

The ZEBRA-MOZART series of experiments was a joint UKAEA/PNC Japan programme carried out using the zero power critical facility, ZEBRA, at the UKAEA establishment at Winfrith in Dorset, UK. The programme was in support of the design of the Japanese sodium cooled, plutonium-uranium oxide fuelled fast reactor, MONJU, and was based on the design for MONJU current in the early 1970s. The measurements were carried out in 1971, 72 and 73, with the MZC Phase being the final series of measurements using arrays of control rods simulating possible designs for the MONJU control rods. The first two phases of the Mozart programme, called MZA and MZB, are detailed in ZEBRA-LMFR-EXP-002. The core element dimensions and compositions and the criticality models are given in that document.

The Mozart programme was divided into three phases called MZA, MZB and MZC. The first assembly was MZA, this being ZEBRA Assembly 11, having a simple one-region core. MZB (ZEBRA Assembly 12) had a two-region core. This assembly was built in three versions which differed in the radial blanket arrangement. The radial blanket in Version 3 used the same type of cell as MZA, comprising natural uranium metal plates plus diluent plates. Versions 1 and 2 had 90^{o} sectors which contained natural uranium oxide and depleted uranium oxide plates, respectively, in place of the natural uranium metal. MZB, in the slightly modified Version 4 (with one ZEBRA control rod repositioned), then provided the basis for the main series of measurements for different patterns of control rods carried out in the MZC phase. A further series of measurements using a rod with a higher boron content, the B80/B90 rod, was made in the Version 5 MZB assembly, which had a further repositioning of the Zebra control rods.

The measurements in the Mozart programme included critical size, reaction rate ratios and distributions, sodium voiding reactivity, and the reactivity worths of small samples and, in the MZC phase, the reactivity worths of different patterns of boron and tantalum control rods. These contained an array of 19 pins. Several different enrichments of boron were used, natural (BN), 30% enriched (B30), 80% enriched (B80), 90% enriched (B90). In addition there was the special B80/B90 rod which contained a close packed array of 19 B90 pins surrounded by a ring of 18 B80 pins. Simulations of the sodium filled control rod channel when the absorber rod was withdrawn were also studied (the "Rod Followers") and partially inserted rods were also simulated.

MZB was designed to be critical at just below the size of MONJU, with the significant reduction in fuel enrichment required relative to the MONJU fuel feed enrichment in the two core regions, because of the absence of absorber rods and fuel burnup. MZA had a single uniform core region having the composition of the outer core of MZB.

The measurements of the reactivity worths of the different configurations of control rods, and control rod followers were critical balances. The balances were obtained by moving the calibrated control rod and by adding extra core elements at the boundary between the outer core and the radial blanket. Although these are critical states of the reactor, the measurements are interpreted here as reactivity worth measurements, the reactivity worth of the added edge element being related to the reactivity scale defined in terms of period measurements interpreted using a chosen set of delayed neutron data. This approach is adopted in order to give the reactivity effects of replacing core elements by follower elements and absorber rods. The procedure involves calculating the reactivity effect of adding the edge elements and then scaling these calculated values using the series of measurements made to relate the calculated worths of edge elements to values measured in terms of the calibrated Zebra control rods. In this way all reactivity worths are related to the delayed neutron reactivity scale. A reactivity scale used in one of the original analyses involved the interrelationship of the Zebra control rod reactivity measurements with the measured and calculated effects of changes to the core plutonium enrichment. Arguments for this latter scale are that one of the purposes of the control rods is to

compensate for the loss of plutonium by burnup and the relative accuracy with which the reactivity effect of plutonium additions can be calculated. However, in the present document the delayed neutron reactivity scale has been used. The evaluation of reactivity scales is an important part of the measurement programme. This procedure involving the calculation of edge element worths and then scaling the calculated values based on measurements of edge element worth is necessary because the measurements of edge element worth were made for only a small set of configurations.

Measurements of reaction rate distributions were made using Pu239 and U238 fission chambers and U235 and U238 foils, and tantalum foils, for different patterns of control rods in the core. Detailed measurements were also made within rods and in the vicinity of the rods.

The document describes the critical cores with the different patterns of rod followers and absorber rods present (together with the positions of the Zebra regulating rod and the edge elements added to the core) and the equivalent reactivity worths of the rod arrays (for a fixed number of edge elements) derived from the measurements. The reaction rate scan measurements are also detailed.

All of these results are recommended as benchmarks:

> **The numbers of edge elements added and the regulating rod insertions in the critical control rod arrays (with the corrections for Pu241 decay).**
> **The results interpreted in terms of the reactivity worths of arrays of rod followers (relative to fuelled elements in cores of the same size, that is, having the same numbers of edge elements) and absorber rods (relative to fuelled elements or rod followers in cores of the same size).**
> **The local and distributed reaction rate scan measurements**

The accuracies of the reactivity worth measurements are dependent on the accuracy of the reactivity scale. In the present document the scale is based on the calibration of the Zebra regulating rod by reactor period measurements interpreted using the FGL5 cross-section set and the Smith-Tomlinson delayed neutron data. People calculating these benchmarks might wish to reanalyse these period measurements using alternative nuclear data. The information to enable this to be done is given in Section 1.4.2C of Part 1 (ZEBRA-LMFR-EXP-002). If this is done it is important to analyse the particular period measurements (or a typical period within the range) used to calibrate the Zebra regulating rods because of the marked difference between the time dependence of delayed neutron emission by U238 and by U235 and Pu239 (see Section 2.4.3). Measurements were made, relative to this scale, of the reactivity effect of plutonium depletion in the inner core, the insertion of a plutonium sample and the addition of edge elements (see the Section: The Reactivity Scale Experiment in MZB/4). This provides a basis for the validation of the delayed neutron scale and possibly its refinement, depending on the relative accuracies of the delayed neutron scale, the calculation of the effects of changes in the plutonium content of the core and the calculation of the reactivity effects of edge elements.

A complete description of the measurements, and the analyses made in the 1970s, can be found in the MTN series of Mozart Technical Notes, available on the dvd.

Description of the ZEBRA zero power critical assembly facility

A description is given in ZEBRA-LMFR-EXP-002, Section 1.01

1.1 Description of the Critical or Subcritical Configurations

The MZA and MZB assemblies are described in ZEBRA-LMFR-EXP-002. Brief summaries follow.

The MZA Assembly.

The reference model of MZA contained a symmetrical array of 213 core elements. The core is surrounded by a region of radial blanket elements outside which is a region of steel bars. There are about 6 rings of radial blanket elements surrounding the core and about 3 rings of steel bars surrounding these, with quadrant symmetry. There are upper and lower axial blanket regions, and plenum regions above and below these. Axially the core cells are not precisely symmetrical but the approximation resulting from treating the core as axially symmetrical in criticality calculations is expected to be negligibly small.

Four different elements were used in the core, differing in the plutonium metal plates and also in the sodium plates used. The effects of these differences are small, however. Two different radial blanket elements are used, the difference being in the sodium plate used, and the element sheath material in the outer ring of the six rings, and the effect of the difference is again negligibly small.

Five types of plate are used in the core region: plutonium metal, natural uranium oxide, sodium, graphite and stainless steel. The same sodium, stainless steel and graphite plates are used in the axial blanket region, together with natural uranium metal plates. Outside the axial blanket regions are plenum regions containing aluminium and mild steel blocks and plates.

The axial region of the radial blanket corresponding in height to the core region contains natural uranium metal, sodium, graphite, stainless steel and mild steel plates. Above and below this axial region are regions containing aluminium plates in place of the sodium plates and outside these are the plenum regions.

The Assembly MZB

Zebra 12, or MZB, was a clean mock-up of a design of the MONJU fast reactor and formed the second assembly in the MOZART programme. The assembly was built in three versions which differed in aspects of the radial blanket. Version 3 used essentially the same type of radial blanket as MZA, containing natural uranium metal plates, whereas Versions 1 and 2 had 90^{o} sectors containing natural uranium oxide and depleted uranium oxide plates respectively. There was also MZB Version 4 but this was essentially just a repositioning of one of the ZEBRA control rods in preparation for the MZC control rod programme and Version 5 a later repositioning of the Zebra control rods for the B80/B90 rod measurements.

The core had two radial regions, an inner core region and an outer core region which contained MZA core elements (supplemented by elements having an equivalent design). The axial blanket regions are those used in MZA, or are equivalent ones, and most of the radial blanket elements are also those used in MZA, or are similar. The radial blanket is surrounded by steel bars, in a similar way to MZA. Full details are given in ZEBRA-LMFR-EXP-002.

MZB/4 and MZB/5, the Assemblies used for the MZC Programme of Measurements.

The MZC programme of measurements using the MONJU Mock-up Rods was carried out in ZEBRA Assembly 12 Version 4 (MZB/4) and consisted of an extensive series of measurements of the reactivity worths of the rods, both singly and in groups. The critical loading of MZB/4, had 413 inner and 264 outer core elements surrounded by a 360 degree simulation of a natural $U0_2$ breeder (simulated using uranium metal, sodium, steel and graphite plates). This served as the reference core for the programme. The positions occupied by the mock-up control rods are shown in Figure 1.2.

The assembly used as the basis for a later series of measurements, using the special B80/B90 control rod, was referred to as MZB/5. This had the Zebra double element control rods 2 and 3 moved to the double element positions (48,56) + (49,56) and (48,42) + (49,42) respectively where (X,Y) denotes the X and Y positions on the plan of the assembly (see Figure 1.2.)

Descriptions of the assemblies are given in ZEBRA-LMFR-EXP-002 Section 1.1.1, the dimensions are detailed in Section 1.1.2 and the material compositions in Section 1.1.3.

1.2 Description of Buckling and Extrapolation Length Measurements

Buckling measurements were made only in MZA and are described in ZEBRA-LMFR-EXP-002 Section 1.2.

1.3 Description of Spectral Characteristics Measurements

These measurements were made in MZA and MZB and are described in ZEBRA-LMFR-EXP-002 Section 1.3.

1.4 Description of Reactivity Effects Measurements

1.4.1 Overview of the MONJU Mock-up Control Rod Measurements

The MONJU Mock-up Control Rods

The MONJU mock-up rods consisted of a 19-pin cluster of absorber pins contained in a sodium-filled calandria. Each rod replaced 4 core elements in MZB/4. Measurements were made on single rods containing natural, 30%, 80% and 90% enriched B_4C and tantalum at various core positions, and for different arrays of up to four natural B_4C rods. These rods were denoted by BN, B30, B80 and TA. Measurements were also made for Rod Followers which were mock-ups of a sodium filled channel from which the absorber rod had been withdrawn. The reduction in reactivity following replacement of fuel by follower, or follower by absorber, was compensated by the addition of fuel elements at the core/ breeder boundary and the repositioning of the regulating Zebra control rod (usually the single rod FR9).

Each MONJU rod and rod follower consisted of an outer stainless steel sheath which replaced a 2 x 2 array of ZEBRA elements and contained control rod calandria, follower calandria and spacers. All absorber calandria and control rod follower calandria were sodium-filled and fabricated in stainless steel. A cross-sectional view of the MONJU rods is shown in Figure 1.1A.

Both fully inserted rods and partially inserted rods were simulated. In the case of the simulation of a fully inserted rod the absorber calandria was axially symmetrically placed about the core mid-plane, with follower calandria above and below the absorber regions (in the axial blanket region). Above and below the follower regions were plenum regions. For the measurements simulating the follower

geometry (a sodium channel through core and breeder) the absorber calandria was removed and replaced by follower calandria. Partially inserted rods were simulated by repositioning the absorber and follower calandria, and making use of follower calandria having different heights.

The B80/B90 Rod.

The range of experiments was extended by means of a rod with a higher content of B10. This was in the form of an array of 19 x 90% enriched B_4C pins (a cluster of 1+6+12 pins) surrounded by a ring of 18 x 80% enriched pins, in tightly packed geometry, in an aluminium block with a central hole of 9 cm diameter to accommodate the pin cluster. The outer boundary of the aluminium block was square of width 10.2 cm and height 91.36 cm. In follower geometry the array of pins was replaced by a cylindrical aluminium block which fitted into this circular hole.

The Arrays of Rods

The lattice positions occupied by the mock-up rods, designated O, P1, P2, P3, P5, Q, R and S, are shown in Figure 1.2, together with the symmetrical 4 rod array, (P2,P2',P5,P5'). Single boron rods were studied at the core centre and at a selection of other positions. Measurements were made on a tantalum rod at the core centre and in the outer core. The interaction between rods was studied for arrays of two, three and four boron rods at different positions.

The Measurement of Rod Reactivity Worth

The primary measured quantity is the excess reactivity of the core (as measured using the Zebra regulating control rod) with the MONJU mock-up rods (or rod followers) present, together with the number of added edge elements. To interpret this in terms of the rod worth in a core of fixed size requires calculations to be made of the worths of the edge elements. These calculated values of the worths of edge elements are compared with measured values for selected numbers of edge elements and the calculated values are scaled to be consistent with the measured values. This procedure involving the calculation of edge element worths and then scaling the calculated values is necessary because the measurements of edge element worth were made for only a small set of configurations.

The reactivity worth of each array of mock-up rods was first determined by a critical balance technique, with edge elements added in order to reach criticality with the Zebra regulating control rod partially inserted. The reactivity loss following the replacement of fuel elements by rod follower, or follower by absorber, was thus compensated by the addition of outer core elements at the outer core/radial breeder boundary so that the assembly was returned to critical. The reactivity worth of the rods was therefore measured in terms of the calculated reactivity change due to the addition of the edge elements (plus the change in position of the regulating Zebra control rod) with a correction factor applied to the calculated values of edge element worths based on the measurement of the edge element worths in a separate experiment (the MZB reactivity scale experiment).

The worth of edge elements was measured relative to the change in position of the calibrated Zebra regulating control rod. The worth of the regulating rod was obtained by means of period measurements interpreted using a chosen set of delayed neutron data using the inhour equation. The reactivity changes resulting from changes in the plutonium content of an inner core region, and from the addition of plutonium samples were also measured. The calculated edge element worth could then be scaled to relate to either the delayed neutron reactivity scale or to the calculated effect of a change in plutonium content. The plutonium worth scale was the one preferred in the original analysis and the adoption of this required a correction to be made to the calculated edge element worth and the regulating rod worth based on the relationship to the worth of the plutonium addition. In the present document the chosen reactivity scale is the one based on the period measurements interpreted using

the Smith-Tomlinson set of delayed neutron data. The regulating rod reactivities and the calculated edge element worths have been scaled to be consistent with this. The calculations of edge element worth can be regarded as a way of interpolating, or extrapolating, the limited set of measured edge element worths.

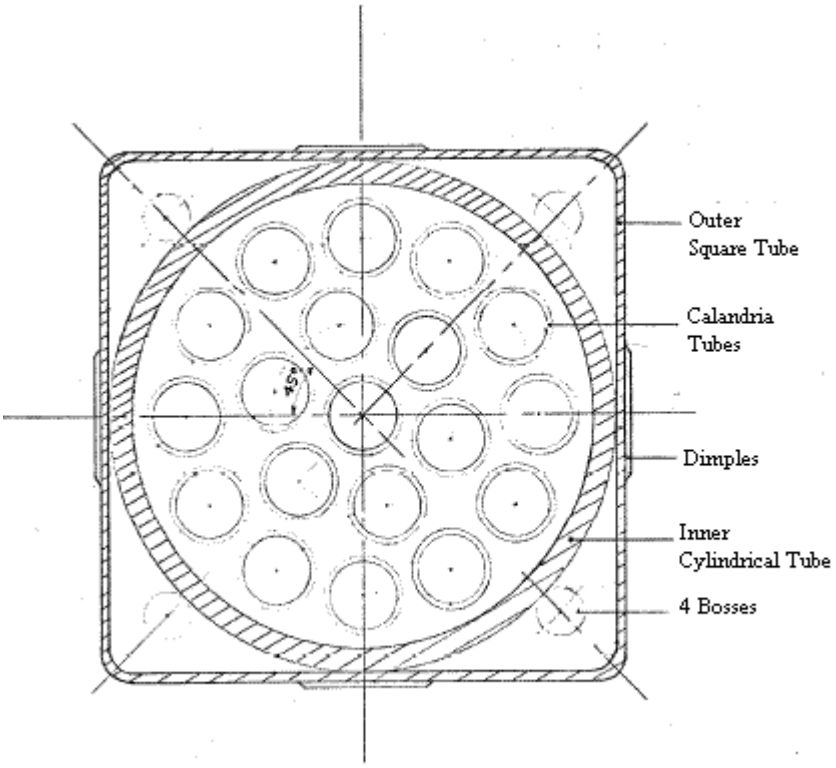

Figure 1.1A Cross-section of a MONJU Mock-up Control Element Calandria.

Some details of the Control Element.
The mock-up control rod Calandria element, illustrated above, is contained in a square stainless steel sheath, or box, having an inner width of 10.47 cm and outer width of 10.623 cm which replaces 2x2 standard elements in the core, the width of the 2x2 lattice cells being 10.7442 cm.
The inner width of the square stainless steel outer Calandria Wall is 9.86 cm and the outer width is 10.402 cm. The stainless steel Cylinder containing the absorber pins has an outer diameter of 9.845 cm and an inner diameter of 9.025 cm. The Calandria is filled with sodium.
The stainless steel Calandria Tubes containing the absorber pins have an outer diameter of 1.55 cm. The centres of the Ring of 6 tubes are on the Diameter of 3.58 cm and the Ring of 12 are on the Diameter of 6.92 cm. The Ring of 6 is rotated so that the centre of the first tube is on a line at 45^o relative to the positive x-axis whereas the Ring of 12 has the centre of the first tube on the x-axis.
The Boron Absorber Pellets (natural boron, 30% enriched, 80% enriched and 90% enriched) are taken to have a Diameter of 1.1 cm and the Tantalum Pins a Diameter of 1.31 cm. The boron pellets are contained in stainless steel cans which are combined with the tubes in the calculational model.
The Inner Height of the Calandria is taken to be 90.5 cm and the Overall Length of the Calandria, including end plates, is taken to be 91.44 cm, making a stainless steel End Plate Region of Thickness 0.47 cm at each end.
The Follower Calandria which replace the Absorber Calandria have the same dimensions but without the tubes for the absorber pins. The Follower Calandria placed above and below the Absorber Calandria, in the axial blanket regions, have an overall height of 35.56 cm.
(Some regions are combined in the calculational model, such as the calandria walls and the containing sheath. Also the cans of the boron pins are combined with the calandria tubes. The cross-sectional form of the Calandria and Sheath are taken to be square, the "dimples" and other shape irregularities being absorbed into the squared off dimensions.)

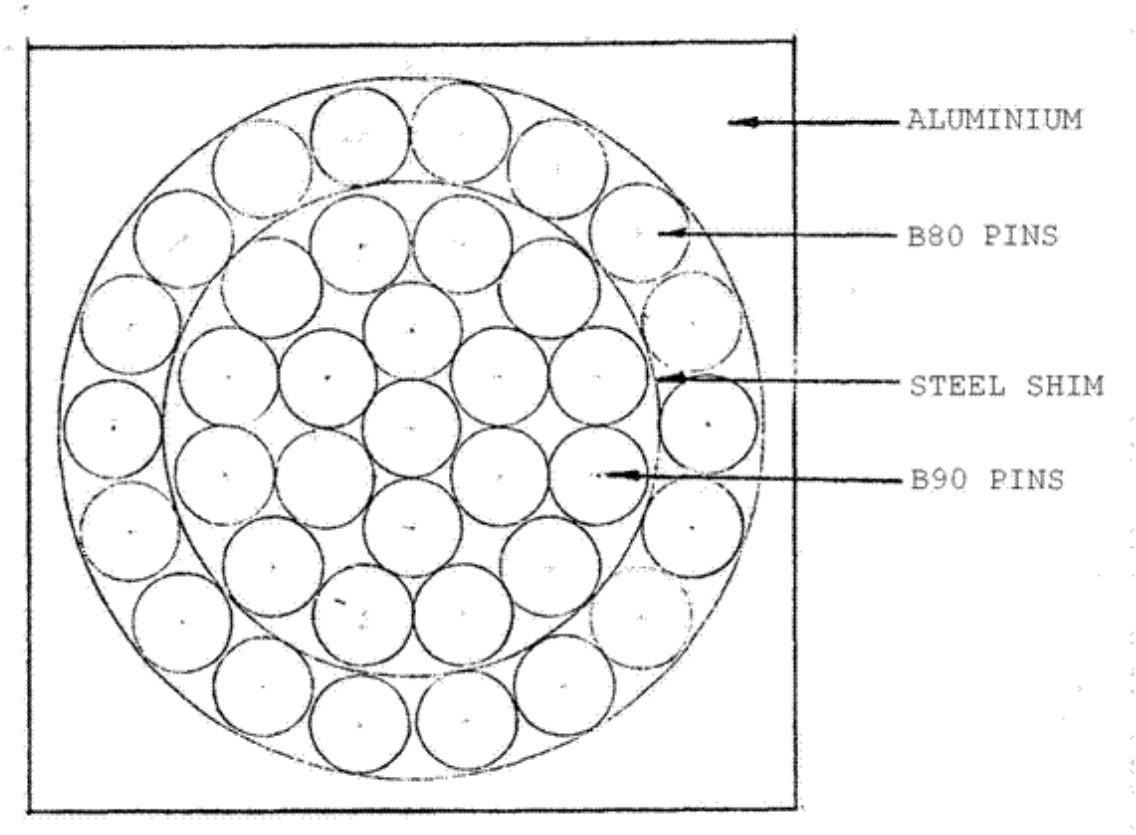

Figure 1.1B Cross-section of a B90/B80 Rod.

There is also the special element B80/B90 which contains a close packed array of 37 pins, the inner array of 19 pins being 90% enriched boron and the outer ring of 18 are 80% enriched.
The array of 37 absorber pins is contained in a square aluminium block having sides 10.2 cm square with a central cylindrical hole of 9 cm diameter which contains the pins. The length of the block is 91.36 cm. The inner array of 19 B90 pins (1+6+12), diameter 1.27 cm, is surrounded by a ring of 18 B80 pins, diameter 1.31 cm, and held in place by means of 7.6 cm long stainless steel shims at either end of the array, between the B90 and B80 pins. The shims are 0.066 cm thick. The cluster of 19 pins has an outer radius of $(3 + \sqrt{3})x1.27$ *cm = 6.01 cm.*
The follower is formed by replacing the absorber pins in the aluminium block with a cylinder of aluminium, 91.34 cm long and 8.95 cm diameter in the central hole.
The aluminium block is contained in the square section stainless steel sheath, which has an inner width of 10.47 cm and outer width of 10.623 cm. (In the calculational model the outer width is assumed to be 10.7442 cm and inner width 10.2 cm, thus eliminating the gaps.)

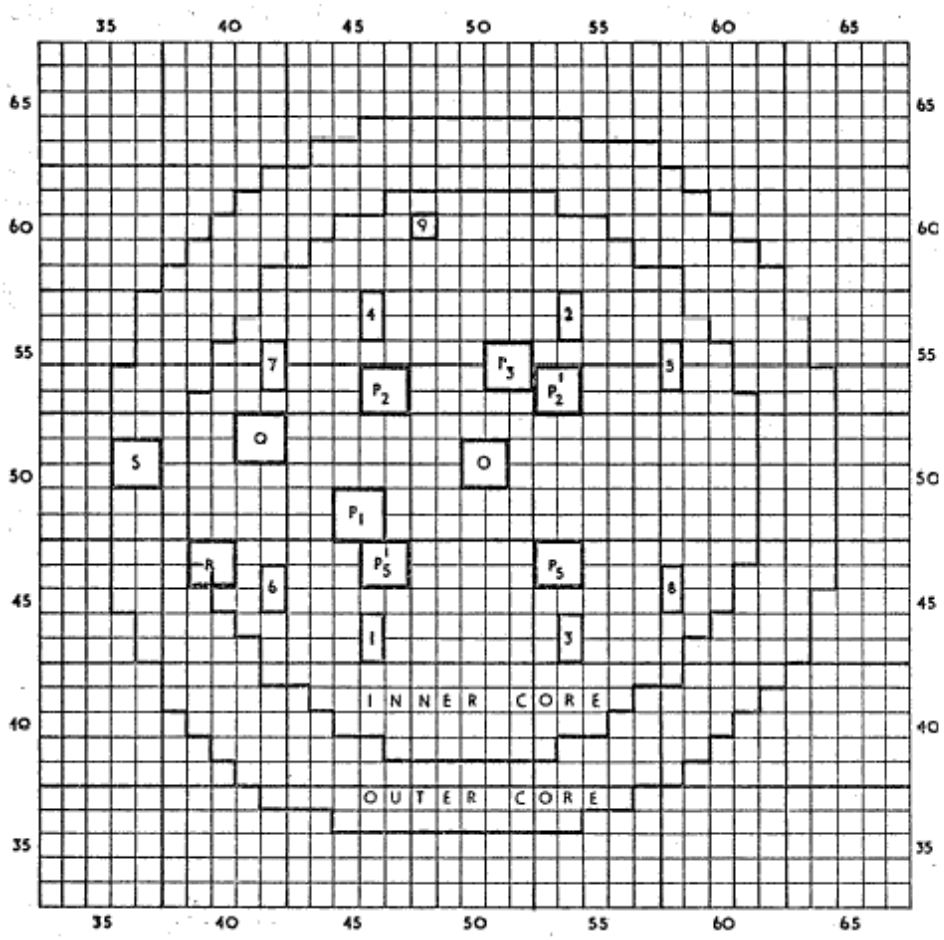

Figure 1.2 The MZB/4 Core showing the Positions of the Mock-up rods.

These are denoted by O, P1, P2, P3, P5, Q, R and S.

The standard ZEBRA control rods are denoted by 1 to 9.
The array (P2.P2',P5,P5') is a symmetrical 4 rod arrangement which was also used.

Reactivity Scales

The reductions in reactivity caused by the introduction of the MONJU mock-up control rods, or rod followers, were balanced by the addition of "edge elements" at the core/breeder boundary, with the residual excess reactivity being measured in terms of the position of the calibrated control rod, FR9. This control rod was calibrated by period measurements and the "Standard centimetres" of movement were then related to reactivity using the inhour equation and the chosen delayed neutron data. The "standard cm" was the reactivity change produced by 1 cm. of movement of the rod at the point of maximum change in reactivity with rod insertion. The reactivity change produced at other rod insertions is obtained relative to the standard cm. via the rod profile and the worth of the insertion of the other Zebra rods is related to the standard cm of FR9. In the present document the reactivity scale used is that based on fission rate ratio and neutron importance calculations made using the FGL5 cross-section set and the Smith-Tomlinson delayed neutron data (MTN/104).

Experiments were performed to relate the calculated worth of edge elements to this delayed neutron reactivity scale so that the worth of the mock-up rods and followers could be given in terms of this reactivity scale, the rod array worth then being the difference between the reactivity of the core with no rods inserted and the worth with the rods inserted in the same size of core (with no edge elements added).

Several reactivity scales were intercompared in the MZB Reactivity Scale Experiment (MTN/76). The edge element scale was related to the worth of plutonium in the core and the standard cm. of the fine control rod FR9. These are described in Section 1.4.2C.

Method used to determine the reactivity worths of control rods and rod followers.

The changes in reactivity resulting from replacing core elements by the MONJU mock-up control rods, or rod followers, were balanced by adding outer core elements to give a critical core. The small excess reactivity of each loading, with all the Zebra control rods fully raised, was measured by critical balance and calibration of the fine control rod, FR9.

To derive a reactivity worth for the mock-up rods, or followers, in the same size of core as the one with no mock-up rods inserted, calculations were made for each of the critical configurations, the standard MZB/4 core, the cores with control rod followers loaded and the cores with absorbers loaded, taking into account the number of outer core elements of the configuration.

The method adopted is described by Broomfield and Carter in MTN/92. First consider the equation involved when no correction is applied for a possible error due to an error in the calculated value of edge element worth. The differences between the measured excess reactivity of a configuration, ρ_E , (as measured using FR9) and the calculated reactivity, ρ_C , for the two configurations being compared, Core 1 and Core 2, gives the discrepancy in the calculation of the change in reactivity resulting from the change in core loading between Core 1 and Core 2:

$$\varepsilon = [\{\rho_E(2) - \rho_E(1)\} - \{\rho_C(2) - \rho_C(1)\}] = [\{\rho_E(2) - \rho_C(2)\} - \{\rho_E(1) - \rho_C(1)\}]$$

An experimental value for the worth of the array of followers or rods would then be obtained by applying this as a correction to the calculated value of the worth of the rod or follower, (calculated with the number of outer elements being the same in the two configurations).

In the case of the worth of an absorbing rod relative to a follower, with the calculated rod worth referred to the critical follower fuel loading, we can define the following:

Calculated rod worth. The two calculations (with the follower present and the rod present) are made

with the same number of outer core elements in the core, the number in the core as measured with the follower present, denoted by (F)

$$R_C(F) = \rho_{CF}(F) - \rho_{CA}(F) \quad (1)$$

where $_C$ denotes the calculated value and $_F$ and $_A$ that the follower or absorber are present in the core. The experimental rod worth is given by

$$R_E(F) = R_C(F) - \varepsilon \quad (2)$$

where

$$\varepsilon = [\{\rho_{EA}(A) - \rho_{EF}(F)\} - \{\rho_{CA}(A) - \rho_{CF}(F)\}] = [\{\rho_{EA}(A) - \rho_{CA}(A)\} - \{\rho_{EF}(F) - \rho_{CF}(F)\}]$$

and it is assumed that the measured excess reactivities of the cores with the absorber loading and the follower loading, $\rho_{EA}(A)$ and $\rho_{EF}(F)$, use a reactivity scale which is accurately known and the worth of the edge elements is being accurately calculated. The corresponding calculated excess reactivities of the cores are $\rho_{CA}(A)$ and $\rho_{CF}(F)$.

The excess reactivities of the critical configurations were measured using the calibrated control rod, FR9, calibrated by means of period measurements and the inhour equation, initially with the delayed neutron data of Stevenson (Internal UKAEA document FRIDWP/P(71)14). This has been revised in the present document to use the Smith-Tomlinson scale, an increase in the measured reactivities of 3.3% (MTN/104).

Equation (2) implies that the calculated worth of the core edge elements added to compensate for the reactivity loss is consistent with this delayed neutron scale. The calculated worth of the additional core elements defines the ‘edge worth’ reactivity scale, and this must be made consistent with the delayed neutron scale (or the chosen scale which could, for example, be based on the calculated worth of plutonium in the inner core related to the measured worth, as was done in the original analysis).

The relationship between the ‘edge worth’ and the ‘delayed neutron’ scales was studied by measuring the worth of up to eight outer core elements added to a variety of follower and absorber arrays.

In the original analysis the edge worths were calculated using XY diffusion theory with group and region dependent axial bucklings, and the mean value of C/E, or ‘edge worth’/’Stevenson delayed neutron’ scale, was 0.963. The C/E values for 76 comparisons were grouped in different ways to look for possible trends in the mean value of C/E with the number of core elements loaded or with the numbers of elements involved in a change. No significant trends were found as can be seen from the data in MTN/92. The analysis of the reactivity scale experiments in MZB (MTN/52), in which inner core fuel depletion was balanced by the addition of edge fuel, gave confidence that this ratio applied to the larger fuel additions made in MZC to an accuracy of ±1%. Relating this ratio to the Smith-Tomlinson delayed neutron scale implies a C/E ratio for the edge element worths 3.3% lower, that is 0.932. The reactivity addition due to the edge elements, as calculated using the XY diffusion theory model in MTN/92, must therefore be increased by the factor 1.073 to be consistent with the Smith-Tomlinson delayed neutron scale, instead of the factor 1.038 used to give consistency with the Stevenson delayed neutron scale.

The revised form of equation (2) given in MTN/92 was therefore used to correct for the difference between the calculated edge element worths and the edge element worths consistent with the ‘delayed neutron’ scale; that is to the measured worths of edge elements on the delayed neutron scale:

$$R_E(F) = R_C(F) - \varepsilon + w(A)\{(1/S) - 1\} \quad (3)$$

where, $w(A) = \rho_{CA}(A) - \rho_{CA}(F)\}$

is the calculated worth of edge fuel elements
and S = {'edge worth' scale}/{'beta-effective scale} = 0.932
S could also be chosen to relate to other reactivity scales such as the plutonium worth scale and this was done in the final analysis included in MTN/92.

As stated above, this procedure of calculating edge element worths and scaling them to be consistent with measurement can be regarded as an interpolation, or extrapolation of the results of the limited set of measurements of edge element worth.

Equation (3) can be rewritten:

$$R_E(F) = \rho_{EF}(F) - \rho_{EA}(A) + w(A)/S \qquad (4)$$

1.4.2A Description of Experimental Configuration.

Detailed descriptions of the basic assembly in which the measurements were made, MZB, are given in ZEBRA-LMFR-EXP-002, Section 3.1. The changes made to the basic MZB/4 core are the additions of the mock-up rods and rod followers and the addition of edge elements. The positions of the rods and rod followers are shown in Figure1.2. The positions of the edge element additions are described here and are shown in Figure 1.3. The components of the additional outer core elements added are described in ZEBRA-LMFR-EXP-002.

The measurements made to investigate the reactivity scale involved the replacement of U-PuO2 (PUIV4) plates by UO2 plates (UO23R4) in a central region of the core and the addition of plutonium metal plates. These components are also described in ZEBRA-LMFR-EXP-002. Measurements made of the reactivity worths of plutonium metal plates are described in ZEBRA-LMFR-EXP-002 Section 1.4.

Elements loaded at the outer core boundary to maintain criticality (MTN/92).

The lattice positions and types of outer core elements added to the MZB/4 reference loading, to make each array of mock-up rods critical, are summarised for the first and second loading sequences, F and S, in Tables 1.1 and 1.2 respectively. These data are taken from MTN/92. The first loading sequence, up to 264 + 34 outer core elements, used at the beginning of the programme, followed the normal Zebra sequence to 264 + 24, and was based on the selection at each step of the next element closest to the core centre. A modified sequence was followed from 264 + 25 to 264 + 34. (The reason for this is said to be to avoid adding small numbers of poorly coupled elements in a new annular ring.) The second loading sequence, up to 264 + 106, followed the normal Zebra sequence throughout and was used primarily for outer core loadings greater than 264 + 35. The use of the two sequences in the control rod worth measurements may be summarised as follows:-

264 to (264 + 29) - Sequence 1 (or Sequence F, Table 1.1)
(264 + 35) to (264 + 106) - Sequence 2 (or Sequence S, Table 1.2)
(264 + 30) to (264 + 34) - In this range Sequence 1 or 2 are used, the choice being indicated by F or S in the tables of experimental results.

Modifications to these loading sequences, made in a few cases during measurements of outer core element worths, are detailed in Table 1.3.

Two points of detail relating to fuel element loadings should be noted. When there was no mock-up rod present in position R, lattice position (X,Y) = (39,46) was filled by an outer core element. When a mock rod was present in position S the practice adopted was to refer to the outer core loading as 264 + X, defining the normal outline of the outer core rather than the actual loading of 260 + X allowing for four elements removed.

The outer core elements added, C11-1G and C11-1D, are described in ZEBRA-LMFR-EXP-002 Section 1.1. In addition, the following element types, which contained a different plutonium plate, were used:

C11-1H	PUX8
C11-1K	PUIX8
C11-1L	PUXI8

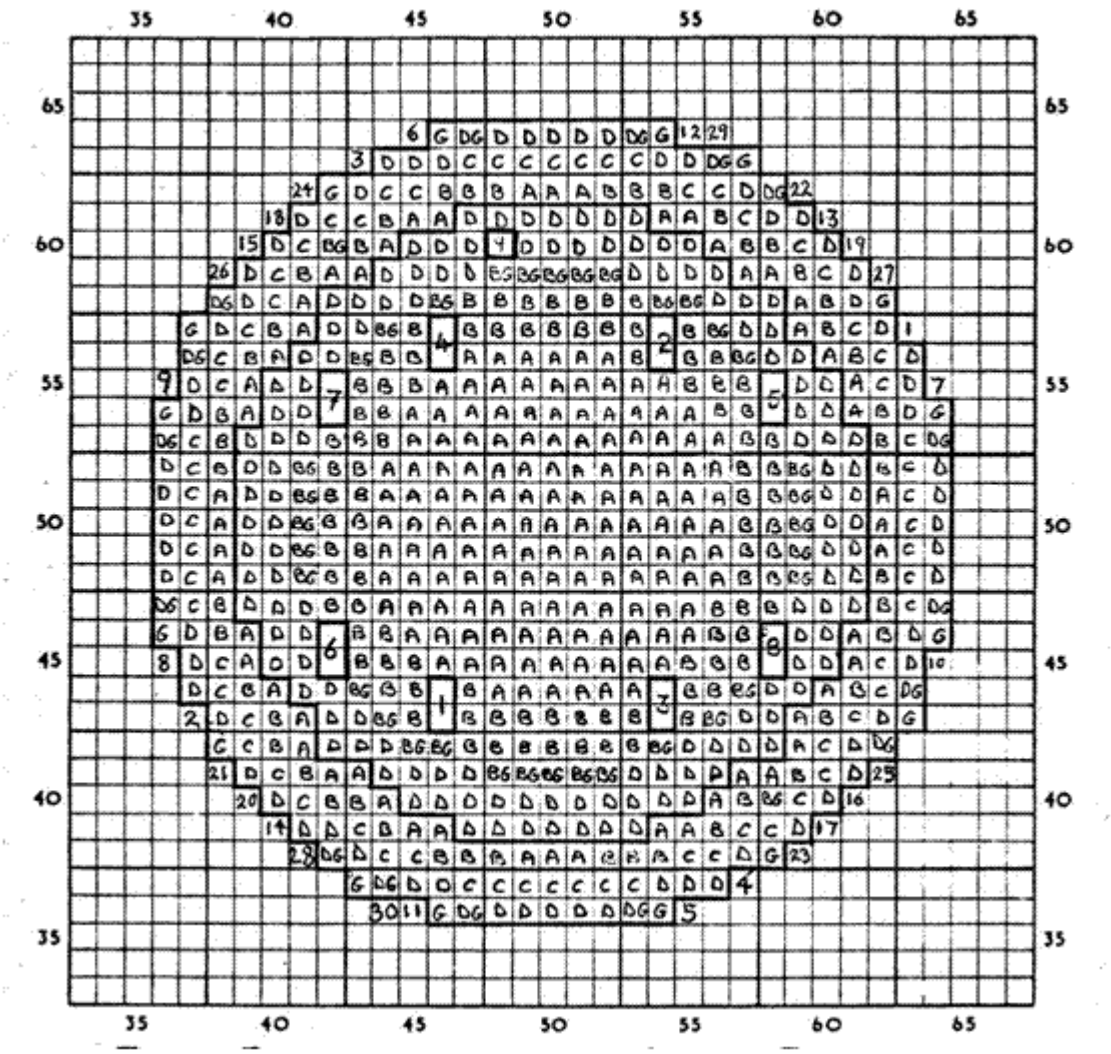

Figure 1.3 The Loading Sequence F with the first 30 Edge Elements Added, Numbered 1 to 30 in Order of Loading.

The Zebra Control Rods are numbered 1 to 9 (1 to 8 being double element rods and 9 a single rod, FR9, the regulating rod).
The element identifiers are described in Part 1 (ZEBRA-LMFR-EXP-02, Section 1.1).

Table 1.1 Outer Core Element Loading - Sequence F (the 1st loading sequence)
The Control Rod Worth calculations were made for a maximum of 30 additional edge elements whereas the critical arrays involved the addition of up to 106 edge elements. The Reactivity Scale Experiment involved the addition of up to 36 elements to the 264 outer core loading (260+40).

264 +	Lattice Position	Element Type	$(Radius)^2$ In units of $(pitch)^2$
1	63-57	Cll-1G	218
2	37-43	Cll-1G	218
3	43-63	Cll-1G	218
4	57-37	Cll-1G	218
5	55-36	Cll-1G	221
6	45-64	CII-1G	221
7	64-55	Cll-1G	221
8	36-45	Cll-1G	221
9	36-55	Cl1-1G	221
10	64-45	Cl1-1G	221
11	45-36	Cll-1G	221
12	55-64	Cll-1G	221
13	60-61	Cll-1G	221
14	40-39	Cl1-1D	221
15	39-60	Cll-1D	221
16	61-40	Cll-1D	221
17	60-39	Cll-1D	221
18	40-61	Cll-1D	221
19	61-60	Cll-1H	221
20	39-40	Cl1-1H	221
21	38-41	Cll-1H	225
22	62-59	Cll-1H	225
23	59-38	Cll-1H	225
24	41-62	Cll-1H	225
25	62-41	Cl1-1H	225
26	38-59	Cll-1H	225
27	59-62	Cll-1H	225
28	41-38	Cl1-1H	225
29	56-64	Cll-1K	232
30	44-36	Cll-1K	232
31.	36-56	Cl1-1K	232
32	64-44	Cll-1K	232
33	56-36	C11-1L	232
34	44-64	Cll-1L	232

The radius squared is in units of the mean element spacing, p.

Table 1.2 Outer Core Element Loading - Sequence S (the 2nd loading sequence)

264 +	Lattice Position	Element Type	$(Radius)^2$ In units of $(pitch)^2$
25	50-65	C11-1ED	225
26	50-35	Cll-1ED	225
27	35-50	Cl1-1ED	225
28	65-50	Cll-1ED	225
29	35-49	Cll-1ED	226
30	65-51	Cll-1ED	226
31	51-35	Cll-1ED	226
32	49-65	Cll-1ED	226
33	51-65	Cll-1ED	226
34	49-35	Cll-1ED	226
35	35-51	Cll-1ED	226
36	65-49	Cll-1ED	226
37	62-41	Cll-1H	225
38	38-59	Cll-1H	225
39	59-62	Cll-1H	225
40	41-38	Cll-1H	225
41	65-48	Cll-1ED	229
42	35-52	Cll-1ED	229
43	52-65	Cll-1ED	229
44	48-35	Cll-1ED	229
45	35-48	Cll-1ED	229
46	65-52	Cll-1ED	229
47	52-35	C11-1ED	229
48	48-65	Cll-1ED	229
49	56-64	Cll-1K	232
50	44-36	Cl1-1K	232
51	36-56	Cll-1K	232
52	64-44	Cl1-1K	232
53	56-36	Cll-1L	232
54	44-64	Cll-1L	232
55	64-56	Cll-1L	232
56	36-44	Cl1-1L	232

Table 1.2 - Continued

264 +	Lattice Position	Element Type	$(Radius)^2$ In units of $(pitch)^2$
57	37-58	Cll-1L	233
58	63-42	Cll-1A	233
59	42-37	Cll-1ED	233
60	58-63	Cll-1ED	233
61	63-58	Cll-1ED	233
62	37-42	Cll-1ED	233
63	42-63	Cll-1ED	233
64	58-37	Cll-1ED	233
65	53-35	Cl1-1ED	234
66	47-65	Cl1-1ED	234
67	65-53	Cll-1ED.	234
68	35-47	Cll-1ED	234
69	35-53	Cll-1ED	234
70	65-47	Cll-1ED	234
72	47-35	Cll-1ED	234
72	53-65	Cll-1ED	234
73	54-65	Cll-1ED	241
74	46-35	Cl1-1ED	241
75	35-54	Cll-1ED	241
76	65-46	Cll-1ED	241
77	54-35	Cll-1ED	241
78	46-65	Cll-1ED	241
79	65-54	Cl1-1ED	241
80	35-46	Cl1-1ED	241
81	39-61	Cl1-1ED	242
82	61-39	Cl1-1ED.	242
83	39-39	Cll-1ED	242
84	61-61	Cll-1ED	242
85	62-60	Cl1-1ED	244
86	38-40	Cl1-1ED	244
87	40-62	C11-1ED	244
88	60-38	Cll-1ED	244
89	40-38	Cll-1ED	244

Table 1.2 - Continued

264 +	Lattice Position	Element Type	(Radius)^2 In units of (pitch)^2
90	60-62	Cll-1M	244
91	62-40	Cll-1M	244
92	38-60	Cl1-1M	244
93	43-64	Cll-1M	245
94	57-36	Cll-1M	245
95	36-43	Cll-1M	245
96	64-57	Cll-1M	245
97	64-43	Cl1-1M	245
98	36-57	Cl1-1M	245
99	57-64	Cll-1M	245
100	43-36	Cll-1M	245
101	41-37	Cll-1M	250
102	59-63	Cll-1M	250
103	63-41	Cll-1M	250
104	37-59	Cll-1M	250
105	41-63	Cll-1M	250
106	59-37	Cl1-1M	250

Table 1.3 Loading Changes not in Sequence

Start-Up Number	Array Number	Specification of Outer Core Loading
531	F15/3	264 + 34F with Cll-1ED's removed from 39-60 from 39-40 from 61-60 from 61-40
590	33/5	264 + 30S with Cll-1ED's transferred from 50-65 to 56-64 from 65-51 to 59-62 from 65-50 to 62-41 from 50-35 to 44-36 from 35-49 to 41-38 from 35-50 to 38-59
637	39/2	264 + 100 with Cll-1ED's transferred from 46-35 to 41-37 from 54-65 to 59-63 from 65-46 to 63-41 from 35-54 to 37-59
662	26/5	264 + 70 with Cll-1ED's removed from 65-53 from 35-47
663	26/6	264 + 70 with Cll-1ED's removed from 34-47 from 35-53
680	23/7	264 + 86 with Cll-.lED's removed from 65-54 from 65-46
681	23/8	264 + 86 with Cll-1ED's removed from 35-54 from 35-46
682	23/9	264 + 86 with Cll-1ED's removed from 46-35 from 54-35

Start-up numbers are sequential in time. An array number is in two parts, M/N. M denotes the type of array and N the particular measurement made for this type of array (1, 2, 3 ..., for the first, second or third measurement, for example). F before the array type number, M, denotes a follower array and so, F15/3 denotes the third measurement for follower array number 15. Measurements for a particular array are made several times, at different stages of the programme.

The positions of the added edge elements belong to either the first or second loading sequence and are denoted by:

F - First loading sequence S - Second loading sequence

and so 264 + 34F denotes 34 edge elements added in the positions of the first sequence. When the loading is the same in both sequences the letter F or S is omitted.

Mock-up Control rod Dimensions

Details of the compositions and dimensions of the ZEBRA-PNC (MONJU) Mock-up Control Rods are given in MTN/39, by C G Campbell and S Kobayashi, and the Supplement, from which the following data have been abstracted. The compositional data used in the original Winfrith analyses, and also adopted here, are those given in MTN/51 by J Marshall.

There were three types of mock-up rods;

(1) arrays of 19 natural and enriched boron absorber pins in sodium filled calandria,
(2) arrays of 19 tantalum pins in the same sodium filled calandria and
(3) a special absorber element consisting of an array of 37 enriched boron absorber pins inside an aluminium block with a cylindrical hole to hold the close packed array of boron pins.

There were also follower elements to simulate withdrawn absorber rods, these being sodium filled calandria without the absorber pin tubes. In the case of the rod with 37 pins in an aluminium block the follower was an aluminium cylinder which fitted into the space of the cluster of 37 pins.

The mock-up control rods of Type (1) and (2) consist of the following main components:

i The Control Rod Sheath which contains the absorber and follower elements, one above the other
ii The Control Absorber Element (Calandria)
iii Follower Elements above and below the Control Absorber Element, or replacing it. These were of different lengths so that partially inserted absorber rods could be simulated.
iv Spacers (Upper and Lower)
v Absorbers
vi Shock Absorber
vii Top Cap
viii Lifting Assembly.
ix Locating Assembly

Each component consists of several parts which are usually welded or assembled with screws. Details are given in MTN/39.

The Control Rod Sheath

The Control Rod Sheath is a 302.414 cm long square section empty stainless steel tube, 10.623 cm outer width and 10.47 cm inner dimension; a top cap and a lifting device are fitted to the top of this tube, and a locating device is fitted at the bottom. This contains three calandria, one above the other. The central one can be either an absorber element or a control rod follower element and the top and bottom elements are follower elements. Partially inserted absorbers were also simulated. The sheath replaces a 2x2 group of normal elements.

Control Absorber and Follower Elements (The Calandria)

The calandria type Control Absorber Element consists of the following stainless steel parts, as shown in Figure1.1A

i an outer square tube which fits inside the control rod sheath
ii an inner cylindrical tube which fits inside the outer square tube
iii 19 calandria tubes which contain the absorber pins
iv 2 end plates
v 1 support plate
vi 1 cover plate
vii 2 filling and venting bosses

The calandria is filled with sodium in an atmosphere of nitrogen gas, at room temperature.

The Follower Element has essentially the same cross-section but without the tubes for the absorber pins. These were available in several different lengths so that partially inserted control rods could be assembled.
(In the calculational model the outer square tube is combined with the control rod sheath and the calandria tubes are combined with the cans of absorber pins when these are canned. The outer dimension of the combined region of sheath plus calandria walls is taken to be 10.7442 cm the width of the 4x4 lattice area which the mock-up rods occupy, that is 2x5.3721cm, the lattice spacing within the groups of 5x5 elements).

Details of the dimensions and weights are given in the Appendix to Section 1.4.3, the following being a summary.

The square section outer calandria tube, which has an inner dimension of 9.86 cm (inside area of 97.2196 cm^2), has 2 groups of 4 dimples on the outside and is welded to an end plate on each end. The end plate has 19 holes, into which the 19 calandria tubes are welded. Two filling and venting bosses, which are used for filling the calandria with sodium, and two locating bosses, to which a cover plate is attached, are located in the four corners of the top end plate, and four locating bosses are provided to secure a support plate in a bottom end plate. ***(In the calculational model the end regions are treated as uniform plates and the dimples are treated as uniform additions to the steel of the calandria walls.)***

In order to get enough stainless steel in a control element, a cylindrical tube of outer diameter 9.845 cm was included in the element, fitting close inside the outer square tube. The wall thickness is 0.41 cm and so the inner diameter is 9.025 cm and the cross-sectional area of the steel tube is 12.1528 cm^2. This cylindrical tube has 6 slots of 0.8 cm width and 0.8 cm depth which are located equidistantly around the periphery at both ends. The array of 19 absorber pins is within this tube. ***(The tube is treated as a uniform cylinder (without the slots) in the calculational model.)***

The overall length of the assembled control element, including the end regions, is 91.44 cm.
The follower elements were in 5 different lengths so that partially inserted elements could be simulated. The lengths of the assembled follower elements, including end regions, were 91.44 cm, 45.72 cm, 35.56 cm, 22.86 cm and 15.00 cm.

The followers occupying the upper and lower axial blanket regions have the height 35.56 cm.

The Calandria Tubes which hold the Absorber Pins

The pattern of the 19 holes for the absorber pins and the 4 holes for the bosses in the end plates, is as follows (see Figure 1.1A).

There is one hole at the centre, 6 with centres on a circle of diameter 3.58 cm, 12 with centres on a circle of diameter 6.92 cm and the four holes for the bosses are centred on a circle of diameter 10.82 cm. ***(The bosses are not represented in the calculational model.)***

The centres of the absorber pins in the ring of 6 are on the lines at an angle of $45^o + n \times 60^o$ to the positive x-axis (where the pins are numbered from 0 to 5) and in the outer ring the centres are on the lines at an angle of $n \times 30^o$ (for the pins numbered from 0 to 11).

The stainless steel calandria tubes (which contain the absorber pins) are of outer diameter 1.55 cm and inner diameter 1.35 cm.

The Absorber Pins

The boron absorber pins consist of a stack of pellets contained in steel cans (the outer diameter of the can being 1.31 cm for the boron absorber pins, other than the 90% enriched pins, which have cans with an outer diameter of 1.27 cm) which fit inside the calandria tubes. The boron enrichments are: natural, 30% enriched, 80% enriched and 90% enriched, the rods containing these being denoted by BN, B30, B80 and B90 respectively. The stainless steel cans are the same for the natural, 30% and 80% enriched pins but are different for the 90% enriched pins. The height of the stack of pellets is taken to be 90.5 cm and the diameter 1.1 cm although the actual dimensions differ from these values (see Table A3 in the Appendix). The corresponding cross-sectional area of boron absorber is then calculated to be 0.95033 cm^2 and for the 19 pins is 18.0563 cm^2. The length of the boron pins with their end regions welded on is 91.36 cm. ***Fuller details of the dimensions and weights are given in the Appendix to Section 1.4.3.***

The diameter of the tantalum absorber pins, which are not contained in cans, is 1.31 cm (the corresponding cross-sectional area of the tantalum pin is calculated to be 1.34782 cm^2 and for the 19 pins is then 25.6086 cm^2). The length of the tantalum pin is 91.337 cm.

The B80/90 Rod and Follower

The data for this element are given in MTN/79. The array of 37 absorber pins is contained in a square aluminium block having sides 10.2 cm square and a central cylindrical void region of 9 cm diameter. The length of the block is 91.36 cm, the volume 3693.02 cm^3 and the weight of aluminium 9.973 kg (density 2.7005 g/cm^3). The inner array of 19 B90 pins (1+6+12), diameter 1.27 cm, is surrounded by a ring of 18 B80 pins, diameter 1.31 cm, and held in place by means of 7.6 cm long stainless steel shims at either end of the array, between the B90 and B80 pins. The shims are 0.066 cm thick and weigh 75 g.

The follower is formed by replacing the absorber pins in the aluminium block with a cylinder of aluminium, 91.34 cm long and 8.95 cm diameter in the central void region, volume 5746.41 cm^3, weight 15.496 kg (density 2.6966 g/cm). ***In the calculational model the B80/90 Follower is assumed to be a solid aluminium region, 10.2 cm x 10.2 cm x 91.36 cm, volume 9505.09cm^3, having the combined weight of 25.433 kg (density 2.6757 g/cm^3)***

The aluminium block is contained in the square section stainless steel sheath, which has an inner width of 10.47 cm and outer width of 10.623 cm. ***In the calculational model the outer width is assumed to be 10.7442 cm and inner width 10.2 cm, thus eliminating the gaps.***

1.4.2B Methods

The Reactivity Scale

The reactivity measurements were made in terms of standard cms. of insertion of the regulating control rod, FR9. This was calibrated by period measurements, the periods being typically about 100 secs. The rod was recalibrated at various stages though the programme of measurements. The reactivities were then expressed in absolute terms via the inhour equation interpreted using fission rates calculated using the FGL5 nuclear data library, the MURAL cell code and diffusion theory whole reactor calculations, together with the Smith-Tomlinson delayed neutron data set. The reactivity scale has an estimated systematic uncertainty of ± 5% (see Section 2.4). There are also random uncertainties in the excess reactivity measurements due to uncertainties in rod profile (the variation of rod worth with rod insertion) and reproducibility of measurements. This random component is about ± 1%.

The reactivity scale is described and evaluated in Section 2.4.

The assemblies containing the mock-up control rods and rod followers were made critical by the addition of core elements at the core edge, as described earlier in Section 1.4. The excess reactivity was balanced by the insertion of the regulating control rod. The critical state of an array of mock-up rods is therefore characterised by the numbers of edge elements and the standard cm of insertion of regulating rod, FR9.

1.4.2C Results

The experimental rod worths were derived from the critical balance results using the method described in Section 1.4.1 above. The rod for which the measurement was made is characterised by the rod (BN, B30, B80, B90, Ta or Na for a follower) and the position (O, P1, P2, Q, R, S). The measurement for a follower at the core centre is denoted by Na(O) and for a natural boron rod at the core centre by BN(O), and a tantalum rod at position S is denoted by Ta(S). Arrays of rods have a similar notation, B80(P1)B90(Q), etc.

The outer core fuel element loading and critical balance results for each of the follower and absorber arrays studied are summarised in Tables 1.7 to 1.12:-

Table 1.7 - Single followers
Table 1.8 - Two, three and four follower arrays
Table 1.9 - Single BN rods
Table 1.10 - Single tantalum and enriched boron rods
Table 1.11 - Two absorber arrays
Table 1.12 - Three and four absorber arrays

The Positions of the Added Edge Elements

The lattice positions and types of outer core elements added to the MZB/4 reference loading to make each array of mock-up rods critical, are summarised in Section 1.4.2A.

Determination of the Excess Reactivities of the Assemblies with Mock-up Rods Present

The reactivity worth profile for FR9 measured in the reference core configuration, MZB/4, was used in the analysis of the MZC measurements. Similarly the technique used to calibrate the worth per standard centimetre of FR9 by period measurements also followed that used in MZB/4.

The measurements made in MZB/3 gave the following result when analysed used the Stevenson delayed neutron data and the FD4 cross-section set:

Table 1.6 The Original Absolute Calibration of FR9 in MZB/3 (using Stevenson delayed neutron data and FD4 cross-sections)

Rod Movement Above Critical	Period (secs)	Reactivity (10^{-4}dk/k)	Reactivity/ std cm (10^{-4}dk/k/cm)
4.99	181.6	1.809	0.362
6.06	143.1	2.215	0.365
7.07	118.5	2.586	0.366
4.07	230.1	1.472	0.362

The average reactivity/std cm is 0.364 x 10^{-4} dk/k. This was later increased to 0.376 x 10^{-4} dk/k, an increase of 3.3%, when the measurements were analysed using the Smith-Tomlinson delayed neutron data and FGL5 cross-sections. The corresponding Smith-Tomlinson/FGL5 value for MZC/4 is 0.437 x 10^{-4} dk/k.

Measurements of FR9 worth were made for the majority of arrays studied in the MZC programme. In those cases for which measurements were not made the worths were either based on measurements in similar arrays or were obtained by the following method: A study of the correlation between the flux squared, (obtained from the standard 9-group XY diffusion theory calculation method that was used in the original analysis), at the FR9 position, and the measured worth of FR9, allowed an estimate to be made of FR 9 worth (from the calculated value of flux squared) in those arrays for which no measurement was made, with an estimated accuracy of ±1%. The worths per standard cm for FR9 used in the analysis of the MZC measurements are summarised in Table 16 of MTN/92 for each array (where the earlier delayed neutron data set of Stevenson was used, subsequently increased by 3.3% to be consistent with analyses made using the Smith-Tomlinson data set), and are included in the detailed summary of experimental data for each array given in the present document. A total of 34 measurements of FR9 worth per standard cm was made in the MZC programme. The highest value was 0.571 x 10^{-4} dk/k with the loading B80(P1) B90(P5), and the lowest was 0.341 x 10^{-4} dk/k with B80(P2), compared with 0.437 x 10^{-4} dk/k in the reference MZB/4 configuration, a range of -22% to +30%.

The excess reactivity for each critical configuration has been corrected for Pu241 decay and referred to 1 May 1972, the date on which the composition of the MZB fuel elements was defined for the calculational model. The Pu241 decay correction for MZB was based on a calculated reactivity decrease of 0.9 x 10^{-4} dk/k per month. To simplify the decay corrections the working day was divided into two periods from 08.30 hours to 14.30 hours and from 14.30 hours to 20.30 hours.

Experimental Excess Reactivities.

The figures in the following Tables are based on the data in MTN/92 with an adjustment of the beta-effective reactivity scale by the factor 1.033 to correspond to the FGL5 cross-sections and Smith-Tomlinson delayed neutron data. A correction has also been made for the difference in the numbers of edge elements from 8 elements (in the case of the Follower loadings, and 4 in the case of the Follower at position S). This is the reason the figure 7 is followed by (8) in the Column headed Added to edge.

Table 1.7 Experimental Excess Reactivities for Single Follower Loadings

Zebra Array Number	Start Up No.	Follower Loading	Added To Edge	Time and Date	Excess Reac. Std. cm	FR9 Worth Per std. cm	Pu241 decay Correct	Edge Elem. Correct *	Exp. Excess Reac.
			264 +			$x10^{-4}$	$x10^{-4}$	$x10^{-4}$	$x10^{-4}$
MZB(4)	437		0	A1.12.72	39.700	0.4370	6.30		23.65
MZB(4)	702		0	P28.3.73	32.580	0.4370	9.82		24.06
MZB(4)	703		0	A29.3.73	32.540	0.4370	9.84		24.06
MZB(4)	773		0	A24.4.73	30.328	0.4370	10.62		23.87
F1/3	691	Na(O)	7 (8)*	A27.3.73	8.580	0.4405	9.78	3.34	16.90
F1/1	490		8	A29.12.72	21.351	0.4405	7.14		16.54
F1/2	534		8	A 16.1.73	20.019	0.4405	7.68		16.50
F1/4	692		8	A 27.3.73	16.077	0.4405	9.78		16.86
F1/5	701		8	P 28.3.73	15.900	0.4405	9.82		16.82
F2/3	694	Na(P_1)	6 (8)*	P 27.3.73	9.850	0.4530	9.79	6.56	20.81
F2/1	489		8	A29.12.72	29.518	0.4530	7.14		20.51
F2/2	693		8	A 27.3.73	24.563	0.4530	9.78		20.91
F3/2	695	Na(P_2)	6 (8)*	P 27.3.73	10.970	0.4277	9.79	6.67	21.15
F3/1	487		8	P28.12.72	31.550	0.4277	7.13		20.62
F3/1	488		8	A29.12.72	31.559	0.4277	7.13		20.63
F3/3	696		8	P 27.3.73	26.320	0.4277	9.79		21.05
F4/3	698	Na(Q)	4 (8)*	A 28.3.73	12.128	0.4411	9.81	13.00	28.16
F4/1	486		8	P28.12.72	46.960	0.4411	7.12		27.83
F4/2	697		8	A 28.3.73	41.674	0.4411	9.81		28.19
F5/2	699	Na(R)	3 (8)*	A28.3.73	11.125	0.4519	9.81	16.00	30.84
F5/1	485		8	A28.12.72	52.221	0.4519	7.11		30.71
F5/3	700		8	A 28.3.73	47.076	0.4519	9.81		31.09
F6/2	482	Na(S)	2 (4)*	A28.12.72	11.935	0.4442	7.11	6.66	19.07
F6/1	481		4	A22.12.72	27.336	0.4442	6.93		19.07
F6/4	690		4	A 23.3.73	21.805	0.4442	9.78		19.47
F6/3	483		8 (4)*	A28.12.72	55.704	0.4442	7.11	-12.65	19.20
MZB(5)									
46/1	826	Al(O)	8	P31.5.73	5.695	0.4405	11.74		14.25
46/2	827		11 (8)*	P 31.5.73	28.732	0.4405	11.74	-9.99	14.41
F1/7	829	Na(O)	8	P 31.5.73	10.150	0.4405	11.74		16.21
F1/8	830		8	A1.6.73	10.150	0.4405	11.76		16.23
F1/6	828		11 (8)*	P 31.5.73	33.145	0.4405	11.74	-10.00	16.34
MZB(5)	777		0	A.26.4.73	29.909	0.4370	10.68		23.75
MZB(5)	831		0	P 1.6.73	26.701	0.4370	11.77		23.44
MZB(5)	832		0	A 4.6.73	26.374	0.4370	11.85		23.37

(In the dates, A - 0830 hours to 1430 hours P - 1430 hours to 2030 hours.)
* Correction added to obtain the value for 4 or 8 edge elements (as shown by the figure in brackets)
The transition from MZB(4) to MZB(5) involved the repositioning of Zebra control rods 2 and 3. The excess reactivity of MZB changed from 23.87 $x10^{-4}$ dk/k (on 24.4.73) to 23.75 $x10^{-4}$ dk/k (on 26.4.73).

The figures in the final column have been adjusted to correct for differences in the numbers of edge elements, using the diffusion theory calculated values of the edge worths given in MTN/92 scaled up by the factor 1.073 to make them consistent with the Smith-Tomlinson delayed neutron reactivity scale. (This factor of 1.073 is the one which is to be applied to the calculated edge element worths to give the value measured on the Smith-Tomlinson reactivity scale.) These corrections are given in the next to last column.

It will be seen that the figures fall into two groups, depending on the date of the measurements. The excess reactivities measured around the date 28.3.73 are about 0.35×10^{-4} dk/k higher than those measured around 28.12.72 and also around 1.6.73 and so it does not appear to be an error in the correction for Pu241 decay. The change in core, from MZB(4) to MZB(5) involved the repositioning of Zebra control rods 2 and 3 but it can be seen that the change in the excess reactivity of MZB was only from 23.87×10^{-4} dk/k (on 24.4.73) to 23.75×10^{-4} dk/k (on 26.4.73), a reduction by 0.12×10^{-4} dk/k. Thus we can take into account the measurements made on MZB(5) in drawing conclusions about this apparent time dependence. The reason why the values measured around 28.3.73 are higher is not understood. However, as a consequence of this, when rod worths are derived the differences between measurements made on dates which are in the same date group are taken.

Table 1.8 Experimental Excess Reactivities for Arrays of Followers

Array Number	Start Up No.	Follower Loading	Outer Core Load 264 +	Time and Date	Excess Reac. Std. cm	FR9 Worth Per Std. cm 10^{-4}dk/k	Pu241 Correct. To 1.5.72, 10^{-4}dk/k	Edge Elem. Correct	Exp. Excess Reac. 10^{-4}dk/k
MZB(4)	437		0	A1.12.72	39.7	0.437	6.3		23.65
MZB(4)	702		0	P28.3.73	32.58	0.437	9.82		24.06
MZB(4)	703		0	A29.3.73	32.54	0.437	9.84		24.06
MZB(4)	773		0	A24.4.73	30.328	0.437	10.62		23.87
F7/1	538	Na(O,P1)	15	A17.1.73	8.17	0.4597	7.71		11.47
F8/1	539	Na(P1,P2)	14	A17.1.73	10.722	0.4361	7.72		12.40
F9/1	540	Na(P1,P5)	14	P17.1.73	8.109	0.4659	7.72		11.50
F9/2	541		18 (14)	P17.1.73	37.619	0.4659	7.72	-13.78	11.47
F9/3	542		20 (14)	P17.1.73	52.81	0.4659	7.72	-20.77	11.55
F10/1	537	Na(P1,Q)	12	A17.1.73	11.169	0.4514	7.71		12.75
F11/1	536	Na(P1,R)	11	A17.1.73	9.255	0.4583	7.71		11.95
F12/1	535	Na(Q,R)	8	P16.1.73	5.056	0.4526	7.69		9.98
F13/2	546	Na(O,P2,P3)	23	P18.1.73	9.725	0.4452	7.75		12.08
F13/1	545		24 (23)	A18.1.73	17.491	0.4452	7.74	-3.44	12.09
F13/3	547		26 (23)	P18.1.73	33.257	0.4452	7.75	-10.40	12.16
F14/1	543	Na(P1P3P5)	22	A18.1.73	5.424	0.4494	7.74		10.18
F14/2	544		26 (22)	A18.1.73	36.918	0.4494	7.74	-14.22	10.11
F15/1	549	Na(P2P2'P5 P5')	30F	P18.1.73	6.612	0.4525	7.75		10.74
F15/3	551		30N (30F)	A19.1.73	-1.759	0.4525	7.77	2.81	9.78
F15/2	550		34F (30 F)	A19.1.73	34.843	0.4525	7.77	-12.85	10.68

A - 0830 hours to 1430 hours P - 1430 hours to 2030 hours

Some FR9 worths are estimated values (see MTN/92)

The Excess Reactivities have been adjusted for differences in the outer core loading for each follower loading, the reference number of edge elements for the array of followers being the figure in brackets.

Table 1.9 Experimental Excess Reactivities for Single Natural Boron Absorber Rods

Array Number	Start Up Number	Follower Loading	Outer Core Loading Increase 264 +	Time and Date	Excess Reactivity, Std. cm	FR9 Worth Per Std. cm , 10^{-4}dk/k	Pu241 Correction To 1.5.72, 10^{-4}dk/k	Experimental Excess Reactivity, 10^{-4}dk/k
1/2	527	BN(O)	29	A12.1.73	7.250	0.4380	7.56	10.74
1/1	526		32 F	A12.1.73	29.501	0.4380	7.56	20.48
1/4	564		32 F	A26.1.73	28.091	0.4380	7.98	20.28
1/5	565		32 F	A26.1.73	28.107	0.4380	7.98	20.29
2/1	521	BN(P1)	26	P10.1.73	16.009	0.4587	7.51	14.85
2/2	522		28	A11.1.73	31.081	0.4587	7.53	21.79
2/3	523		31 F	A11.1.73	50.778	0.4587	7.53	30.82
2/4	524		32 F	A11.1.73	58.643	0.4587	7.53	34.43
3/1	519	BN(P2)	24	A10.1.73	3.723	0.3801	7.50	8.92
3/2	520		26	A10.1.73	21.759	0.3801	7.50	15.77
4/1	503	BN(Q)	16	A3.1.73	0.540	0.4297	7.29	7.52
4/2	504		20	A3.1.73	32.534	0.4297	7.30	21.28
4/3	505		22	P 3.1.73	48.562	0.4297	7.30	28.17
5/3	686	BN(R)	13	A26.3.73	14.525	0.4607	9.75	16.44
5/1	501		16	P 2.1.73	39.705	0.4607	7.28	25.57
5/2	502		16	A 3.1.73	39.592	0.4607	7.28	25.52
6/5	497	BN(S)	6	A 2.1.73	9.254	0.4411	7.26	11.34
6/7	688		7	P26.3.73	12.185	0.4411	9.76	15.13
6/1	492		8	P29.12.2	23.320	0.4411	7.15	17.44
6/2	493		8	A 1.1.73	23.062	0.4411	7.23	17.40
6/3	495		8	P 1.1.73	22.926	0.4411	7.24	17.35
6/4	496		8	A 2.1.73	22.957	0.4411	7.26	17.39
6/6	498		12	A 2.1.73	51.459	0.4411	7.26	29.96

F denotes the first and S the second edge element loading sequences, when these differ (see Tables 1.1 and 1.2 respectively)

Table 1.10 Experimental Excess Reactivities for Single Enriched Boron and Tantalum Rods

Array Number	Start Up Number	Follower Loading	Outer Core Loading Increase, 264 +	Time and Date	Excess Reactivity, Std. cm	FR9 Worth Per Std. cm 10^{-4} dk/k	Pu241 Correction To 1.5.72, 10^{-4}dk/k	Experimental Excess Reactivity, 10^{-4}dk/k
07/1	571	B30(O)	34 F	P29.1.73	4.231	0.4401	8.08	9.94
07/2	572		36	A30.1.73	19.111	0.4401	8.10	16.51
08/1	525	B30(P1)	32 F	P11.1.73	26.585	0.4566	7.54	19.68
09/2	507	B30(Q)	20	P 3.1.73	8.710	0.4225	7.30	10.98
09/1	506		22	P 3.1.73	24.890	0.4225	7.30	17.82
09/3	508		26	A 4.1.73	56.229	0.4225	7.32	31.08
10/2	579	B80(O)	48	A 31.1.73	8.870	0.4421	8.13	12.05
10/3	623		48	P 23.2.73	7.420	0.4421	8.82	12.10
10/4	624		48	A 26.2.73	7.242	0.4421	8.91	12.11
10/1	578		52	A 31.1.73	40.535	0.4421	8.13	26.05
11/2	574	B80(P1)	42	P 30.1.73	12.100	0.4681	8.11	13.77
11/1	573		44	P 30.1.73	26.540	0.4681	8.11	20.53
12/2	567	B80(Q)	28	A 26.1.73	6.994	0.4124	7.99	10.87
12/1	566		30F	A 26.1.73	22.053	0.4124	7.98	17.07
13/3	687	B80(S)	11	A 26.3.73	7.800	0.4432	9.75	13.21
13/1	499		12	A 2.1.75	20.546	0.4432	7.27	16.38
13/2	500		16	P 2.1.73	50.223	0.4432	7.27	29.53
14/1	580	B90(O)	51	P 31.1.73	11.969	0.4421	8.14	13.43
15/1	568	B90(Q)	30 F	P 26.1.73	9.420	0.4173	7.99	11.92
15/2	569		34F	A 29.1.73	37.738	0.4173	8.07	23.82
16/4	518	Ta(O)	24	P 9.1.73	7.186	0.4432	7.48	10.66
16/1	509		26	P 4.1.73	23.455	0.4432	7.33	17.72
16/2	516		28	P 9.1.73	39.656	0.4432	7.48	25.05
16/3	517		30 F	P 9.1.73	54.035	0.4432	7.48	31.43
17/2	689	Ta(S)	6	P 26.3.73	11.960	0.4411	9.76	15.04
17/1	491		8	P29.12.72	31.233	0.4411	7.15	20.93
43/l	683	B90(P2)	44	A 23.2.73	14.310	0.3414	9.66	14.55
44/2	685	B80(P2)	41	A 23.3.73	8.332	0.3414	9.66	12.50
44/1	684		46	A 23.3.75	56.955	0.3414	9.66	29.10
45/1	824	B80/B90(0)	63	A 30.5.73	1.379	0.4386	11.70	12.30
45/2	825		67	A 30.5.73	34.419	0.4386	11.70	26.80

F denotes the first and S the second edge element loading sequences, when these differ (see Tables 1.1 and 1.2 respectively). When no letter is attached the sequence numbers are the same.

Table 1.11 Experimental Excess Reactivities for Arrays of Two Absorbers

Array No.	Start Up No.	Follower Loading	Outer Core Loading Increase, 264 +	Time and Date	Excess Reactivity, Std.cm.	FR9 Worth Per Std. cm , 10^{-4} dk/k	Pu241 Correction To 1.5.72, 10^{-4}dk/k	Experimental Excess Reactivity, 10^{-4}dk/k
23/1	674	B80(P1) B90(O)	84	A19.3.73	1.510	0.4637	9.54	10.24
23/7	680		86 N	P20.3.73	13.360	0.4637	9.58	15.78
23/8	681		86 N	P20.3.73	19.011	0.4637	9.58	18.40
23/9	682		86 N	P20.3.73	15.995	0.4637	9.58	17.00
23/2	675		88	P19.3.73	31.625	0.4637	9.55	24.21
23/3	676		88	A20.3.73	31.406	0.4637	9.57	24.13
23/6	679		88	A20.3.73	31.361	0.4637	9.57	24.11
23/5	678		90	A20.3.73	46.942	0.4637	9.57	31.34
23/4	677		92	A20.3.73	62.940	0.4637	9.57	38.76
24/3	672	B80(P1) B90(P2)	76	P 16.3.73	2.250	0.3654	9.46	10.28
24/2	671		79	A16.3.73	34.100	0.3654	9.45	21.91
24/1	670		82	A16.3.73	59.340	0.3654	9.45	31.13
25/1	667	B80(P1) B90(P5}	83	A15.3.73	-0.124	0.5717	9.42	9.35
25/2	668		88	P 15.3.73	31.236	0.5717	9.43	27.29
25/3	669		88	A16.3.73	31.006	0.5717	9.45	27.17
26/2	659	B80(P1) B90(Q)	64	P 12.3.73	-0.265	0.4407	9.34	9.22
26/3	660		66	A13.3.73	16.343	0.4407	9.36	16.56
26/1	658		68	A12.3.73	31.285	0.4407	9.33	23.12
26/5	662		68 N	A13.3.73	23.720	0.4407	9.36	19.81
26/6	663		68 N	A13.3.73	39.246	0.4407	9.36	26.65
26/4	661		70	A13.3.73	46.743	0.4334	9.36	29.62
27/2	610	B80(P1) BN(Q)	56	P 15.2.73	8.205	0.4535	8.59	12.31
27/3	657		56	A12.3.73	6.388	0.4535	9.33	12.23
27/1	609		60	P 15.2.73	38.442	0.4535	8.59	26.02
28/2	608	B80(P1) BN(R)	52	A15.2.73	4.480	0.4862	8.58	10.76
28/1	607		54	A15.2.73	19.231	0.4862	8.58	17.93
29/2	612	BN(P1) B80(P2)	62	A16.2.73	1.567	0.3605	8.61	9.17
29/1	611		64	A16.2.73	20.885	0.3605	8.61	16.14
30/2	605	BN(P1) B80(Q)	51	P 14.2.73	3.180	0.4370	8.56	9.95
30/3	606		54	A15.2.73	28.978	0.4370	8.58	21.24
30/1	604		56	14.2.73	44.013	0.4370	8.55	27.78
31/2	595	BN(P1) BN(Q)	42	A 8.2.73	5.760	0.4432	8.37	10.92
31/1	594		46	A 8.2.73	36.511	0.4432	8.37	24.55
32/1	593	BN(P1) BN(R)	38	P 7.2.73	7.191	0.4778	8.35	11.79

Table 1.11 continued. Experimental Excess Reactivities for Arrays of Two Absorbers

33/3	587	BN(Q) BN(R)	30 S	P 5.2.73	8.430	0.4535	8.29	12.11
33/6	591		30 S	P 7.2.73	7.610	0.4535	8.35	11.80
33/5	590		30 N	P 7.2.73	11.974	0.4535	8.35	13.78
33/1	585		32 S	A 5.2.73	23.812	0.4535	8.28	19.08
33/2	586		34 S	A 5.2.73	38.936	0.4535	8.28	25.94
33/7	592		36	P 7.2.73	51.410	0.4535	8.35	31.66
41/2	576	B80(P1) Na(P2)	48	P 30.1.73	7.042	0.4535	8.11	11.30
41/1	575		52	P 30.1.73	37.388	0.4535	8.11	25.06

F denotes the first and S the second edge element loading sequences, when these differ (see Tables 1.1 and 1.2 respectively). N denotes a non-standard loading detailed in Table 1.3.

Table 1.12 Experimental Excess Reactivities for Arrays of Three or More Absorbers

Array Number	Start Up Number	Follower Loading	Outer Core Loading Increase, 264 +	Time and Date	Excess Reactivity, Std.cm.	FR9 Worth Per Std. cm 10^{-4} dk/k	Pu241 Correction To 1.5.72, 10^{-4}dk/k	Experimental Excess Reactivity, 10^{-4}dk/k
34/2	630	BN(O,P2,P5)	77	P 27.2.73	7.420	0.4312	8.95	12.15
34/1	629		82	A 27.2.73	47.099	0.4312	8.94	29.25
35/1	631	B30(O)BN(P2,P5)	82	P 27.2.73	17.810	0.4312	8.95	16.63
36/1	632	B80(O)BN(P2,P5)	92	A 28.2.73	18.637	0.4311	8.97	17.00
36/2	633		94	A 28.2.73	34.654	0.4311	8.97	23.91
36/3	634		96	A 28.2.73	52.205	0.4311	8.97	31.47
37/4	618	BN(P_1P3,P5)	78	A 20.2.73	7.375	0.4525	8.73	12.07
37/2	615		80	A 19.2.73	22.978	0.4525	8.70	19.10
37/3	617		80	A 20.2.73	23.251	0.4525	8.73	19.25
37/1	614		82	A 19.2.73	38.153	0.4525	8.70	25.96
37/5	619		82	P 20.2.73	38.105	0.4525	8.74	25.98
39/1	636	BN(P2,P2',P5,P5')	100	A 28.2.73	7.010	0.4370	9.00	12.06
39/2	637		100 N	A 1.3.73	5.120	0.4370	9.00	11.24
39/3	638		103	A 1.3.73	31.779	0.4370	9.00	22.89
39/5	640		104	P 1.3.73	39.446	0.4370	9.01	26.25
39/4	639		106	P 1.3.73	55.690	0.4370	9.01	33.34
42/2	626	BN(P2,P5)Na(O)	60	P 26.2.73	2.328	0.4373	8.92	9.94
42/1	625		62	P 26.2.73	19.499	0.4373	8.92	17.45
42/3	627		64	P 26.2.73	34.980	0.4373	8.92	24.22

N denotes a non-standard loading detailed in Table 1.3.

Derived Reactivity Worth Values for Followers and Rods

From the critical balance measurements and calculations of rod worths, corresponding measured values of the worths have been deduced in MTN/92. These derived reactivity worths are the values deduced for cores having the same size as reference cores containing either fuel in place of the rod or followers in place of the rod. The values given in the present document have been scaled to refer to a reactivity scale based on the period measurements for FR9 interpreted using the Smith-Tomlinson delayed neutron data and FGL5 cross-sections.

The calculations in MTN/92 were made using 2D diffusion theory models with group and region dependent axial bucklings used to treat axial leakage and a simple homogenisation method used for the rod and follower regions. These models can result in discrepancies of up to 14% in the calculated rod worths but it was concluded in MTN/92 that the procedure results in accurate values for the effect of the change in core size on the measured reactivity worths, with random uncertainties (relative plus absolute) typically about (±1% combined with $\pm$ 0.5 x 10^{-4} dk/k).

The random uncertainties given in MTN/92 have been adopted here. These have to be combined with the systematic uncertainty in the reactivity scale, which was given as ± 5%. We note the consistency with the plutonium reactivity scale (the comparison of the measured and calculated reactivity worth of plutonium additions). However a large correction of 7.3% has to be applied to the calculated worth of edge elements to give consistency with the delayed neutron scale and the reason for this has not been investigated.

Components of the uncertainty (as given in MTN/92).

1. The worth per standard cm of FR9 in each array has an estimated uncertainty of ±1%, based on consideration of error sources in the period measurements, including rod movement, and from a consideration of the accuracy of values obtained by the (flux squared) correlation method for those arrays in which control rod calibration measurements were not made.

2. Errors in the correction from actual to standard cm of FR9 were assessed from an examination of profiles obtained from counters at the core centre and in the top shield doors, and from a measurement of the profile in array BN(P1,P3,P5). Pairs of balances with different
FR9 heights have an uncertainty assigned of ±1% of the difference in standard cm. An additional error component varying from zero standard cm, for pairs of balances at mid-rod height, to ±0.2 standard cm, for pairs of balances close to the fully raised position, has been assigned to allow for possible small changes in profile with change in core loading. The profile uncertainty is a maximum of ±1% of rod worth for low worth mock-up rod and follower loadings at position S.

3. Examination of all repeat balances for the same core loadings made throughout the MZC programme, following major rearrangements of the core and changes in the state of the core temperature distribution, indicates an uncertainty in comparing two balances of about ±1 standard cm. For a small number of loadings, 13/3 B80(S), 17/2 Ta(S) and 6/7 BN(S) referred to F6/4 Na(S), the uncertainty in the comparison was reduced to ±0.5 standard cm. (Here, 13/3 denotes the array number, the third measurement for array 13.) The uncertainty in reproducibility is the dominant contribution to the random error. In comparing balances for small changes in the edge loading for a particular array this figure is reduced to ±0.2 standard cm.

4. Each calculated eigenvalue has an uncertainty of $\pm$ 0.1 x 10^{-4} dk/k. An uncertainty of $\pm$ 0.14 x 10^{-4} dk/k has been assigned to each experimental absorber and follower worth to allow for the uncertainty in the edge fuel worth.

These four error components have been combined to give the random uncertainties in absorber and follower array worths. To simplify the error analysis a standard cm worth of 0.43 x 10^{-4} dk/k was used. This random error component is the major uncertainty for single sodium follower worths relative to fuel and is a maximum of 3.2% of the follower worth at position S.

5. The correction factor S, which relates the ‘edge worth’ and ‘beta-effective’ reactivity scales, has an estimated uncertainty of ±1%, based on the analysis of the reactivity scale measurements in MZB.

6. The uncertainty in the Pu241 decay correction has been assigned a value of ±20% of the correction between absorber loading balance and follower loading balance, or between follower loading balance and reference loading. The error in absorber and follower worths contributed by the Pu241 decay uncertainty is less than ±1%. The maximum error contributed in the case of the first measurement of Na(S) is just less than ±1%.

Table 1.13 Worths of Single Rod Followers and Single Rods relative to Followers
(Core 264 +8 elements, in units of 10^{-4} dk/k).

The measurements have been modified to relate to a Core with a 264 element loading plus 8 edge elements. The rod reactivities are relative to the core with the follower inserted.
The uncertainties (s.d.%) do not include the uncertainty in the reactivity scale of ± 5% due to the uncertainty in the effective delayed neutron yield data and FGL5 cross-section set.

Position	Follower relative to Core (10^{-4} dk/k)	s.d. (%)	TA Rod relative to Follower (10^{-4} dk/k)	s.d. (%)	B80/B90 Rod relative to AL(O) Follower (10^{-4} dk/k)	s.d. (%)
O	32.9	1.7	62.5	1.3		
P1	28.9	2.0				
P2	28.7	2.0				
Q	21.7	2.4				
R	18.8	2.9				
AL(O)	34.6	1.6			213.6	2.3

Table 1.14 Reactivity Worths of Rods relative to Followers (Core 264 +8 elements)

Position	BN Rod relative to Follower (10^{-4} dk/k)	s.d. (%)	B30 Rod relative to Follower (10^{-4} dk/k)	s.d. (%)	B80 Rod relative to Follower (10^{-4} dk/k)	s.d. (%)	B90 Rod relative to Follower (10^{-4} dk/k)	s.d. (%)
O	80.6	1.3	99.2	1.4	153.2	1.8	163.8	1.9
P1	68.5	1.3	84.0	1.5	128.0	1.6		
P2	67.3	1.3			126.6	1.6	134.9	1.6
Q	46.5	1.4	57.1	1.3	85.0	1.3	90.5	1.4
R	31.2	1.4						

Table 1.15 Measurements in Position S related to a 264+4 Core Loading

Position	Na Follower (10^{-4} dk/k)	s.d. (%)	BN Rod relative to Follower (10^{-4} dk/k)	s.d. (%)	B80 Rod relative to Follower (10^{-4} dk/k)	s.d. (%)	TA Rod relative to Follower (10^{-4} dk/k)	s.d. (%)
S	17.7	1.7	14.3	1.4	27.7	1.4	10.9	2.9

Table 1.16 Arrays of Two or More Rods
The numbers of edge elements for which the reactivities are derived differ from case to case. (in units of 10^{-4} dk/k)

Positions	Number of edge elements	Followers relative to Core	s.d. (%)	(B80, B90) Rods relative to Followers	s.d. (%)	(B80, BN) Rods relative to Followers	s.d. (%)	(BN, B80) Rods relative to Followers	s.d. (%)
P1, O	15	60.3	1.4	276.0	2.9				
P1, P2	14	56.1	1.4	237.9	2.5			180.0	2.0
P1, P5	14	57.0	1.4	268.1	2.8				
P1, Q	12	49.4	1.5	190.6	2.1	157.7	1.8	137.7	1.7
P1, R	11	47.0	1.5			147.0	1.7		
Q, R	8	39.4	1.7						

Positions	Number of edge elements	Followers relative to Core	s.d. (%)	(BN, BN) Rods relative to Followers	s.d. (%)	(B80, NA) Rods relative to Followers	s.d. (%)
P1, O	15						
P1, P2	14	56.1	1.4			124.4	1.6
P1, P5	14						
P1, Q	12	49.4	1.5	105.7	1.5		
P1, R	11	47.0	1.5	92.9	1.4		
Q, R	8	39.4	1.7	69.8	1.4		

Positions	Number of edge elements	Followers relative to Core	s.d. (%)	(BN, BN, BN) Rods relative to Followers	s.d. (%)
O,P2,P5	23	85.8	1.4	206.0	2.2
P1,P3,P5	22	84.6	1.4	210.3	2.3
P2,P2',P5,P5'	30	109.5	1.5	271.1	2.8

Positions	Number of edge elements	Followers relative to Core	s.d. (%)	(NA, BN, BN) Rods relative to Followers	s.d. (%)	(B30, BN, BN) Rods relative to Followers	s.d. (%)	(B80, BN, BN) Rods relative to Followers	s.d. (%)
O,P2,P5	23	85.8	1.4	137.6	1.7	221.7	2.4	266.8	2.8

Table 1.17 Reactivity Worth of Single Rods relative to Core Elements
(Core 264 +8 elements)
(The uncertainties are taken to be the same as for rod relative to follower.)

Position	BN Rod relative to Core elements (10^{-4} dk/k)	s.d. (%)	B30 Rod relative to Core elements (10^{-4} dk/k)	s.d. (%)	B80 Rod relative to Core elements (10^{-4} dk/k)	s.d. (%)	B90 Rod relative to Core elements (10^{-4} dk/k)	s.d. (%)
O	113.50	1.3	132.10	1.4	186.10	1.8	196.70	1.9
P1	97.40	1.3	112.90	1.5	156.90	1.6		
P2	96.00	1.3			155.30	1.6	163.60	1.6
Q	68.20	1.4	78.80	1.3	106.70	1.3	112.20	1.4
R	50.00	1.4						
S	32.00	1.4			45.40	1.4		

Table 1.18 Reactivity Worth of Pairs of Rods relative to Core Elements
(in units of 10^{-4} dk/k)

Positions	Number of edge elements	B80, B90 Rods relative to Core Elements	s.d. (%)	B80, BN Rods relative to Core Elements	s.d. (%)	BN, B80 Rods relative to Core Elements	s.d. (%)	(BN, BN) Rods relative to Core Elements	s.d. (%)
P1, O	15	336.3	2.9						
P1, P2	14	294.0	2.5			236.1	2.0		
P1, P5	14	325.1	2.8						
P1, Q	12	240	2.1	207.1	1.8	187.1	1.7	155.1	1.5
P1, R	11			194.0	1.7			139.9	1.4
Q, R	8	336.3						109.2	1.4

Table 1.19 Interaction Coefficients and Fitted Values.
Values calculated using the formula W(X,Y) = W(X)+W(Y) +A(X,Y)*W(X)*W(Y) where A(X,Y) are the interaction coefficients derived from the fit. (in units of 10^{-4} dk/k)

Positions of the Rod Pair, X,Y	Interaction Coefficient A(I,J)		Rods relative to Core Elements B80, B90	Rods relative to Core Elements B80, BN	Rods relative to Core Elements BN, B80	Rods relative to Core Elements BN, BN
P1, O	-0.00056		336.3			
P1, P2	-0.00107		293.2		236.6	
P1, P5						
P1, Q	-0.00164		240.2	207.55	187.1	165.3
P1, R	-0.0016			194.35		147.2
Q, R	0.0041					118.7

The interaction coefficients must be considered approximate because the number of edge elements is greater for the multiple rods than for the single rods. This will tend to reduce the worths of the multiple rods relative to the single rods.

Table 1.20 MZC Control Rod Interaction Effects (MTN/92)
Sum of single rod worths/Array worth

Array number	Absorber Loading	Experiment	MTN/92 Calculation	C/E interaction
26	B80(P1) B90(Q)	1.152	1.173	1.018
23	B80(P1) B90(O)	1.063	1.077	1.013
24	B80(P1) B90(P2)	1.112	1.127	1.013
25	B80(P1) B90(P5)	0.988	0.987	0.999
27	B80(P1) BN(Q)	1.108	1.117	1.008
28	B80(P1) BN(R)	1.086	1.089	1.003
29	BN(P1) B80(P2)	1.088	1.091	1.003
30	BN(P1) B80(Q)	1.120	1.131	1.010
31	BN(P1) BN(Q)	1.091	1.099	1.007
32	BN(P1) BN(R)	1.075	1.080	1.005
33	BN(Q) BN(R)	1.116	1.121	1.004
41	B80(P1) Na(P2)	1.029	1.033	1.004
34	BN(O, P2,P5)	1.051	1.041	0.990
35	B30(O) BN(P2,P5)	1.062	1.069	1.007
36	B80(O) BN(P2,P5)	1.085	1.098	1.012
25	B80(O) B90(P5)	0.988	0.987	0.999
39	BN(P2,P2',P5,P5')	1.003	1.002	0.999
42	Na(O) BN(P2,P5)	0.982	0.987	1.005
37	BN(P1,P3,P5)	0.978	0.976	0.998
	Mean			1.0051
	S.D.%			±0.66%

It should be noted that the array worths are related to a larger core loading than the single rods and thus the experimental and calculated ratios in the third and fourth columns are a little too high. Since both columns are similarly affected there will be little effect on the C/E values in the final column.

The Reactivity Scale Experiment in MZB/4

Different ways to provide a reactivity scale were intercompared in MZB/4 (the measurements are described in MTN/52 and the analysis in MTN/76). The objective was to compare reactivity scales based on the control rod calibrations (calculated using period measurements together with the inhour equation and a chosen set of delayed neutron data), the calculated effect of reducing the inner core enrichment (or plutonium content), the calculated effect of adding edge elements and the calculated value of the central worth of a plutonium sample. The method used to reduce the plutonium content of a group of inner core elements was to replace the PuO_2-UO_2 plates (PUIV4) by the very similar thickness UO_2 plates (UO23R4) in each of the eleven core cells, the other contents of the elements remaining unchanged.

The basic assembly for these experiments was the standard loading of MZB/4 as described in MTN/49, reduced by four outer core elements in positions (37,57), (63,43), (43,37) and (57,63) (replaced by radial blanket elements), to give a just critical loading, containing 260 outer core elements. When extra core elements were added these four elements were replaced first. Then the sequence F (Table 1.1) was followed, involving the elements of type C11-1G, D, H, K and L making a total number of additions of 4 + 34 =38, followed by two elements of type C11-1L at (64,56) and (36,44) to bring the total number of possible additions to 40.

A total of 45 inner core elements were depleted in two stages. These elements were in an array of one in every nine elements in the inner core, centred on the position (50,50) and then moving outwards 3 in each direction, to (47,50), (53,50) etc. the outer positions being (41,44), etc. (their positions are shown in Figure 1 of MTN/52). The central nine elements of this set were depleted first and ten outer core elements were added (replacing radial blanket elements) to retain a just-critical assembly. The remaining 36 elements were then depleted and a further 24 outer core elements added in two steps, again to give a just-critical assembly. The worths of adding six outer core elements to the basic assembly and to this enlarged core were measured in terms of the compensating movement of the regulating control rod FR9. An extra measurement was included with only five depleted elements in positions (50,50), (50,47), (47,50), (50,53) and (53,50) and with six extra outer core elements to give a direct comparison of the reactivities of the depletion and of a standard cm of FR9.

The worth of the standard cm of FR9 was calibrated in the loading containing the 45 depleted inner core elements and the 40 extra outer core elements using the technique described for MZB/3 in MTN/42. Three periods were run with movements of about 4.1, 5.1 and 6.1 std cms above critical and the three worths per std cm agreed well to give an average of 0.435×10^{-4} dk/k/std cm (when corrected using the adjustment of +3.3% to bring into consistency with the Smith-Tomlinson delayed neutron data). The result compares with the adjusted value of 0.437×10^{-4} dk/k/std cm found for the standard loading of MZB/4.

Table 1.21 shows all the balances taken during these measurements, as a function of date, and the numbers of elements depleted and added at the edge of the outer core.

A correction was made to the measured reactivity of a core to allow for decay of Pu241 from the reference date for the experiment. The reactivity decrease due to Pu241 decay was calculated to be 0.9×10^{-4} dk/k per month in MZB.

Using the worth of a std cm FR9 in MZB/4, an increase of 0.07 std cm FR9 per day is required to compensate for this reactivity loss of 0.03×10^{-4} dk/k per day. Corrections were made to the results to give equivalent values on the first day of the sequence of measurements and these are given in Table 1.21.

The results in Table 1.21 have been compared to give the net reactivity effects of the depletions and outer core additions in Table 1.22 and edge worths in Table 1.23.

Uncertainties

a Because of the large number of element movements required for some of the changes to the core loadings, and the necessity of having empty sheaths in core positions while elements were depleted, it was not possible to ensure that the core temperature distribution had reached an equilibrium condition for each balance. Analysis of the repeated balances indicated a standard deviation for a single balance of about 0.4 std cm of FR9, although comparison of the first three results with the corresponding balances at the end of the measurements suggests a systematic change caused by the intervening reactor alterations. Therefore uncertainties of ±0.4 std cm FR9 were assigned to the movement of FR9 based on a pair of balances, except for the last result in Table 1.22 where an uncertainty of ±1.0 std cm FR9 is given for the mean value.

b The simple subtraction of balance positions is only correct if the worth of the std cm FR9 is the same in the two loadings. This can be safely assumed in all cases except the depletion of the 45 elements. However the excess reactivity in the 45/34 loading is only 2 std cm and therefore a difference of 1% in the std cm worth in this loading only alters the effective change in balance position of FR9 by 0.02 std cm.

c Comparison of corrections from actual to std cms. FR9, obtained from counters at the core centre and between the top shield doors suggested that errors of up to 0.2 std cms. might be possible in the larger changes of balance position.

d The reactivity uncertainty associated with unloading an element and reassembling it with the same contents was found to be ~ 0.01 std cm FR9 at the centre of MZB (see MTN/54). Assuming random effects, even the reloading of 45 elements will have an uncertainty of less than 0.1 std cms. FR9.

e The systematic uncertainty in the Pu239 content of the PUIV4 plates is about 0.3% arising from the uncertainties in the chemical and isotopic analyses. The results in MTN/26 showed the plutonium in a central PUIV4 plate to be worth 1 std cm. FR9 in MZB/4. Hence, after some allowance for the variation of worth with position, the uncertainties associated with 55, 99 and 495 plates were therefore about 0.15, 0.3 and 1.2 std cm. FR9 respectively.
The random uncertainty in the Pu239 content of these plates arises from the individual weight variations and is ~ 0.2%. The uncertainties associated with 55, 99 and 495 plates were about 0.01, 0.02 and 0.04 std cm FR9. The plates were returned to the depleted elements in a random way rather than to their original elements, but the associated reactivity changes would be similar to these figures.

The effects of systematic and random uncertainties (or errors) in the uranium contents of the mixed oxide and UO_2 plates will be significantly smaller than those from the plutonium.

f The average thicknesses of the PUIV4 and UO23R4 plates are 6.278 mm and 6.313 mm respectively. Thus replacing 11 PUIV4 plates by UO23R4 plates increases the average core height by almost 0.4 mm. The top shims in each element were kept the same and under pressure during the measurements so this change was compensated by compression of the sodium plates in the core and blanket sections. Moreover, calculations reported in MTN/36 showed that an increase of 1 mm in core height for a central element produced a reactivity decrease of 0.30×10^{-6} dk/k requiring a compensating movement of 0.007 std cm FR9 in MZB/4. Thus an increase of 0.4 mm in 45 elements required ~ 0.1 std cm FR9 to compensate. This correction was ignored.

Only the uncertainties from the reproducibility of the balance positions and in the conversion from actual rod insertion to std cm. were applied to the edge worth measurements. All the uncertainties were combined to obtain the values given in Table 1.23.

Table 1.21 Balance Positions of the Control Rod FR9 following the Depletion of Inner Core Elements and the Addition of Outer Core Elements

Date (1972)	I/C Elements Depleted	O/C Elements added	FR9 (std cm)	Correction for Pu241 decay from 4/12	Correction for the difference in subcriticality	Final value in std cm FR9
4/12	0	0	72.90	0	0	72.9
	0	6	27.84	0	0	27.8
	9	10	70.15	0	0	70.2
6/12	45	34	80.7	-0.14	+0.18	80.7
	45	40	38.29	-0.14	+0.18	38.3
7/12	45	40	38.66	-0.21	+0.18	38.6
	45	34	81.4	-0.21	+0.18	81.4
11/12	9	10	70.33	-0.49	0	69.8
12/12	5	6	69.85	-0.56	0	69.3
	0	6	27.67	-0.56	0	27.1
	0	0	72.76	-0.56	0	72.2

Notes:
1. The 5 elements depleted were in positions 50,50, 50,53, 50,47, 53,50 and 47,50 and the additional 4 elements of the 9 element depletion were at 47,47, 47,53, 53,47, 53,53.
2. The positions of outer core elements added are given in the Table 1.1 and Figure 1.3 (see also MTN/52).

Table 1.22 Reactivity Changes produced by Depleting Inner Core Elements and adding Edge Elements

Number of Elements Depleted	Number of Edge Elements added	Change in Balance Position of FR9 (std cm)	Change in Reactivity x 10^{-4} dk/k
0	6	-45.1	19.7 ± 0.2
5	0	42.2 ± 0.5	-18.4 ± 0.2
9	10	-2.6 ± 0.4	1.1 ± 0.2
45	34	+8.5 ± 1.6	-3.7 ± 0.7

Notes:

1. The change in reactivity produced by depleting inner core elements and adding edge elements has been obtained by multiplying the change in the balance position by -0.437 x 10^{-4} dk/k. The uncertainty in this delayed neutron scale (± 5%) has not been included.

2. The number of edge elements added is relative to the basic loading of 260 outer core elements except for the first result when the loading was unchanged at 266 outer core elements.

Table 1.23 Edge Element Worths

Number of Depleted Elements in the Core	Number of O/C Elements	Number of O/C Elements added	Change in Balance Position of FR9 (std cm)	Reactivity worth of an added O/C element dk/k.(x 10^{-4})
0	260	6	-45.1 ± 0.4	3.28 ± 0.03
45	294	6	-42.6 ± 0.4	3.09 ± 0.03

Note: The reactivity worth of adding the edge elements (on the Smith-Tomlinson delayed neutron scale) has been obtained by multiplying the first result by -0.437 x 10^{-4} and the second by -0.435 x 10^{-4} dk/k, although the difference between these figures is not statistically significant.

Period-Reactivity Relationships.

The excess reactivity of a core and small changes in reactivity were measured in terms of a "standard centimeter" of movement of a calibrated control rod, usually the rod FR9. This in turn was related to an absolute reactivity scale by measuring the relationship between control rod movement and reactor period and calculating the period-reactivity relationship using a chosen set of cross-sections and delayed neutron data. The relationships were measured for periods typically in the range 100 to 300 secs. In most of the reported analyses of the MOZART programme measurements the calculations of the relationship were made using the FD4 cross-section set and the ZEBRA (Stevenson) delayed neutron data. Towards the end of the program the FGL5 fine group cross-section set was used together with the Smith-Tomlinson delayed neutron data. This was also used in the later ZEBRA programmes, Zebra Cores 13 and 14 and the BIZET and CADENZA programmes. In MTN/104 the change in the period-reactivity relationship resulting from the change in cross-sections and delayed neutron data is described. There is a 1.9% increase in the reactivity per standard.cm in MZA and a 3.3% increase in MZB, the revised relationships for FR9 being as follows:

Table 1.24 Standard cm of FR9 calculated using FGL5 and Smith-Tomlinson delayed neutron data

	Standard cm of FR9 (in units of 10^{-4} dk/k)
MZA	-0.502
MZB/1	-0.383
MZB/2	-0.380
MZB/3	-0.376
MZB/4	-0.437

For the analyses of central plutonium worth, inner core depletion and edge worth given in MTN/76, the Analysis of the Reactivity Scale Experiment in MZB using FGL5 Data and Theory, the following results are presented:

Table 1.25 C/E values calculated using FGL5 and Smith-Tomlinson delayed neutron data

Reactivity effect	Uncertainty	C/E values on the Smith-Tomlinson Delayed neutron Reactivity Scale
Central plutonium plate sample	4%	1.03
Inner core depletion	4%	1.00
Core edge element	(larger)	0.95

The uncertainty in the calculation of the core edge element worth was considered to be larger than that of the other effects because diffusion theory was used in the calculations. This is not necessarily the explanation because the MONK Monte Carlo calculations of edge element worth, although not made for the above measurements, show a similar discrepancy.

The reactivity scales used in the present document are those corresponding to the FGL5 nuclear data set and the Smith-Tomlinson delayed neutron data. (In the later MTN documents a scale corresponding to the calculated worth of plutonium was used, and this is about 0.7% higher.) The Smith Tomlinson data are presented in Tables 1.26 to 1.28.

Smith-Tomlinson Delayed Neutron Data

Table 1.26 Smith-Tomlinson total yields and six group relative abundances

	Relative abundances					
	U-235	U-238	Pu-239	Pu-240	Pu-241	Pu-242
Time group						
1	0.038	0.013	0.038	0.025	0.010	0.004
2	0.213	0.137	0.280	0.270	0.229	0.195
3	0.188	0.162	0.216	0.184	0.173	0.162
4	0.407	0.388	0.329	0.358	0.390	0.411
5	0.128	0.225	0.103	0.135	0.182	0.218
6	0.026	0.075	0.035	0.027	0.016	0.010
Total yield n/100F	0.0165	0.0458	0.00633	0.0088	0.0159	0.015

Table 1.27 Smith-Tomlinson six group decay constants

	6 time group decay constants (sec^{-1})					
	U-235	U-238	Pu-239	Pu-240	Pu-241	Pu-242
Time group						
1	0.0127	0.0132	0.0129	0.0129	0.0128	0.0129
2	0.0317	0.0321	0.0311	0.0313	0.0299	0.0295
3	0.115	0.139	0.134	0.135	0.124	0.131
4	0.311	0.358	0.331	0.333	0.352	0.338
5	1.40	1.41	1.26	1.36	1.61	1.39
6	3.87	4.02	3.21	4.04	3.47	3.65

The recommended relative abundances in the Smith-Tomlinson evaluation are Keepin's 1957 fission spectrum averaged data for U235, U238 and Pu239. The data are summarised in the above Tables.

Table 1.28 Smith-Tomlinson energy spectra for the 6 time groups.

		Group1	Group2	Group3	Group4	Group5	Group6
Lower energy (MeV)	Upper energy (MeV)						
2.2313	3.6788	0	0.01	0	0.02	0.01	0.01
1.3534	2.2313	0.03	0.04	0.03	0.04	0.04	0.04
0.82085	1.3534	0.06	0.12	0.08	0.12	0.14	0.14
0.49787	0.82085	0.13	0.27	0.22	0.24	0.23	0.23
0.30197	0.49787	0.20	0.26	0.30	0.24	0.23	0.23
0.18316	0.30197	0.23	0.15	0.19	0.19	0.17	0.17
0.11109	0.18316	0.16	0.08	0.09	0.09	0.11	0.11
0.06738	0.11109	0.19	0.07	0.09	0.06	0.07	0.07

The Control Rod Reactivity Worth Measurements described in this section, and the Reactivity Worth Measurements for Plutonium and Edge Elements are recommended as suitable for consideration as benchmark measurements.

1.4.3 Material Data.

Compositions of the Control Rod Components

Weights per unit length for the sheath, outer square calandria walls the inner cylinder, the calandria tubes and the canning of the BN, B30 and B80 pins.

These components are made from stainless steel (304S of BS1449).

The Sheath	23.1281 g/cm
The Calandria outer square tube	47.8874 g/cm
The inner cylinder of stainless steel	98.0309 g/cm.
The 19 calandria tubes	68.9589 g/cm.
The cans of the 19 BN, B30 and B80 pins	57.8758 g/cm

The corresponding weights for the Follower Elements

The weights (per unit height) of the calandria square tube and the cylinder are greater for the Follower Elements, 48.5549 g/cm and 99.1729 g/cm respectively, making the weight of the sheath plus calandria tube 71.683 g/cm (0.94% higher than for the Absorber Element) the value for the inner cylinder being 1.16% higher.

The composition of the steel (304S of BS1449) used in the sheath, the calandria walls, the inner cylinder, the calandria tubes and the BN, B30 and B80 pins is given in Table 1.M1.

Table 1.M1 Composition of the steel (304S of BS1449) used in the sheath, the calandria outer walls, the inner cylinder, the calandria tubes which hold the absorber pins and the cans of the BN, B30 and B80 pins.

	Weight %
C	0.03
Si	0.49
P	0.021
S	0.015
Cr	19.24
Mn	1.74
Fe	67.864
Ni	10.60

The steel of the canning of the B90 absorber pins.

In the case of the B90 pins the weight of stainless steel in the 19 cans is 28.8230 g/cm and the composition of the steel is different. The composition of the steel is compared with that of the canning of the BN, B30 and B80 pins in Table. 1.M2.

Weights per unit length of absorber.

These are given in Table 1.M3.

Table 1.M2 Weight per unit length of the steel tubes and boron pin canning

	Calandria tube	BN, B30, B80 can	B90 can	BN, B30, B80 tube+can	B90 tube+can
C	0.0206	0.0174	0.0145	0.0380	0.0351
Si	0.3379	0.2836	0.1412	0.6215	0.4791
P	0.0145	0.0121	0.0086	0.0266	0.0231
S	0.0103	0.0087	0.0035	0.0190	0.0138
Cr	13.2677	11.1353	5.0642	24.4030	18.3319
Mn	1.1999	1.007	0.5044	2.2069	1.7043
Fe	46.7983	39.2769	19.5529	86.0752	66.3512
Ni	7.3097	6.1348	3.3262	13.4445	10.6359
Nb			0.2075		0.2075
Total (g/cm)	68.9589	57.8758	28.8230	126.8347	97.7819

Table 1.M3 The weights per unit length for the absorbers

	BN	B30	B80	B90	TA
Area (cm^2)	18.0563	18.0563	18.0563	18.0563	25.6086
Boron Absorber					
Weight of Boron g/cm	34.2328	34.0277	32.6838	33.1246	
B10 % atoms	19.806	29.889	79.914	90.16	
Boron atomic weights	10.8120	10.7115	10.2130	10.1109	
B10	6.2791	9.5072	25.6071	29.5755	
B11	27.9537	24.5205	7.0767	3.5491	
C	9.6316	9.4456	9.2441	9.0147	
Al				0.0213	
Si				0.085	
Fe	0.0351	0.0348	0.0336	0.0553	
Total	43.8995	43.5081	41.9615	42.3009	
Tantalum Absorber					
H					0.0011
N					0.0075
Nb					0.2357
Ta					428.1052
W					0.1071
				Total	428.4566

Sodium density

The area enclosed by the 19 calandria tubes is 35.8514 cm^2 and so the area occupied by sodium is (inside area of calandria minus cross-sectional area of the inner tube minus the area of the 19 calandria tubes):

$$97.2196 - 12.1528 - 35.8514 = 49.2154\ cm^2.$$

The sodium weight per unit length is 44.8940 g/cm and so the density is calculated to be 0.91219 g/cm^3.

In the case of the follower component the area of sodium is 97.2196 - 12.1528 = 85.0668 cm^2 and the weight of sodium per unit length is 77.6577 g/cm, and so the density is calculated to be 0.91290 g/cm^3 (essentially the same as that for the absorber element).

The sodium contains the following trace quantities (in parts per million by weight):
H 1.2 ppm; B 0.46 ppm; O 197 ppm; Fe 20 ppm
The Fe can be neglected in comparison with the steel present in the element structure and the quantities of H and B are also negligible. The O is to be taken into account in the calculational model.

Overall length of the elements and the end regions

The height of the boron absorber section is taken to be 90.5 cm and the length of the inner cylinder is assumed to be the same (actually 90.6 cm). The overall length of the calandria, including end plates, is 91.44 cm, making an end region of width 0.47 cm at each end which contains the steel and any other materials in the end region.

The weight, estimated here, for the steel in the end region is very approximate.

The steel of the sheath and 0.42 cm of the steel of the calandria walls and the calandria tubes and boron pins are components of this end region. (This figure of 0.42 cm is a result of the length of the calandria walls and the calandria tubes being 91.34 cm, that is 0.84 cm longer than the 90.5 cm of the boron absorber section.)

Steel of the Sheath	= 0.47 x 23.1281 g = 10.87 g
Steel of the Calandria walls	= 0.42 x 47.8874 g = 20.11 g
Steel of the Calandria tubes	= 0.42 x 68.9590 g = 28.96 g
Steel of the Canning	= 0.42 x 57.8759 g = 24.31 g (BN, B30 and B80)
	= 0.42 x 28.823 g = 12.11 g (B90)

These components contribute a total of 84.25 g for the BN, B30 and B80 elements, 72.05 g for the B90 element and 59.94 g for the Ta element.

The End Plate is 0.38 cm thick and the Support Plate and Cover Plate 0.04 cm thick, a total of 0.42 cm. The weight of the Top End Plate plus 4 Bosses is 163.6 g and the Support Plates and Cover Plates 59.2 g (2 x 29.6 g) giving a total of 193.2 g. There are also end regions above and below the absorber columns in the cans.

Combining all the components gives 277.45 g for the BN, B30 and B80 elements, 265.25 g for the B90 element and 253.14 g for the Ta element (although these estimates might be low because there are also end caps in the absorber tubes).

The tantalum absorber pin extends 0.4185 cm into this end volume, having a length of 91.337 cm. The end regions are divided into two parts, one of thickness 0.4185 which contains the continuation of the tantalum rods surrounded by a uniform region of steel and the other a slab of steel of thickness

0.0515 cm.

In this case the total weight of steel in the two regions is divided over the volume of the end region minus the volume of the end of the tantalum pins, that is 54.2558 - 0.4185 x 25.6086 = 43.5386 cm^3.

Lengths of the assembled follower elements and their end regions

The lengths of the assembled follower elements, including end regions, are 91.44 cm, 45.72 cm, 35.56 cm, 22.86 cm and 15.00 cm. The followers occupying the upper and lower axial blanket regions have the height 35.56 cm. The end regions are assumed to be the same as for the BN elements, being 0.47 cm thick, and thus reducing the size of the cylinder and outer walls by 0.94 cm to 90.5 cm, 44.78 cm, 34.62 cm 21.92 cm and 14.06 cm.

Representation of the B80/90 element
The aluminium is assumed to have the same composition as that of the ZEBRA aluminium block, ALSC3, (Al 99.847%, Si 0.01%, Mn 0.004%, Fe 0.13%, Cu 0.009%).

The B10 loading for the (B80/B90) element was 4.88kg.

APPENDIX TO SECTION 1.4.3. Details of the Materials and Dimensions

In this Appendix the full specification of the mock-up control rods is reproduced.

Detailed information on control element dimensions and compositions and their uncertainties

The following is more detailed background information giving the sources of the dimensions and compositions of the components of the rods as presented in MTN/39 by C G Campbell and S Kobayashi.

Location of the absorber pins and the bosses in the end plates.

1 hole is at the centre

6 holes are on 3.58 cm PCD

12 holes are on 6.92 cm PCD

4 holes for bosses are on 10.82 cm PCD

Table A1. Control Rod Sheath

A. Material:	Stainless Steel: 304S of BS 1449	
B. Dimensions:		
	Length	302.414 cm
	Inside dimensions	10.47 cm (square)
	Thickness of Steel	0.0765 cm
	Outside dimensions	10.623 cm
Dimples:	there are 3 groups of 8 dimples on 4 sides of this tube.	
	Diameter:	25 cm
	Thickness:	0.0518 cm
	Corner Radius	0.10 cm
C Weight:		11.727 Kg

Table A2. Calandria Elements

A	**Materials:**	i Stainless Steel	
		ii Sodium	
B	**Dimensions:**		
	i	**Outer square tube:**	
		Length:	91.26 ± 0.013 cm
		Inside dimensions:	9.86 ± 0.01 cm (square)
		Outside dimensions:	l0.402 ± 0.067 cm (square, across dimples)
		Wall thickness of stainless steel	0.15 cm
		Corner radius:	0.5 ± 0.01 cm
		Diameter of dimple:	2.5 cm (ϕ)
	ii	**Inner cylindrical tube:**	
		Length:	90.6 ± 0.013 cm
		Outer diameter:	9.845 ± 0.013 cm (ϕ)
		Wall thickness:	0.41 cm
	iii	**19 Calandria tubes**	
		Length:	91.26 ± 0.073 cm
		Outer diameter:	l.55 ± 0.0025 cm
		Wall thickness:	0.1 ± 0.005 cm
	iv	**End plate:**	
		Thickness:	0.38 cm (Thickest)
		Side:	9.86 ± 0.01 cm (square)
		Hole diameter:	1.55 ± 0.005 cm (ϕ) for 19 holes 0.79 ± 0.005 cm for 4 holes of Bosses
		Corner radius:	0.5 ± 0.01 cm
	v.	**Support plate and Cover plate:**	Four corners are removed by a straight cut at 45^0 0.5 ± 0.05 cm from the corner
		Thickness:	0.04 cm
		Side:	9.5 ± 0.05 cm (square)
	vi	**Filling and Venting Boss:**	(see Figs 3, 4 and 5 in MTN/39)
	vii	**Length of assembled control elements, after welding:**	
		without cover and support plates	91.36 ± 0.013 cm
		with cover and support plate	91.44 ± 0.013 cm
C.	**Weights of Stainless Steel**		
	i	Outer tube + bottom end plate + 4 bosses	4534.8 g
	ii	Inner tube:	8881.6 g
	iii	Top end plates + 4 bosses:	163.6 g
	iv	Calandria tubes (19):	6293.2 g
	v	Control Element without support and cover plates after welding:	19864.8 g
	vi	Control Element with support and cover plates (Total Control Element);	19924.0 g

D	**Weight and Volumetric Fraction of Sodium:**		
		Na weight:	4067.4 g
		Volumetric Fraction (VF):	94.54%

Definition of VF:
VF = 100* (weight of Na poured into the element) / (density of Na at 20°C)* (Volume of the space in the element)
Density of Na at 20°C = 0.9684 gm/cm3

Follower Elements
A follower element consists of the following parts:
i an outer tube
ii an inner tube
iii two end plates
iv sodium
Follower elements of several lengths are provided to change the position of the absorber section in the core.
A Materials:
i Stainless Steel: All parts are made from stainless steel, Type 304S of BS 1449
ii Sodium: The same material as in the control element.
B Dimensions:
i Outer tubes (square) (Dimensions as for the control element)
Lengths: 91.34 ± 0.013 cm
45.62 ± 0.013 cm
35.46 ± 0.013 cm
22.76 ± 0.013 cm
14.90 ± 0.013 cm
ii Inner tubes. (Dimensions as for the control element, except for the lengths)
Lengths: 90.68 ± 0.013 cm
44.96 ± 0.013 cm
34.80 ± 0.013 cm
22.l0 ± 0.013 cm
14.24 ± 0.013 cm
iii End plate. (Dimensions as for control element)
Four filler holes of 0.79 ± 0.05 cm diameter are located in the four corners of this plate.
iv Lengths of the assembled follower elements
1 91.44 ± 0.013 cm
2 45.72 ± 0.013 cm
3 35.56 ± 0.013 cm
4 22.86 ± 0.013 cm
5 15.00 ± 0.013 cm

Absorber Pins

The absorber pins are divided into two groups: B_4C absorber pins and Tantalum absorber pins. A B_4C absorber pin consists of a stack of 20 B_4C pellets in an absorber tube, or 60 pellets in the case of 90% B10 pellets. A tantalum absorber is a single long solid rod.
Some special absorber pins, which are called "demountable pins", are provided for both B_4C and Ta absorber pins to insert activation foils into the pins.

B_4C absorber pin

Materials

B_4C pellets: B_4C pellets have four different enrichments of B10 as follows:

Natural boron pellet
30% B10 enrichment boron pellet
80% B10 enrichment boron pellet
90% B10 enrichment boron pellet

The isotopic analysis and chemical analysis of these pellets are summarised in the Table A3.

Boron carbide cans

Material: Stainless steel, Type 304s of BS1449 excepting for the 90% B10 absorber pin tube for which the composition is given in Table 1.M2.

Dimensions

Length: 91.337 ± 0.013 cm (before welding)
91.36 ± 0.013 cm (after welding)

Inner diameter (excepting for the 90%B10 absorber pin): 1.11 ± 0.0025 cm (ϕ)
Outer diameter (excepting for the 90%B10 absorber pin): 1.31 ± 0.0025 cm
Inner diameter of the 90%B10 absorber pin: 1.1786 cm
Outer diameter of the 90%B10 absorber pin: 1.27 cm
Wall thickness (excepting for the 90%B10 absorber pin) : 0.1 ± 0.005 cm
Wall thickness of 90%B10 absorber : 0.0457 cm
Thickness of end cap: 0.362 ± 0.007 cm

Weights

Boron Absorber tube and end caps

283.24 g for the welded tube, excepting for the 90%B10 absorber pin tube
147.18 g for the welded 90%B10 absorber pin tube (138.6 g before welding).
The weights per unit length of the tubes for 19 pins are
282.9 g for demountable tube

Tantalum absorber pin

Materials: Pure Ta metal, (see Table A5 giving the analysed composition)

Dimensions:

Length: 91.337 ± 0.013 cm

Diameter 1.31 ± 0.0025cm (ϕ)

Weights: 2060.2 g for single solid rod
Mean weight per unit length: 22.5560 g/cm
Mean density: 16.7357 g/cm^3

B_4C pellets and column.

Detailed data for the pellets are given in MTN/39. The following Table A3 summarises the derived average data for use in calculations.

Table A3. Dimensions and Weights of the Boron Components

	Natural	30%	80%	90%
Dimensions and weights				
Mean diameter of pellet (cm)	1.09142	1.09305	1.09362	1.1033
Mean height of pellet (cm)	4.52467	4.52754	4.52810	1.5024
Mean weight of pellet (g)	10.4545	10.3674	10.0002	3.361
Mean volume of pellet (cm^3)	4.2331	4.2485	4.2534	1.4364
Mean density of pellet (g/cm^3)	2.4697	2.4403	2.3511	2.337
No. of pellets in stack	20	20	20	60
Mean weight/unit length of stack (gm/cm)	2.3105	2.2899	2.2085	2.238
*Assumed density (g/cm^3)**	2.1957	2.1762	2.0988	2.1268
B10 percentage (1) (atomic percent)	19.806 ± 0.0166	29.889 ± 0.004	79.914 ± 0.0037	90.16 ± 0.02
Mean length of pellet stack (cm)	90.493	90.551	90.562	90.148
Compositions (weight %)				
B	77.88	77.48	77.95	77.9
C	21.77	22.27	21.65	21.2
Al				0.05
Si				0.20
Ti			0.03	
Fe	0.08		0.08	0.13
Remainders individually < 100 ppm				

***** *The assumed density corresponds to the weight per unit length and the pellet diameter of 1.1 cm used in the calculational model*

(1) Several analyses of the boron compositions were carried out. These are the atomic percentage figures provided by Partiot.

Table A4. Stainless Steel Composition in Weight %

	304S of BS1449	B90 tube
C	0.03	0.05
Si	0.49	0.49
P	0.021	0.03
S	0.015	0.012
Cr	19.24	17.57
Mn	1.74	1.75
Fe	67.864	67.838
Ni	10.60	11.54
Nb		0.72

Table A5. Tantalum. Trace Elements in Weight ppm.

	Weight ppm.
H	2.2 - 3.0
N	15 - 20
Nb	360 - 740
W	225 - 272
C	< 30
O	< 50
Al	< 20
Si	< 10
Ca	< 10
Ti	< 10
Cr	< 10
Co	< 15
Ni	< 10
Zr	< 50
Mo	< 10

Table A6. Chemical Analysis of Sodium

Elements	(ppm)
Ca	< 100
Fe	20
O	197
Li	< 2.0
B	0.46
H	1.2
Total assay (%)	99.3

Table A7. Weights per Unit Length of Components (from MTN/51)

Component	Weight, g	Length cm	Weight per unit length.(g/cm)
Calandria			
Outer square tube	4370.2 (1)	91.26	47.8874
Inner round tube	8881.6	90.6 (2)	98.0309
19 Calandria tubes	6293.2	91.26	68.9590
Sodium	4067.4	90.6	44.8940
Follower 90 cm			
Outer square tube	4435.0 (3)	91.34	48.5549
Inner round tube	8993.0	90.68	99.1729
Sodium	7042.0	90.68	77.6577
Control Rod Sheath			
Square tube			23.1281 (4)
Absorber Pins			
BN 19 pins			43.8995 (5)
B30 19 pins			43.5081 (5)
B80 19 pins			41.9615 (5)
B90 19 pins			42.522 (7)
Ta 19 pins	39143.8	91.36	428.4566
Boron Cans (except B90)			57.8759 (6)
Cans for B90			28.823 (7)

1 MTN/39 Section 8C Item (i) - Item (iii)

2 End slots ignored, also taken as length of sodium

3 MTN/39 Table 3 Item (i) - Item (iii)

4 Data in MTN/51 were supplied by P Mason, Design Group. Weight given in MTN/39 is for total assembly which included end fittings.

5 Weight per cm quoted in MTN/39, Table 8

6 Data in MTN/51 were supplied by P Mason. Weight quoted in MTN/39 section 15 c does not separate tube and end caps

7 Based on the figures in MTN/39 Supplement

Table A8. Weights per Unit Length of Materials in the Components (from MTN/51) Region 1 - Calandria with absorber.

The 19 absorber pins, 19 calandria tubes and associated sodium inside the Region 1 boundary (a circle of radius 4.235 cm which just encloses the absorber pins).

	BN g/cm	B30 g/cm	B80 g/cm	B90 g/cm	Ta g/cm
Sodium					
H	0.000022	0.000022	0.000022	0.000022	0.000022
O	0.0037	0.0037	0.0037	0.0037	0.0037
Na	18.6902	18.6902	18.6902	18.6902	18.6902
Steel (Cans + Calandria)	126.8349	126.8349	126.8349	97.782	68.9590
C	0.0380	0.0380	0.0380	0.0351	0.0206
Si	0.6215	0.6215	0.6215	0.4791	0.3379
P	0.0266	0.0266	0.0266	0.0231	0.0145
S	0.0190	0.0190	0.0190	0.0138	0.0103
Cr	24.4030	24.4030	24.4030	18.3319	13.2677
Mn	2.2069	2.2069	2.2069	1.7043	1.1999
Fe	86.0752	86.0752	86.0752	66.3512	46.7983
Ni	13.4445	13.4445	13.4445	10.6359	7.3097
Nb				0.2075	
Boron Absorber					
Boron (Partiot Analysis)	34.2328	34.0277	32.6838	33.1246	
B10 % atoms	19.806	29.889	79.914	90.16	
Boron atomic weights	10.8120	10.7115	10.2130	10.1109	
B10 g/cm	6.2791	9.5072	25.6071	29.5755	
B11 g/cm	27.9537	24.5205	7.0767	3.5491	
C	9.6316	9.4456	9.2441	9.0147	
Al				0.0213	
Si				0.085	
Fe	0.0351	0.0348	0.0336	0.0553	
Tantalum Absorber					
H					0.0011
N					0.0075
Nb					0.2357
Ta					428.1052
W					0.1071

Note:- Chemical analyses used are from MTN/39

Table A9. Calandria Region 2 and Follower

	Calandria Region 2. g/cm	Follower (90 cm). g/cm
Sodium		
Na	26.1949	77.6424
O	0.0052	0.0153
H	0.000031	0.000093
Steel	169.0464	170.8559
Fe	114.7216	115.9496
C	0.0507	0.0512
Si	0.8283	0.8372
Mn	2.9414	2.9729
S	0.0254	0.0256
P	0.0355	0.0359
Ni	17.9189	18.1107
Cr	32.5249	32.8727

1.4.4 Temperature

The temperature was not recorded for individual measurements. We note that the temperature during measurements made in MZB was up to ~ 50°C.

1.4.5 Additional Information Relevant to the Reactivity Measurements

None.

1.5 Description of Reactivity Coefficient Measurements in MZC.

Not measured

1.6 Description of Kinetics Measurements in MZC.

Not measured apart from the period measurements described above.

1.7 Description of Reaction Rate Distributions Measurements in MZC.

1.7.1 Overview

The results of the foil measurements are given in MTN/97 and of the fission chamber measurements in MTN/89. Comparisons with calculation are given in MTN/93 and /100.

Pu239 and U238 fission rate distributions were measured using fission chambers in four of the control rod configurations. Radial distributions were measured along the radial centre line ("flight tube direction") in the BN (Q, R), BN(P1,P3,P5), BN/2 (P1,P3,P5) and B90(Q)B80(P) arrangements. In addition axial scans were measured at positions (53,48) and (50,50) in the BN/2 (P1,P3,P5) arrangement and at position (50,50) in the BN (P1,P3,P5) arrangement.

Reaction rate distributions were measured using foils in cores with single rods at the core centre, TA(O), BN(O) and B80(0), and with groups of three natural boron rods fully inserted, BN(P1,P3,P5), and half inserted, BN/2(P1,P3,P5). Measurements were made of the U235 and U238 fission rate distributions across the central plane of the reactor in the inner region of the core. These extended through centrally located rods and were supplemented by similar Ta scans when the TA rod was present. The flux gradients adjacent to the control rods were measured using closely spaced U235 foils. For the 3-rod arrays the fission rate distributions were measured between the rods.

A measurement was also made of the ratio of tantalum capture to U235 fission in the inner core, relative to the ratio in the NESTOR thermal column.

A fuller description of the measurement techniques used for the foil and fission chamber measurements is given in Part 1 (ZEBRA-LMFR-EXP-02).

1.7.2A Description of Experimental Configurations.

The dimensions of the basic assembly, MZB, are given in ZEBRA-LMFR-EXP-02, and the dimensions of the mock-up control rods in Section 1.4.2 of the present document.

Details of the foil dimensions, and compositions, and their locations within the cells are given in Table 1.29 and the central region cell plate numbering system in Table 1.30. Details of the fission chambers are given in the document on MZA and MZB, ZEBRA-LMFR-EXP-002, Section 1.7.

The positions of the MONJU Mock-up rods and the Zebra control rods are shown in Figure 1.2. The core loadings used for the foil measurements are shown in Figures 1.4 to 1.9 (reproduced from MTN/97). The inner core contained 413 elements and the outer core contained 264 +23, +32, +48, +80 and +54 elements for the Ta(O), BN(O), B80(0), BN(Pl,P3,P5) and BN/2(Pl,P3,P5) loadings respectively.

All the Zebra control rods were fully raised except Rod 9 which was at 60, 54, 78, 60 and 61 cm respectively. The ends of the absorber sections of the Zebra control rods were located at 7.6 cm above the top of the core for rods 3 and 4 and at 15.2 cm for the remaining rods (MTN/100).

Figures 1.10 to 1.13 show the core loadings for the fission chamber measurements and the positions of the measurements. The measurements were made with two natural boron rods, BN(Q,R), two enriched boron rods, B80(P1)B90(Q)), an array of three natural boron rods fully inserted (P1,P3,P5), and an array with the rods half inserted.

The same elements were used for the axial and radial fission chamber scans as in the unperturbed MZB core (See MTN/80).

Table 1.29 - Foil Locations and Foil Types

Reaction rate	Location	Foil Size (mm)	Material
U235 fission, F25	Inner core UO2 plate No. 16	13.10 dia x 0.13	93% U235 metal, located using 0.025 mm Al
	UO2 plate No. 16 adjacent to control rod	6.35 x 5.51 x 0.076	93% U235 metal
	Boron rods BN(O) and B80(O)	10.87 dia x 0.13	93% U235 metal
	Inner core with 3 BN rods		93% U235 metal, located using 0.025 mm Al
	Ta rods	Outer foil 13.10 dia x 0.13 Inner foil 8.64 x 0.13	93% U235 metal
U238 fission, F28	UO2 plate No. 13	13.10 dia x 0.076	0.04% U235 metal, wrapped in 0.025 mm Al
	Boron rods BN(O) and B80(O)	10.87 dia x 0.076	0.04% U235 metal, wrapped in 0.025 mm Al
	Inner core with 3 BN rods, BN(P1,P3,P%) and BN/2(P1,P3,P5)	24.4 dia x 0.076	0.04% U235 metal, wrapped in 0.025 mm Al
	Ta rod	Outer foil 13.10 dia x 0.076 Inner foil 8.64 x 0.13	0.04% U235 metal, wrapped in 0.025 mm Al
Ta(n,γ)	SS plate No22	13.10 dia x 0.13	Tantalum metal, located using 0.025 mm Al
	Ta rods	Outer foil 13.10 dia x 0.13 Inner foil 8.64 x 0.13	Tantalum metal

Table 1.30 Inner Core Cell Plate Numbering

Plate Number	Inner Core Cell
28	NASTDL4
27	UO23R4
26	NASTDL4
25	PUIV4
24	NASTDL4
23	UO23R4
22	STSTBR8
21	NASTDL4
20	UO23R4
19	NASTDL4
18	PUX8
17	NASTDL4
16	UO23R4
15	NASTDL4
14	NASTDL4
13	UO23R4
12	NASTDL4
11	PUIV4
10	NASTDL4
9	UO23R4
8	STSTBR8
7	NASTDL4
6	UO23R4
5	NASTDL4
4	PUX8
3	NASTDL4
2	UO23R4
1	NASTDL4

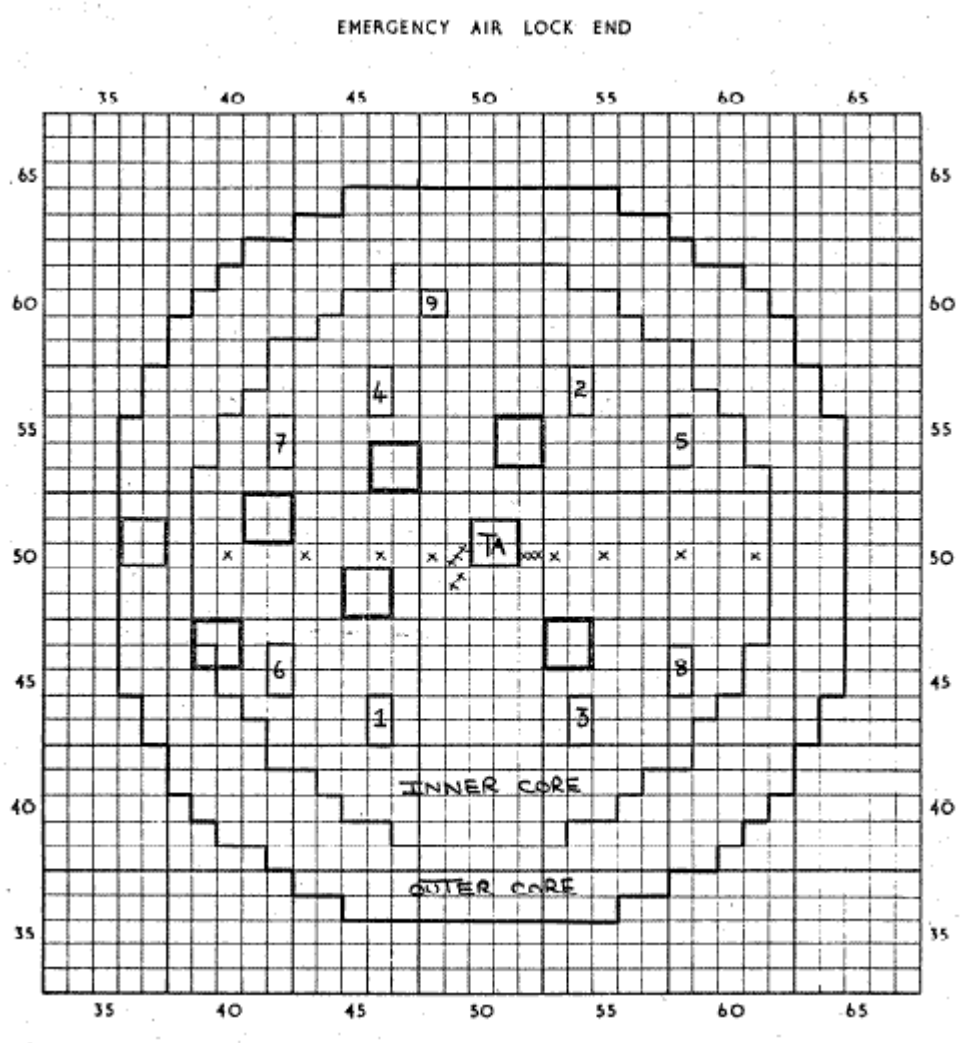

Figure 1.4 The Core with the Tantalum Mock-up Rod at the Centre showing the Positions of the Foil Measurements.

The 2x2 element squares show the positions which can be occupied by Mock-up Rods. Numbers 1 to 9 denote the Zebra control rods.

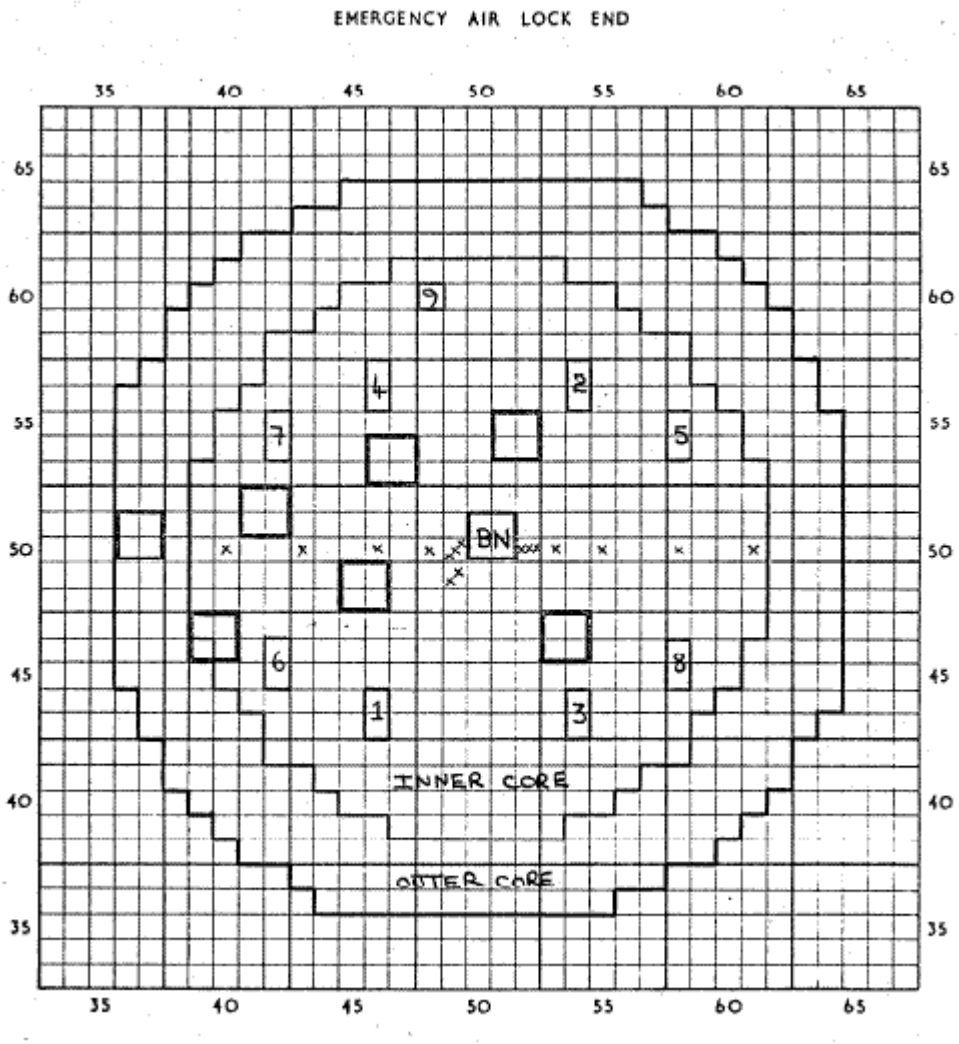

Figure 1.5 The Core with the Natural Boron Mock-up Rod at the Centre, showing the Positions of the Foil Measurements

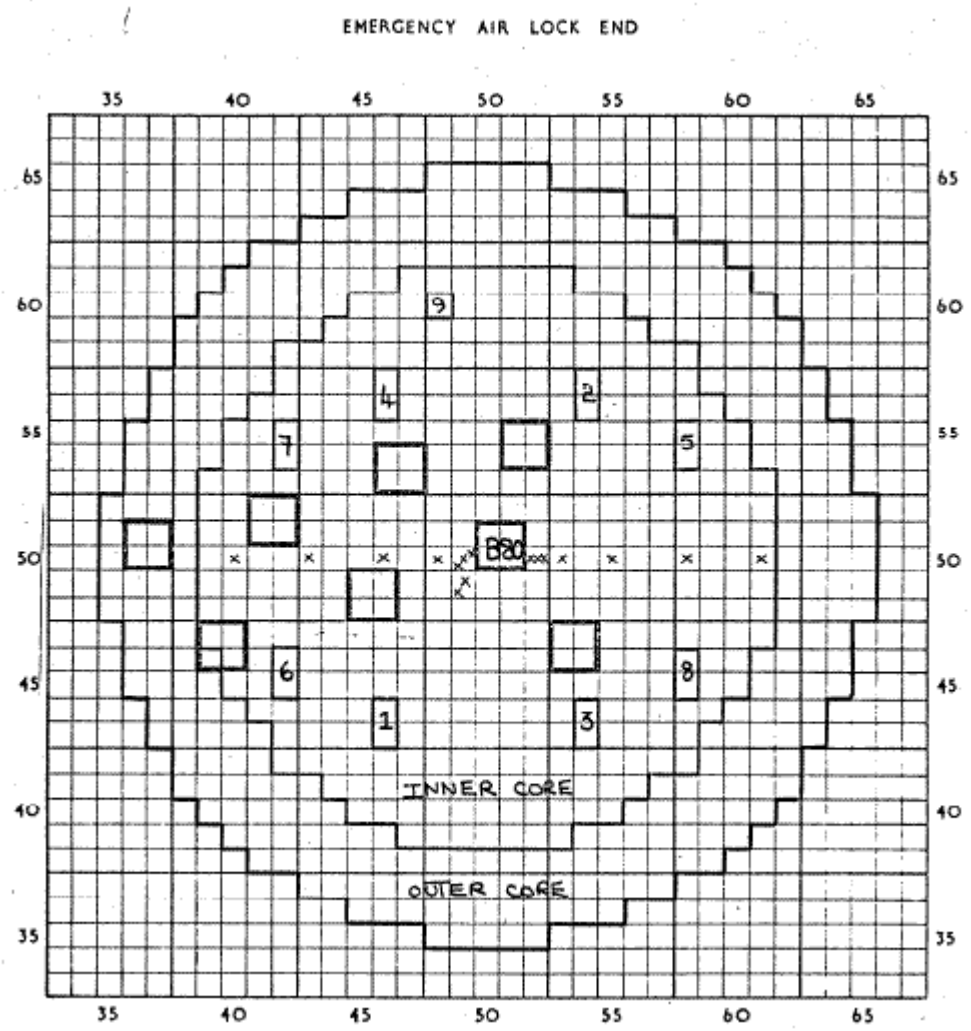

Figure 1.6 The Core with the 80% Enriched Boron Mock-up Rod at the Centre, showing the Positions of the Foil Measurements

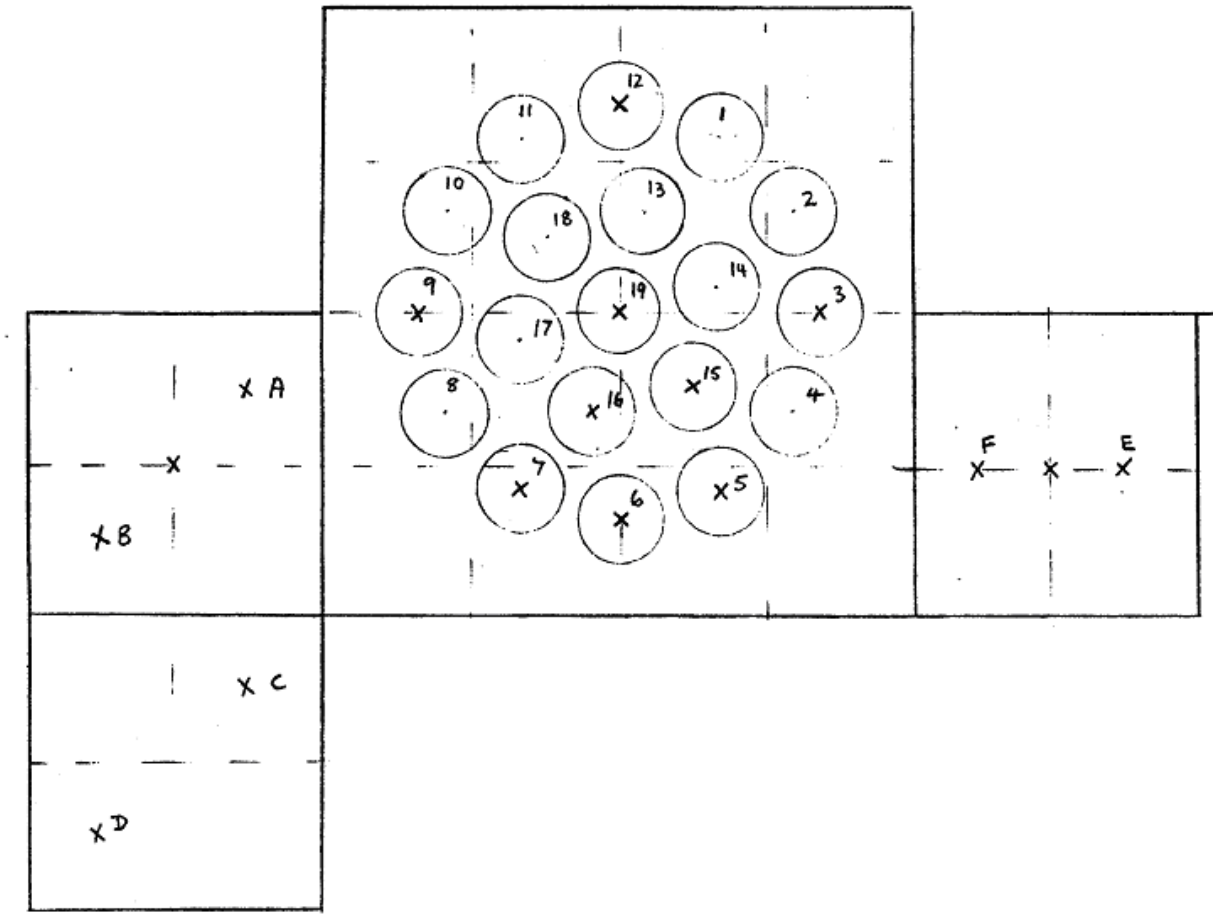

Figure 1.7 Reaction Rate Measurements Within and Adjacent to the TA, BN and B80 Rods.

X marks the position of the measurements

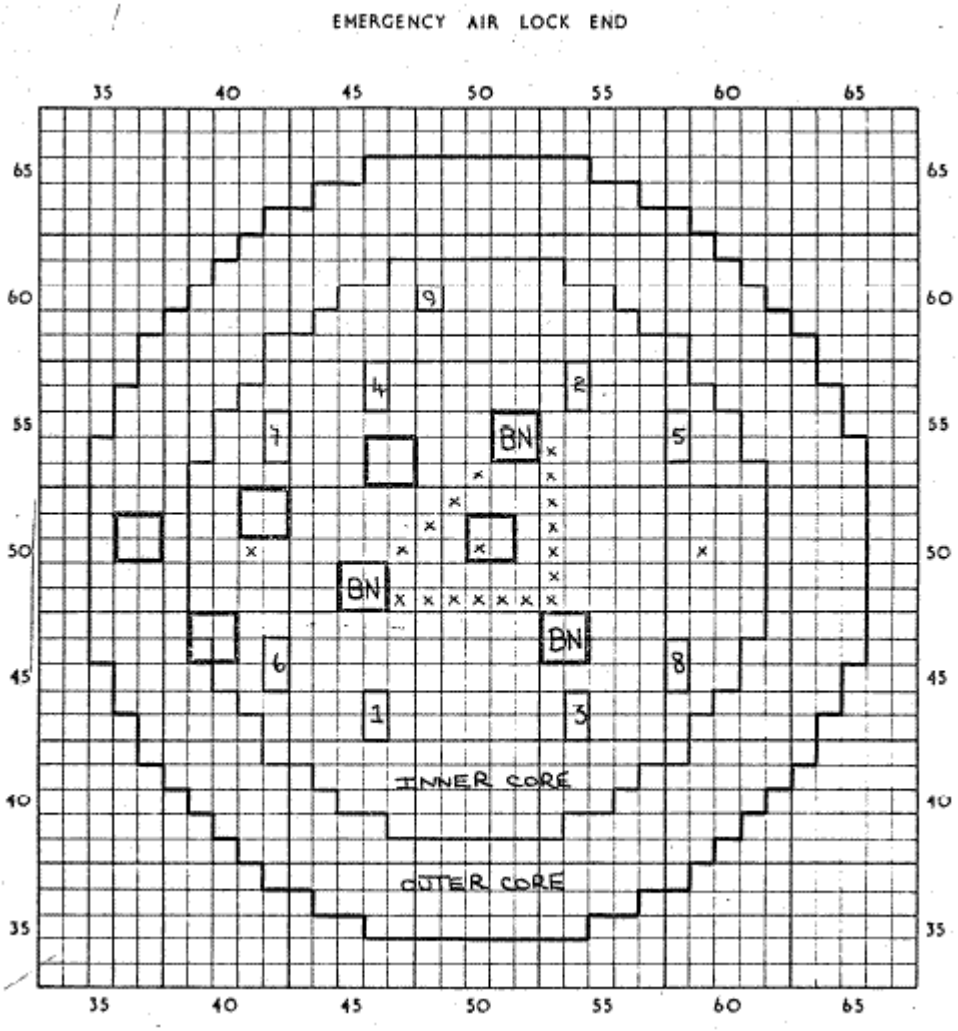

Figure 1.8 The Core with Three Natural Boron Mock-up Rods Fully Inserted, showing the Positions of the Foil Measurements

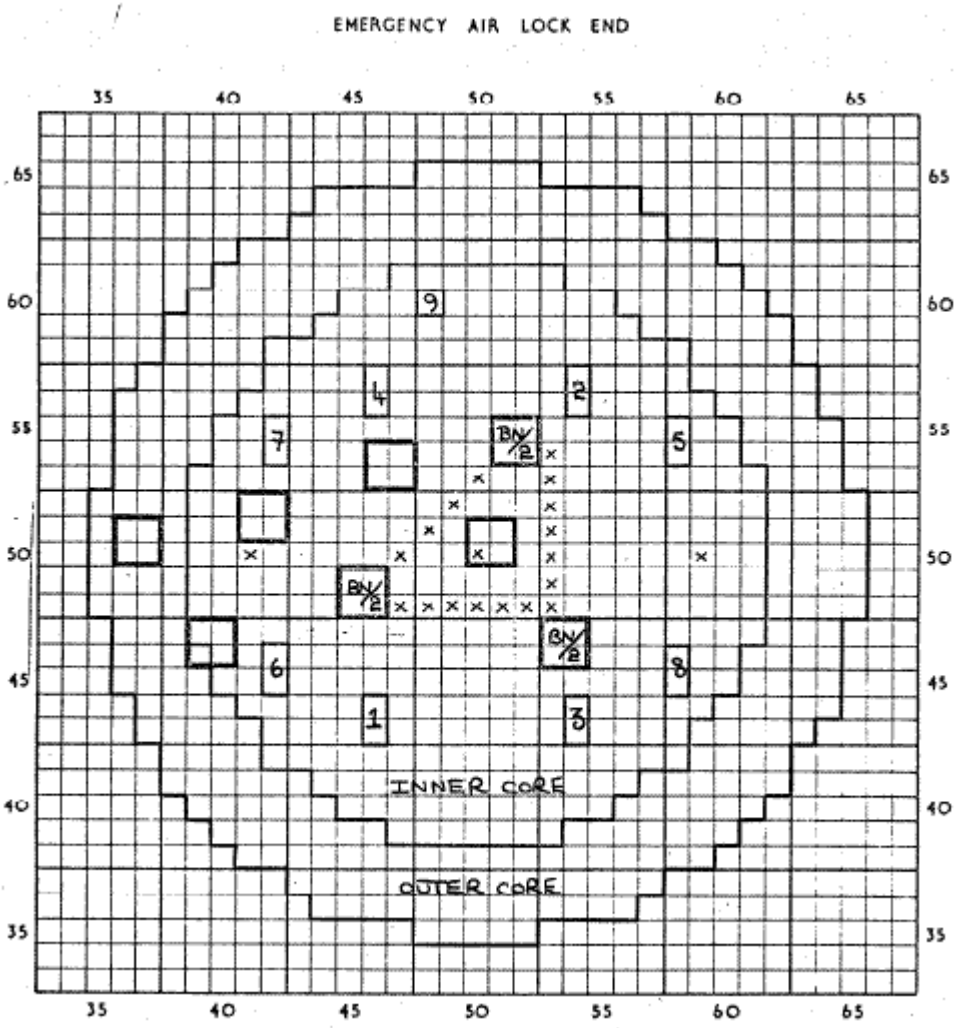

Figure 1.9 The Core with Three Natural Boron Mock-up Rods Half Inserted, showing the Positions of the Foil Measurements.

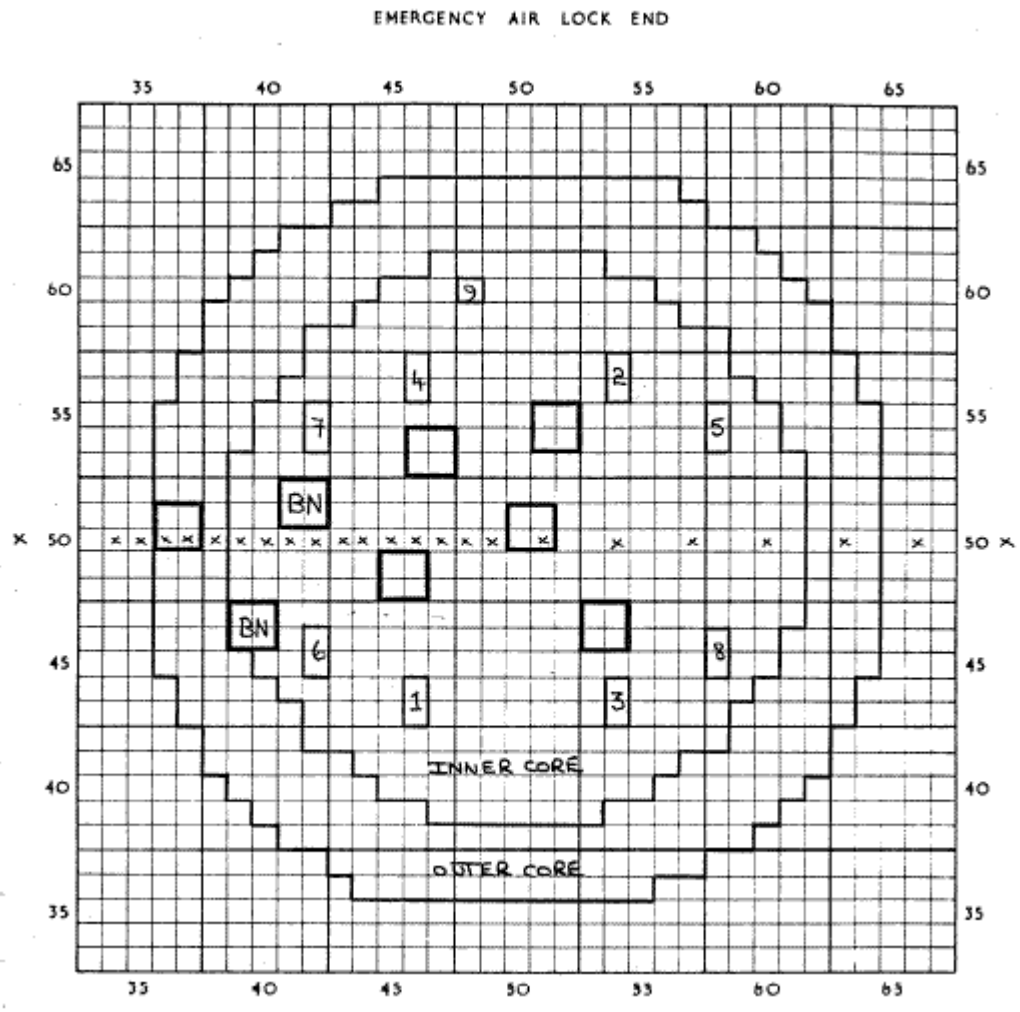

Figure 1.10 The Core with Two Natural Boron Mock-up Rods Inserted in Locations Q and R, showing the Positions of the Radial Chamber Measurements

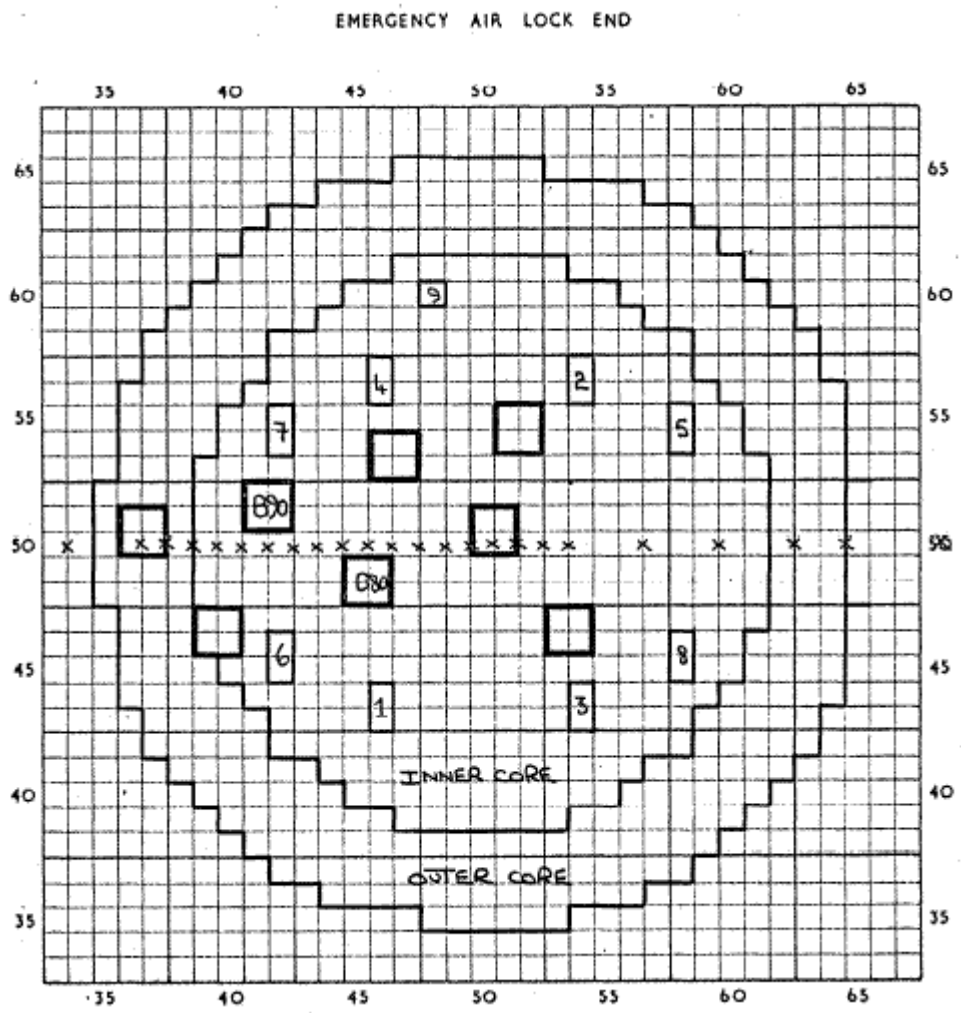

Figure 1.11 The Core with Enriched Boron Mock-up Rods Inserted, B80 at Location P1 and B90 at Location Q, showing the Positions of the Radial Chamber Measurements

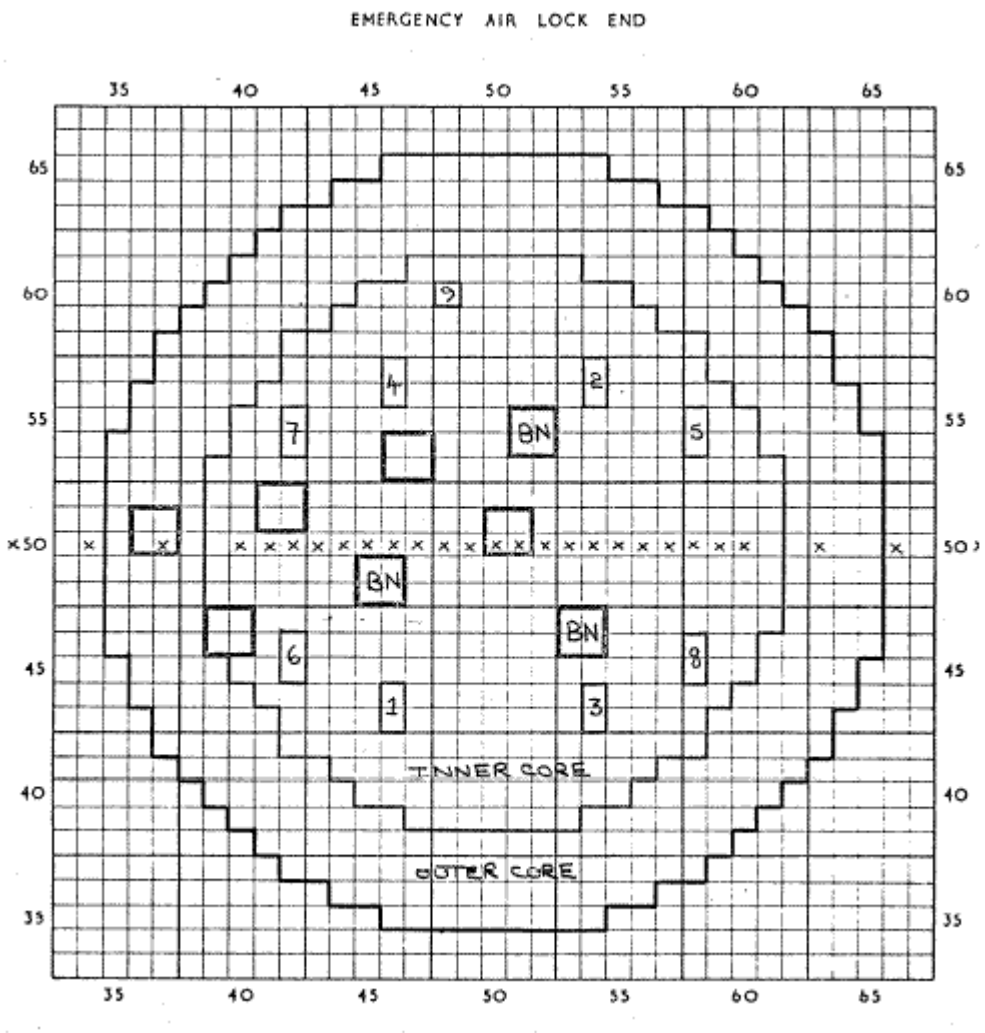

Figure 1.12 The Core with the Array of Three Natural Boron Mock-up Rods Inserted at Positions P1, P3, P5, showing the Positions of the Radial Chamber Measurements.

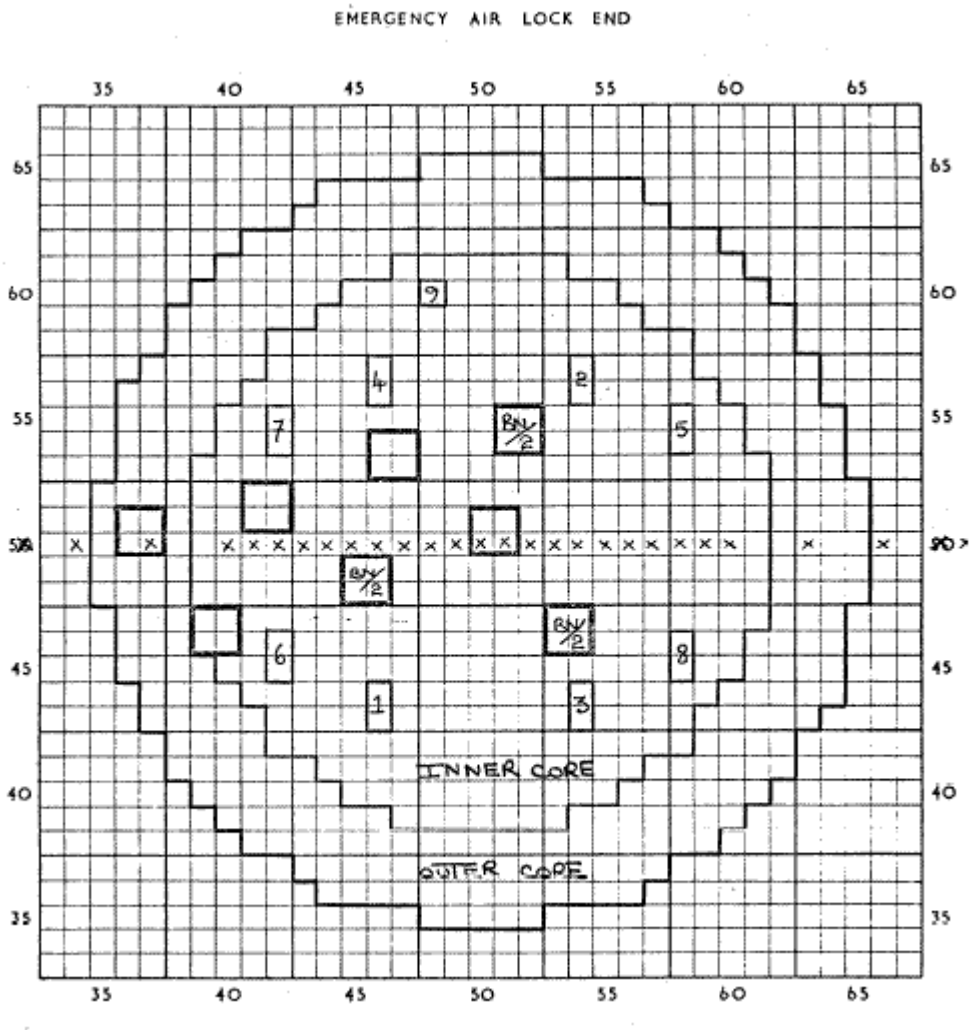

Figure 1.13 The Core with the Array of Three Natural Boron Mock-up Rods Half Inserted at Positions P1, P3, P5, showing the Positions of the Radial Chamber Measurements.

1.7.2B Methods

Measurements were made using both fission chambers and foils.

Radial fission rate scans were made in the core, for fission in U235 and U238, with Ta, BN and B80 rods at the core centre. Measurements were also made within the rings of absorber pins. In the case of the tantalum rod at the core centre, Ta(O), tantalum reaction rates were also measured, both in the core and within the rings of absorber pins (Tables 1.32 to 1.34).

Radial U235 and U238 fission rate scans were made in the core for the array of three BN rods, BN(P1,P3,P5), and for the array of half-inserted rods, BN/2 (P1,P3,P5) (Tables 1.35 and 1.36).

1.7.2C Results

Tantalum Capture to U235 Fission Ratio

A measurement was made of the ratio of tantalum capture to U235 fission in the inner core, relative to the ratio in the NESTOR thermal column, (Zebra/Nestor), (Z/N). The U235 foils were located in the UO_2 plate number 16 and the tantalum foils in the SS plate number 22. (See Table 1.30 for the plate numbering.)

Table 1.31 Tantalum Capture Relative to U235 Fission in the Inner Core of MZB.

Ratio Zebra/Nestor	Ratio, corrected for flux depression in the Ta foil in Nestor (4.5 ± 0.4)%	Ratio of Thermal Maxwellian values in JEF-2.2	Ratio in the inner core spectrum
13.05 ± 1.2%	12.46 ± 1.3%	0.03727	0.464

Foil Measurements

Typical uncertainties associated with the foil measurements are summarised in Table 1.37. They range from ±0.2% to ±0.7% for tantalum capture, ±0.3% to ±1.4% for U235 fission and ±0.6% to ±2.1% for U238 fission. More details of the foil measurements are given in MTN/97.

Confidence in the accuracy of the measurements can be gained from the comparison of Foil and Solid State Track Recorder (SSTR) U238 and U235 Fission Scans in Boron Rods at the Core Centre (Table 1.38 and 1.39). (See Section 1.3.2C of ZEBRA-LMFR-EXP-002 for more information on these techniques.)

Table 1.32 U235, U238 and Ta(n,γ) Radial Scans - tantalum rod at the core centre, Ta(O) (see Figure 1.4)

Element Position	Distance from Centre (cm)		F28	Total s.d. (%)	F25	Total s.d. (%)	Ta	Total s.d. (%)
	X	Y						
40-50	54.25	0	1.000	0.6	1.000	0.3	1.000	0.2
43-50	37.87	0	1.122	0.8	1.170	0.5	1.178	0.2
46-50	21.75	0	1.173	1.1	1.240	0.8	1.258	0.2
48-50	10.74	0	-	-	1.219	1.1	-	-
49-50	6.73	-1.36	-	-	1.197	1.2	-	-
49-50	5.37	0	1.028	1.6	1.160	1.2	1.154	0.5
49-50	4.02	1.36	-	-	1.130	1.3	-	-
49-49	6.73	-6.73	-	-	1.220	1.2	-	-
49-49	4.02	-4.02	-	-	1.183	1.3	-	-
52-50	-9.39	0	-	-	1.136	1.2	-	-
52-50	-10.74	0	1.010	1.4	1.154	1.1	1.141	0.5
52-50	-12.10	0	-	-	1.175	1.2	-	-
53-50	-16.38	0	-	-	1.191	1.0	-	-
55-50	-27.12	0	1.129	1.0	1.209	0.8	1.223	0.2
58-50	-43.50	0	1.059	0.7	1.112	0.5	1.115	0.2
61-50	-59.62	0	0.975	0.6	0.917	0.5	0.904	0.2

Measurements within the rod (see Figure 1.7)

Pin Position	Distance from Centre (cm)		F28	Total s.d. (%)	F25	Total s.d. (%)	Ta	Total s.d. (%)
	X	Y						
3	-6.15	2.69	0.727	1.7	0.963	1.4	0.632	0.7
5	-4.42	-0.31	-	-	0.972	1.4	0.643	0.7
6	-2.69	-0.77	0.734	1.7	0.968	1.4	0.640	0.7
7	-0.96	-0.31	-	-	0.965	1.4	0.635	0.7
9	0.77	2.69	0.720	1.7	0.964	1.4	0.636	0.7
12	-2.69	6.15	0.727	1.7	0.962	1.4	0.629	0.7
15	-3.95	1.42	-	-	0.914	1.4	0.571	0.4
16	-2.22	0.96	0.664	1.7	0.904	1.4	0.571	0.4
19	-2.69	2.69	0.637	1.7	0.894	1.4	0.557	0.2

Note: The tantalum results have not been corrected for self-shielding.

The pin numbering is clockwise, with the outer ring of 12 following the numbering of the clock, from 1 to 12, the inner ring of 6 being numbered with 13 being between 12 and 1. The central pin is number 19.

Table 1.33 U235 and U238 Radial Scans - BN(O)
(see Figure 1.5)

Element Position	Distance from Centre (cm)		F28	Total S.d. (%)	F25	Total S.d. (%)
	X	Y				
40-50	54.25	0	1.000	0.6	1.000	0.3
43-50	37.87	0	1.106	0.8	1.151	0.5
46-50	21.75	0	1.142	1.1	1.216	0.8
48-50	10.74	0	-	-	1.191	1.1
49-50	6.73	-1.36	-	-	1.163	1.2
49-50	5.37	0	1.024	1.5	1.136	1.2
49-50	4.02	1.36	-	-	1.114	1.2
49-49	6.73	-6.73	-	-	1.194	1.2
49-49	4.02	-4.02	-	-	1.158	1.2
52-50	-9.39	0	-	-	1.113	1.1
52-50	-10.74	0	0.999	1.4	1.128	1.1
52-50	-12.10	0	-	-	1.140	1.1
53-50	-16.38	0	-	-	1.173	1.0
55-50	-27.12	0	1.112	1.0	1.190	0.7
58-50	-43.50	0	1.060	0.7	1.102	0.4
61-50	-59.62	0	0.963	0.6	0.924	0.4

Measurements within the rod (see Figure 1.7)

Pin Position	Distance from Centre (cm)		F28	Total S.d. (%)	F25	Total S.d. (%)
	X	Y				
3	-6.15	2.69	0.808	1.7	0.939	1.3
5	-4.42	-0.31	-	-	0.940	1.3
6	-2.69	-0.77	0.807	1.7	0.945	1.3
7	-0.96	-0.31	-	-	0.943	1.3
9	0.77	2.69	0.802	1.7	0.943	1.4
12	-2.69	6.15	0.800	1.7	0.936	1.3
15	-3.95	1.42	-	-	0.889	1.4
16	-2.22	0.96	0.770	1.7	0.893	1.3
19	-2.69	2.69	0.752	1.7	0.870	1.3

Table 1.34 U235 and U238 Radial Scans - B80(O)
(see Figure 1.6)

Element Position	Distance from Centre (cm)		F28	Total S.d. (%)	F25	Total S.d. (%)
	X	Y				
40-50	54.25	0	1.000	0.7	1.000	0.3
43-50	37.87	0	1.065	1.2	1.117	0.5
46-50	21.75	0	1.068	1.3	1.131	0.8
48-50	10.74	0	-	-	1.032	1.1
49-50	6.73	-1.36	-	-	0.976	1.2
49-50	5.37	0	0.882	1.6	0.922	1.3
49-50	4.02	1.36	-	-	0.865	1.4
49-49	6.73	-6.73	-	-	1.039	1.2
49-49	4.02	-4.02	-	-	0.953	1.3
52-50	-9.39	0	-	-	0.872	1.3
52-50	-10.74	0	0.888	1.6	0.911	1.3
52-50	-12.10	0	-	-	0.945	1.1
53-50	-16.38	0	-	-	1.018	1.0
55-50	-27.12	0	1.033	1.1	1.091	0.7
58-50	-43.50	0	1.009	0.8	1.056	0.4
61-50	-59.62	0	0.970	0.7	0.913	0.3

Measurements within the rod (see Figure 1.7)

Pin Position	Distance from Centre (cm)		F28	Total S.d. (%)	F25	Total S.d. (%)
	X	Y				
3	-6.15	2.69	0.686	2.1	0.531	1.4
5	-4.42	-0.31	-	-	0.541	1.4
6	-2.69	-0.77	0.687	1.8	0.534	1.4
7	-0.96	-0.31	-	-	0.538	1.4
9	0.77	2.69	0.690	1.7	0.532	1.4
12	-2.69	6.15	0.687	1.7	0.528	1.4
15	-3.95	1.42	-	-	0.465	1.4
16	-2.22	0.96	0.647	1.9	0.466	1.4
19	-2.69	2.69	0.638	1.9	0.446	1.3

Table 1.35 U235 and U238 Radial Scans - BN(P1,P3,P5)
(see Figure 1.8)

Element Position	Distance from Centre (cm)		F28	Total S.d. (%)	F25	Total S.d. (%)
	X	Y				
47-50	16.38	0.00	0.928	1.4	0.971	1.2
48-51	10.74	5.37	0.979	1.1	0.980	0.9
49-52	5.37	10.74	0.987	1.1	0.992	0.9
50-53	0.00	16.38	0.930	1.4	0.954	1.2
53-54	-16.38	21.75	0.878	1.4	0.913	1.2
53-53	-16.38	16.38	0.922	1.4	0.942	1.2
53-52	-16.38	10.74	0.969	1.2	0.978	1.1
53-51	-16.38	5.37	0.993	1.1	0.981	0.9
53-50	-16.38	0.00	0.986	1.1	0.985	0.9
53-49	-16.38	-5.37	0.965	1.2	0.966	1.1
53-48	-16.38	-10.74	0.897	1.4	0.922	1.2
52-48	-10.74	-10.74	0.939	1.4	0.949	1.2
51-48	-5.37	-10.74	0.978	1.2	0.973	1.1
50-48	0.00	-10.74	0.988	1.1	0.988	0.9
49-48	5.37	-10.74	0.988	1.1	0.992	0.9
48-48	10.74	-10.74	0.963	1.2	0.964	1.1
47-48	16.38	-10.74	0.897	1.4	0.922	1.2
41-50	48.88	0.00	0.972	0.9	0.929	0.8
50-50	0.00	0.00	1.000	1.1	1.000	0.9
59-50	-48.88	0.00	0.987	0.9	0.938	0.7

Table 1.36 U235 and U238 Fission Radial Scans - Half-inserted Array BN/2 (P1,P3,P5)
(see Figure 1.9)

Element Position	Distance from centre (cm)		F28	Total S.d. (%)	F25	Total S.d. (%)
	X	Y				
47-50	16.38	0.00	0.938	1.4	0.978	1.2
48-51	10.74	5.37	0.985	1.1	1.002	0.9
49-52	5.37	10.74	0.983	1.1	1.004	0.9
50-53	0.00	16.38	0.944	1.4	0.981	1.2
53-54	-16.38	21.75	0.895	1.4	0.954	1.2
53-53	-16.38	16.38	0.930	1.4	0.964	1.2
53-52	-16.38	10.74	0.963	1.3	0.976	1.1
53-51	-16.38	5.37	0.984	1.1	0.986	0.9
53-50	-16.38	0.00	0.990	1.1	0.985	0.9
53-49	-16.38	-5.37	0.968	1.3	0.979	1.1
53-48	-16.38	-10.74	0.920	1.4	0.975	1.2
52-48	-10.74	-10.74	0.957	1.4	0.978	1.2
51-48	-5.37	-10.74	0.986	1.2	0.982	1.1
50-48	0.00	-10.74	0.992	1.1	0.987	0.9
49-48	5.37	-10.74	0.992	1.1	0.988	0.9
48-48	10.74	-10.74	0.968	1.3	0.981	1.1
47-48	16.38	-10.74	0.913	1.4	0.971	1.2
41-50	48.88	0.00	0.901	1.0	0.861	0.8
50-50	0.00	0.00	1.000	1.1	1.000	0.9
59-50	-48.88	0.00	0.909	0.8	0.872	0.7

Table 1.37 Typical Uncertainties Associated with the Foil Measurements in the Core and in the Three Rings of the Control Rods

Rod	Reaction Rate	Position	% Uncertainties				
			Total	Foil Posn.	Foil Counting	Axial Buckling	Gammas per Fission
Ta	F25	Core	0.8	0.1	0.2	0.2	0.8
		Outer Ring	1.1	0.2	0.3	0.2	1.3
		Inner Ring	1.4	0.1	0.3	0.2	1.3
		Central Pin	1.4	0.0	0.3	0.2	1.3
	F28	Core	1.1	0.1	0.5	0.3	0.9
		Outer Ring	1.7	0.4	0.6	0.2	1.5
		Inner Ring	1.7	0.2	0.6	0.2	1.5
		Central Pin	1.7	0.0	0.6	0.2	1.5
	Ta	Core	0.3	0.1	0.2	0.1	-
		Outer Ring	0.7	0.7	0.2	0.1	-
		Inner Ring	0.5	0.4	0.2	0.1	-
		Central Pin	0.2	0.0	0.2	0.1	-
BN(O)	F25	Core	0.8	0.1	0.2	0.2	0.8
		Outer Ring	1.3	0.2	0.2	0.1	1.3
		Inner Ring	1.3	0.1	0.2	0.1	1.3
		Central Pin	1.3	0.0	0.2	0.1	1.3
	F28	Core	1.1	0.1	0.5	0.3	0.9
		Outer Ring	1.7	0.2	0.6	0.3	1.5
		Inner Ring	1.7	0.1	0.6	0.3	1.5
		Central Pin	1.7	0.0	0.7	0.3	1.5
B80(0)	F25	Core	0.8	0.1	0.2	0.1	0.8
		Outer Ring	1.4	0.5	0.2	0.1	1.3
		Inner Ring	1.4	0.3	0.3	0.1	1.3
		Central Pin	1.3	0.0	0.3	0.1	1.3
	F28	Core	1.2	0.1	0.7	0.3	0.9
		Outer Ring	1.9	0.2	1.0	0.3	1.5
		Inner Ring	1.9	0.1	1.0	0.3	1.5
		Central Pin	1.9	0.0	1.1	0.3	1.5
3BN	F25	Core	0.9	0.0	0.2	0.0	0.9
	F28	Core	1.1	0.0	0.3	0.0	1.1
3BN/2	F25	Core	0.9	0.0	0.2	0.0	0.9
	F28	Core	1.1	0.0	0.3	0.0	1.1

Table 1.38 Comparison of Foil and SSTR U238 Fission Scans in Boron Rods at the Core Centre (SSTR denotes measurements made using Solid State Track Recorders.)

Rod Type	Position	Mean SSTR Value	Mean Foil Value	Foil/SSTR	Mean Foil/SSTR in Rod Relative to Core
BN	Pin 19	1.000 ± 1.2%	1.000 ± 0.7%	1.000 ± 1.4%	0.986 ± 1.1%
	Pin 16	1.029 ± 1.2%	1.024 ± 0.7%	0.995 ± 1.4%	
	Pin 6	1.072 ± 1.2%	1.073 ± 0.7%	1.001 ± 1.4%	
	46-50	1.481 ± 1.0%	1.519 ± 0.6%	1.026 ± 1.2%	
	43-50	1.472 ± 1.0%	1.471 ± 0.6%	0.999 ± 1.2%	
B80	Pin 19	1.000 ± 1.5%	1.000 ± 1.2%	1.000 ± 1.9%	1.003 ± 1.5%
	Pin 16	1.006 ± 1.5%	1.014 ± 1.1%	1.008 ± 1.9%	
	Pin 6	1.076 ± 1.5%	1.077 ± 1.0%	1.001 ± 1.8%	
	46-50	1.689 ± 1.1%	1.674 ± 0.9%	0.991 ± 1.4%	
	43-50	1.653 ± 1.1%	1.669 ± 1.1%	1.010 ± 1.6%	

Table 1.39 Comparison of Foil and SSTR U235 Fission Scans in Boron Rods at the Core Centre

Rod Type	Position	Mean SSTR Value	Mean Foil Value	Foil/SSTR	Mean Foil/SSTR in Rod Relative to Core
BN	Pin 19	1.000 ± 1.2%	1.000 ± 0.3%	1.000 ± 1.25%	1.012 ± 1.0%
	Pin 16	1.021 ± 1.2%	1.026 ± 0.3%	1.005 ± 1.25%	
	Pin 6	1.098 ± 1.2%	1.086 ± 0.3%	0.989 ± 1.25%	
	46-50	1.412 ± 1.0%	1.397 ± 0.3%	0.989 ± 1.04%	
	43-50	1.344 ± 1.0%	1.322 ± 0.3%	0.983 ± 1.04%	
B80	Pin 19	1.000 ± 1.2%	1.000 ± 0.3%	1.000 ± 1.4%	1.005 ± 1.1%
	Pin 16	1.004 ± 1.3%	1.045 ± 0.5%	1.041 ± 1.4%	
	Pin 6	1.206 ± 1.3%	1.197 ± 0.6%	0.993 ± 1.4%	
	46-50	2.542 ± 0.9%	2.536 ± 0.3%	0.998 ± 0.95%	
	43-50	2.466 ± 0.9%	2.504 ± 0.3%	1.015 ± 0.95%	

Fission Chamber Scans

Pu239 and U238 fission rate distributions were measured using fission chambers in four control rod configurations. Radial distributions were measured along the radial centre line, in the "flight tube direction". That is they are along the line of elements with Y=50 and are positive for X greater than 50. Measurements were made for the BN(Q, R), BN(P1,P3,P5), BN/2(P1,P3,P5) and B90(Q)B80(P1) arrangements. In addition axial scans were measured in the elements at positions (53,48) and (50,50) in the arrangement with the half inserted array BN/2(P1,P3,P5) and at position (50,50) in the BN(P1,P3,P5) arrangement. The results of the measurements are given in Tables 1.40 to 1.46 with a comparison between the fission chamber and foil measurements of U238 fission in Table 1.47.

The same elements and chambers were used as for the measurements in the unperturbed version of MZB, that is, the version without mock-up rods inserted (see Part 1, ZEBRA-LMFR-EXP-002, Section 1.7, for a description).

A correction was made to the U238 fission chamber measurements for fission in the 0.036% of U235 in the U238 deposit of the chamber. No U235 measurements were available to make the correction and so a correction was calculated based on the Pu239 scans, which have a sufficiently similar variation with position, normalised to the central U235/Pu239 fission ratio measurements.

A problem was found in the case of the Pu239 radial fission chamber scan in the BN/2(P1,P3,P5) case. The radial position appeared to be incorrect and it was suggested that this was due to the position recorded having jumped by 2 cm. In MTN/100 a correction is made on this basis and the corrected values are the ones given in Table 1.41.

The uncertainty of the measurements ranged from 0.3% to 1.0% for the Pu239 scans and from 0.5% to 2.5% for the U238 scans (see Part 1, ZEBRA-LMFR-EXP-002, Section 1.7, and MTN/89, for a summary and discussion of the sources of uncertainty).

Table 1.40 Radial Scans with Rods BN(Q,R) Present
(see Figure 1.10)

Pu239			U238		
Distance from Centre (cm)	Normalised Count Rate	S.D. (%)	Distance from Centre (cm)	Normalised Count Rate	S.D. (%)
102.92	0.2438	0.90	102.92	0.0220	2.73
86.57	0.3679	0.73	86.57	0.1077	1.48
81.21	0.3933	0.70	81.21	0.2053	1.26
75.85	0.4045	0.34	75.85	0.3834	0.77
70.49	0.4438	0.34	70.50	0.4929	0.62
64.87	0.4808	0.35	64.87	0.5322	0.57
59.50	0.5191	0.34	59.50	0.5260	0.57
54.14	0.5495	0.34	54.14	0.5306	0.57
48.77	0.5861	0.34	48.78	0.5441	0.57
43.42	0.6416	0.35	43.41	0.5996	0.56
37.79	0.7105	0.34	37.79	0.6838	0.52
32.43	0.7728	0.34	32.43	0.7613	0.49
27.06	0.8347	0.34	27.06	0.8202	0.47
21.69	0.8830	0.33	21.70	0.8701	0.45
16.34	0.9269	0.34	16.34	0.9112	0.44
10.71	0.9523	0.34	10.71	0.9544	0.43
5.35	0.9836	0.33	5.35	0.9881	0.42
-5.37	1.0164	0.32	-5.37	1.0119	0.42
-21.71	1.0178	0.32	-21.72	1.0162	0.42
-37.81	0.9561	0.34	-37.81	0.9504	0.43
-54.15	0.8266	0.34	-54.16	0.8491	0.45
-70.51	0.6467	0.35	-70.51	0.7503	0.52
-86.59	0.5179	0.63	-86.59	0.1652	1.39
-102.94	0.3376	0.78	-102.94	0.0321	2.60

Table 1.41 Radial Scans with Rods BN/2(P1,P3,P5) Present
(see Figure 1.13)

Pu239			U238		
Distance from Centre (cm)	Normalised Count Rate (Adjusted, see MTN/100)	S.D. (%)	Distance from Centre (cm)	Normalised Count Rate	S.D. (%)
97.56	0.4044	0.87	97.56	0.0795	2.42
86.58	0.4939	0.79	86.57	0.2979	1.38
70.50	0.6758	0.37	70.49	0.8605	0.57
54.14	0.8409	0.35	54.14	0.8778	0.53
48.78	0.8761	0.35	48.78	0.9065	0.54
43.41	0.9104	0.36	43.42	0.9201	0.56
37.79	0.9228	0.36	37.79	0.9290	0.56
32.43	0.9364	0.33	32.44	0.8995	0.57
27.06	0.9543	0.33	27.06	0.8980	0.57
21.69	0.9561	0.33	21.70	0.9098	0.57
16.34	0.9794	0.39	16.34	0.9477	0.58
10.71	0.9961	0.36	10.71	0.9913	0.60
5.35	1.0011	0.36	5.35	0.9986	0.57
-0.01	1.0003		-0.01	1.0052	0.56
-5.37	1.0015		-5.37	0.9962	0.60
-10.73	0.9852		-10.73	0.9942	0.60
-16.36	0.9858		-16.36	0.9835	0.60
-21.72	0.9804		-21.72	0.9777	0.60
-27.09	0.9566		-27.08	0.9698	0.57
-32.45	0.9510		-32.45	0.9672	0.57
-37.81	0.9259		-37.81	0.9512	0.58
-43.43	0.9059		-43.43	0.9234	0.59
-48.80	0.8786		-48.80	0.9174	0.59
-54.16	0.8356		-54.16	0.8877	0.60
-70.51	0.6615		-70.51	0.8646	0.65
-86.59	0.5210		-86.59	0.3014	1.38
-97.58	0.3959		-97.58	0.0807	2.00
-102.94			-102.94	0.0500	2.32

Table 1.42 Axial Scans in the element at (53,48) for BN/2(P1,P3,P5)

Pu239			U238		
Distance from Centre (cm)	Normalised Count Rate	S.D. (%)	Distance from Centre (cm)	Normalised Count Rate	S.D. (%)
-75.05	0.1869	1.04	-75.05	0.0206	2.69
-66.30	0.2511	1.06	-66.29	0.0440	2.02
-57.53	0.3505	1.00	-57.53	0.0885	1.72
-48.77	0.4575	0.87	-48.77	0.1974	1.40
-40.64	0.5298	0.44	-40.65	0.4246	0.76
-32.53	0.6422	0.42	-32.53	0.6122	0.59
-24.42	0.7523	0.36	-24.44	0.7502	0.40
-16.32	0.8547	0.26	-16.32	0.8536	0.53
-8.22	0.9340	0.34	-8.22	0.9471	0.51
-0.10	1.0000	0.33	-0.10	1.0000	0.51
8.00	1.0336	0.34	8.00	1.0154	0.51
16.11	1.0134	0.33	16.11	0.9767	0.52
24.22	0.9398	0.35	24.22	0.8924	0.52
32.32	0.8387	0.27	32.33	0.7807	0.55
40.43	0.7268	0.37	40.43	0.5950	0.66
49.17	0.6658	0.72	49.17	0.2931	1.31
57.94	0.5710	0.78	57.94	0.1306	1.51
66.70	0.4628	0.86	66.70	0.0640	1.78
75.45	0.3796	0.95	75.45	0.0338	2.14

Note: The coordinates shown are relative to the centre of the element in which measurements are made. To make them relative to the mean core centre plane they should be modified by -0.25 cm (as has been done in Tables 4.24 et seq.).

In comparing with calculation (Tables 4.24 et seq.) the axial distributions calculated using homogenised core cross-sections have been adjusted downwards by 0.85 cm to compensate for the asymmetry of the inner core cells (see MTN/100). The measured values have also been renormalised in MTN/100 and these values are the ones given in Tables 4.24 et seq.

Table 1.43 Axial Scans in the element at (50,50) for BN/2(P1,P3,P5)

Pu239			U238		
Distance from Centre (cm)	Normalised Count Rate	s.d. (%)	Distance from Centre (cm)	Normalised Count Rate	s.d. (%)
-75.05	0.2177	1.02	-75.05	0.0201	2.80
-66.28	0.2947	1.01	-66.29	0.0426	2.04
-57.53	0.3901	0.96	-57.53	0.0875	1.61
-48.77	0.4871	0.36	-48.77	0.1853	1.53
-40.65	0.5573	0.51	-40.65	0.4358	0.81
-32.53	0.6649	0.47	-32.52	0.6291	0.59
-24.43	0.7732	0.46	-24.42	0.7751	0.45
-16.32	0.8797	0.44	-16.32	0.8963	0.52
-8.22	0.9546	0.42	-8.22	0.9596	0.50
-0.1	1	0.44	-0.09	1	0.56
8.00	1.0109	0.43	8	1.0067	0.52
16.12	0.9705	0.42	16.11	0.9687	0.54
24.23	0.8954	0.44	24.21	0.8760	0.54
32.34	0.7884	0.45	32.33	0.7627	0.59
40.43	0.6794	0.5	40.43	0.5843	0.71
49.17	0.6219	0.72	49.17	0.2747	1.32
57.94	0.5304	0.79	57.94	0.1219	1.41
66.70	0.4260	0.87	66.7	0.0617	1.74
75.45	0.3568	0.94	75.45	0.0302	4.14

Note: The coordinates shown are relative to the centre of the core region of the element in which measurements are made. To make them relative to the mean core centre plane -0.25 cm should be added to the axial height (i.e. 0.25 should be subtracted).

Table 1.44 Radial Scans with Rods BN(P1,P3,P5) Present
(see Figure 1.12)

Pu239			U238		
Distance from Centre (cm)	Normalised Count Rate	s.d. (%)	Distance from Centre (cm)	Normalised Count Rate	s.d. (%)
103.11	0.4046	0.73	103.11	0.0595	2.71
96.73	0.6017	0.83	96.73	0.3449	1.15
70.61	0.7620	0.26	70.62	0.9692	0.56
54.24	0.9202	0.33	54.24	0.9621	0.51
46.87	0.9415	0.33	46.87	0.9727	0.39
43.49	0.9502	0.33	43.49	0.9706	0.51
37.86	0.9519	0.33	37.87	0.9574	0.52
32.49	0.9440	0.33	32.49	0.9182	0.53
27.11	0.9251	0.35	27.09	0.8874	0.50
21.74	0.9257	0.35	21.74	0.8901	0.50
16.37	0.9569	0.34	16.37	0.9483	0.52
10.73	0.9832	0.35	10.73	0.9886	0.54
5.36	1.0028	0.35	5.36	0.9997	0.50
-0.01	1.0019	0.35	-0.01	1.0063	0.50
-5.38	0.9953	0.34	-5.38	0.9940	0.51
-10.75	0.9904	0.34	-10.75	0.9904	0.51
-16.39	0.9942	0.34	-16.39	0.9919	0.51
-21.76	0.9887	0.34	-21.76	0.9881	0.51
-27.13	0.9960	0.34	-27.13	1.0063	0.50
-32.51	0.9959	0.34	-32.51	1.0033	0.50
-37.87	0.9841	0.34	-37.88	1.0060	0.50
-43.51	0.9761	0.34	-43.51	0.9962	0.43
-48.89	0.9536	0.34	-48.89	0.9931	0.51
-54.26	0.9174	0.35	-54.26	0.9833	0.48
-70.64	0.7610	0.38	-70.64	0.9770	0.53
-86.75	0.5973	0.83	-86.75	0.3519	1.13
-103.13	0.4046	1.00	-103.13	0.0612	2.60

Table 1.45 Axial Scans in the Element at Position (50,50) for Rods BN(P1,P3,P5)

Pu239			U238		
Distance from Centre (cm)	Normalised Count Rate	s.d. (%)	Distance from Centre (cm)	Normalised Count Rate	s.d. (%)
-75.41	0.2607	0.98	-75.41	0.0238	2.69
-66.63	0.3438	0.98	-66.63	0.0466	2.16
-57.86	0.4561	0.96	-57.86	0.0917	1.78
-49.09	0.5600	0.05	-49.09	0.1995	1.75
-40.94	0.6055	0.45	-40.94	0.4510	0.78
-32.82	0.7016	0.45	-32.82	0.6607	0.59
-24.70	0.8125	0.43	-24.69	0.7950	0.54
-16.57	0.9076	0.44	-16.57	0.9035	0.52
-6.45	0.9715	0.42	-6.45	0.9699	0.52
-0.33	1.0000	0.3	-0.33	1.0000	0.36
7.80	0.9914	0.41	7.80	0.9853	0.52
15.92	0.9389	0.41	15.92	0.9357	0.51
24.04	0.8647	0.54	24.04	0.8546	0.51
32.16	0.7569	0.45	32.16	0.7266	0.56
40.30	0.6472	0.52	40.30	0.5482	0.69
49.05	0.5939	0.83	49.05	0.2633	1.64
57.82	0.5112	0.9	57.82	0.1161	1.79
66.61	0.4163	0.99	66.60	0.0571	2.07
75.37	0.3552	1.06	75.37	0.0292	2.46

Note: The coordinates shown are relative to the centre of the core region of the element in which measurements are made. To make them relative to the mean core centre plane they should be modified by:

-2.5 mm.

Table 1.46 Radial Scans with Rods B90(Q) B80(P1) Present
(see Figure 1.11)

Pu239			U238		
Distance from Centre (cm)	Normalised Count Rate	S.D. (%)	Distance from Centre (cm)	Normalised Count Rate	S.D. (%)
89.27	0.3306	0.87	89.25	0.1329	2.04
72.89	0.4120	0.70	72.89	0.5109	0.95
67.52	0.4512	0.75	67.52	0.5548	0.90
62.16	0.4714	0.32	62.15	0.5567	0.76
56.78	0.4772	0.32	56.78	0.5178	0.74
51.14	0.4657	0.31	51.14	0.5024	0.75
45.77	0.4727	0.32	45.77	0.4942	0.76
40.40	0.5096	0.33	40.40	0.5392	0.77
35.03	0.5519	0.33	35.03	0.5720	0.75
29.65	0.5810	0.33	29.65	0.5940	0.74
24.02	0.6250	0.34	24.02	0.6302	0.77
18.65	0.7157	0.36	18.65	0.7295	0.79
13.27	0.8187	0.34	13.27	0.8162	0.76
7.90	0.9016	0.33	7.90	0.9031	0.74
2.53	0.9715	0.32	2.53	0.9678	0.77
-3.11	1.0285	0.32	-3.11	1.0322	0.75
-8.48	1.0635	0.31	-8.48	1.0653	0.74
-13.84	1.0915	0.21	-13.85	1.0907	0.63
-19.21	1.1104	0.31	-19.22	1.1066	0.73
-35.60	1.1080	0.32	-35.60	1.1050	0.73
-51.72	1.0204	0.32	-51.72	1.0487	0.74
-68.10	0.8330	0.33	-68.10	1.0396	0.75
-84.49	0.6165	0.34	-84.48	0.4796	0.88
-100.59	0.4464	0.76	-100.59	0.0718	2.25
-116.97	0.3417	0.66	-116.97	0.0108	3.60

Table 1.47 Comparison of Foil and Fission Chamber U238 Results

Rod Arrangement	Position	Fission Chamber	S.d. %	Foil	S.d. %	FC/Foil	S.d. %
BN/2(P1,P3,P5)	41-50	0.9014	0.54	0.9006	0.46	1.0009	0.71
	47-50	0.9425	0.58	0.9377	0.25	1.0051	0.63
	50-50	1.0000	0.56	1.0000	0.32	1.0000	0.64
	53-50	0.9783	0.60	0.9903	0.28	0.9879	0.66
	59-50	0.9123	0.59	0.9092	0.23	1.0031	0.63
BN(P1,P3,P5)	41-50	0.9666	0.39	0.9721	0.27	0.9943	0.47
	47-50	0.9423	0.52	0.9281	0.26	1.0153	0.58
	50-50	1.0000	0.50	1.0000	0.40	1.0000	0.64
	53-50	0.9857	0.51	0.9865	0.55	0.9992	0.75
	59-50	0.9869	0.51	0.9874	0.36	0.9995	0.62

Note: All scans have been normalised to 1.0 at the element in the central position, (50,50).

The reaction rate distribution measurements presented in this section are recommended as suitable for consideration for use as benchmarks, in conjunction with the control rod reactivity worth measurements.

1.7.3 Description of Material Data.

As stated above, in 1.7.2A.

1.7.4 Temperature

The temperature was not recorded and no temperature corrections were made.

1.7.5 Additional Information Relevant to the Reaction Rate Distribution Measurements

None.

1.8 Description of Power Distributions Measurements in MZC.

Not measured.

1.9 Description of Isotopic Measurements in MZC.

Not measured.

1.10 Description of other Miscellaneous Measurements in MZC.

Note the measurement of the tantalum (n,γ) reaction rate relative to the U235 fission rate described in Section 1.7.

2. EVALUATION OF EXPERIMENTAL DATA

2.1 Evaluation of Critical or Subcritical Configuration Data

The evaluation of the criticality measurements made in the Mozart Cores is documented in ZEBRA-LMFR-EXP-002.

2.2 Evaluation of Buckling and Extrapolation Length Data

There were no bucklings derived from the reaction rate scan measurements made in MZB.

2.3 Evaluation of Spectral Characteristics Data

The measurements made in MZA and MZB are documented and evaluated in ZEBRA-LMFR-EXP-002.

2.4 Evaluation of Reactivity Effects Data

2.4.1 The Mock-up Control Rod Reactivity Worth Measurements.

The measurements were critical balances, with the reduction in reactivity resulting from the insertion of the mock-up rod in the core being balanced by the addition of edge elements and with the residual excess reactivity being balanced by the insertion of the regulating rod, FR9.

To relate the measurements to the worth of the absorber rod displacing a rod follower, calculations were made of the reactivity difference due to the different numbers of edge elements between the core containing the rod and the reference core containing the rod follower. In this first stage the reactivity worth of the rod relative to the rod follower is expressed in terms of the calculated reactivity worth of the additional edge elements (plus the reactivity effect of any difference in the insertion of the regulating rod, FR9). There is then a further stage which involves the choice of a reactivity scale. Several reactivity scales were evaluated and in this document the data have been standardised on the calibration of FR9 by means of period measurements using the chosen delayed neutron data (Smith-Tomlinson). ***Thus the calculated reactivity effect of the added edge elements must then be scaled to be consistent with this reactivity scale. The correction is a substantial one, an increase of 7.3%, as described in Section 1.4.1, and a key question is to try to understand this difference.***

In the original analyses several different approaches were explored and a slightly different reactivity scale was used in the final analysis, one based on the measured and calculated worths of plutonium, but this scale is very little different from the delayed neutron scale adopted here. Different approaches gave results within about ±1% of each other, although the uncertainty in the reactivity scale is taken to be ±5%.

One can be confident that the approach used to derive the reactivity worths of rods relative to fuelled elements or followers, in cores of the same size, is a sound one by looking at the results given in Table 1.20, comparing measured and calculated rod interaction effects. The measured interaction effects are based on the measurements for single rods compared with the measurements for arrays. One sees that there is an overall consistency in the ratio of calculation to measurement (C/E), with a mean value of 1.0051 and a standard deviation of 0.66%. The overall consistency is good even though there is a significant discrepancy between these homogenised diffusion theory calculations and experiment for individual rods and arrays, a discrepancy which increases with rod worth and is considered to be due to the use of these homogenisation methods and diffusion theory. There is an overall consistency in the MONK JEF-2.2 Monte Carlo C/E values presented in Section 4, with no evidence of a significant bias in the reactivity scale (when account is taken of the uncertainty in the Monte Carlo results and the discrepancy for the follower measurements, noting that JEF-2.2 sodium data have been shown elsewhere to be unsatisfactory).

On the basis of these considerations the measurements presented in Section 1.4, in Tables 1.13 to 1.19, are recommended as suitable benchmarks for validating methods for calculating the reactivity effects of control rods and rod followers.

2.4.2 Uncertainties in the Weights and Dimensions of the Absorber Pins.

Details of all components are given in MTN/39. Uncertainties in weights and dimensions are generally below 0.2% excepting for the enrichment of the B30 rod for which the difference between two measurements is 0.5%. However, the effect of these uncertainties on rod worths are about one half of the percentage uncertainties and so are considered to be negligible.

For the Tantalum pins the dimensions are:

length	91.337 ± 0.013 cm (±0.014%)
diameter	1.31 ± 0.0025 cm (±0.2%)
weight	2060.2 range 2058.0 to 2062.5 (range ±0.11%)

For the Boron pins two values are given for the percentage enrichments in B10, the first as measured by Partiot and the second by the UKAEA. The two sets of figures are quoted as

BN	19.806 ±0.0166 and	19.76 ±0.04	
B30	29.88 ±0.004	and	30.03
B80	79.914 ±0.0037 and	79.78	
B90	90.16 ±0.02		

The differences between the two measurements are a maximum for the B30 pin and is 0.5% in this case.

The weight figures are difficult to interpret. For the B90 pin the mean value is given as 201.75 g with a range from 201.63 to 201 86 g, a range of 0.06%

2.4.3 The Reactivity Scale and its Uncertainty.

Because it is key to understanding the systematic uncertainty in the reactivity scale, and the discrepancy in calculating the edge element worths, these measurements should be reanalysed using the latest nuclear data. They are considered to be part of the control rod reactivity benchmark and the measurements are recommended as part of this benchmark.

As is illustrated in Table 2.1 below, the JEFF-3 data for yields and relative abundances in U235, U238 and Pu239 (D'Angelo and Rowlands, Prog Nucl Energy, 2002) would result in a value of beta (for the fast reactor core calculated by Stevenson[1] - Proc Specialists' Mtg on Delayed Neutron Properties, Univ. of Birmingham, Sept. 1986, page 1) which is 1.8 % higher and a 100 sec period-reactivity calibration value which gives a reactivity 3.7% higher. However, there are other differences between the data and calculations which have not been taken into account here - the effect of differences in relative fission rates, in prompt neutron yields, and in the delayed neutron energy spectra and neutron importance calculations. The Reviewer, Atsushi Zukeran, has studied the uncertainties and has contributed the Appendix attached to this Section, 2.4. He concludes that the uncertainty due to the delayed neutron yields is ±2.5%, that due to the uncertainties in the energy dependence is ± 1.7%, that due to uncertainties in the fission cross-sections is ± 1.6%, that due to reaction rate ratios is ± 0.1%, that due to uncertainties in the delayed neutron spectra ± 0.1%, etc. giving an overall uncertainty of ±5.2%.

Table 2.1 Isotopic Contributions to Reactivity for a 100 sec Period Calculated for a ZEBRA Core
(units 10^{-4} dk/k)

	Smith-Tomlinson (1973) data				JEFF-3 data			
	% Yield	Time factor	Beta	Reactivity	% Yield	Time factor	Beta	Reactivity
U-235F	1.65	0.0965	1.951	0.188	1.63	0.0994	1.927	0.192
U-238F	4.58	0.0613	14.40	0.883	4.65	0.0613	14.620	0.896
Pu-239F	0.633	0.110	14.66	1.613	0.651	0.1129	15.077	1.702
Pu-240F	0.88	0.101	1.136	0.115	0.891	0.1027	1.150	0.118
Pu-241F	1.59	0.0866	1.893	0.164	1.565	0.0876	1.863	0.163
Pu-242F	1.5	0.076	0.042	0.003	1.94	0.0738	0.054	0.004
Total			34.082	2.965			34.692	3.075

(The total percentage yields per fission given above for Pu240, 241 and 242 are the JEF-2.2 values.) The time dependent data used to calculate the JEFF-3 time factors are the 8 time group parameters recommended by Spriggs, Campbell and Piksaikin (Prog Nucl. Energy, 2002).

It can be seen that it is not sufficient to compare beta-effective values, the time dependence factor also has an important effect.

Appendix to Section 2.4. Reviewer's Comments on the Reactivity Scale based on the Delayed Neutron Data of Smith-Tomlinson.

Atsushi Zukeran [1]

The reactivity scale based on period measurements, interpreted by means of the inhour equation and the Smith-Tomlinson delayed neutron data, is the most important problem in the present work. The delayed neutron data themselves have been revised several times since these data were used in the analysis and thus the experimental reactivity data should be revised using up-to-date data. The Smith-Tomlinson data, however, are not significantly different from the current evaluated data as shown in Table Rev-A1

The "Smith-Tomlinson" data set is quite the same as "Tuttle" for the first three nuclei, U235, U238 and Pu239, and for the others nearly equal. The Tuttle data is not the newest one since some new evaluations of delayed neutron data have been reported such as JEFF-3, JENDL-3.3 and the 8 time group parameters recommended by Spriggs, Campbell and Piksaikin as referred to in the present document in Section 1.4. This last 8 group method is the advanced method being able to interpret the experimental data of delayed neutrons in detail. However, the Tuttle data is not so far from the current recommended data and the Smith-Tomlinson data is willingly accepted.

As is well known, the effective delayed neutron yield β_{eff} and its sensitivity coefficient with respect to delayed neutron yield and perturbation denominator γ_i^m are briefly reviewed as follows

$$\beta_{eff} = \sum_m \sum_i \left[\beta_i \gamma_i \right]^m \tag{1}$$

The component $\left[\beta_i \gamma_i \right]^m$ and perturbation denominator D_p are defined by

$$\left[\beta_i \gamma_i \right]^m = \frac{\int_V \int_{E'} \chi_{d,i}^m(E') \varphi^*(E', \vec{r}) dE' \int_E \nu_{d,i}^m(E) \Sigma_f^m \varphi(E, \vec{r}) dE dV}{D_p} \tag{2}$$

$$D_p = \sum_n \int_V \int_{E'} \chi^n(E') \phi^*(E', \vec{r}) dE' \int_E \nu^n(E) \Sigma_f^n \phi(E, \vec{r}) dE dV \tag{3}$$

$$\cong \sum_n \int_V \int_{E'} \chi_p^n(E') \phi^*(E', \vec{r}) dE' \int_E \nu_p^n(E) \Sigma_f^n \phi(E, \vec{r}) dE dV \tag{4}$$

where the delayed neutron contribution to the perturbation denominator D_p is dropped in Eq.(4) for simplicity, since its magnitude (at most 0.65%) is negligibly small relative to the total neutron yield of about 2.49. The other parameters or variables are as follows,

E : incident neutron energy (eV),
E' : secondary neutron energy (eV),
V : reactor volume,

[1] A. Zukeran et al.: J. Nucl. Sci. and Technol., 36(1), 61, (1999). In this paper a generalized perturbation treatment is used and more detailed information will be needed as a supplement.

ν_p^m : prompt neutron yield of fuel isotope m

$\nu_{d,i}^m$: delayed neutron yield of fuel isotope m and family i

ν^m : total neutron yield of fuel isotope m, i.e. $\nu^m = \nu_p^m + \sum_i \nu_{d,i}^m$,

χ_p^m : prompt neutron spectrum of fuel isotope m

$\chi_{d,i}^m$: delayed neutron spectrum of fuel isotope m and family i

χ^m : average neutron spectrum, i.e., $\chi^m = \chi_p^m \cdot (1-\beta^m) + \sum_i \chi_{d,i}^m \beta_i^m$

β^m : total β for isotope m, i.e., $\beta^m = \sum_i \beta_i^m$

ϕ, ϕ^* : neutron direct and adjoint fluxes,

Σ_f^m : macroscopic fission cross section of fuel isotope m

$\vec{r}$: spatial position,

D_p : perturbation denominator.

In the present work, the first order approximation is adopted by omitting the energy dependence of the delayed neutron yield, i.e.,

$$\nu_d^m \cong \nu_d^{m0} \tag{5}$$

and the effect of the energy dependence is treated as a separate term of systematical error.

By using the approximation Eq.(5), $\left[\beta_i \gamma_i \right]^m$ defined by Eq.(2) takes a simplified form as the result of variable separation,

$$\left[\beta_i \gamma_i \right]^m \cong \nu_{d,i}^{m0} \cdot \frac{\gamma_i^m}{D_p} \tag{6}$$

where the factor γ_i^m is defined by

$$\gamma_i^m = \int_V \int_{E'} \chi_{d,i}^m(E') \phi^*(E', \vec{r}) dE' \int_E \Sigma_f^m \phi(E, \vec{r}) dE dV \tag{7}$$

The γ_i^m has the same dimensions as the perturbation denominator (D_p) defined by Eq.(3) and means the fractional importance of the delayed neutrons relative to whole (prompt and delayed) neutrons in a reactor as implied by the second term of the right-hand side of Eq.(6). The component β_i^m is defined by,

$$\beta_i^m = \frac{\nu_{d,i}^m}{\nu^m} \tag{8}$$

Finally, the effective delayed neutron fraction β_{eff} can be expressed as a linear sum of fuel isotope m and family i components $\left[\beta_i \gamma_i \right]^m$ as follows,

$$\beta_{eff} = \frac{\sum_{m=1}^{M} \sum_{i=1}^{I} \nu_i^m \gamma_i^m}{D_p} \tag{9}$$

where M and I ($\cong 6$) indicate the numbers of fuel isotopes and delayed neutron families. By using this simplified expression, the error of β_{eff} due to errors of delayed neutron parameters can be expressed in terms of several error sources as,

$$\frac{\delta\beta_{eff}}{\beta_{eff}} = -\frac{\delta D_p}{D_p} + \frac{\sum_{m=1}^{M} \sum_{i=1}^{6} \left\{ \frac{\delta\nu_{d,i}^m}{\nu_{d,i}^m} + \frac{\delta\gamma_i^m}{\gamma_i^m} \right\} \cdot \nu_{d,i}^m \gamma_i^m}{\sum_{m=1}^{M} \sum_{i=1}^{6} \nu_{d,i}^m \gamma_i^m} \tag{10}$$

The sensitivity coefficient $S_{\nu_{d,i}^m}^{\beta_{eff}}$ of β_{eff} with respect to the change of delayed neutron yield $\nu_{d,i}^m$ can be defined by,

$$S_{\nu_{d,i}^m}^{\beta_{eff}} = \frac{\nu_{d,i}^m}{\beta_{eff}} \cdot \frac{\partial\beta_{eff}}{\partial\nu_{d,i}^m} = \frac{\nu_{d,i}^m \gamma_i^m}{\sum_{m=1}^{M} \sum_{i=1}^{6} \nu_{d,i}^m \gamma_i^m} \tag{11}$$

This implies that the sensitivity coefficient is the fractional contribution of $\nu_{d,i}^m$ to β_{eff} and can be obtained as a part of the calculated β_{eff} -values.

The error of $\nu_{d,i}^m$ is the sum of errors due to total delayed neutron yield ν_d^m and due to the fractional delayed neutron yield $a_{d,i}^m$; i.e.,

$$\nu_{d,i}^m = \nu_d^m \cdot a_{d,i}^m \tag{12}$$

Therefore

$$\frac{\delta\nu_{d,i}^m}{\nu_{d,i}^m} = \frac{\delta\nu_d^m}{\nu_d^m} + \frac{\delta a_{d,i}^m}{a_{d,i}^m} \tag{13}$$

The error components $\delta a_{d,i}^m / a_{d,i}^m$ and $\delta\lambda_i^m / \lambda_i^m$ are taken from the recommended values by Tuttle, shown in Table Rev.-A1, respectively. Since the family sum of $a_{d,i}^m$ (i=1 to 6) is unity, the error $\delta a_{d,i}^m / a_{d,i}^m$ has an anti-correlation with the other terms, $\delta a_{d,j}^m / a_{d,j}^m$ ($i \neq j$). However, the anti-correlation is omitted and thus the resultant error tends to be overestimated, which is preferred from a statistical viewpoint.

The statistical error of β_{eff}, denoted by $\delta\beta_{eff}/\beta_{eff}$, as functions of generalized parameters $\chi_{d,i}^{m}$ of delayed neutron parameters and fission cross sections is estimated by the error propagation law as,

$$\frac{\delta\beta_{eff}}{\beta_{eff}} = \sqrt{\sum_{m}\sum_{i}\left\{W_{d,i}^{m}\cdot S_{x_{d,i}^{m}}^{\beta_{eff}}\cdot\left(\frac{\delta x_{d,i}^{m}}{x_{d,i}^{m}}\right)\right\}^{2}} + \left(\frac{\delta\beta_{eff}}{\beta_{eff}}\right)^{St.} \tag{14}$$

where the mutual correlation, i.e. the off-diagonal term in the covariance matrix in the assemblage $\chi_{d,i}^{m}$ of all delayed neutron related quantities , is neglected. When there are some systematic errors $\left(\delta\beta_{eff}/\beta_{eff}\right)^{St}$, the total error of β_{eff} is decreased or increased by the amount of the systematic errors depending on their statistical natures as shown by the second term in the right-hand side of Eq.(14). Uncertainties due to calculational methods are generally systematic errors which do not obey a normal distribution of errors. The weight $W_{d,i}^{m}$ defined by the fractional contribution $\left[\beta_i\gamma_i\right]^{m}$ to β_{eff} is introduced for the uncertainty due to the fission cross section (discussed in Section II.4), while the magnitudes for the basic delayed neutron parameters discussed in this section are unity since their weights are automatically introduced into the second term of Eq.(10).

The error of the perturbation denominator D_p is mainly due to uncertainties of the fission cross sections as discussed in Section II.4 of the original paper. Strictly speaking, it is also a function of the prompt neutron spectrum as well as neutron and adjoint fluxes, and a feed-back loop must be made between the changes of cross section and fluxes in the outer iteration of the flux calculation. Therefore, generalized perturbation theory is unavoidable for such a feedback effect as used in II.4.

Using the same approach as for β_{eff}, the error evaluation formula of reactivity worth ρ for a step insertion of reactivity as a function of period T can be obtained. The final forms are shown below,

$$\rho = \rho_p + \sum_{m=1}^{M}\sum_{i=1}^{I}\rho_i^m \tag{15}$$

$$\frac{\delta\rho}{\rho} = \frac{\rho_p}{\rho}\cdot\left(\frac{\delta l_p}{l_p} - \frac{\delta k}{k} - \frac{\delta T}{T}\right) + \frac{\sum_{m=1}^{M}\sum_{i=1}^{6}\left\{-\frac{\delta D_p}{D_p} + \frac{\delta\nu_{d,i}^{m}}{\nu_{d,i}^{m}} + \frac{\delta\gamma_i^m}{\gamma_i^m} - \frac{\lambda_i^m T}{1+\lambda_i^m T}\cdot\left(\frac{\delta\lambda_i^m}{\lambda_i^m} + \frac{\delta T}{T}\right)\right\}\cdot\rho_i^m}{\rho_p + \sum_{m=1}^{M}\sum_{i=1}^{6}\rho_i^m} \tag{16}$$

$$\rho_p = \frac{l_p}{\kappa T} \tag{17}$$

$$\rho_i^m = \frac{\gamma_i^m\beta_i^m}{1+\lambda_i^m T} \tag{18}$$

where the newly introduced parameters have the following meanings:

K : effective multiplication factor,
l_p : prompt neutron life-time (s),

λ_i^m : decay constant of fuel element m and family i (s^{-1}),
T : reactor period (s),
ρ_p : reactivity worth component for prompt neutrons,
ρ_i^m : reactivity worth component for fuel isotope m and family i.

The sensitivity coefficient for the reactivity worth ρ with respect to the variation of the delayed neutron parameters can also be obtained. The uncertainty of ρ is evaluated in Section IV in comparison with that of β_{eff} .

The resulting β_{eff} of the MONJU full core including blankets is 0.3446% for Tuttle delayed neutron data, while those for Smith-Tomlinson and JEFF-3 are 0.34082% and 0.34692%, respectively. Considering the difference of cores of interest, reasonable agreement is obtained.

The evaluated β_{eff} uncertainty and the percentage contribution of each error source is shown in Table Rev-A2:

Therefore, the uncertainty of β_{eff} due to all sources of errors expected is about ±5.2% which agrees fairly well with the figure adopted in the present document.

The uncertainty of reactivity ρ is shown in Figure Rev-A1 as function of period, whose magnitude shown by "(10) Overall Statistical Treatment" is about 3% around 70 sec of period and decreasing with period. The "increase of reactivity of 3.3%" relative to the earlier Stevenson/FGL data described above is in the range of the uncertainty.

As mentioned previously, the delayed neutron data have been re-evaluated and recommended data will be released. General reactivity experimental data including the present MOZART Data will be obliged to be up-dated to take account of the advances of delayed neutron data. Then, the basic information such as the period data are required to up-date the reactivity scale. The Tables giving the periods used are very important since as shown in Eqs.(15), (17) and (18) the reactivity can be up-dated if the periods are known.

Table Rev.-A1 Comparison of evaluated delayed neutron data.

Fuel Element	Family No	Tuttle		Smith-Tomlinson		Keepin	
		a_{di}	λ_i	a_{di}	λ_i	a_{di}	λ_i
^{235}U	1	0.038 ±0.004	0.017 ±0.0003	0.038	0.0127	0.086 ±0.003	0.0126 ±0.0002
	2	0.213 ±0.007	0.0317 ±0.0012	0.213	0.0317	0.299 ±0.004	0.0337 ±0.0006
	3	0.188 ±0.024	0.115 ±0.004	0.188	0.0115	0.252 ±0.040	0.139 ±0.0006
	4	0.407 ±0.010	0.311 ±0.012	0.407	0.311	0.278 ±0.020	0.325 ±0.030
	5	0.128 ±0.012	1.40 ±0.12	0.128	1.41	0.051 ±0.024	1.13 ±0.40
	6	0.026 ±0.004	3.84 ±0.55	0.026	3.87	0.034 ±0.014	2.50 ±0.42
^{238}U	1	0.013 ±0.001	0.0132 ±0.0004	0.013	0.0132	0.033 ±0.003	0.0124 ±0.0003
	2	0.137 ±0.003	0.0321 ±0.0009	0.137	0.0321	0.219 ±0.009	0.0305 ±0.0010
	3	0.162 ±0.030	0.139 ±0.007	0.162	0.139	0.196 ±0.022	0.111 ±0.004
	4	0.388 ±0.018	0.358 ±0.021	0.388	0.358	0.395 ±0.011	0.301 ±0.012
	5	0.225 ±0.019	1.41 ±0.10	0.225	1.41	0.115 ±0.009	1.13 ±0.15
	6	0.075 ±0.007	4.02 ±0.32	0.075	4.02	0.042 ±0.008	3.00 ±0.33
^{239}Pu	1	0.038 ±0.004	0.129 ±0.0003	0.038	0.0129	0.035 ±0.009	0.0128 ±0.0005
	2	0.280 ±0.006	0.0311 ±0.0007	0.280	0.0311	0.298 ±0.035	0.0301 ±0.0022
	3	0.216 ±0.027	0.134 ±0.004	0.216	0.134	0.211 ±0.048	0.124 ±0.009
	4	0.328 ±0.015	0.331 ±0.018	0.329	0.331	0.326 ±0.033	0.325 ±0.036
	5	0.103 ±0.013	1.26 ±0.17	0.103	1.26	0.086 ±0.029	1.12 ±0.39
	6	0.035 ±0.007	3.21 ±0.38	0.035	3.21	0.044 ±0.016	2.69 ±0.47
^{240}Pu	1	0.028 ±0.004	0.0129 ±0.0005	0.025	0.0129		
	2	0.273 ±0.006	0.0313 ±0.0007	0.270	0.0313		
	3	0.192 ±0.078	0.135 ±0.016	0.184	0.135		
	4	0.350 ±0.030	0.333 ±0.046	0.358	0.333		
	5	0.128 ±0.027	1.36 ±0.30	0.135	1.36		
	6	0.029 ±0.009	4.04 ±1.16	0.027	4.04		
^{241}Pu	1	0.010 ±0.003	0.0128 ±0.0002	0.010	0.0128		
	2	0.229 ±0.006	0.0299 ±0.0006	0.229	0.0299		
	3	0.173 ±0.025	0.124 ±0.013	0.173	0.124		
	4	0.390 ±0.050	0.352 ±0.018	0.390	0.352		
	5	0.182 ±0.019	1.61 ±0.15	0.182	1.61		
	6	0.016 ±0.005	3.47 ±1.1	0.016	3.47		
^{242}Pu	1	0.004 ±0.001	0.0128 ±0.0003	0.004	0.0129		
	2	0.195 ±0.032	0.0314 ±0.0013	0.195	0.0295		
	3	0.161 ±0.048	0.128 ±0.009	0.162	0.131		
	4	0.412 ±0.153	0.325 ±0.020	0.411	0.338		
	5	0.218 ±0.037	1.35 ±0.09	0.218	1.39		
	6	0.010 ±0.003	3.70 ±0.44	0.010	3.65		

a_{di} and λ_i : Fractional yield and decay constant, respectively.
Tuttle : Tuttle, R.J. Nucl Sci Eng., **56**, 37 (1975)
Smith-Tomlinson: Cited from the Table in Section 2.4 of the present work (Part 2)
Keepin : Keepin, G.R., Wimett, T.F. and Ziegler, R.K., Phys. Rev. **107**, 1044 (1957)

Table Rev.-A2 Evaluated β_{eff} uncertainty and the percentage contribution of each error source.

Item	Error source		Method-1[i]		Method-2	
			Stat.	Syst.	Stat.	Syst.
(1)	$\nu_{d,i}$ error		±2.5		±2.5	
(2)	ν_d energy dependence			+1.4		+1.7
(3)	Fission cross section		±1.6		±1.6	
(4)	Reaction rate ratio		±0.1		±0.1	
(5)	χ_d choice		±0.5		±0.5	
(6)	Transport effect[ii]	(a)		-0.3		-0.3
		(b)		0.0		0.0
(7)	Energy group effect	(a)	0.0[iii]		0.0	
		(b)	±1.3		±1.3	
(8)	Control rod effect	(a)	0.0		±0.03[iv]	
		(b)	0.0		±1.1[v]	
(9)	Cell homogenization		0.0		±0.3[v]	
	Statistical treatment					
(A-1)	Simple sum	(a)	±4.7	+1.0	±5.0	+1.4
		(b)	±6.0	+1.4	±7.4	+1.7
(A-2)	Overall simple sum[vi]	(a)	±5.7		±6.4	
		(b)	±7.4		±9.1	
(B)	Overall statistical sum	(a)	±3.3		±3.5	
		(b)	±3.6		±3.9	
(C)	Statistical sum	(a)	±3.0	+1.0	±3.0	+1.4
		(b)	±3.3	+1.4	±3.5	+1.7
(D)	Overall uncertainty	(a)	±4.0[vii]		±4.4[viii]	
		(b)	±4.7[vii]		±5.2[viii]	

i) Method-1 has a smaller ν dm energy dependence and no items (8) and (9) which are considered in Method-2. "Stat." abd "Syst." stand for statistical (random) error and systematical error, respectively.
ii) Treated as systematical error.
iii) For number of energy groups larger than 18. The ±1.2% of (b) for 6 group calculation.
iv) For fully inserted central control rod
v) From Ref.(5)
vi) Extreme case when all errors additionally contribute
vii) (a) does not have the energy group effect (7), but (b) has the 1.2% energy group effect.
viii) (a) does not have the energy group (7) and control rod (8) effects, but (b) has both effects.

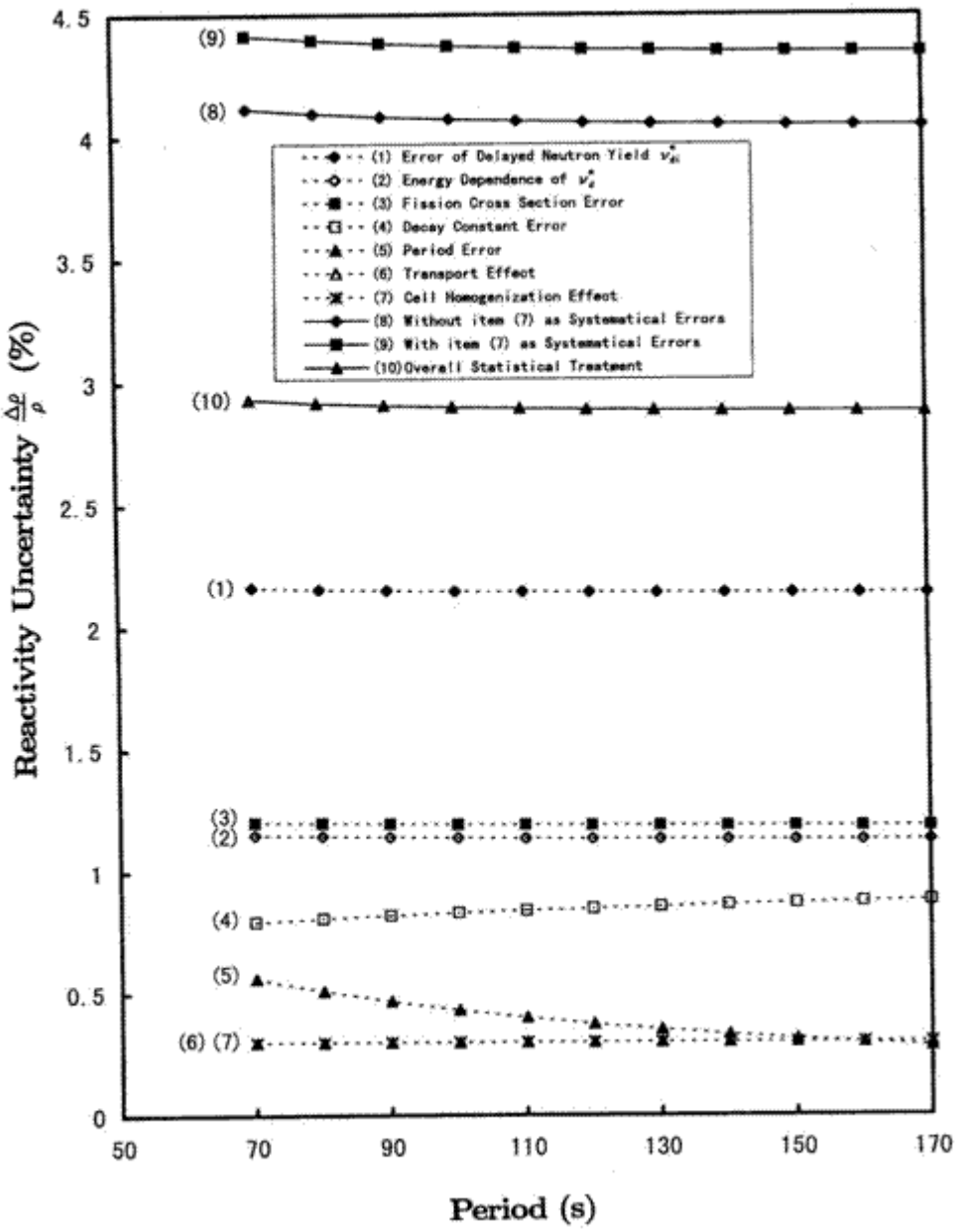

Figure Rev.- A1. Uncertainties of reactivity ρ and its components as a function of reactor period.

2.5 Evaluation of Reactivity Coefficient Data

There were no reactivity coefficient measurements

2.6 Evaluation of Kinetics Data

No kinetics measurements were made, other than the period measurements used to calibrate the reactivity scale.

2.7 Evaluation of Reaction Rate Distributions

Measurements are made both in the assembly as a whole (for both single rods and arrays of rods) and within the rings of absorber pins in a rod.

The sources of uncertainty are summarised in Section 1.7. A detailed description of the sources of experimental uncertainties can be found in the MTN documents referenced in Section 1.7 (namely MTN/97 for the foil measurements and MTN/89 for the fission chamber measurements; these documents also refer to other MTNs for aspects of the measurements). The magnitude of the experimental uncertainties associated with the measurements is given in the Tables.

A particular problem concerning the axial measurements must be noted. Firstly, for their accurate interpretation account must be taken of the absorber sections of the Zebra control rods in the upper axial blanket area and the axial asymmetry of the core cells. Also the alignment between the elements in which the chamber measurements were made and the neighbouring elements must be noted. This necessitated an adjustment to the axial positions of the measurements when comparing with calculation.

There was a problem with one of the radial fission chamber scan measurements, the Pu239 radial fission chamber measurement in the BN/2(P1,P3,P5) case. The radial position appeared to be incorrect and it was adjusted by 2 cm.

By intercomparing the foil, SSTR (Tables 1.38 and 1.39) and fission chamber scan measurements (Table 1.47) (and also the C/E values in the MTN documentation, MTN/93 and /100) it can be seen that the measurements are consistent.

The reaction rate scan measurements given in Tables 1.31 to 1.36 and Tables 1.40 to 1.46 are recommended as benchmark measurements to be used in conjunction with the rod worth measurements.

2.8 Evaluation of Power Distribution Measurements

There were no power distribution measurements.

2.9 Evaluation of Isotopic Measurements

No isotopic measurements were performed.

2.10 Evaluation of Other Miscellaneous Types of Measurements

Note the measurement of the tantalum (n,γ) reaction rate relative to the U235 fission rate described in Section 1.7.

3. BENCHMARK SPECIFICATIONS

3.1 Critical or Subcritical Configuration Benchmark Specifications

(The Mozart Programme criticality benchmark models are detailed in ZEBRA-LMFR-EXP-002).

3.2 Benchmark-Model Specifications for Buckling and Extrapolation Length Measurements

(see ZEBRA-LMFR-EXP-002 for the measurements made in MZA)

3.3 Benchmark-Model Specifications for Spectral Characteristics Measurements

(see ZEBRA-LMFR-EXP-002 for the measurements made in MZA and MZB)

3.4 Benchmark-Model Specification for Reactivity Effects Measurements

3.4.1 Description of the Calculational Methodology and Model

Notes on the Calculational Methods to be used

The control rod reactivity worths are to be derived from the criticality calculations for the cores with and without the control rods (or followers) and with the number of additional outer core edge elements chosen appropriately, as given in Tables 1.13 to 1.18. The Zebra control rods are not modelled in the calculations, these being replaced by standard core elements in the models (as described for criticality calculations in ZEBRA-LMFR-EXP-002). The calculations use 3D XYZ geometry models with the XY plan geometry cells of the models occupied by inner core, outer core, radial blanket or reflector elements which are described in detail in Section 3.1 of ZEBRA-LMFR-EXP-002. Different modelling approximations are described there, in particular the models which represent the 5x5 element super-lattice structure and the approximation to this which uses a regular lattice structure.

The preparation of the macroscopic cross-sections for the control rods should preferably take into account the individual pin structure of the rods. Using the cylindrical model of the rod introduces errors ranging from about 1.3% for the BN rod to 3% for the B80 rod (MTN/98). The resonance shielding calculation for the tantalum rod should also be done at the individual pin level; using the cylindrical model results in an overestimate of rod worth by about 4.5%. If the whole reactor calculation involves the homogenisation of the control rod regions advanced homogenisation methods should be used, and not simple flux averaging of region cross-sections.

Three dimensional XYZ geometry transport theory should be used for the whole reactor calculations. It is shown in MTN/85 that diffusion theory can introduce errors in the reactivity worth of the follower of 8% unless a special treatment of the low density channel, such as direction dependent diffusion coefficients, calculated using a transport theory method which treats the streaming effects, is used. The overestimate of the absorber rod worth can be up to about 6% if simple homogenisation methods are used.

The Models

The basic model is the 3D XYZ criticality model of MZB described in ZEBRA-LMFR-EXP-002, Section 3.1 with the addition of the extra outer core elements, as indicated, for the particular array, using the data for these elements as given in ZEBRA-LMFR-EXP-002. In the present document only

the details of the Mock-up Control Rods to be used in conjunction with this model are given. In Appendix A an XYZ geometry MONK input is given which can be used as a guide to setting up models.

Cylindrical models of the rods are also given here and these can be used together with the cylindrical criticality models given in ZEBRA-LMFR-EXP-002, Section 3.1, to treat a Mock-up rod at the core centre, but the accuracy of these has not been assessed (but see MTN/98 for an indication of the approximations involved).

Finally a MONK Monte Carlo model of a rod is given in this section because this provides the data in a form more convenient for some applications and shows the angular orientation of the pins in the rings of 6 and 12.

Mock-up Control rod Compositions and Dimensions

More details of the compositions and dimensions of the (MONJU) Mock-up Control Rods than are given in Sections 1.4.2 and 3 (and the associated Appendix) are given in MTN/39 and the Supplement, from which the following data have been abstracted. The compositional data used in the original Winfrith analyses, and also adopted here, are those given in MTN/51.

As described in Section 1.4.2, the following modelling approximations are made:

The outer square tube of the calandria is combined with the control rod sheath and the calandria tubes are combined with the cans of absorber pins (when these are canned). The outer dimension of the combined region of sheath plus calandria walls is taken to be 10.7442 cm the width of the 4x4 lattice area which the mock-up rods occupy, that is, 2x5.3721cm, the lattice spacing within the groups of 5x5 elements).
The end regions are treated as uniform plates and the dimples are treated as uniform additions to the steel of the calandria walls.
The wide tube in the calandria is treated as a uniform cylinder (without the slots)
The bosses are not represented.
The corresponding Followers differ in that the absorber pins and calandria tubes are replaced by sodium.

The B80/90 Follower is assumed to be a solid aluminium region, 10.2 cm x 10.2 cm x 91.36 cm, volume 9505.09cm^3, having the combined weight of 25.433 kg (density 2.6757 g/cm^3). The outer width is assumed to be 10.7442 cm and inner width 10.2 cm, thus eliminating the gaps.

3.4.2 Dimensions

Detailed Model of the Monju Mock-up Control Rod and Follower.

Calandria per control rod
The absorber element in a simulation of a "fully inserted" control rod, has a height of 91.44 cm. Above and below are Follower elements. These Follower elements, occupying the upper and lower axial blanket regions, have a height of 35.56 cm. Above and below the follower regions are plenum regions of height 33.0048 cm. The overall height of the region to be modelled is therefore:

91.44 +2*(35.56 +33.0048) = 228.5696 cm

The end plate regions at the two ends of the absorber and follower calandria have a thickness of 0.47 cm and so the components within have a correspondingly reduced height of 90.50 cm (and 34.62 cm in the case of the followers in the upper and lower blanket regions).

The components of a rod follower are similar but the central calandria contains no absorber pins or calandria tubes. The weights of steel in the calandria walls and inner cylinder of a follower element are also slightly different.

The Calandria Walls plus the Sheath.
In the calculational model the outer wall of the mini-calandria is combined with the control rod sheath to form a square section region of steel of outer width 10.7442 cm (twice the lattice spacing of 5.3721 cm within a group of 5x5 positions in the superlattice) and inner width 9.86 cm, and height 90.5 cm. Above and below this is the end-plate region of thickness 0.47 cm making a total height of 90.5 + 2x0.47 cm = 91.44 cm.

The Inner Cylinder.
Inside this outer square section region is the Inner Cylinder having outer diameter 9.845 cm, inner diameter 9.025 cm, and height = 90.50 cm.

(The heights are reduced correspondingly in the shorter length Follower Elements)

Calandria Tubes + Cans and the absorber regions
The arrangement of the absorber pins is illustrated in Figure 1.1A. In the case of the boron absorber pins the calandria tubes are combined with the cans of the boron pins. The outer diameter of the calandria tubes is l.55 cm, and inner diameter assumed for the boron cans 1.1 cm, height 90.5 cm
The boron absorber regions have a diameter of 1.1 cm and length 90.5 cm.
The inner diameter assumed for tantalum tubes is 1.31 cm, Height 90.5 cm.
The tantalum pins have a diameter of 1.31 cm.
The centres of the Ring of 6 tubes are on the Diameter of 3.58 cm and the Ring of 12 are on the Diameter of 6.92 cm. The Ring of 6 is rotated so that the centre of the first tube is on a line at 45^{o} relative to the positive x-axis whereas the Ring of 12 has the centre of the first tube on the x-axis.
The End plate regions
These are square section slabs which fit to the top and bottom of the calandria walls plus sheath. The Inner Cylinder and Boron Absorber Pins and Calandria Tubes also fit between them. Dimensions 10.7442 cm x 10.7442 cm x 0.47 cm.
When combined with the other components they form a square section region of length 91.44 cm.

The B80/B90 Rods

The Cans of the Pins in the B80/B90 Rods

The B80 pins in the B80/B90 rods have cans with outer diameter 1.31 cm, inner diameter 1.1 cm, and the B90 pins have cans with an outer diameter of 1.27 cm, inner diameter 1.1 cm.

The Sheath for the B80/90 Rod

In the case of the B80/90 Element the sheath is smeared over the area between the aluminium block and the lattice boundary, outer width 10.7442 cm, inner width 10.2 cm, area 11.3978 cm^2 and the height is 91.36 cm. There are end-plate regions only above and below the absorber pins.

The Aluminium Block containing the cluster of boron pins has a square outer boundary of width 10.2 cm, and an inner circular boundary of diameter 9.0 cm. The height of the block is 91.36 cm. There are no end-plate regions above and below the aluminium, only above and below the absorber regions.

The Pin Cluster in the B80/90 rod.

This is treated as two concentric cylindrical regions of boron plus steel (an inner region of 19 B90 pins, diameter 6.38 cm (the model specified in MTN79), and an outer region of 18 B80 pins, diameter 9.0 cm) with steel "end-plate" regions at the top and bottom. The length of the absorber section of the pin cluster is the length of the column of boron pellets, 90.5 cm. Above and below are cylindrical steel end-plate regions of diameter 9.0 cm and thickness 0.43 cm making a total height of 91.36 cm.

Cylindrical Model of the Control Rods.

In this simplified model the array of absorber pins is homogenised within the circle surrounding the array. In MTN/98 comparisons were made between rod worths calculated using the PIJ pin cluster geometry collision probability code to represent the individual pins and a cylindrical model. The simplified model gave reactivity worths larger by 1.3% for the BN rod and 3% larger for the B80 rod. These possible corrections have not been evaluated in the present document. This simplified model is included because it could be used to derive condensed cross-section sets for use in a more detailed geometrical representation or to assess the effects of changing nuclear data or reactor parameters.

In the case of the BN, B30, B60, B80, B90 and Ta rods the diameter of the cylinder containing the absorber pins is taken to be equal to the diameter of the centres of the outer ring of pins, plus the diameter of the steel calandria tubes, (6.92 + 1.55) cm = 8.47 cm, an area of 56.3452 cm^2 (this being the model also adopted in the original Winfrith analysis). The weighting of the constituent materials is proportional to their areas.
For the boron absorbers the region weights are:
Boron carbide region region weighting factor = 18.0563/56.3452 = 0.32046
Tubes plus canning region weighting factor = 17.7952/56.3452 = 0.31582
Sodium = 20.4937/56.3452 = 0.36372
For the tantalum absorbers the region weights are:
Tantalum region weighting factor = 25.6086/56.3452 = 0.45449
Tubes region weighting factor = 10.2429/56.3452 = 0.18179
Sodium region weighting factor = 0.36372

If the square outer boundary is also cylindricalised it is done so as to preserve areas (and hence the weights of the materials), the inner diameter being 11.1258 cm and outer diameter 12.1235 cm.

For the B80/90 absorber the dimensions and region weights are as follows:
The dimensions adopted in the original analysis of the experiments are given in MTN/79 and are radii of 3.19 cm and 4.5 cm for the inner group of 19 B90 pins and outer ring of 18 B80 pins. These are

areas of 31.9692 cm^2 and 31.6481 cm^2 into which the 19 B90 pins and 18 B80 pins are to be smeared. The region weighting factors used to calculate the atomic densities for the homogenised regions are as follows:

Inner region

B90 absorber region weighting factor = 18.0563/31.9692 = 0.56480

Canning region weighting factor = 6.01230/31.9692 = 0.18807; density = 4.794 g/cm^3

smeared density = 0.9016 g/cm^3

Outer region

B80 absorber region weighting factor = 17.1060/31.6481 = 0.54051

Canning region weighting factor = 7.15482 /31.6481 = 0.22607 density = 7.6633 g/cm^3

smeared density = 1.7324 g/cm^3

The Geometrical Model of the Rods used in the MONK Monte Carlo Calculations

This information, although relating to the way the data are specified for this particular Monte Carlo code, describes the positions of the absorber pins in the array, in terms of radius and angular offset.

The Absorber Calandria

The rings of pins, and enclosing cylinder, can be represented using a "Hole Routine". The "Hole Region" is placed within the square box representing the calandria walls and enclosing sheath.

PART XXX NEST

* The inner cylinder and array of pins is represented by a "hole", BH1

ZROD BH1 0.0 0.0 -45.25 4.9225 90.5

(That is, a cylinder with axis in the z direction and

origin of the axis at (x,y,z) = (0.0,0.0,-45.25 cm) and with radius 4.9225 cm, height 90.5 cm)

* The sodium between the cylinder and the calandria walls

BOX Mat4 -4.93 -4.93 -45.25 9.86 9.86 90.5

(that is, a box, containing the material Mat4, with coordinates of the corner which has the lowest values of (x,y,z) = (-4.93,-4.93,-45.25) and dimensions (dx,dy,dz) = (9.86,9.86,90.5))

* The side walls of the calandria

BOX Mat5 -5.3721 -5.3721 -45.25 10.744210.744290.5

* The end plates of the Calandria

BOX Mat6 -5.3721 -5.3721 -45.72 10.744210.744291.44

BEGIN HOLE DATA

* Array of absorber pins in a stainless steel cylinder

GLOBE

5 ! number of cylindrical regions

4.9225 Mat1 ! outer radius of cylinder and Material number of Cylinder

4.5125 SUB ! inner radius of cylinder . Array of subunits is to follow

12 ! 12 equally spaced pins

1 ! no angular offset

3.46 ! radius of circle location of the centres of the pins

Mat 2 Mat3 ! material numbers of the pin constituents, tube+can and boron

0.775 0.55 ! outer radius of pin tube and radius of boron absorber

* Note, the radius of the Ta absorber pin is 0.655 cm

2.625 SUB ! radius separating the ring of 12 and ring of 6

6 ! 6 equally spaced pins

1.5 ! angular offset of 45^{o}

1.79 ! radius of circle location of the centres of the pins

Mat 2 Mat3 ! material numbers of the pin constituents, tube+can and boron

0.775 0.55 ! outer radius of pin tube and radius of boron absorber

0.775 Mat2 ! outer radius of tube containing the central pin, Mat number

0.55 Mat3 ! outer radius of absorber region of pin

Mat 4 ! the sodium filling the calandria

The Follower Calandria having the same length as the Absorber Calandria
PART YYY NEST

* The sodium within the Cylinder

ZROD Mat4 0.0 0.0 -45.25 4.5125 90.5

* the steel of the Cylinder, a slightly different composition from that of the Absorber

ZROD Mat1 0.0 0.0 -45.25 4.9225 90.5

* The sodium between the cylinder and the calandria walls

BOX Mat4 -4.93 -4.93 -45.25 9.86 9.86 90.5

* The side walls of the calandria

BOX Mat5 -5.3721 -5.3721 -45.25 10.744210.744290.5

* The end plates of the Calandria

BOX Mat6 -5.3721 -5.3721 -45.72 10.744210.744291.44

In the case of the smaller calandria occupying the upper and lower axial blanket regions the overall height is 35.56 cm (half height 17.78 cm) and the height between the end plates is 34.62 cm (half height, 17.31cm).

PART ZZZ NEST

* The sodium within the Cylinder

ZROD Mat4 0.0 0.0 -17.31 4.5125 34.62

* the steel of the Cylinder, a slightly different composition from that of the Absorber

ZROD Mat1 0.0 0.0 -17.31 4.9225 34.62

* The sodium between the cylinder and the calandria walls

BOX Mat4 -4.93 -4.93 -17.31 9.86 9.86 34.62

* The side walls of the calandria

BOX Mat5 -5.3721 -5.3721 -17.31 10.744210.744234.62

* The end plates of the Calandria

BOX Mat6 -5.3721 -5.3721 -17.78 10.744210.744235.56

Plenum regions

Above and below the follower regions are plenum regions of height 33.0048 cm. The overall height of the assembly is therefore: 91.44 +2*(35.56 +33.0048) = 228.5696 cm

In the MONK model the overall height is 230 cm and so steel "packing pieces" of width 0.7152 cm are included in the model at either end.

3.4.3 Material Data

Atomic Densities are in units of Atoms/barn.cm, weights in g and densities in g/cm^3. Areas are in cm^2. Weights associated with an area are the weights per unit length, in g/cm.

Table 3.1 Dimensions and Atomic Densities of the Control Rod and Follower Components.
Stainless Steel Regions
Outer square region: Outer width = 10.7442 cm, Inner width = 9.86 cm, Height = 90.5 cm.
Inner Cylinder: Outer diameter 9.845 cm, Inner diameter of 9.025 cm, Height = 90.5 cm
(The heights are reduced correspondingly in the shorter length Follower Elements)

In the case of the B80/90 element the sheath is smeared over the area between the aluminium block and the lattice boundary, inner width 10.2 cm, area 11.3978 cm^2.

	Outer Square region			Inner Cylinder	
	For an Absorber	For a Follower	B80/90 sheath	For an Absorber	For a Follower
Weight	71.0155	71.683	23.1281	98.0309	99.1729
Area	18.2182	18.2182	11.3978	12.1528	12.1528
Density	3.89805	3.93469	2.02917	8.06653	8.16050
C	5.8633E-05	5.9184E-05	3.0522E-05	1.2133E-04	1.2275E-04
Si	4.0956E-04	4.1341E-04	2.1320E-04	8.4752E-04	8.5740E-04
P31	1.5916E-05	1.6065E-05	8.2850E-06	3.2935E-05	3.3319E-05
S	1.0980E-05	1.1083E-05	5.7156E-06	2.2721E-05	2.2986E-05
Cr	8.6863E-03	8.7679E-03	4.5217E-03	1.7975E-02	1.8185E-02
Mn55	7.4349E-04	7.5048E-04	3.8703E-04	1.5386E-03	1.5565E-03
Fe	2.8526E-02	2.8794E-02	1.4849E-02	5.9031E-02	5.9718E-02
Ni	4.2398E-03	4.2796E-03	2.2070E-03	8.7736E-03	8.8758E-03
Total	4.2690E-02	4.3092E-02	2.2223E-02	8.8343E-02	8.9372E-02

Table 3.2 Calandria Tubes + Cans

Atomic Densities are in units of Atoms/barn.cm, weights in g and densities in g/cm^3. Areas are in cm^2. Weights associated with an area are the weights per unit length, in g/cm.

Outer diameter of tube = l.55 cm, Inner diameter assumed for the boron cans 1.1 cm,
Inner diameter assumed for tantalum tubes = 1.31 cm: Height 90.5 cm.
The B80 pins in the B80/B90 rod have cans with outer diameter = 1.31 cm and the B90 cans have an outer diameter of 1.27 cm.

	BN,B30,B80 tubes+cans	B80 cans	TA tubes
Weight	126.8347		68.9589
Area	17.7952		10.2429
Density	7.12748	7.6633	6.73237
C	1.0721E-04	1.1527E-04	1.0127E-04
Si	7.4886E-04	8.0516E-04	7.0735E-04
P31	2.9101E-05	3.1289E-05	2.7488E-05
S	2.0076E-05	2.1585E-05	1.8963E-05
Cr	1.5883E-02	1.7077E-02	1.5002E-02
Mn55	1.3595E-03	1.4617E-03	1.2841E-03
Fe	5.2159E-02	5.6080E-02	4.9267E-02
Ni	7.7523E-03	8.3351E-03	7.3225E-03
Total	7.8058E-02	8.3926E-02	7.3731E-02

B90 Tubes and Canning

	B90 tube+can	B90 cans
Weight	97.7819	28.823
Area	17.7952	6.0123
Density	5.49485	4.794
C	9.8895E-05	1.2019E-04
Si	5.7729E-04	5.0358E-04
P31	2.5239E-05	2.7873E-05
S	1.4562E-05	1.0794E-05
Cr	1.1931E-02	9.7542E-03
Mn55	1.0498E-03	9.1947E-04
Fe	4.0207E-02	3.5069E-02
Ni	6.1328E-03	5.6767E-03
Nb93	7.5582E-05	2.2371E-04
Total:	6.0112E-02	5.2306E-02

Table 3.3 End Plate Regions

Atomic Densities are in units of Atoms/barn.cm, weights in g and densities in g/cm^3. Areas are in cm^2. Weights associated with an area are the weights per unit length, in g/cm.

(Dimensions 10.7442 cm x 10.7442 cm x 0.47 cm)

	BN element	B90 element	TA element
Weight	277.45	265.25	253.14
Volume	54.2558	54.2558	43.5386
Density	5.11374	4.88888	5.81415
C	7.6919E-05	7.3536E-05	8.7454E-05
Si	5.3728E-04	5.1366E-04	6.1087E-04
P31	2.0879E-05	1.9961E-05	2.3739E-05
S	1.4404E-05	1.3771E-05	1.6377E-05
Cr	1.1395E-02	1.0894E-02	1.2956E-02
Mn55	9.7536E-04	9.3247E-04	1.1090E-03
Fe	3.7422E-02	3.5777E-02	4.2548E-02
Ni	7.6919E-05	5.3174E-03	6.3238E-03
Total	5.6004E-02	5.3542E-02	6.3675E-02

Table 3.4 Absorber Regions: Boron Pins

(Diameter = 1.1 cm, length = 90.5 cm)

PIN	BN	B30	B80
Weight	43.8995	43.508	41.9615
Area	18.0563	18.0563	18.0563
Density	2.43126	2.40957	2.32393
B10	2.0915E-02	3.1668E-02	8.5295E-02
B11	8.4684E-02	7.4283E-02	2.1438E-02
C	2.6745E-02	2.6228E-02	2.5669E-02
Fe	2.0962E-05	2.0783E-05	2.0066E-05
Total	1.3237E-01	1.3220E-01	1.3242E-01

PIN	B90
Weight	42.3009
Area	18.0563
Density	2.34272
B10	9.8513E-02
B11	1.0752E-02
C	2.5032E-02
Al27	2.6329E-05
Si	1.0094E-04
Fe	3.3025E-05
Total:	1.3446E-01

Table 3.5 Tantalum Pin

Atomic Densities are in units of Atoms/barn.cm, weights in g and densities in g/cm^3. Areas are in cm^2. Weights associated with an area are the weights per unit length, in g/cm.

(Diameter = 1.31 cm, Length = 91.337 cm, extending into the end-plate regions)

Weight	428.4566
Area	25.6086
Density	16.73097
H	2.5665E-05
N	1.2592E-05
Nb93	5.9659E-05
Ta	5.5637E-02
W	1.3699E-05
Total	5.5748E-02

Table 3.6 Sodium

Weight	44.894
Volume	49.2154
Density	0.91219
O	6.7640E-06
Na23	2.3890E-02
Fe	1.9673E-07
Total	2.3897E-02

Table 3.7 Aluminium regions of the B80/90 Absorber and Follower Elements
Atomic Densities are in units of Atoms/barn.cm, weights in g and densities in g/cm^3. Areas are in cm^2. Weights associated with an area are the weights per unit length, in g/cm.

Outer aluminium region of the B80/90 rod.
Square outer boundary, 10.2 cm x 10.2 cm. Inner circular boundary, diameter 9.0 cm.
The length of the block, 91.36 cm, volume 3693.02 cm^3, weight of aluminium 9.973 kg (density 2.7005 g/cm^3).

Follower region 10.2 cm x 10.2 cm x 91.36 cm, **(**density 2.6757 g/cm3)

	Outer block	Follower
Density	2.7005	2.6757
AL	6.0181E-02	5.9628E-02
SI	5.7905E-06	5.7373E-06
MN	1.1841E-06	1.1732E-06
FE	3.7856E-05	3.7509E-05
CU	2.3033E-06	2.2821E-06
TOTAL	6.0228E-02	5.9675E-02

Table 3.8 Cylindrical Model of the Absorber Region of the B80/B90 Rod (height 90.5 cm)

B80/B90 absorber region (with radii of 3.19 cm and 4.5 cm for Region 1 and Region 2)

	B90 pins Region 1	**B80 pins Region 2**
B10	5.5640E-02	4.6103E-02
B11	6.0727E-03	1.1587E-02
C	1.4161E-02	1.3900E-02
Al27	1.4871E-05	
Si	1.5172E-04	1.8202E-04
P31	5.2419E-06	7.0733E-06
S	2.0300E-06	4.8797E-06
Cr	1.8345E-03	3.8605E-03
Mn55	1.7292E-04	3.3044E-04
Fe	6.6141E-03	1.2689E-02
Ni	1.0676E-03	1.8843E-03
Nb	4.2072E-05	
Total	8.5779E-02	9.0547E-02

(See the Table in MTN/79 for comparison)

Table 3.9 Cylindrical Models of the Control Rods

Atomic Densities are in units of Atoms/barn.cm, weights in g and densities in g/cm^3. Areas are in cm^2. Weights associated with an area are the weights per unit length, in g/cm.

Atomic Densities for the Cylindrical Models of the Boron Rods
The cylindrical region representing the array of calandria tubes containing the absorber pins has diameter = 8.47 cm.

	BN	B30	B80	B90
B10	6.7024E-03	1.0148E-02	2.7334E-02	3.1569E-02
B11	2.7138E-02	2.3805E-02	6.8700E-03	3.4456E-03
C	8.6046E-03	8.4389E-03	8.2597E-03	8.0530E-03
O	2.4602E-06	2.4602E-06	2.4602E-06	2.4602E-06
Na23	8.6893E-03	8.6893E-03	8.6893E-03	8.6893E-03
Al27				8.4374E-06
Si	2.3650E-04	2.3650E-04	2.3650E-04	2.1467E-04
P31	9.1907E-06	9.1907E-06	9.1907E-06	7.9710E-06
S	6.3404E-06	6.3404E-06	6.3404E-06	4.5990E-06
Cr	5.0162E-03	5.0162E-03	5.0162E-03	3.7680E-03
Mn55	4.2936E-04	4.2936E-04	4.2936E-04	3.3155E-04
Fe	1.6480E-02	1.6480E-02	1.6480E-02	1.2709E-02
Ni	2.4483E-03	2.4483E-03	2.4483E-03	1.9369E-03
Nb				2.3870E-05
Total	7.5762E-02	7.5709E-02	7.5780E-02	7.0765E-02

(see Table 3 in MTN/51 for comparison)

Table 3.10 Atomic Densities for the Cylindrical Model of the Tantalum Rod
The cylindrical region containing the tantalum pins has diameter = 8.47 cm

H	1.1664E-05
C	1.8410E-05
N	5.7229E-06
O	2.4602E-06
Na23	8.6893E-03
Si	1.2859E-04
P31	4.9970E-06
S	3.4473E-06
Cr	2.7272E-03
Mn55	2.3344E-04
Fe	8.9563E-03
Ni	1.3312E-03
Nb93	2.7114E-05
Ta	2.5286E-02
W	6.2261E-06
Total	4.7432E-02

(see Table 3 in MTN/51 for comparison)

Atomic Compositions (in atoms/barn.cm) used in the MONK calculations

Table 3.11 Compositions for the BN Absorber Elements

Outer Square Region, Absorber					
C	5.8633E-05	Si	4.0956E-04	P31	1.5916E-05
S	1.0980E-05	Cr	8.6863E-03	Mn55	7.4349E-04
Fe	2.8526E-02	Ni	4.2398E-03		
Cylinder, Absorber					
C	1.2133E-04	Si	8.4752E-04	P31	3.2935E-05
S	2.2721E-05	Cr	1.7975E-02	Mn55	1.5386E-03
Fe	5.9031E-02	Ni	8.7736E-03		
Tube+Cans, BN, B30, B80					
C	1.0721E-04	Si	7.4886E-04	P31	2.9101E-05
S	2.0076E-05	Cr	1.5883E-02	Mn55	1.3595E-03
Fe	5.2159E-02	Ni	7.7523E-03		
Absorber Region, BN					
B10	2.0915E-02	B11	8.4684E-02	C	2.6745E-02
Fe	2.0962E-05				
EndPlate Regions, BN, B30, B80					
C	7.6919E-05	Si	5.3728E-04	P31	2.0879E-05
S	1.4404E-05	Cr	1.1395E-02	Mn55	9.7536E-04
Fe	3.7422E-02	Ni	7.6919E-05		
Sodium					
O	6.7640E-06	Na23	2.3890E-02	Fe	1.9673E-07

Table 3.12 Compositions for the B30, B80 Absorber Elements

Absorber Region, B30			
B10	3.1668E-02	B11	7.4283E-02
C	2.6228E-02	Fe	2.0783E-05
Absorber Region, B80			
B10	8.5295E-02	B11	2.1438E-02
C	2.5669E-02	Fe	2.0066E-05

Table 3.13 Compositions for the B90 Absorber Elements

Tube+Cans, B90					
C	9.8895E-05	Si	5.7729E-04	P31	2.5239E-05
S	1.4562E-05	Cr	1.1931E-02	Mn55	1.0498E-03
Fe	4.0207E-02	Ni	6.1328E-03	Nb93	7.5582E-05
Absorber Region, B90					
B10	9.8513E-02	B11	1.0752E-02	C	2.5032E-02
Al27	2.6329E-05	Si	1.0094E-04	Fe	3.3025E-05
EndPlate Regions, B90					
C	7.3536E-05	Si	5.1366E-04	P31	1.9961E-05
S	1.3771E-05	Cr	1.0894E-02	Mn55	9.3247E-04
Fe	3.5777E-02	Ni	5.3174E-03		

Table 3.14 Compositions for the Tantalum Absorber Elements

Tube+Cans, TA

C	1.0127E-04	Si	7.0735E-04	P31	2.7488E-05
S	1.8963E-05	Cr	1.5002E-02	Mn55	1.2841E-03
Fe	4.9267E-02	Ni	7.3225E-03		

Absorber Region, TA, ***Note the Radius is 0.655 cm***

H	2.5665E-05	N	1.2592E-05	Nb93	5.9659E-05
Ta	5.5637E-02	W	1.3699E-05		

EndPlate Regions, TA

C	8.7454E-05	Si	6.1087E-04	P31	2.3739E-05
S	1.6377E-05	Cr	1.2956E-02	Mn55	1.1090E-03
Fe	4.2548E-02	Ni	6.3238E-03		

Table 3.15 Compositions for the Follower Elements

Outer Square Region, Follower

C	5.9184E-05	Si	4.1341E-04	P31	1.6065E-05
S	1.1083E-05	Cr	8.7679E-03	Mn55	7.5048E-04
Fe	2.8794E-02	Ni	4.2796E-03		

Cylinder, Follower

C	1.2275E-04	Si	8.5740E-04	P31	3.3319E-05
S	2.2986E-05	Cr	1.8185E-02	Mn55	1.5565E-03
Fe	5.9718E-02	Ni	8.8758E-03		

(The End plate is assumed to be the same as that of the BN Calandria.)

Table 3.16 Compositions for the B80/B90 Elements

Length taken to be the same as the Absorber Calandria, 91.44 cm.

B90 pins, Cylindrical Region 1, Radius 3.19 cm

B10	5.5640E-02	B11	6.0727E-03	C	1.4161E-02
Al27	1.4871E-05	Si	1.5172E-04	P31	5.2419E-06
S	2.0300E-06	Cr	1.8345E-03	Mn55	1.7292E-04
Fe	6.6141E-03	Ni	1.0676E-03	Nb	4.2072E-05

B80 pins, Cylindrical Region 2, Radius 4.5 cm

B10	4.6103E-02	B11	1.1587E-02	C	1.3900E-02
Si	1.8202E-04	P31	7.0733E-06	S	4.8797E-06
Cr	3.8605E-03	Mn55	3.3044E-04	Fe	1.2689E-02
Ni	1.8843E-03				

Aluminium Outer Region. Outer square boundary 10.2 cm x 10.2 cm.
Inner circular boundary, radius 4.5 cm.

AL	6.0181E-02	SI	5.7905E-06	MN	1.1841E-06
FE	3.7856E-05	CU	2.3033E-06		

Aluminium Follower. Outer square boundary 10.2 cm x 10.2 cm

AL	5.9628E-02	SI	5.7373E-06	MN	1.1732E-06
FE	3.7509E-05	CU	2.2821E-06		

Outer Square Region. The sheath of the B80/B90 Element, 10.7442 cm outer width

C	3.0522E-05	Si	2.1320E-04	P31	8.2850E-06
S	5.7156E-06	Cr	4.5217E-03	Mn55	3.8703E-04
Fe	1.4849E-02	Ni	2.2070E-03		

3.4.4 Temperature Data

Records of the temperature at which the measurements were performed are not available. For the purposes of the calculations, the temperatures of the MZB criticality models, 21.4^0C, should be used.

3.4.5 Experimental and Benchmark Control Rod Reactivity Worth Measurements

The recommended values are given in Section 1.4, Tables 1.13 to 1.19.

3.5 Benchmark-Model Specification for Reactivity Coefficient Measurements

No reactivity coefficient measurements were made.

3.6 Benchmark-Model Specification for Kinetics Measurements

No kinetic measurements, other than the period measurements for the calibration of the control rods, were made.

3.7 Benchmark-Model Specification for Reaction Rate Distribution Measurements

3.7.1 Description of the Calculational Methodology and Model

The benchmark model to be used to calculate reaction rate distributions is the 3D XYZ model described in Section 3.4, based on the 3D XYZ model of MZB (see ZEBRA-LMFR-EXP-002 Section 3.1). In calculations of axial distributions, account should also be taken of the absorber regions at the tops of the Zebra control rods, these being detailed in ZEBRA-LMFR-EXP-002. It should also be noted that if homogenised cell macroscopic cross-sections are used there is an axial bias in the results because the cells do not have axial symmetry, as is described in Section 4.7. It should also be noted that Zebra has a 5x5 super-lattice structure and that, if a uniform lattice cell structure is used in the calculations (as was done in the original analyses described in the MTNs) account should be taken of this.

3.7.2 Dimensions

The dimensions of the benchmark model are those for the 3D XYZ core model described in Section 3.4 (and see also ZEBRA-LMFR-EXP-002 Section 3.1 for the MZB model). The numbers of edge elements for the particular array of rods and their positions are those given in Figures 1.4 to 1.10.

3.7.3 Material Data

Identical material specifications were used for the 3D whole core model used in Section 3.4. Atom densities for the control rod materials are given above, in Section 3.4.

3.7.4 Temperature Data

Records of the temperature at which the measurements were performed are not available. For the purposes of calculation the temperatures specified for the criticality models in ZEBRA-LMFR-EXP-002 should be used (or a room temperature figure - the value is not critical).

3.7.5 Experimental and Benchmark Reaction Rate Distributions

The recommended benchmark measured reaction rate distributions are given in Tables 1.34 to 1.47.

3.8 Benchmark-Model Specifications for Power Distribution Measurements

No power distribution measurements were performed.

3.9 Benchmark-Model Specifications for Isotopic Measurements

No isotopic measurements were performed.

3.10 Benchmark Specifications for Other Miscellaneous Types of Measurements

No other types of measurement were performed.

4. RESULTS OF SAMPLE CALCULATIONS

4.4 Results of Calculations of the Control Rod Reactivity Worths

MONK Monte Carlo Calculations.
In the following Tables the results of the MONK Monte Carlo 3D hyperfine group calculations are presented for a selection of the cases in which the reactivity differences between two cases can be calculated sufficiently well using the MONK code (the best accuracy being $\pm 1 \times 10^{-4}$ dk/k in each calculation).

Calculations have been made (for a selection of cases only) using both the JEF-2.2 and JENDL-3.2 nuclear data libraries.

Table 4.1 MONK-JEF-2.2 Calculations for Single Followers and Control Rods at the Core Centre
(Reactivity in units of 10^{-4} dk/k)

Reference cores	**1-1/k**	**C**	**E**	**(C-E)/E%**
MZB Model BS	77±2			
		Edge Element worths		
MZB+8	99±1	22		
Component		**Worth of followers relative to (MZB+8) fuel elements**		
NA	69±1	30±4.7%	33±1.7%	-9%±5%
AL	63±2	36±6.2%	34.6±1.6%	+4%±6.4%
		Worth of absorber rods relative to NA or AL followers		
BN	-18±2	87±2.6%	81±1.3%	+7%±3%
B30	-32±2	101±2.2%	99±1.4%	+2%±2.6%
B80	-81±2	150±1.5%	153±1.8%	-2%±2.3%
B90	-84±2	153±1.5%	164±1.9%	-7%±2.4%
TA (old data)	-5±2	74±3%	62.5±1.3%	+18% ±3.3%
TA shielded	-2±2	71 ±3.1%	62.5±1.3%	+14% ±3.4%
B80/B90 *	-138±2	201±1.4%	214±2.3%	-6%±2.7%

* Relative to the AL follower.

The TA (old data) did not include a subgroup representation in the unresolved resonance region whereas the TA shielded data do.
The systematic uncertainty in the reactivity scale has not been included in the measurement uncertainty estimates.

MZB Model BS is the uniform model in which the superlattice structure of the array of elements has been replaced by a uniform array of equally spaced elements. In addition, the steel of the element sheaths has been smeared over the space between the plates and the lattice cell boundaries, thus eliminating the void gaps.

The uncertainties of the Monte Carlo calculations are the statistical uncertainties.

Table 4.2 MONK-JEF-2.2 Worths of Rods Relative to the Fuel Elements Replaced
(Reactivity in units of 10^{-4} dk/k)
The random uncertainties on the measured values, E, have been taken to be those applying to the measurements relative to a follower.

Reference cores	1-1/k	C	E	(C-E)/E%
MZB Model BS	77±2			
MZB+8	99±1			
Component				
BN	-18±2	117±1.9%	114±1.3%	+3% ±2.3%
B30	-32±2	131±1.7%	132±1.4%	-1% ±2.2%
B80	-81±2	180±1.2%	186±1.8%	-3% ±2.2%
B90	-84±2	183±1.2%	197±1.9%	-7% ±2.2%
TA (old data)	-5±2	104±2.2%	95±1.3%	+9% ±2.6%
TA shielded	-2±2	101 ±2.2%	95±1.3%	+6% ±2.6%
B80/B90	-138±2	237±0.9%	248±2.3%	-4% ±2.5%

Table 4.3 MONK-JEF-2.2 Calculations for Single Rods in Positions P1, P2 and Q
(Reactivity in units of 10^{-4} dk/k)

Reference cores	1-1/k	C	E	(C-E)/E%
MZB+8	99 ± 1			
Component				
P1		**Worth of NA follower relative to fuel elements**		
NA	71 ± 2	28±8%	28.9±2.0%	-3%±8%
		Worth of absorber rod relative to NA follower		
BN	0 ± 2	71±4%	69±1.3%	+3% ±4%
B30	-16 ± 2	87±3.3%	84±1.5%	+4% ±3.6%
B80	-48 ± 2	119±2.4%	128±1.6%	-7% ± 2.9%
P2		**Worth of NA follower relative to fuel elements**		
NA	73 ± 2	26±9%	28.7±2.0%	-9% ± 9%
		Worth of absorber rod relative to NA follower		
BN	-2 ± 2	75±3.8%	67.3±1.3%	+11% ± 4%
B80	-46 ± 2	119±2.4%	126.6±1.6%	-6% ± 2.9%
B90	-58 ± 2	131±2.2%	134.9±1.6%	-3% ± 2.7%
Q		**Worth of NA follower relative to fuel elements**		
NA	79 ± 2	18±12%	21.7±2.4%	-17% ± 12%
		Worth of absorber rod relative to NA follower		
BN	29 ± 2	50±5.6%	46.5±1.4%	+8% ± 6%
B30	17 ± 2	62±4.6%	57.1±1.3%	+8.6% ± 4.8%
B80	-4 ± 2	83±3.4%	85±1.3%	-2% ± 3.6%

The systematic uncertainty in the reactivity scale has not been included in the measurement uncertainty estimates.

Table 4.4 Worths of Single Rods at Positions P1, P2 and Q, Relative to the Fuel Elements Replaced

(Reactivity in units of 10^{-4} dk/k)

The random uncertainties on the measured values, E, have been taken to be those applying to the measurements relative to a follower.

Reference core	1-1/k	C	E	(C-E)/E%
MZB+8	99 ± 1			
Component				
P1				
BN	0 ± 2	99±2.3%	97 ±1.3%	+2% ±2.6%
B30	-16 ± 2	115±1.9%	112.9 ±1.5%	+2% ±2.4%
B80	-48 ± 2	147±1.5%	157 ±1.6%	-6% ±2.2%
P2				
BN	-2 ± 2	101±2.2%	96 ±1.3%	+5% ±2.6%
B80	-46 ± 2	145±1.5%	155.3 ±1.6%	-7% ±2.2%
B90	-58 ± 2	157±1.4%	163.6 ±1.6%	-4% ±2.1%
Q				
BN	29 ± 2	70±3.2%	68 ±1.4%	+3% ±3.5%
B30	17 ± 2	82±2.7%	78.8 ±1.3%	+4.1% ±3.0%
B80	-4 ± 2	103±2.2%	107 ±1.3%	-4% ±2.6%

Table 4.5 MONK-JEF-2.2 Calculations for Arrays of Two, Three and Four Rods

Reference core	**1-1/k**	**C**	**E**	**(C-E)/E%**
MZB 12	110 ± 2			
Components				
P1+Q		**Worth of NA followers relative to fuel elements**		
NA	68 ± 2	42±6.7%	49.4±1.4%	-15% ± 7%
		Worth of rods relative to NA followers		
BN BN	-49 ± 2	117±2.4%	105.7±1.5%	+11% ± 3%
BN B80	-78 ± 2	146±2.4%	137.7±1.7%	+6% ± 3%
B80 BN	-90 ± 2	158±1.8%	157.7±1.8%	+0.2 ± 2.5%
B80 B90	-120 ± 2	188±1.5%	190.6±2.1%	-1.4% ± 2.6%
Reference core				
MZB+23	145 ± 2			
Components				
O,P2,P5		**Worth of NA followers relative to fuel elements**		
NA	62 ± 2	83 ± 3.4%	85.8 ±1.4	-3% ± 3.7%
		Worth of rods relative to NA followers		
BN BN BN	-148 ± 2	210±1.3%	206±2.2%	+2% ± 2.6%
B30(O)BNBN	-163 ± 2	225±1.3%	221.7±2.4%	+1.5%± 2.7%
B80(O)BNBN	-202 ± 2	264±1.1%	266.8±2.8%	-1.0% ± 3%
Reference core				
MZB+30	162 ± 2			
Components				
P2,P2'P5,P5'		**Worth of NA followers relative to fuel elements**		
NA	59 ± 2	103±2.7%	109.5±1.5%	-6% ± 3%
		Worth of rods relative to NA followers		
BN	227 ± 2	286±1.0%	271±2.8%	+5.5% ± 3%

The systematic uncertainty in the reactivity scale has not been included in the measurement uncertainty estimates.

Table 4.6 MONK-JEF-2.2 Worths of Rods Relative to the Fuel Elements Replaced
(Reactivity in units of 10^{-4} dk/k)

Reference core	**1-1/k**	**C**	**E**	**(C-E)/E%**
MZB 12	110 ± 2			
P1+Q				
Components				
BN BN	-49 ± 2	159 ±1.8%	155.1 ±1.5%	+3% ±2.3%
BN B80	-78 ± 2	188 ±1.5%	187.1 ±1.7%	+0.5% ±2.3%
B80 BN	-90 ± 2	200 ±1.4%	207.1 ±1.8%	-3.5% ±2.3%
B80 B90	-120 ± 2	230 ±1.2%	240 ±2.1%	-4% ±2.4%
Reference core				
MZB+23	145 ± 2			
O,P2,P5				
Components				
BN BN BN	-148 ± 2	293 ±1.0%	292 ±2.2%	+0.3% ±2.4%
B30(O)BNBN	-163 ± 2	308 ±0.9%	307.5 ±2.4%	+0.2% ±2.6%
B80(O)BNBN	-202 ± 2	347 ±0.8%	352.6 ±2.8%	-1.6% ±2.9%
Reference core				
MZB+30	162 ± 2			
P2,P2'P5,P5'				
Components				
BN	227 ± 2	389 ±0.7%	381 ±2.8%	+2% ±2.9%

Note: The broadly satisfactory agreement for the worth of boron rods relative to fuel elements gives confidence in the reactivity scale.

Table 4.7 MONK-JENDL-3.2 Calculations for a Selection of Cases

Worths of followers replacing fuel elements and rods replacing followers (in units of 10^{-4} dk/k)

	1-1/k	**C**	**E**	**(C-E)/E%**
Rod at the Core Centre				
Reference core				
MZB+8	62 ± 1			
Components		**Worth of follower relative to MZB+8** (x 10^{-4} dk/k)		
NA	33 ± 1	29 ± 4.9%	33 ± 1.7%	-12% ±5%
AL	29 ± 2	33±6.8%	34.6±1.6%	-5%±7%
		Worth of absorber rod relative to NA or AL*		
BN	-54 ± 2	87±2.6%	81±1.3%	+7%±3%
B30	-72 ± 2	105±2.1%	99±1.4%	+6%±3%
B80	-116 ± 2	149±1.5%	153±1.8%	-3% ±2.3%
B90	-129 ± 2	162±1.4%	164±1.9%	-1% ±2.4%
B80/B90*	-173 ± 2	202±1.4%	214±2.3%	-6% ±2.7%
Array of 4 rods				
Reference core				
MZB+30	124 ± 2			
Components		**Worth of follower array relative to MZB+30**		
NA P2P2'P5P5'	22 ± 1.5	102±2.5%	109.5±1.5%	-7% ±3%
		Worth of BN rods relative to NA		
BN P2P2'P5P5'	-262±2%	284±1.0%	271±2.8%	+5% ±4.3%

*Relative to AL

Table 4.8 Worths of Absorber Rods Relative to the Fuel Elements Replaced (x 10^{-4} dk/k)

	1-1/k	**C**	**E**	**(C-E)/E%**
Single rods at the core centre				
Reference core				
MZB+8	62 ± 1			
Components				
BN	-54 ± 2	116±1.9%	114 ±1.3%	+2% ±2.3%
B30	-72 ± 2	134±1.7%	132 ±1.4%	+2% ±2.2%
B80	-116 ± 2	178±1.3%	186 ±1.8%	-4% ±2.2%
B90	-129 ± 2	191±1.2%	197 ±1.9%	-3% ±2.2%
B80/B90	-173 ± 2	235±1.0%	248 ±2.3%	-5% ±2.5%
Array of four BN rods				
Reference core				
MZB+30	124 ± 2			
Components				
BN P2P2'P5P5'	-262±2%	386±0.7%	381 ±2.8%	1.3% ±2.9%

Table 4.9 The MONK-JEF-2.2 calculated values of the reactivity effect of additions of N edge elements.
(reactivity in units of 10^{-4} dk/k)

Number of edge elements added to MZB	N	1-1/k	Edge element effect C	Reactivity change per element C/N
MZB		77 ± 2		
MZB+8	8	99 ± 1	22	2.8
MZB +12	12	110 ± 2	33	2.8
MZB +23	23	145 ± 2	68	3.0
MZB+30	30	162 ± 2	85	2.8

Calculations made in the original analysis.

It is interesting to see the calculations based on 2D diffusion theory (using region and energy group dependent axial multi-bucklings) carried out for the original interpretation of the measurements (MTN/92). (Other Mozart Technical Notes provide corrections for the use of 2D diffusion theory and for homogenisation of the structure of the rods. These enabled more accurate results to be obtained.)

Table 4.10 Summary of Calculated and Experimental Results for Single Rods
(Based on MTN/92 data)

Absorber or Follower Loading	Outer Core Loading for Worth Calcs	Calc. Worth rel foll. 2D diff. theory	Calc. Worth rel fuel 2D diff theory	Exp. Worth rel foll. DN Scale	Exp. Worth rel fuel DN Scale	C/E rel foll. DN scale	C/E rel fuel DN scale	Exp. Std Dev (%).
	264 +	10^{-4}	10^{-4}	10^{-4}	10^{-4}			
Na(O)	8	37.4		32.9		1.14		1.7
Na(P1)	8	33.0		28.9		1.14		2.0
Na(P2)	8	32.7		28.7		1.14		2.0
Na(Q)	8	24.4		21.7		1.12		2.4
Na(R)	8	20.6		18.8		1.10		2.9
Na(S)	4	18.3		17.7		1.03		3.0
Al(O)	8	34.4		34.6		0.99		1.6
BN(O)	8	84.3	121.7	80.6	113.5	1.05	1.07	1.3
BN(P1)	8	71.2	104.2	68.5	97.40	1.04	1.07	1.3
BN(P2)	8	70.2	102.9	67.3	96.00	1.04	1.07	1.3
BN(Q)	8	47.5	71.9	46.5	68.20	1.02	1.05	1.4
BN(R)	8	31.3	51.9	31.2	50.00	1.00	1.04	1.4
BN(S)	4	14.2	32.5	14.3	32.00	0.99	1.02	2.3
B30(O)	8	106.4	143.8	99.2	132.1	1.07	1.09	1.4
B30(P1)	8	89.7	122.7	84.0	112.9	1.07	1.09	1.5
B30(Q)	8	59.8	84.2	57.1	78.80	1.05	1.07	1.3
B80(O)	8	173.5	210.9	153.2	186.1	1.13	1.13	1.8
B80(P1)	8	144.1	177.1	128.0	156.9	1.13	1.13	1.6
B80(P2)	8	141.8	174.5	126.6	155.3	1.12	1.12	1.6
B80(Q)	8	94.9	119.3	85.0	106.7	1.12	1.12	1.3
B80(S)	4	30.6	48.9	27.7	45.4	1.10	1.08	1.4
B90(O)	8	184.8	222.2	163.8	196.7	1.13	1.13	1.9
B90(P2)	8	150.7	183.4	134.9	163.6	1.12	1.12	1.6
B90(Q)	8	100.6	125.0	90.5	112.2	1.11	1.11	1.4
Ta(O)	8	68.7	103.1	62.5	97.1	1.10	1.06	1.3
Ta(S)	4	11.2		10.9		1.03		2.9
B80/B90(O)	8	243.5	280.9	213.6	251.0	1.14	1.12	2.3

Calculations made using volume averaged compositions for the control rods overestimate rod worths by up to about 13% for the highly enriched boron rods.

Table 4.11 Summary of Calculated and Experimental Results for Multiple Rod Arrays
(Based on MTN/92 data)

Core Loading	Added Edge Elements	MTN/92 Calc. rel. follower	MTN/92 Calc. rel. fuel	Measured relative to follower	Measured relative to fuel	C/E (Pu worth scale)	C/E	S.D. (%)
	264 +	$x10^{-4}$		$x10^{-4}$	$x10^{-4}$			
Na(O,P1)	15	68.8		60.3		1.14		1.4
Na(P1,P2)	14	64.1		56.1		1.14		1.4
Na(P1,P5)	14	65.2		57.0		1.14		1.4
Na(P1,Q)	12	56.1		49.4		1.14		1.5
Na(P1,R)	11	52.7		47.0		1.12		1.5
Na(Q,R)	8	44.0		39.4		1.12		1.7
Na(O,P2,P5)	23	98.6		85.8		1.15		1.4
Na(P1,P3,P5)	22	97.1		84.6		1.15		1.4
Na(P2,P2',P5,P5')	30	125.8		109.5		1.15		1.5
B80(P1)B90(O)	15	305.5	374.3	276.0	336.3	1.11	1.11	2.9
B80(P1)B90(P2)	14	261.6	325.7	237.9	294.0	1.10	1.11	2.5
B80(P1)B90(P5)	14	298.7	363.9	268.1	325.1	1.11	1.12	2.8
B80(P1)B90(Q)	12	208.6	264.7	190.6	240.0	1.09	1.10	2.1
B80(P1)BN(Q)	12	171.6	227.7	157.7	207.1	1.09	1.10	1.8
B80(P1)BN(R)	11	161.0	213.7	147.0	194.0	1.10	1.10	1.7
BN(P1)B80(P2)	14	195.3	259.1	180.0	236.1	1.09	1.10	2.0
BN(P1)B80(Q)	12	146.9	203.0	137.7	187.1	1.07	1.08	1.7
BN(P1)BN(Q)	12	108.0	164.1	105.7	155.1	1.02	1.06	1.5
BN(P1)BN(R)	11	94.9	147.6	92.9	139.9	1.02	1.06	1.4
BN(Q)BN(R)	8	70.3	114.3	68.8	108.2	1.02	1.06	1.4
B80(P1)Na(P2)	14	139.5		124.4				1.6
BN(O,P2,P5)	23	215.8	314.4	206.0	291.8	1.05	1.08	2.2
B30(O)BN(P2,P5)	23	230.9	329.5	221.7	307.5	1.04	1.07	2.4
B80(O)BN(P2,P5)	23	285.9	384.5	266.8	352.6	1.07	1.09	2.8
BN(P1,P3,P5)	22	217.9	315.0	210.3	294.9	1.04	1.07	2.3
BN(P2,P2',P5,P5')	30	280.1	405.9	271.1	380.6	1.03	1.07	2.8
BN(P2,P5)Na(O)	23	142.3		137.6		1.11		1.7

4.7 Results of Calculations of the Reaction Rate Distributions

Comparisons of the measured values with the original calculations (carried out in the early 1970s) are given in MTN/93 and /100. These calculations were made using the MURAL cell code, the SCRAMBLE and TIGAR diffusion theory codes and the TWOTRAN 2D transport theory code, together with the FGL5 and FD5 cross-section sets (MTN/81). Different methods of calculation, and approximations, are also compared. The following are summaries of the conclusions of these two papers.

Cell averaged cross-sections were used in the whole reactor calculations and thus the effect of the axial asymmetry of the cells was not represented. Also the ZEBRA control rods were replaced by core elements and so the axial asymmetry due to the absorber sections at the tops of the rods was not represented. To allow for this in the comparisons made with the axial scan measurements the centre of the calculated scan was moved downwards by 0.85 cm. The number of outer core elements corresponded to that of the core on which the measurements were made (see MTN/93 and MTN/100).

4.7.1 Radial Reaction Rate Distributions Calculated for Control Rods Fully Inserted

The calculations and description are those presented by Marshall and Samways in MTN/93 (1973).

Methods of Calculation.

Most reaction rates were calculated using fluxes obtained from the MZC standard analysis method (described by Collins, Marshall and Sugawara in MTN/58). This was an XY diffusion theory calculation in 9 energy-groups using cross-sections modified to include region and energy group dependent axial bucklings, to treat axial leakage from the core. Thus the calculated fluxes are values appropriate to some average over the core height rather than being values for the centre plane of the reactor, where the measurements were made. In the standard analysis method the cross-sections used to represent the absorbers in the standard diffusion theory reactivity analysis were obtained from a cylindrical geometry MURAL collision probability super-cell calculation, whereas for reaction rates PIJ-MURAL pin-cluster collision probability super-cell calculations were used to obtain the cross-sections for the absorber region. This was so that the use of PIJ disadvantage factors for pin-to-pin reaction rate variations was consistent with the cross-sections used to provide the basic reactor fluxes. A comparison of a small number of absorber reactivity worths based on MURAL cylindrical and PIJ-MURAL pin-cluster models is given in MTN/98. Reaction rates for one case, B80 at position O, based on these two models are compared in Table 4.23.

The reaction rate foil measurements in the inner core region of the reactor were made by placing U235 and U238 metal foils in uranium oxide plates and tantalum foils in steel plates. MURAL calculations for the inner core cells of the reactor with U235 and U238 foils represented were carried out by Nakano (MTN/70) to provide microscopic foil cross-sections. Similarily microscopic tantalum cross-sections were obtained for a tantalum foil in a steel plate from a MURAL calculation of the inner core cell, C12-30A. Microscopic cross-sections for the U235, U238 and tantalum foils in the absorber pins were obtained by Collins from the PIJ-MURAL pin-cluster geometry super-cell calculations for the PNC control rods (MTN/98).

For fission chamber scans, effective cross-sections were obtained by averaging the microscopic cross-sections of the appropriate isotope over 1.3 cm on each side of the centre plate of the reactor. This included the 1.3 cm aluminium block carrying the scan tube and the plate on either side of it.

37 group cross-sections were obtained using MURAL for regions of the assembly and then condensed to 9 groups. The spectra used to condense the detector cross-sections were chosen to be consistent with the macroscopic data used for the standard diffusion theory reactivity analysis. Thus different spectra were used for the detectors in each region within the inner and outer cores and the appropriate infinite cylinder spectra were used for the absorber as described in MTN/58.

Reaction rates within the absorber pins were calculated by taking the average reaction rate over the absorber and using cross-sections which included the pin disadvantage factors. That is, microscopic cross-sections were available for each ring of pins (including the disadvantage factor for that ring relative to the average).

In general, measurements in the reactor core were made at the centre of each fuel element (in the XY plane). Exceptions to this were foil measurements near absorbers, when extra positions were used to give finer detail, as shown in Figure 4.1. The numbering system for absorber pin identification is also shown. In most cases the diffusion theory calculation had four mesh points for each fuel element and these have simply been averaged to give the calculated value at the centre of the fuel element.

A problem arises because the average Zebra fuel element pitch, 5.42544 cm, was used in the calculations and so the fuel element centres in this model differed from the true positions in the reactor. For foil measurements, these positional discrepancies varied from element to element, being at worst 0.11 cm ,and generally the error introduced was small in comparison with the experimental uncertainty. For some positions near the absorber, in particular position 52-50F, the error due to this effect was similar in magnitude to the experimental uncertainty and so corrections, based on the slope of the reaction rate at that position, were applied. In the case of fission chamber measurements, discrepancies in position, due partly to flux scanner tape inaccuracy (MTN/94), were up to 0.24 cm. Significant errors were only introduced in the radial blanket region where corrections of up to 3.9% were applied.

For one configuration, B80(P1)+B90(O), the fission chamber measurements were not made at the element centres and so third order Neville-Aitken interpolation was used to determine the calculated flux at the measuring positions.

Discussion of Results - Radial Reaction Rates calculated using Diffusion Theory.

For reaction rates within the absorber pins, the calculations give values for the centre pin, an inner ring pin, and an outer ring pin only. The measured values within a ring of pins were therefore averaged, the error introduced being less than 0.3%.

Comparisons of the measured reaction rates with calculated reaction rates obtained from XY diffusion theory are presented in Tables 4.12 to 4.18. The calculated reaction rates have been normalised to unity at the same positions as the measured values, in general at some distance from absorbers. The quoted s.d.s are the contribution from the experimental uncertainty only.

Tables 4.12, 4.13 and 4.14 give (C/E-1)% values for the diffusion theory calculations for U235 and U238 foil fission rates for the Ta, BN and B80 absorbers at position O. Tantalum foil reaction rates are also quoted for the Ta absorber. Throughout the inner core of the reactor the agreement is good, discrepancies being generally less than 2% for all detectors. Significant discrepancies are apparent within the absorber, U235 fission rates being between 5% and10% in error and U238 fission rates being 10% to 14% in error. The tantalum reaction rates also show discrepancies of about 9% in the Ta absorber.

The U235 and U238 foil fission rate measurements between the absorbers in the BN(P1,P3,P5) case are also well predicted as shown in Table 4.15, discrepancies being again less than 2%.

(C/E-1)% values for the Pu239 and U238 fission chamber scans are given in Tables 4.16, 4.17 and 4.18. Generally agreement within the inner core is good except for Pu239 fission rates in the elements adjacent to the absorber (Q), which neighbours the centre line of elements, and the neighbouring elements towards the outer core, where discrepancies of up to 6% occur. In the outer core and radial blanket regions significant discrepancies occur similar to the effects found in the diffusion theory analysis of MZB. This overestimation of the flux dip is probably associated with the overestimation of rod worth resulting from the method of rod homogenisation used in the standard method.

Transport Theory.

Some calculations were repeated using the general-geometry transport theory code TWOTRAN. Again an XY model, with axial buckling-modified cross-sections, was used but for these cases with only one mesh point per element. Two cases, BN(P1,P2,P3), and B80(P1) + B90(Q) were reported by Sugawara in MTN/85 and one additional case B80(O) has been calculated in MTN/93.

A comparison of these calculated reaction rates with the measured values is shown in Tables 4.20 to 4.23. The foil measurements made in the BN(P1,P3,P5) case are well predicted by both transport and diffusion theory. In the case of fission chambers, transport theory gives a better prediction of the reaction rates in the outer regions of the reactor as can be seen by comparing Table 4.20 with 4.17. Table 4.21 shows the transport theory comparison for the B80(P1) + B90(Q) case. At positions within about 10 cm of the absorber rod Q discrepancies of up to 7% occur for both U235 and U238 reaction rates. Comparison of Table 4.21 with Table 4.18 shows that this is in some cases worse by about 2% than for diffusion theory.

The most interesting effects are however apparent in Table 4.22 for the case of B80 at position O. Compared with diffusion theory (Table 4.14) transport theory apparently gives a worse prediction by some 3% for the inner core reaction rates near the B80 absorber. In the absorber pins, however, the (C/E-1)% value is improved slightly by about 2% for U235 but there is a significant improvement by 8% for the U238 reaction rate.

Intercomparison of Calculation Models.

In one particular case, B80 at position O, reaction rates were calculated using transport theory with different supercell calculation methods to derive the cross-sections for the absorber region. In the diffusion theory analysis reaction rates were calculated using the PIJ-MURAL pin-cluster based cross-sections. In the second set of calculations the reaction rates were calculated using the MURAL cylindrical model cross-sections of the standard reactivity analysis. Also reaction rates were obtained from a calculation using MURAL data with axial bucklings appropriate to the centre plane of the reactor. This gives a better representation of the reaction rate distribution along the centre plane of the reactor where the measurements were made, Table 4.23 gives values of (C/E-1)% for these cases together with the "standard" PIJ pin-cluster model for comparison. Comparison of the PIJ and MURAL-cylinder cases shows that in the core region MURAL cylinder cross-sections give slightly worse agreement whereas in the absorber they are slightly improved. The use of centre plane axial bucklings shows little effect in the core region, as might be expected, but increases the within absorber discrepancy by about 2%. These variations on the diffusion theory analysis show differences of about 2%.

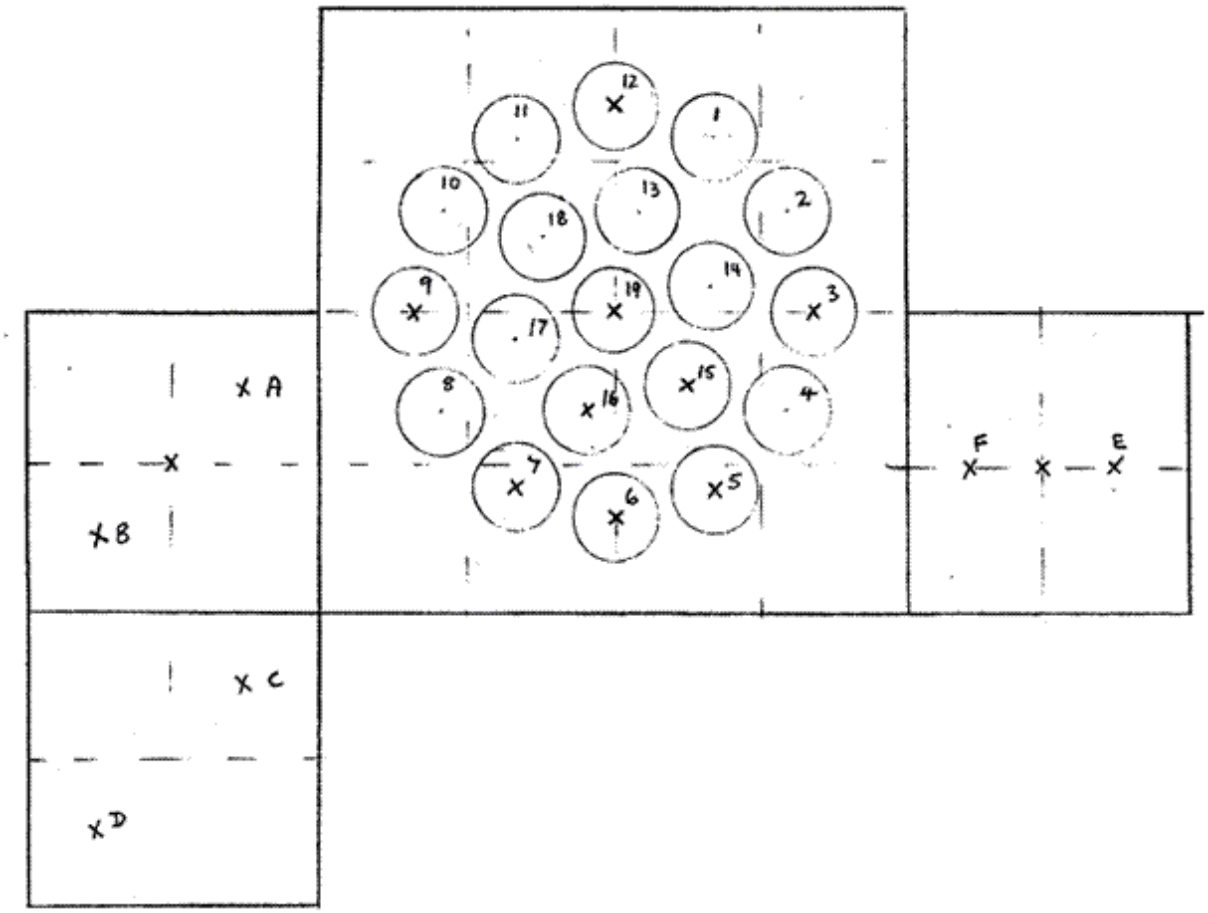

Figure 4.1 Reaction Rate Measurements Within and Adjacent to the Mock-up Rods.

X marks the position of the measurements

Table 4.12 Reaction Rate Comparisons for the Mock-up Rod Ta at Position (O), Ta(O), Foil Measurements in the Inner Core and Mock-up Rod. Diffusion Theory Calculations
(Mock-up Rod Position O occupies element positions 50-50, 50-51, 51-50 and 51-51)

			U235			
			Calc.	Exp	(C/E-1)%	s.d. %
40-50	542.5	0.0	1.0000	1.0000	Normalise	0.3
43-50	378.7	0.0	1.1708	1.1697	0.1	0.5
46-50	217.5	0.0	1.2472	1.2397	0.6	0.8
48-50	107.4	0.0	1.2278	1.2188	0.7	1.1
49-50B	67.3	- 13.6	1.2012	1.1972	0.3	1.2
49-50	53.7	0.0	1.1795	1.1595	1.7	1.2
49-50A	40.2	13.6	1.1516	1.1303	1.9	1.3
52-50F	- 93.9	0.0	1.1516	1.1363	1.3	1.2
52-50	- 107.4	0.0	1.1667	1.1542	1.1	1.1
52-50E	- 121.0	0.0	1.1818	1.1746	0.6	1.2
53-50	- 163.8	0.0	1.2062	1.1914	1.2	1.0
55-50	- 271.2	0.0	1.2081	1.2087	0.0	0.8
58-50	- 435.0	0.0	1.1297	1.1123	1.6	0.5
61-50	- 596.2	0.0	0.9088	0.9169	-0.9	0.5
49-49D	67.3	- 67.3	1.2282	1.2204	0.6	1.2
49-49C	40.2	- 40.2	1.1934	1.1832	0.9	1.3
Centre pin			0.9681	0.8940	8.3	1.4
Inner ring			0.9841	0.9093	8.2	1.4
Outer ring			1.0350	0.9657	7.2	1.4

			U238			
			Calc.	Exp	(C/E-1)%	s.d. %
40-50	542.5	0.0	1.000	1.000		0.6
43-50	378.7	0.0	1.1114	1.1217	-0.9	0.8
46-50	217.5	0.0	1.1613	1.1731	-1.0	1.1
48-50	107.4	0.0				
49-50B	67.3	- 13.6				
49-50	53.7	0.0	1.0219	1.0275	-0.5	1.6
49-50A	40.2	13.6				
52-50F	- 93.9	0.0				
52-50	- 107.4	0.0	1.0101	1.0099	0.0	1.4
52-50E	- 121.0	0.0				
53-50	- 163.8	0.0				
55-50	- 271.2	0.0	1.1263	1.1294	-0.3	1.0
58-50	- 435.0	0.0	1.0757	1.0587	1.6	0.7
61-50	- 596.2	0.0	0.9537	0.9750	-2.2	0.6
49-49D	67.3	- 67.3				
49-49C	40.2	- 40.2				
Centre pin			0.6978	0.6366	9.6	1.7
Inner ring			0.7250	0.6643	9.1	1.7
Outer ring			0.8152	0.7269	12.1	1.7

Position	X (mm)	Y (mm)	**Ta foil**			
			Calc	Exp	(C/E-1)%	s.d. %
40-50	542.5	0.0	1.0000	1.0000		0.2
43-50	378.7	0.0	1.1875	1.1782	0.8	0.2
46-50	217.5	0.0	1.2723	1.2584	1.1	0.2
49-50	53.7	0.0	1.1733	1.1540	1.7	0.5
52-50	- 107.4	0.0	1.1569	1.1410	1.4	0.5
55-50	- 271.2	0.0	1.2307	1.2229	0.6	0.2
58-50	- 435.0	0.0	1.1180	1.1149	0.3	0.2
61-50	- 596.2	0.0	0.9003	0.9043	-0.4	0.2
Centre pin			0.6085	0.5567	9.3	0.2
Inner ring			0.6198	0.5708	8.6	0.4
Outer ring			0.6557	0.6359	3.1	0.7

Table 4.13 Reaction Rate Comparison for BN(O).
Foils in the Inner Core and Mock-up Rod. Diffusion Theory

Position	X (mm)	Y (mm)	**U235**			
			Calc.	Exp	(C/E-1)%	S.d. %
40-50	542.5	0.0	1.0000	1.0000		0.3
43-50	378.7	0.0	1.1639	1.1509	1.1	0.5
46-50	217.5	0.0	1.2307	1.2160	1.2	0.8
48-50	107.4	0.0	1.2052	1.1912	1.2	1.1
49-50B	67.3	- 13.6	1.1767	1.1633	1.2	1.2
49-50	53.7	0.0	1.1539	1.1362	1.6	1.2
49-50A	40.2	13.6	1.1282	1.1137	1.3	1.2
52-50F	- 93.9	0.0	1.1214	1.1132	0.7	1.1
52-50	- 107.4	0.0	1.1408	1.1281	1.1	1.1
52-50E	- 121.0	0.0	1.1568	1.1403	1.4	1.1
53-50	- 163.8	0.0	1.1826	1.1730	0.8	1.0
55-50	- 271.2	0.0	1.1912	1.1904	0.1	0.7
58-50	- 435.0	0.0	1.0984	1.1023	-0.4	0.4
61-50	- 596.2	0.0	0.9078	0.9235	-1.7	0.4
49-49D	67.3	- 67.3	1.2055	1.1937	1.0	1.2
49-49C	40.2	- 40.2	1.1685	1.1576	0.9	1.2
Centre pin	- 26.9		0.9216	0.8698	6.0	1.3
Inner ring			0.9369	0.8911	5.1	1.3
Outer ring			0.9873	0.9411	4.9	1.3

Position	X (mm)	Y (mm)	**U238**			
			Calc.	Exp	(C/E-1)%	S.d. %
40-50	542.5	0.0	1.0000	1.0000		0.6
43-50	378.7	0.0	1.1055	1.1064	-0.1	0.8
46-50	217.5	0.0	1.1509	1.1416	0.8	1.1
48-50	107.4	0.0				
49-50B	67.3	- 13.6				
49-50	53.7	0.0	1.0367	1.0242	1.2	1.5
49-50A	40.2	13.6				
52-50F	- 93.9	0.0				
52-50	- 107.4	0.0	1.0247	0.9990	2.6	1.4
52-50E	- 121.0	0.0				
53-50	- 163.8	0.0				
55-50	- 271.2	0.0	1.1155	1.1120	0.3	1.0
58-50	- 435.0	0.0	1.0524	1.0603	-0.7	0.7
61-50	- 596.2	0.0	0.9528	0.9630	-1.1	0.6
49-49D	67.3	- 67.3				
49-49C	40.2	- 40.2				
Centre pin	- 26.9		0.8447	0.7519	12.3	1.7
Inner ring			0.8627	0.7695	12.1	1.7
Outer ring			0.9169	0.8041	14.0	1.7

Table 4.14 Reaction Rate Comparison for B80(O)
Foils in the Inner Core and Mock-up Rod. Diffusion Theory

Position	X (mm)	Y (mm)	**U235**			
			Calc	Exp	(C/E-1)%	s.d. %
40-50	542.5	0.0	1.0000	1.0000		0.3
43-50	378.7	0.0	1.1267	1.1174	0.8	0.5
46-50	217.5	0.0	1.1354	1.1305	0.4	0.8
48-50	107.4	0.0	1.0347	1.0317	0.3	1.1
49-50B	67.3	- 13.6	0.9641	0.9758	-1.2	1.2
49-50	53.7	0.0	0.9141	0.9219	-0.8	1.3
49-50A	40.2	13.6	0.8583	0.8647	-0.7	1.4
52-50F	- 93.9	0.0	0.8561	0.8725	-1.9	1.3
52-50	- 107.4	0.0	0.9006	0.9109	-1.1	1.3
52-50E	- 121.0	0.0	0.9385	0.9454	-0.7	1.1
53-50	- 163.8	0.0	1.0117	1.0181	-0.6	1.0
55-50	- 271.2	0.0	1.0939	1.0912	0.2	0.7
58-50	- 435.0	0.0	1.0586	1.0557	0.3	0.4
61-50	- 596.2	0.0	0.9042	0.9127	-0.9	0.3
49-49D	67.3	- 67.3	1.0316	1.0391	-0.7	1.2
49-49C	40.2	- 40.2	0.9447	0.9526	-0.8	1.3
Centre pin	- 26.9	26.9	0.4908	0.4460	10.0	1.3
Inner ring			0.5112	0.4651	9.9	1.4
Outer ring			0.5835	0.5341	9.2	1.4

Position	X (mm)	Y (mm)	**U238**			
			Calc	Exp	(C/E-1)%	s.d. %
40-50	542.5	0.0	1.0000	1.0000		0.7
43-50	378.7	0.0	1.0642	1.0651	-0.1	1.2
46-50	217.5	0.0	1.0630	1.0678	-0.4	1.3
48-50	107.4	0.0				
49-50B	67.3	- 13.6				
49-50	53.7	0.0	0.9038	0.8818	2.5	1.6
49-50A	40.2	13.6				
52-50F	- 93.9	0.0				
52-50	- 107.4	0.0	0.8912	0.8879	0.4	1.6
52-50E	- 121.0	0.0				
53-50	- 163.8	0.0				
55-50	- 271.2	0.0	1.0260	1.0327	-0.6	1.1
58-50	- 435.0	0.0	1.0096	1.0089	0.1	0.8
61-50	- 596.2	0.0	0.9556	0.9696	-1.4	0.7
49-49D	67.3	- 67.3				
49-49C	40.2	- 40.2				
Centre pin	- 26.9	26.9	0.7124	0.6380	11.7	1.9
Inner ring			0.7291	0.6470	12.7	1.9
Outer ring			0.7796	0.6876	13.4	1.8

Table 4.15 Reaction Rate Comparison for BN(P1,P3,P5)
Foil measurements in the Inner Core. Diffusion Theory

Position	X (mm)	Y (mm)	**U235**			
			Calc	Exp	(C/E-1)%	S.d. %
47-48	163.8	- 107.4	0.9277	0.9219	0.6	1.2
48-48	107.4	- 107.4	0.9708	0.9639	0.7	1.1
49-48	53.7	- 107.4	0.9887	0.9924	-0.4	0.9
50-48	0.0	- 107.4	0.9902	0.9883	0.2	0.9
51-48	- 53.7	- 107.4	0.9779	0.9732	0.5	1.1
52-48	- 107.4	- 107.4	0.9524	0.9490	0.4	1.2
53-48	- 163.8	- 107.4	0.9222	0.9218	0.0	1.2
53-49	- 163.8	- 53.7	0.9659	0.9655	0.0	1.1
53-50	- 163.8	0.0	0.9853	0.9846	0.1	0.9
53-51	- 163.8	53.7	0.9883	0.9813	0.7	0.9
53-52	- 163.8	107.4	0.9767	0.9785	-0.2	1.1
53-53	- 163.8	163.8	0.9501	0.9415	0.9	1.2
53-54	- 163.8	217.5	0.9164	0.9134	0.3	1.2
50-53	0.0	163.8	0.9609	0.9543	0.7	1.2
49-52	53.7	107.4	0.9966	0.9921	0.5	0.9
48-51	107.4	53.7	0.9966	0.9797	1.7	0.9
47-50	163.8	0.0	0.9608	0.9714	-1.1	1.2
41-50	488.8	0.0	0.9186	0.9289	-1.1	0.8
50-50	0.0	0.0	1.0000	1.0000		0.9
59-50	- 488.8	0.0	0.9251	0.9382	-1.4	0.7

Position	X (mm)	Y (mm)	**U238**			
			Calc	Exp	(C/E-1)%	S.d. %
47-48	163.8	- 107.4	0.8995	0.8970	0.3	1.4
48-48	107.4	- 107.4	0.9603	0.9632	-0.3	1.2
49-48	53.7	- 107.4	0.9858	0.9885	-0.3	1.1
50-48	0.0	- 107.4	0.9881	0.9880	0.0	1.1
51-48	- 53.7	- 107.4	0.9710	0.9782	-0.7	1.2
52-48	- 107.4	- 107.4	0.9353	0.9388	-0.4	1.4
53-48	- 163.8	- 107.4	0.8940	0.8972	-0.4	1.4
53-49	- 163.8	- 53.7	0.9560	0.9648	-0.9	1.2
53-50	- 163.8	0.0	0.9834	0.9865	-0.3	1.1
53-51	- 163.8	53.7	0.9877	0.9930	-0.5	1.1
53-52	- 163.8	107.4	0.9717	0.9693	0.2	1.2
53-53	- 163.8	163.8	0.9352	0.9223	1.4	1.4
53-54	- 163.8	217.5	0.8908	0.8776	1.5	1.4
50-53	0.0	163.8	0.9443	0.9301	1.5	1.4
49-52	53.7	107.4	0.9947	0.9870	0.8	1.1
48-51	107.4	53.7	0.9948	0.9791	1.6	1.1
47-50	163.8	0.0	0.9445	0.9281	1.8	1.4
41-50	488.8	0.0	0.9678	0.9721	-0.4	0.9
50-50	0.0	0.0	1.0000	1.000		1.1
59-50	- 488.8	0.0	0.9779	0.9874	-1.0	0.9

Table 4.16 Reaction Rate Comparison for BN(Q + R).
Rod Q is at 41-51, 41-52, 42-51, 42-52
Fission Chamber Scan along the X axis.

Position		X (mm)	**Pu239** Calc	Exp	(C/E-1)%	S.d.
31-50		1029.2	0.1688	0.2438	-30.8	0.90
34-50	Blanket	865.7	0.3264	0.3679	-11.3	0.73
35-50		812.1	0.3621	0.3933	-7.9	0.70
36-50		758.5	0.3547	0.4045	-12.3	0.34
37-50	Outer Core	704.9	0.3914	0.4438	-11.8	0.34
38-50		648.7	0.4352	0.4808	-9.5	0.35
39-50		595.0	0.4799	0.5191	-7.6	0.34
40-50		541.4	0.5180	0.5495	-5.7	0.34
41-50		487.7	0.5571	0.5861	-4.9	0.34
42-50		434.2	0.6134	0.6416	-4.4	0.35
43-50		377.9	0.6871	0.7105	-3.3	0.34
44-50		324.3	0.7580	0.7728	-1.9	0.34
45-50	Inner	270.6	0.8196	0.8347	-1.8	0.34
46-50	Core	216.9	0.8724	0.8830	-1.2	0.33
47-50		163.4	0.9169	0.9269	-1.1	0.34
48-50		107.1	0.9535	0.9523	0.1	0.34
49-50		53.5	0.9824	0.9836	-0.1	0.33
51-50		- 53.7	1.0176	1.0164	0.1	0.32
54-50		-217.1	1.0145	1.0178	-0.3	0.32
57-50		-378.1	0.9447	0.9561	-1.2	0.34
60-50		-541.5	0.8100	0.8266	-2.0	0.34
63-50	Outer Core	-705.1	0.6085	0.6467	-5.9	0.35
66-50		-865.9	0.5009	0.5179	-3.3	0.63
69-50	Blanket	-1029.4.	0.2573	0.3376	-23.8	0.78

Table 4.16 continued. - Reaction Rate Comparison for BN(Q + R). Fission Chamber Scan along the X axis.

Position		X (mm)	U238			
			Calc	Exp	(C/E-1)%	S.d.
31-50		1029.2	0.0216	0.0233	-7.3	2.77
34-50	Blanket	865.7	0.1155	0.1077	7.2	1.54
35-50		812.1	0.2117	0.2053	3.1	1.33
36-50		758.5	0.3577	0.3834	-6.7	0.87
37-50	Outer Core	705.0	0.4544	0.4929	-7.8	0.74
38-50		648.6	0.5064	0.5322	-4.8	0.70
39-50		595.0	0.5130	0.5260	-2.5	0.70
40-50		541.4	0.5236	0.5306	-1.3	0.70
41-50		487.8	0.5437	0.5441	-0.1	0.70
42-50		434.1	0.5946	0.5996	-0.8	0.69
43-50		377.9	0.6734	0.6838	-1.5	0.66
44-50		324.3	0.7498	0.7613	-1.5	0.64
45-50	Inner	270.6	0.8150	0.8202	-0.6	0.62
46-50	Core	217.0	0.8699	0.8701	0.0	0.61
47-50		163.4	0.9156	0.9112	0.5	0.60
48-50		107.1	0.9529	0.9544	-0.2	0.59
49-50		53.5	0.9822	0.9881	-0.6	0.59
51-50		- 53.7	1.0178	1.0119	0.6	0.58
54-50		-217.2	1.0156	1.0162	-0.1	0.58
57-50		-378.1	0.9529	0.9504	0.3	0.59
60-50		-541.6	0.8535	0.8491	0.5	0.61
63-50	Outer Core	-705.1	0.7162	0.7503	-4.5	0.66
66-50		-865.9	0.1805	0.1652	9.3	1.45
69-50	Blanket	-1029.4	0.0333	0.0321	3.7	2.65

Table 4.17 Reaction Rate Comparison for BN(P1,P3,P5).
Fission Chamber Scan along the X axis. Diffusion Theory

Position		X	**Pu239**			
			Calc	Exp	(C/E-1)%	s.d. %
31-50		1031.1	0.3436	0.4046	-15.1	0.73
34-50	Blanket	867.3	0.5879	0.6017	-2.3	0.83
37-50	Outer Core	706.1	0.7294	0.7620	-4.3	0.26
40-50		542.4	0.8996	0.9202	-2.2	0.33
41-50		488.7	0.9298	0.9415	-1.2	0.33
42-50		434.9	0.9473	0.9502	-0.3	0.33
43-50		378.6	0.9515	0.9519	0.0	0.33
44-50		324.9	0.9415	0.9440	-0.3	0.33
45-50		271.1	0.9252	0.9251	0.0	0.35
46-50		217.4	0.9319	0.9257	0.7	0.35
47.50		163.7	0.9622	0.9569	0.6	0.34
48-50	Inner	107.3	0.9872	0.9832	0.4	0.35
49-50	Core	53.6	0.9996	1.0028	-0.3	0.35
50-50		- 0.1	1.0020	1.0019	0.0	0.35
51-50		- 53.8	0.9983	0.9953	0.3	0.34
52-50		- 107.5	0.9923	0.9904	0.2	0.34
53-50		- 163.9	0.9875	0.9942	-0.7	0.34
54-50		- 217.6	0.9858	0.9887	-0.3	0.34
55-50		- 271.3	0.9861	0.9960	-1.0	0.34
56-50		- 325.1	0.9843	0.9959	-1.2	0.34
57-50		- 378.7	0.9765	0.9841	-0.8	0.34
58-50		- 435.1	0.9612	0.9761	-1.5	0.34
59-50		- 488.9	0.9369	0.9536	-1.8	0.34
60-50		- 542.6	0.9026	0.9174	-1.6	0.35
63-50	Outer Core	- 706.4	0.7277	0.7610	-4.4	0.38
66-50	Blanket	-.867.5	0.5854	0.5973	-2.0	0.83
69-50		- 1031.3	0.3419	0.4046	-15.5	1.00

Table 4.17 continued. Reaction Rate Comparison for BN(P1,P3,P5). Fission Chamber Scan along the X axis. Diffusion Theory

Position		X	U238			
			Calc	Exp	(C/E-1)%	s.d. %
31-50		1031.1	0.0573	0.0595	-3.7	2.76
34-50	Blanket	867.3	0.3616	0.3449	4.8	1.24
37-50	Outer Core	706.1	0.9302	0.9892	-6.0	0.74
40-50		542.4	0.9680	0.9621	0.6	0.71
41-50		488.7	0.9705	0.9727	-0.2	0.62
42-50		434.9	0.9700	0.9706	-0.1	0.70
43-50		378.6	0.9590	0.9574	0.2	0.71
44-50		324.9	0.9326	0.9182	1.6	0.72
45-50		271.1	0.9010	0.8874	1.5	0.70
46-50		217.4	0.9059	0.8901	1.8	0.70
47.50		163.7	0.9471	0.9483	-0.1	0.71
48-50	Inner	107.3	0.9817	0.9886	-0.7	0.73
49-50	Core	53.6	0.9990	0.9997	-0.1	0.70
50-50		- 0.1	1.0027	1.0063	-0.4	0.70
51-50		- 53.8	0.9983	0.9940	0.4	0.70
52-50		- 107.5	0.9911	0.9904	0.1	0.70
53-50		- 163.9	0.9861	0.9919	-0.6	0.70
54-50		- 217.6	0.9865	0.9881	-0.2	0.70
55-50		- 271.3	0.9910	1.0063	-1.5	0.70
56-50		- 325.1	0.9951	1.0033	-0.8	0.70
57-50		- 378.7	0.9951	1.0060	-1.1	0.70
58-50		- 435.1	0.9897	0.9962	-0.7	0.68
59-50		- 488.9	0.9806	0.9931	-1.3	0.70
60-50		- 542.6	0.9725	0.9833	-1.1	0.68
63-50	Outer Core	- 706.4	0.9281	0.9770	-5.0	0.72
66-50	Blanket	-.867.5	0.3596	0.3519	2.2	1.23
69-50		- 1031.3	0.0567	0.0612	-7.4	2.65

Table 4.18 Reaction Rate Comparison for B80(P1) + B90(Q)
Q is located between X= 408 and 516 mm and is adjacent to the central line of elements.
Fission Chamber Scans along the X axis. Diffusion Theory

The measurement positions in the X direction correspond approximately to the position between the two elements M and N denoted by M/N

Element		X	**Pu239**			
approx. X coordinate		(mm)	Calc	Exp	(C/E-1)%	s.d. %
33/34	Blanket	892.7	0.3155	0.3306	-4.6	0.87
36/37	Outer	728.9	0.3838	0.4120	-6.8	0.78
37/38	Core	675.2	0.4178	0.4512	-7.4	0.75
38/39		621.6	0.4419	0.4714	-6.3	0.32
39/40		567.8	0.4505	0.4772	-5.6	0.32
40/41		511.4	0.4427	0.4657	-4.9	0.31
41/42		457.7	0.4487	0.4727	-5.1	0.32
42/43		404.0	0.4899	0.5096	-3.9	0.33
43/44		350.3	0.5377	0.5519	-2.6	0.33
44/45		296.5	0.5655	0.5810	-2.7	0.33
45/46	Inner	240.2	0.6103	0.6258	-2.5	0.34
46/47	Core	186.5	0.7020	0.7157	-1.9	0.36
47/48		132.7	0.8095	0.8187	-1.1	0.34
48/49		79.0	0.8990	0.9016	-0.3	0.33
49/50		25.3	0.9706	0.9715	-0.1	0.32
50/51		- 31.1	1.0294	1.0285	0.1	0.32
51/52		- 84.8	1.0718	1.0635	0.8	0.31
52/53		-138.4	1.1023	1.0915	1.0	0.21
53/54		-192.1	1.1216	1.1104	1.0	0.31
56/57		-356.0	1.1162	1.1080	0.7	0.32
59/60		-517.2	1.0204	1.0204	0.0	0.32
62/63	Outer Core	-681.0	0.8201	0.8330	-1.5	0.33
65/66	Blanket	-844.9	0.6341	0.6165	2.9	0.34
68/69		-1005.9	0.3962	0.4464	-11.2	0.76

Table 4.18. continued. Reaction Rate Comparison for B80(P1) + B90(Q) Fission Chamber Scans along the X axis. Diffusion Theory

Element		X	**U238**			
approx. X coordinate		(mm)	Calc	Exp	(C/E-1)%	s.d. %
33/34	Blanket	892.5	0.1390	0.1329	4.6	2.01
36/37	Outer	728.9	0.4749	0.5109	-7.0	0.89
37/38	Core	675.2	0.5208	0.5548	-6.1	0.8
38/39		621.5	0.5194	0.5567	-6.7	0.68
39/40		567.8	0.4996	0.5178	-3.5	0.66
40/41		511.4	0.4840	0.5024	-3.7	0.67
41/42		457.7	0.4868	0.4941	-1.5	0.67
42/43		404.0	0.5185	0.5392	-3.8	0.69
43/44		350.3	0.5586	0.5720	-2.3	0.67
44/45		296.5	0.5895	0.5940	-0.8	0.66
45/46	Inner	240.2	0.6376	0.6301	1.2	0.70
46/47	Core	186.5	0.7214	0.7295	-1.1	0.71
47/48		132.7	0.8178	0.8161	0.2	0.68
48/49		79.0	0.9018	0.9031	-0.1	0.65
49/50		25.3	0.9710	0.9678	0.3	0.68
50/51		- 31.1	1.0290	1.0322	-0.3	0.67
51/52		- 84.8	1.0714	1.0653	0.6	0.66
52/53		-138.5	1.1021	1.0907	1.0	0.53
53/54		-192.2	1.1220	1.1066	1.4	0.65
56/57		-356.0	1.1239	1.1050	1.7	0.65
59/60		-517.2	1.0661	1.0487	1.7	0.66
62/63	Outer Core	-681.0	1.0195	1.0396	-1.9	0.67
65/66	Blanket	-844.8	0.4703	0.4796	-1.9	0.81
68/69		-1005.9	0.0723	0.0718	0.7	2.22

Table 4.19 Reaction Rate Comparison for BN(P1,P3,P5)
Foil measurements in the Inner Core. Transport Theory

Position	X (mm)	Y (mm)	**U235**			
			Calc	Exp	(C/E-1)%	s.d. %
47-48	163.8	-107.4	0.9181	0.9219	-0.4	0.31
48-48	107.4	-107.4	0.9715	0.9639	0.8	0.22
49-48	53.7	-107.4	0.9881	0.9924	-0.4	0.18
50-48	0.0	-107.4	0.9903	0.9883	0.2	0.17
51-48	-53.7	-107.4	0.9769	0.9732	0.4	0.21
52-48	-107.4	-107.4	0.9463	0.9490	-0.3	0.20
53-48	-163.8	-107.4	0.9141	0.9218	-0.8	0.24
53-49	-163.8	- 53.7	0.9683	0.9655	0.3	0.21
53-50	-163.8	0.0	0.9867	0.9846	0.2	0.21
53-51	-163.8	53.7	0.9904	0.9813	0.9	0.16
53-52	-163.8	107.4	0.9775	0.9785	-0.1	0.18
53-53	-163.8	163.8	0.9459	0.9415	0.5	0.20
53-54	-163.8	217.5	0.9103	0.9134	-0.3	0.24
50-53	0.0	163.8	0.9549	0.9547	0.0	0.20
49-52	53.7	107.4	0.9968	0.9921	0.5	0.18
48-51	107.4	53.7	0.9965	0.9797	1.7	0.17
47-50	163.8	0.0	0.9538	0.9714	-1.8	0.17
41-50	488.8	0.0	0.9254	0.9289	-0.4	0.25
50-50	0.0	0.0	1.0000	1.0000	0.0	0.16
59-50	-488.8	0.0	0.9365	0.9382	-0.2	0.17

Position	X (mm)	Y (mm)	**U238**			
			Calc	Exp	(C/E-1)%	s.d. %
47-48	163.8	-107.4	0.8836	0.8970	-1.5	0.34
48-48	107.4	-107.4	0.9689	0.9632	0.6	0.28
49-48	53.7	-107.4	0.9843	0.9885	-0.4	0.42
50-48	0.0	-107.4	0.9897	0.9880	0.2	0.36
51-48	-53.7	-107.4	0.9728	0.9782	-0.6	0.27
52-48	-107.4	-107.4	0.9260	0.9388	-1.4	0.28
53-48	-163.8	-107.4	0.8788	0.8972	-2.1	0.29
53-49	-163.8	- 53.7	0.9670	0.9648	0.2	0.31
53-50	-163.8	0.0	0.9848	0.9865	-0.2	0.55
53-51	-163.8	53.7	0.9913	0.9930	-0.2	0.27
53-52	-163.8	107.4	0.9737	0.9693	0.5	0.27
53-53	-163.8	163.8	0.9270	0.9223	0.5	0.28
53-54	-163.8	217.5	0.8800	0.8776	0.3	0.25
50-53	0.0	163.8	0.9364	0.9301	0.7	0.27
49-52	53.7	107.4	1.0033	0.9870	1.7	0.19
48-51	107.4	53.7	1.0033	0.9791	2.5	0.42
47-50	163.8	0.0	0.9352	0.9281	0.8	0.26
41-50	488.8	0.0	0.9670	0.9721	-0.5	0.27
50-50	0.0	0.0	1.0000	1.0000	0.0	0.40
59-50	-488.8	0.0	0.9833	0.9874	-0.4	0.36

Table 4.20 Reaction Rate Comparison for BN(P1,P3,P5)
Fission Chamber Scans along the X axis. Transport Theory

Position		X	**Pu239**			
			Calc	Exp	(C/E-1)%	s.d. %
31-50		1031.1	0.3527	0.4046	-12.8	0.73
34-50	Blanket	867.3	0.5888	0.6017	-2.1	0.83
37-50	Outer Core	706.1	0.7476	0.7620	-1.9	0.26
40-50		542.4	0.9072	0.9202	-1.4	0.33
41-50		488.7	0.9358	0.9415	-0.6	0.33
42-50		434.9	0.9519	0.9502	0.2	0.33
43-50		378.6	0.9530	0.9519	0.1	0.33
44-50		324.9	0.9361	0.9440	-0.8	0.33
45-50		271.1	0.9161	0.9251	-1.0	0.35
46-50		217.4	0.9221	0.9257	-0.4	0.35
47.50		163.7	0.9550	0.9569	-0.2	0.34
48-50	Inner	107.3	0.9855	0.9832	0.2	0.35
49-50	Core	53.6	0.9986	1.0028	-0.4	0.35
50-50		- 0.1	1.0019	1.0019	0.0	0.35
51-50		- 53.8	0.9994	0.9953	0.4	0.34
52-50		- 107.5	0.9931	0.9904	0.3	0.34
53-50		- 163.9	0.9886	0.9942	-0.6	0.34
54-50		- 217.6	0.9880	0.9887	-0.1	0.54
55-50		- 271.3	0.9900	0.9960	-0.6	0.34
56-50		- 325.1	0.9907	0.9959	-0.5	0.34
57-50		- 378.7	0.9849	0.9841	0.1	0.34
58-50		- 435.1	0.9711	0.9761	-0.5	0.34
59-50		- 488.9	0.9476	0.9536	-0.6	0.34
60-50		- 542.6	0.9144	0.9174	-0.3	0.35
63-50	Outer Core	- 706.4	0.7499	0.7610	-1.5	0.38
66-50	Blanket	-.867.5	0.5898	0.5973	-1.3	0.83
69-50		- 1031.3	0.3532	0.4046	-12.7	1.00

Table 4.20 continued. Reaction Rate Comparison for BN(P1,P3,P5). Fission Chamber Scans along the X axis. Transport Theory

Position		X	U238			
			Calc	Exp	(C/E-1)%	s.d. %
31-50		1031.1	0.0581	0.0595	-2.4	2.76
34-50	Blanket	867.3	0.3485	0.3449	1.0	1.24
37-50	Outer Core	706.1	0.9746	0.9892	-1.5	0.74
40-50		542.4	0.9606	0.9621	-0.2	0.71
41-50		488.7	0.9675	0.9727	-0.5	0.62
42-50		434.9	0.9709	0.9706	0.0	0.70
43-50		378.6	0.9562	0.9574	-0.1	0.71
44-50		324.9	0.9204	0.9182	0.2	0.72
45-50		271.1	0.8845	0.8874	-0.3	0.70
46-50		217.4	0.8889	0.8901	-0.1	0.70
47.50		163.7	0.9357	0.9483	-1.3	0.71
48-50	Inner	107.3	0.9813	0.9886	-0.7	0.73
49-50	Core	53.6	0.9976	0.9997	-0.2	0.70
50-50		- 0.1	1.0005	1.0063	-0.6	0.70
51-50		- 53.8	1.0018	0.9940	0.8	0.70
52-50		- 107.5	0.9904	0.9904	0.0	0.70
53-50		- 163.9	0.9853	0.9919	-0.7	0.70
54-50		- 217.6	0.9868	0.9881	-0.1	0.70
55-50		- 271.3	0.9938	1.0063	-1.2	0.70
56-50		- 325.1	1.0024	1.0033	-0.1	0.70
57-50		- 378.7	1.0017	1.0060	-0.4	0.70
58-50		- 435.1	0.9979	0.9962	0.2	0.68
59-50		- 488.9	0.9838	0.9931	-0.9	0.70
60-50		- 542.6	0.9691	0.9833	-1.4	0.68
63-50	Outer Core	- 706.4	0.9778	0.9770	0.1	0.72
66-50	Blanket	-.867.5	0.3493	0.3519	-0.7	1.23
69-50		- 1031.3	0.0582	0.0612	-4.9	2.65

Table 4.21 Reaction Rate Comparison for B80(P1) + B90(Q)
Fission Chamber Scans along the X axis. Transport Theory

Element	X		**Pu239**			
approx. X coordinate	(mm)		Calc	Exp	(C/E-1)%	s.d. %
33/34	892.7	Blanket	0.3145	0.3306	-4.9	0.87
36/37	728.9	Outer	0.3912	0.4120	-5.0	0.78
37/38	675.2	Core	0.4237	0.4512	-6.1	0.75
38/39	621.6		0.4443	0.4714	-5.7	0.32
39/40	567.8		0.4454	0.4772	-6.7	0.32
40/41	511.4		0.4324	0.4657	-7.2	0.31
41/42	457.7		0.4377	0.4727	-7.4	0.32
42/43	404.0		0.4760	0.5096	-6.6	0.33
43/44	350.3		0.5203	0.5519	-5.7	0.33
44/45	296.5		0.5484	0.5810	-5.6	0.33
45/46	240.2	Inner	0.5953	0.6258	-4.9	0.34
46/47	186.5	Core	0.6873	0.7157	-4.0	0.36
47/48	132.7		0.7999	0.8187	-2.3	0.34
48/49	79.0		0.8962	0.9016	-0.6	0.33
49/50	25.3		0.9697	0.9715	-0.2	0.32
50/51	- 31.1		1.0303	1.0285	0.2	0.32
51/52	- 84.8		1.0740	1.0635	1.0	0.31
52/53	-138.4		1.1054	1.0915	1.3	0.21
53/54	-192.1		1.1259	1.1104	1.4	0.31
56/57	-356.0		1.1236	1.1080	1.4	0.32
59/60	-517.2		1.0311	1.0204	1.0	0.32
62/63	-681.0	Outer Core	0.8403	0.8330	0.9	0.33
65/66	-844.9	Blanket	0.6257	0.6165	1.5	0.34
68/69	-1005.9		0.4057	0.4464	-9.1	0.76

Table 4.21 continued. Reaction Rate Comparison for B80(P1) + B90(Q) - Fission Chamber Scans along the X axis. Transport Theory

Element	X		U238			
approx. X coordinate	(mm)		Calc	Exp	(C/E-1)%	s.d. %
33/34	892.7	Blanket	0.1309	0.1329	-1.5	2.01
36/37	728.9	Outer	0.4998	0.5109	-2.2	0.89
37/38	675.2	Core	0.5390	0.5548	-2.8	0.8
38/39	621.6		0.5284	0.5567	-5.1	0.68
39/40	567.8		0.4930	0.5178	-4.8	0.66
40/41	511.4		0.4694	0.5024	-6.6	0.67
41/42	457.7		0.4739	0.4941	-4.1	0.67
42/43	404.0		0.5047	0.5392	-6.4	0.69
43/44	350.3		0.5440	0.5720	-4.9	0.67
44/45	296.5		0.5736	0.5940	-3.4	0.66
45/46	240.2	Inner	0.6213	0.6301	-1.4	0.70
46/47	186.5	Core	0.7061	0.7295	-3.2	0.71
47/48	132.7		0.8101	0.8161	-0.7	0.68
48/49	79.0		0.9017	0.9031	-0.2	0.65
49/50	25.3		0.9702	0.9678	0.2	0.68
50/51	- 31.1		1.0298	1.0322	-0.2	0.67
51/52	- 84.8		1.0740	1.0653	0.8	0.66
52/53	-138.4		1.1050	1.0907	1.3	0.53
53/54	-192.1		1.1262	1.1066	1.8	0.65
56/57	-356.0		1.1288	1.1050	2.2	0.65
59/60	-517.2		1.0677	1.0487	1.8	0.66
62/63	-681.0	Outer Core	1.0659	1.0396	2.5	0.67
65/66	-844.9	Blanket	0.4749	0.4796	-1.0	0.81
68/69	-1005.9		0.0745	0.0718	3.8	2.22

Table 4.22 Reaction Rate Comparison for B80(O) Foils. Transport Theory.

Position	X	Y	**U235**			
	(mm)	(mm)	Calc	Exp	(C/E-1)%	s.d. %
40-50	542.5	0.0	1.000	1.0000		0.32
43-50	379.8	0.0	1.1208	1.1174	0.3	0.31
46-50	217.0	0.0	1.1237	1.1305	-0.6	0.26
48-50	108.5	0.0	1.0193	1.0317	-1.2	0.32
49-50	54.3	0.0	0.8740	0.9219	-5.2	0.60
52-50	-108.5	0.0	0.8608	0.9109	-5.5	0.39
53-50	-162.8	0.0	0.9947	1.0181	-2.3	0.32
55-50	-271.3	0.0	1.0792	1.0912	-1.1	0.27
58-50	-434.0	0.0	1.0494	1.0557	-0.6	0.27
61-50	-596.8	0.0	0.9008	0.9127	-1.3	0.53
Centre Pin			0.4835	0.4460	8.4	0.34
Inner Ring			0.5042	0.4651	8.4	0.46
Outer Ring			0.5774	0.5341	8.1	0.58

Position	X	Y	**U238**			
	(mm)	(mm)	Calc	Exp	(C/E-1)%	s.d. %
40-50	542.5	0.0	1.0000	1.0000		0.67
43-50	379.8	0.0	1.0683	1.0651	0.3	1.07
46-50	217.0	0.0	1.0646	1.0678	-0.3	0.90
48-50	108.5	0.0				
49-50	54.3	0.0	0.8721	0.8818	-1.1	0.76
52-50	-108.5	0.0	0.8604	0.8879	-3.1	1.03
53-50	-162.8	0.0				
55-50	-271.3	0.0	1.0255	1.0327	-0.7	0.75
58-50	-434.0	0.0	1.0099	1.0089	0.1	0.68
61-50	-596.8	0.0	0.9667	0.9696	-0.3	0.72
Centre Pin			0.6622	0.6380	3.8	1.18
Inner Ring			0.6774	0.6470	4.7	1.09
Outer Ring			0.7247	0.6876	5.4	0.80

Table 4.23 Comparison of MURAL Supercell Methods for B80(O). U235 Foils

Position	Exp	MURAL-PIJ		MURAL (cylindrical)		MURAL at Centre Plane	
		Calc	C/E	Calc	C/E	Calc	C/E
40-50	1.0000	1.0000	0.0	1.0000	0.0	1.0000	0.0
43-50	1.1174	1.1267	0.8	1.1253	0.7	1.1236	0.6
46-50	1.1305	1.1354	0.4	1.1308	0.0	1.1293	-0.1
48-50	1.0317	1.0347	0.3	1.0246	-0.7	1.0245	-0.7
49-50B	0.9758	0.9641	-1.2	0.9501	-2.6	0.9508	-2.6
49-50	0.9219	0.9141	-0.8	0.8973	-2.7	0.8985	-2.5
49-50A	0.8647	0.8583	-0.7	0.8386	-2.3	0.8403	-2.8
52-50F	0.8725	0.8561	-1.9	0.8436	-3.3	0.8453	-3.1
52-50	0.9109	0.9006	-1.1	0.8838	-3.0	0.8851	-2.8
52-50E	0.9454	0.9385	-0.7	0.9239	-2.3	0.9250	-2.2
53-50	1.0181	1.0117	-0.6	1.0014	-1.6	1.0017	-1.6
55-50	1.0912	1.0939	0.2	1.0890	-0.2	1.0881	-0.3
58-50	1.0557	1.0586	0.3	1.0567	0.1	1.0560	0.0
61-50	0.9127	0.9042	-0.9	0.9036	-1.0	0.9051	-0.8
49-49D	1.0391	1.0316	-0.7	1.0211	-1.7	1.0210	-1.7
49-49C	0.9526	0.9447	-0.8	0.9296	-2.4	0.9504	-2.3
Centre Pin	0.4460	0.4908	10.0	0.4800	7.6	0.4907	10.0
Inner Ring	0.4651	0.5112	9.9	0.4994	7.4	0.5099	9.6
Outer Ring	0.5341	0.5835	9.2	0.5673	6.2	0.5767	8.0

4.7.2 Comparison of Measurement with Calculation for the Axial Scans. The array BN(P1,P3,P5) fully inserted and half inserted.

These calculations and description are from MTN/100 by P J Collins.

Axial fission chamber scans were measured in two of the control rod configurations. These have three natural boron rods in a triangular array. In the first configuration, BN(P1,P3,P5), the rods were fully inserted in the core and in the second BN/2(P1,P3,P5) the rods were half inserted. The calculations for these cases, described in MTN/100, were made used the TIGAR diffusion theory code in XYZ geometry, with 9 group data as in the standard control rod analysis method. A radial scan calculation is also made for the BN/2(P1,P3,P5) case.

Calculation Method

The calculations were made for the critical loading in each case, 264 + 54 outer core elements for the 3 x BN/2 Array (Experiment 38/1) and 264 + 80 outer core elements for the 3 x BN Array (Experiment 37/2). A full-plan full-height XYZ model was used in the TIGAR calculations with one mesh point per element in the XY plane compared with four mesh points per element in the standard XY geometry model (the standard method). The axial mesh, starting at the top of the reactor (cm), was
2*11.04 10.95 3*6.58 2*7.60 16*5.575 2*7.60 3*6.58 3*11.01

The 9 group data generated for the standard method control rod calculations was used. The ZEBRA control rod followers were included in the models for rods 1 to 8 but not for rod 9. FD5 data was used for these (MTN/81) instead of the FGL5 2000 fine group data library which was used in the MURAL cell calculations made to produce the cross-sections for the core cells and the absorber rods. The ends of the absorber section of the rods were located at 7.6 cm above the top of the core for rods 3 and 4 and at 15.2 cm for the remaining rods. Effective anisotropic diffusion coefficients were used for the MONJU mock-up followers. These were generated by the method described by Sugawara in the Addendum to MTN/85 and are compared with the isotropic values in this reference. The steel end-caps of the MONJU rods were not included in the model and the top of the absorber section was positioned at the mid-plane in the half-inserted case and at the bottom of the core in the fully inserted case. The height of the radial blanket was increased slightly to avoid a small mesh step. Otherwise the zone heights (but not the mesh sizes) were the same as for the standard model of MZB (MTN/43).

The TIGAR runs were converged to accuracy of 0.00001. The eigenvalues obtained were:
BN (P1,P3,P5) : 0.99786
BN/2 (P1,P3,P5) : 0.99770
The standard method, XY calculation, with region and energy group dependent axial bucklings to treat axial leakage, gave a value of 0.99547 for this first case. The TIGAR 3D calculations had one mesh point per element whereas the XY geometry calculations with axial bucklings had 4 mesh points per element. Using 1 mesh point per element and an explicit representation of the axial dimension is resulting in a difference in k_{eff} of 0.00239.

The reaction rates were computed using the microscopic cross-sections for radial and axial chambers described by Nakano in MTN/70, condensed to nine groups with the same spectra as for the macroscopic data. The reaction rates at the mesh intervals of the calculation model were interpolated to the experimental positions. The three nearest points to the required position were used for interpolation except near the core/blanket boundary, where points within the same zone were used.

Axial Scans in BN(P1,P3,P5)

The calculated and experimental scans along the central axis, for the configuration with the three rods fully inserted, are compared in Tables 4.24 and 4.25. **The experimental co-ordinates in the Tables of Section 1.7 (from MTN/85) have been modified by -0.25 cm to make them relative to the mean core-centre plane, as described in this reference. The calculated distributions have been displaced 0.85 cm downwards to adjust the effective centres to those of the experiments, to allow for the axial asymmetry of the inner core cell, based on the analysis of the axial scans described in MTN/70**. In the tables, the axial distances are relative to the mean core centre plane and are negative in the top half of the core to conform with the tables in MTN/89. The experimental values have been renormalised so that the mean square deviation between C and E, weighted with the statistical errors, is minimised over the height over the core. The factor employed is given by the experimental value at the position, nearest to the mid-plane, where the calculation is normalised to unity. This normalisation was chosen because of the marked asymmetry in the scans for the case with the rods half inserted.

Comparison of the Measurements in BN(P1,P3,P5) with the MZB Scans without Mock-up Rods.

The BN(P1,P3,P5) scans (Tables 4.24 and 4.25) can be compared with those for MZB, with no mock-up rods inserted, as given in MTN/70 (Tables 17 and 19). For both the Pu239 and U238 scans the C/E values, with and without the rods inserted, are in broad agreement (~ ± 6%), the differences being largest at the outermost positions in the axial blanket, 30 cm from the core boundary (apart from the discrepancy for U238 in the lower axial blanket, near the boundary). In MTN/70 corrections, of up to 2% in the outer regions, were derived for the mesh size effect. No corrections have been applied for this approximation in Tables 4.24 and 4.25. The comparison shows that the introduction of the rods results in no significant increase in the calculational error over the core region and inner part of the blanket, but that larger differences occur at positions deep in the blanket.

Axial Scans with the Array of Half Inserted Rods, BN/2(P1,P3,P5)

Fission rate distributions for the configuration with the three rods half inserted in the core are compared in Tables 4.26 and 4.27, for the central axis (position 50-50), and in Tables 4.28 and 4.29, for position 53-48 in the element adjacent to one of the rods. The calculated distributions have been displaced 8.5 mm downwards, as described above, and the normalisation has been chosen to minimise the calculational error over the core height. Each scan is normalised separately.

Over the core region, the C/E values are similar for the positions along the central axis (Tables 4.26, 4.27) or in element (53-48) adjacent to the absorbing rod (Tables 4.28, 4.29). The Pu239 fission rate is calculated about 2% low for the positions between 3 cm and 4 cm from the core boundary (± 44.6 cm), but otherwise is within 1% of experiment. The U238 fission rate is calculated 1% high at the top of the core but 2% low at the bottom of the core. These results are similar to those for the rods fully inserted (Tables 4.24 and 4.25).

The calculated Pu239 fission rates at positions deep in the axial blanket (30 cm from the core boundary) are 10% low at the top of the reactor near the mock-up rods and about 15% low at the bottom. These discrepancies are a few percent worse than those with the rods fully inserted. The U238 fission rates are calculated up to 10% too high in both the upper and lower blankets and are 5% to 10% worse than with the rods fully inserted when the maximum discrepancy is about 4% (as can be seen by comparing Tables 4.27 and 4.29 with Table 4.25). These results change by less than 0.6% if the scans are normalised near the core centre rather than over the core height.

Radial Scans in BN/2(P1,P3,P5)

Radial reaction rate scans at the reactor mid plane, with the mock-up rods half inserted are compared in Table 4.30. The calculations were interpolated axially to give values for the mid plane, since this position was not contained in the basic mesh. In the XY plane, small differences arise between the mean element positions, used in the calculation model, and the actual positions in ZEBRA. These were insignificant near the centre where the flux gradients are small, but the calculations were interpolated to the true positions for the outermost points, beyond 50 cm from the centre.

The results in Table 4.30 may be compared with those for the three rods fully inserted (MTN/93 Table 7). The calculations in this latter case were made with the standard method, XY geometry, multi-bucklings and doubled mesh in the core and part of the blanket. For U238(n,f), the C/E values are in close agreement in the core. For the blanket positions differences of a few percent could be due to the different diffusion theory methods and models used in the calculations.

However, for the Pu239 fission rate distribution significant differences in C/E are obtained in the core zone. Examination of the results shows that both sets of calculations are radially symmetric in the outer parts of the core, away from the rods, and in the blanket. On the other hand the experimental results in the half-inserted rod case are markedly asymmetric while those in the fully-inserted case are again symmetric. **Thus the experimental results for Pu239 in the 3 x BN/2 case are suspect.** After completion of the Pu239 radial scan in the BN/2(P1,P3,P5) arrangement, a change in the datum reading of 1.98 cm was noticed. No such change was observed in any other scan. It was believed at the time that this change occurred whilst removing the chamber at the end of the scan and the analysis proceeded on this basis. Comparison of the C/E values for Pu239(n,f) in Table 4.30 with those from similar scans (MTN/93) suggests that the change in datum reading occurred near the beginning of the scan. The most likely fault in the scanner mechanism is for the measuring tape to jump one or more sprockets on the digitiser drive wheel which would result in changes to the apparent measuring position in multiples of (1.00 ± 0.02) cm which is consistent with the change of 1.98 cm. If it is assumed that the change occurred before the start of the scan all positions would be wrong by 2.0 ± 0.03 cm. In Table 4.31 the results have been altered to allow for the chamber being 2.0 cm closer to the scanner than indicated. This results in C/E values closer to those observed in similar scans although there are still anomalies, particularly near the positive extremity. In view of this it is recommended that the experimental results in Table 4.31 are the preferred values, but, since the reason for the fault is not entirely clear, **low weight should be attached to these in comparisons made with calculation**.

Summary of the Axial Scan Comparisons

For the mock-up rods fully inserted, the results compare well with experiment within the core, but discrepancies, of up to 13%, arise for Pu239 fission at positions deep in the axial blanket. The results are similar to axial scan comparisons for a core with no mock-up rods present, except at the extremities of the scan. The results with the rods half inserted are similarly good within the core but tend to be in worse agreement within the blanket than with the rods fully inserted.

Significant transport theory corrections to the diffusion theory whole assembly calculations were found in other axial scan analyses (MTN/70). These are expected to be important in the present case, particularly for scans immediately adjacent to a mock-up rod.

Table 4.24 Pu239 Fission Axial Scan in the Element at Position (50-50) for Rods BN(P1,P3,P5)

Pu239					
Distance from Centre (cm)		Renormalised Fission Rate	Calc	(C/E-1)%	S.D. (%)
-75.66		0.2591	0.2653	2.4	0.98
-66.88	Axial	0.3417	0.3529	3.3	0.98
-58.11	Blanket	0.4533	0.4754	4.9	0.96
-49.34		0.5566	0.5847	5.0	0.85
-41.19		0.6018	0.5890	-2.1	0.45
-33.07		0.6973	0.6970	0.0	0.45
-24.95		0.8075	0.8140	0.8	0.43
-16.82		0.9021	0.9093	0.8	0.44
-6.70		0.9656	0.9732	0.8	0.42
-0.58		0.9939	1.0000	0.6	0.30
7.55		0.9854	0.9881	0.3	0.41
15.67		0.9332	0.9384	0.6	0.41
23.79		0.8594	0.8542	-0.6	0.54
31.91		0.7523	0.7445	-1.0	0.45
40.05		0.6433	0.6316	-1.8	0.52
48.80		0.5903	0.6210	5.2	0.83
57.57	Axial	0.5081	0.5221	2.8	0.90
66.36	Blanket	0.4138	0.4033	-2.5	0.99
75.12		0.3530	0.3060	-13.3	1.06

Note: -0.25 cm has been added to the axial coordinates given in the Tables of Section 1.7.
The measured fission rates have also been renormalised, in this case by the factor 0.9939.

Table 4.25 U238 Fission Axial Scan in the Element at Position (50-50) for Rods BN(P1,P3,P5)

U238					
Distance from Centre (cm)		Renormalised Fission Rate	Calc	(C/E-1)%	S.D. (%)
-75.66		0.0238	0.0243	2.1	2.69
-66.88	Axial	0.0468	0.0482	3.0	2.02
-58.11	Blanket	0.0916	0.0935	2.1	1.72
-49.34		0.1995	0.2076	4.1	1.40
-41.19		0.4509	0.4619	2.4	0.76
-33.07		0.6606	0.6585	-0.3	0.59
-24.94		0.7948	0.8019	0.9	0.40
-16.82		0.9033	0.9059	0.3	0.53
-6.70		0.9696	0.9724	0.3	0.51
-0.58		0.9998	1.0000	0.0	0.51
7.55		0.9851	0.9878	0.3	0.51
15.67		0.9354	0.9364	0.1	0.52
23.79		0.8544	0.8464	-0.9	0.52
31.91		0.7264	0.7173	-1.3	0.55
40.05		0.5481	0.5422	-1.1	0.66
48.80		0.2632	0.2531	-3.8	1.31
57.57	Axial	0.1161	0.1165	0.3	1.51
66.35	Blanket	0.0571	0.0577	1.1	1.78
75.12		0.0292	0.0304	4.1	2.14

Note: -0.25 cm has been added to the axial coordinates given in the Tables of Section 1.7.
The measured fission rates have also been renormalised, in this case by the factor 0.9998.

Table 4.26 Pu239 Fission Axial Scan in the Element at Position (50-50) for Rods BN/2(P1,P3,P5)

Pu239					
Distance from Centre (cm)		Renormalised Fission Rate	Calc	(C/E-1)%	S.D. (%)
-75.30		0.2168	0.1968	-9.2	1.02
-66.53	Axial	0.2935	0.2773	-5.5	1.01
-57.78	Blanket	0.3885	0.3876	-0.2	0.96
-49.02		0.4851	0.4927	1.6	0.86
-40.90		0.5550	0.5454	-1.7	0.51
-32.78		0.6622	0.6589	-0.5	0.47
-24.68		0.7700	0.7795	1.2	0.46
-16.57		0.8761	0.8816	0.6	0.44
-8.47		0.9507	0.9573	0.7	0.42
-0.35		0.9959	1.0000	0.4	0.44
7.75		1.0068	1.0047	-0.2	0.43
15.87		0.9666	0.9679	0.1	0.42
23.98		0.8917	0.8918	0.0	0.44
32.09		0.7852	0.7837	-0.2	0.45
40.18		0.6767	0.6685	-1.2	0.50
48.92		0.6194	0.6221	0.4	0.72
57.69	Axial	0.5282	0.5186	-1.8	0.79
66.45	Blanket	0.4243	0.3967	-6.5	0.87
75.20		0.3554	0.2979	-16.2	0.94

Note: -0.25 cm has been added to the axial coordinates given in the Tables of Section 1.7.
The measured fission rates have also been renormalised, in this case by the factor 0.9959.

Table 4.27 U238 Fission Axial Scan in the Element at Position (50-50) for Rods BN/2(P1,P3,P5)

U238					
Distance from Centre (cm)		Renormalised Fission Rate	Calc	(C/E-1)%	S.D. (%)
-75.30		0.0200	0.0220	10.0	2.80
-66.54	Axial	0.0423	0.0448	5.9	2.04
-57.78	Blanket	0.0873	0.0899	3.0	1.61
-49.02		0.1842	0.2039	10.7	1.53
-40.90		0.4333	0.4377	1.0	0.81
-32.77		0.6255	0.6261	0.1	0.59
-24.67		0.7706	0.7689	-0.2	0.45
-16.57		0.8912	0.8789	-1.4	0.52
-8.47		0.9541	0.9569	0.3	0.50
-0.34		0.9942	1.0000	0.6	0.56
7.75		1.0009	1.0040	0.3	0.52
15.86		0.9631	0.9650	0.2	0.54
23.96		0.8710	0.8824	1.3	0.54
32.08		0.7583	0.7533	-0.7	0.59
40.18		0.5810	0.5718	-1.6	0.71
48.92		0.2731	0.2766	1.3	1.32
57.69	Axial	0.1212	0.1272	5.0	1.41
66.45	Blanket	0.0613	0.0628	2.4	1.74
75.20		0.0300	0.0330	10.0	4.14

Note: -0.25 cm has been added to the axial coordinates given in the Tables of Section 1.7.
The measured fission rates have also been renormalised, in this case by the factor 0.9942.

Table 4.28 Pu239 Fission Axial Scans in the element at position (53-48) for Rods BN/2(P1,P3,P5)

Pu239					
Distance from Centre (cm)		Renormalised Fission Rate	Calc	(C/E-1)%	S.D. (%)
-75.30		0.1858	0.1638	-11.8	1.04
-66.55	Axial	0.2497	0.2372	-5.0	1.06
-57.78	Blanket	0.3485	0.3400	-2.4	1.00
-49.02		0.4548	0.4469	-1.7	0.87
-40.89		0.5268	0.5201	-1.3	0.44
-32.78		0.6385	0.6373	-0.2	0.42
-24.67		0.7480	0.7572	1.2	0.36
-16.57		0.8498	0.8588	1.1	0.26
-8.47		0.9287	0.9380	1.0	0.34
-0.35		0.9943	1.0000	0.6	0.33
7.75		1.0277	1.0336	0.6	0.34
15.86		1.0076	1.0055	-0.2	0.33
23.97		0.9344	0.9298	-0.5	0.35
32.07		0.8339	0.8221	-1.4	0.27
40.18		0.7227	0.7049	-2.5	0.37
48.92		0.6619	0.6560	-0.9	0.72
57.69	Axial	0.5678	0.5483	-3.4	0.78
66.45	Blanket	0.4602	0.4235	-8.0	0.86
75.20		0.3774	0.3209	-15.0	0.95

Note: -0.25 cm has been added to the axial coordinates given in the Tables of Section 1.7.
The measured fission rates have also been renormalised, in this case by the factor 0.9943.

Table 4.29 U238 Fission Axial Scans in the element at position (53-48) for Rods BN/2(P1,P3,P5)

U238					
Distance from Centre (cm)		Renormalised Fission Rate	Calc	(C/E-1)%	S.D. (%)
-75.30		0.0206	0.0224	8.7	2.69
-66.54	Axial	0.0441	0.0462	4.8	2.02
-57.78	Blanket	0.0886	0.0927	4.6	1.72
-49.02		0.1976	0.2058	4.1	1.40
-40.90		0.4250	0.4294	1.0	0.76
-32.78		0.6128	0.6135	0.1	0.59
-24.69		0.7509	0.7551	0.6	0.40
-16.57		0.8544	0.8656	1.3	0.53
-8.47		0.9481	0.9465	-0.2	0.51
-0.35		1.0010	1.0000	-0.1	0.51
7.75		1.0164	1.0156	-0.1	0.51
15.86		0.9778	0.9807	0.3	0.52
23.97		0.8932	0.8972	0.4	0.52
32.08		0.7814	0.7655	-2.0	0.55
40.18		0.5956	0.5827	-2.2	0.66
48.92		0.2934	0.2944	0.3	1.31
57.69	Axial	0.1307	0.1411	8.0	1.51
66.45	Blanket	0.0641	0.0709	10.6	1.78
75.20		0.0339	0.0374	10.3	2.14

Note: -0.25 cm has been added to the axial coordinates given in the Tables of Section 1.7.
The measured fission rates have also been renormalised, in this case by the factor 1.0010.

Table 4.30 Radial Reaction Rate Comparison for BN/2(P1,P3,P5) - Fission Chambers

Position	X (mm)	Pu239 (n,f)			X (mm)	U238 (n,f)		
		Calc	Exp[a]	(C/E-1)%		Calc	Exp[b]	(C/E-1)%
32-50	975.6	0.3698	0.4206	1.2	975.6	0.0841	0.0795	5.8
34-50	865.8	0.5200	0.5137	-6.5	865.7	0.2944	0.2979	-1.2
37-50	705.0	0.6520	0.6970	-2.9	704.9	0.8249	0.8605	-4.1
40-50	541.4	0.8304	0.8554	-2.2	541.4	0.8871	0.8778	1.1
41-50	487.8	0.8691	0.8884	-2.1	487.8	0.9036	0.9065	-0.3
42-50	434.1	0.8994	0.9182	-1.3	434.2	0.9173	0.9201	-0.3
43-50	377.9	0.9175	0.9298	-0.9	377.9	0.9238	0.9290	-0.6
44-50	324.3	0.9333	0.9416	-1.8	324.4	0.9181	0.8995	2.1
45-50	270.6	0.9395	0.9570	-0.9	270.6	0.9022	0.8980	0.5
46-50	216.9	0.9528	0.9615	-1.1	217.0	0.9141	0.9098	0.5
47-50	163.4	0.9744	0.9849	-0.8	163.4	0.9545	0.9477	0.7
48-50	107.1	0.9908	0.9989	-0.1	107.1	0.9839	0.9913	-0.7
49-50	53.5	0.9998	1.0011	0.1	53.5	0.9990	0.9986	0.0
50-50	-0.1	1.0017	1.0003	0.0	-0.1	1.0026	1.0052	-0.3
51-50	-53.7	0.9985	0.9987	1.0	-53.7	0.9984	0.9962	0.2
52-50	-107.3	0.9919	0.9825	0.1	-107.3	0.9900	0.9942	-0.4
53-50	-163.6	0.9836	0.9830	0.0	-163.6	0.9810	0.9835	-0.2
54-50	-217.2	0.9750	0.9749	1.5	-217.2	0.9743	0.9777	-0.3
55-50	-270.9	0.9651	0.9513	0.6	-270.8	0.9688	0.9698	-0.1
56-50	-324.5	0.9515	0.9457	1.5	-324.5	0.9608	0.9672	-0.7
57-50	-378.1	0.9322	0.9180	1.2	-378.1	0.9482	0.9512	-0.3
58-50	-434.3	0.9064	0.8957	1.1	-434.3	0.9307	0.9234	0.8
59-50	-488.0	0.8730	0.8637	1.7	-488.0	0.9102	0.5174	-0.8
60-50	-541.6	0.8323	0.8181	1.7	-541.6	0.8904	0.8870	0.4
63-50	-705.1	0.6523	0.6414	3.6	-705.1	0.8238	0.8646	-4.7
66-50	-865.9	0.5188	0.5010	-1.9	-865.9	0.2932	0.3014	-2.7
68-50	-975.8	0.3684	0.3755	-11.1	-975-8	0.0836	0.0807	3.5
69-50	-1029.4	0.2904	0.3267	1.2	-1029.4	0.0474	0.0490	-3.3

a Statistical errors typically 0.35% except near the ends of the scan (see MTN/89)
b Statistical errors typically 0.60% except near the ends of the scan (see MTN/89)

Table 4.31 Pu239(n,f) Distribution Calculated for BN/2(P1.P3,P5) Compared with Adjusted Experimental Values

X (mm)		Pu239(n,f)		
		Experiment Adjusted	Calc	(C/E-1)%
975.6		0.4044	0.3698	-8.6
865.8	Blanket	0.4939	0.5200	5.3
705.0	Outer Core	0.6758	0.6520	-3.5
541.4		0.8409	0.8304	-1.2
487.8		0.8761	0.8691	-0.8
434.1		0.9104	0.8994	-1.2
377.9		0.9228	0.9175	-0.6
324.3		0.9364	0.9333	-0.3
270.6		0.9543	0.9395	-1.6
216.9		0.9561	0.9528	-0.3
163.4		0.9794	0.9744	-0.5
107.1	Inner	0.9961	0.9908	-0.5
53.5	Core	1.0011	0.9998	-0.1
-0.1		1.0003	1.0017	0.1
-53.7		1.0015	0.9985	-0.3
-107.3		0.9852	0.9919	0.7
-165.6		0.9858	0.9836	-0.2
-217.2		0.9804	0.9750	-0.6
-270.9		0.9566	0.9651	0.9
-324.5		0.9510	0.9515	0.1
-378.1		0.9259	0.9322	0.7
-434.3		0.9059	0.9064	0.1
-488.0		0.8786	0.8730	-0.6
-541.6		0.8368	0.8323	-0.5
-705.1	Outer Core	0.6615	0.6523	-1.4
-865.9	Blanket	0.5210	0.5188	-0.4
-975.8		0.3959	0.3684	-6.9

REFERENCES

MOZART TECHNICAL NOTE SERIES (Documents on the dvd available from the OECD-NEA)

Authors	Title	Number
J. M. Stevenson, S. F. Swoboda	Revised Proposal for Mozart Assemblies	MTN1
J. E. Sanders	Outline Programme of Control Rod Measurements in MZC	MTN2
J. L. Butler	Proposals for the Kochel Programme of Energy-Deposition and Penetration Measurements on the Zebra Mozart Cores	MTN3
C. McCombie	Calculations in support of Spectrum Measurements in MZA	MTN4
J. M. Stevenson, S. F. Swoboda	Description of Subcritical and Standard Critical Loadings of Zebra 11 (MZA)	MTN5
J. Marshall, J. M. Stevenson, S. F. Swoboda	Control Rod Calibrations in Zebra 11 (MZA)	MTN6
T. Konishi, J. Marshall	Zebra Core 11 (MZA) Number Densities (Computer Print - Out) Volume 1, 2 And 3	MTN7
J. M. Stevenson, S. F. Swoboda	Further Information on the Experimental Reactivity of the 213 Core Element Loading of Zebra 11 (MZA)	MTN8
J. M. Stevenson, S. F. Swoboda	Further Information on the Experimental Reactivity of the 213 Core Element Loading Of Zebra 11 (MZA)	MTN8-ADD
J. M. Stevenson, S. F. Swoboda	Reactivity Measurements with Plate Samples in Zebra 11 (MZA)	MTN9
M. D. Carter, J. Samways	Spectrum Measurements with Proton -Recoil Counters In Zebra 11 (MZA)	MTN10
J. P. Hardiman, B. Franklin	Re-Evaluation of Time-Of-Flight Spectra in Zebra Core 11 (MZA)	MTN11
J. M. Stevenson	Experiment B10 (3) (Comparison of Reactivity Scales)	MTN12
J. M. Stevenson, S. F. Swoboda	Sodium Removal Reactivity Measurements in Zebra 11 (MZA)	MTN13
B. L. M. Burbidge, G. Ingram, D. Jowitt, Miss M. P. Smith, Miss P. A. Smart, D. Sweet	Central Reaction Rate Ratio Measurements in Zebra Core 11	MTN14
H. Yoshida	Analyses of Central Perturbation Measurements in Zebra 10	MTN15
J. M. Stevenson, S. F. Swoboda	The Final Design of MZB	MTN16
A. Sugawara	An Estimate of the MZC Reactivity Requirements and the Number of Outer Core Elements to be added to MZB	MTN17
J. M. Stevenson, S. F. Swoboda	Description of the Standard Loading of Zebra Assembly 12(1) - The First Version Of MZB	MTN18
H. Yoshida	Analysis of Sodium Removal Reactivity Measurements in Zebra 11 (MZA)	MTN19
H. Yoshida	Analysis Of Central Perturbation Measurements In Zebra 11 (Mza)	MTN20
A. K. McCracken, A. Packwood	Details of the Irradiations in the Kochel Programme on the MZB Core	MTN21
A. K. McCracken	MTN/21 Amendment 1	MTN21-AM1
A. K. McCracken	MTN/21 Amendment 2	MTN21-AM2

M. D. Carter, J. Samways	Energy Uncertainties near 30 Kev in Proton Recoil Counter Spectrum Measurements in Zebra 11 (MZA)	MTN22
J. Marshall, J. M. Stevenson, S. F. Swoboda	Control Rod Calibrations in Zebra 12(1) - The First Version of MZB	MTN23
B. L. H. Burbidge, G. Ingram, D. W. Sweet, W. H. Taylor	Reaction Rate Scans Using Foils in Zebra Core 11	MTN24
J. M. Stevenson, S. F. Swoboda	The Experimental Reactivity of the Standard Loading of Zebra 12/1 - The First Version of MZB	MTN25
J. M. Stevenson, S. F. Swoboda	Additional Perturbation Measurements in MZB/1	MTN26
G. Ingram	Simulated Vapour Explosion and Melt Down Measurements in Zebra Core 12 (MZB/2)	MTN27
B. L. H. Burbidge, G. Ingram, D. Jowitt, Miss M. P. Smith, Miss P. A. Smart, D. W. Sweet	Results of Further Central Reaction Rate Ratio Measurements in Zebra Core 11	MTN28
D. Jowitt, Miss P. A. Smart	Reaction Rate Scans using Fission Chambers in Zebra Core 11	MTN29
B. L. H. Burbidge, G. Ingram, D. Jowitt, Miss M. P. Smith, Miss P. A. Smart, D. W. Sweet	Central Reaction Rate Ratio Measurements in Zebra Core 12 (MZB/1)	MTN30
J. M. Stevenson, S. F. Swoboda	Zebra Assembly 12/2 - The Second Version Of MZB Description of Standard Loading, Control Rod Calibrations, Experimental Reactivity	MTN31
M. Nakano	Zebra Core 12 (MZB) Number Densities	MTN32
D. Jowitt, B. Franklin, Miss P. A. Smart, G. Ingram	Reaction Rate Scans using Fission Chambers in the Natural Uranium Oxide and Depleted Uranium Oxide Sector Versions Of MZB	MTN33
J. E. Sanders	A Revised Programme of Control Rod Measurements in MZC	MTN34
A. Sugawara	Application of the Twotran(XY) Code to Fast Reactor Analysis	MTN35
J. M. Stevenson, S. F. Swoboda	Reactivity Worths of Special Assemblies in Various Radial Positions in Zebra Core 12 (Mzb)	MTN36
M. Nakano, R. W. Smith	Mural/FGL4 Cell Calculations For MZB (Zebra Core 12)	MTN37
M. Nakano	A Note on the Calculation of Reaction Rate Distributions in MZA	MTN38
C. G. Campbell, S. Kobayashi	Data On PNC 90 % B4C And Ta Absorbers	MTN39
I. C. Rickard	Lithium-6 Spectrometer Measurements in Zebra Core 11 (MZA)	MTN40
W. J. Paterson, J. Redfern	Double Scintillator Spectrometry on Zebra Core11, MZA	MTN41
J. M. Stevenson, S. F. Swoboda	Third Version of MZB Description of Standard Loading, Control Rod Calibrations, Experimental Reactivity, Comparisons with Assemblies 12/1 And 12/2	MTN42
J. M. Stevenson, M. Nakano, H. Yoshida, J. Hardiman	Proposals for the Standard Reactor Models and the Analytical Methods for Comparison of Calculations and Experiments in MZB	MTN43

B. M. Franklin, J. P. Hardiman	The Buckling of Zebra Core 11 (MZA)	MTN44
T. Konishi	Diffusion Theory Calculations of the Reactivity, Reaction Rate Ratios and Reaction Rate Distributions in MZA	MTN45
J. Butler	Theoretical Interpretation of the Kochel Experiments on MZB	MTN46
A. M. Broomfield, G. Ingram	The Experimental Programme for MZC	MTN47
R. W. Smith	Mural/FGL5 Cell Calculations for MZB (Zebra Core 12)	MTN48
J. Marshall, J. M. Stevenson, S. F. Swoboda	Zebra Assembly 12/4 Description of Standard Loading, Control Rod Calibrations, Experimental Reactivity Comparison with Assembly 12/3	MTN49
M. D. Carter, J. Samways	Neutron Spectrum Measurements with Proton-Recoil Counters in a Beam from Zebra 11, (MZA)	MTN50
J. Marshall	Atomic Number Densities for Calculations on PNC Absorbers used in MZC	MTN51
J. M. Stevenson	The Reactivity Scale Experiment in Assembly MZB/4	MTN52
A. Sugawara	Studies of the Standard Methods for the MZC Control Rod Worth Analysis	MTN53
J. M. Stevenson, S. F. Swoboda	Sodium Removal Measurements in Plate and Pin Geometry in Zebra Assembly 12/2, the Second Version Of MZB	MTN54
P. J. Collins, J. D. Macdougall	Control Rod Fine Structure Studies in MZC	MTN55
M. Nakano	A Further Study of the Material Buckling of Zebra Core 11 (MZA)	MTN56
J. D. Macdougall	Reaction Rate Scans using Foils in the Natural Uranium Oxide and Depleted Uranium Oxide Sector Versions of MZB	MTN57
J. D. Macdougall	Reaction Rate Scans using Foils in the Natural Uranium Oxide and Depleted Uranium Oxide Sector Versions of MZB	MTN57 ADD
P. J. Collins, J. Marshall, A. Sugawara	The Standard Method for the Analysis of MZC	MTN58
M. D. Carter, A. D. Knipe, A. K. McCracken, A. Packwood, I. C. Rickard	The Kochel Experiments on MZB Part I: Measurements with Activation Detectors, Hydrogen-Filled Proportional Counters, 6Li Sandwich Spectrometer, Gamma-Ray Ionisation Chambers and Thermoluminescent Detectors	MTN59
J. M. Stevenson, S. F. Swoboda	Calculations of the Reactivity and Central Reaction Rate Ratios for MZB with FGL5 Data, and Comparison with Experimental Results	MTN60
A. Sugawara, A. N. Broomfield	Summary of Calculations made in Support of the Design of the MZC Experiment	MTN61
J. H Spanton	A Study of the Effect of Transients in the Spectrum on the Group Constants and Reaction Rates Calculated in MZA	MTN62
T. Konishi	Investigations of Some of the Approximations made in the Standard Diffusion Theory Analysis of MZA Reactivity and Reaction Rate Scans	MTN63
H. Yoshida	Analysis of Central Perturbation Measurements in Zebra 11 (MZA) and Zebra 12 (MZB)	MTN64
H. Yoshida	Analysis of Sodium Removal Experiment in Zebra 11 (MZA) (2) Using the FGL5 Cross-Section Data Set	MTN65
C. J. Dean	One-Group Capture and Fission Cross-Sections for MZA	MTN66
G. Ingram, D. W. Sweet	Vapour Explosion and Fuel Melt-Down Simulations in Zebra Core 12 (MZB/2)	MTN67

R. W. Smith	Calculation of the Reactivity and Central Reaction Rate Ratios for MZA using the FGL5 Library of Cross-Sections, and their Comparison with the Measured Values	MTN68
R. W. Smth	Calculated Perturbation Cross Sections and Reactivity Worths of the Constituent Isotopes at the Core Centres of MZA and MZB using the FGL5 Data Set	MTN69
M. Nakano	Calculations of the Reaction Rate Distributions in MZB with FGL5 Data, and Comparison with Experimental Results	MTN70
R. W. Smith	A Comparison of FGL5 - Transport Theory Calculations of Reaction Rate Distributions in MZA with Experiment	MTN71
J. H. Spanton	Preliminary Results of a Study of the Effect of Heterogeneity on Fission Rate Scans in MZA Blanket Cells	MTN72
J. P. Hardiman	Analysis of Sodium Removal Experiments in MZB/2 Part1	MTN73
M. D. Carter, J. Samways	A Comparison of the High Energy Neutron Spectrum Measurements made with Double Scintillator, Proton Recoil Counter and Lithium - 6 Spectrometers in Zebra 11 (MZA)	MTN74
B. L.H. Burbidge, G. Ingram, Miss M. P. Smith	Reaction Rate Scans using Foils in Zebra Core 12/3	MTN75
J. M. Stevenson, S. F. Swoboda	Analysis of the Reactivity Scale Experiment in MZB using FGL5 Data and Theory	MTN76
J. M. Stevenson	A Note on the Measurement of the Interaction of Sodium Voiding and Rod Worths in MZC	MTN77
M. D. Carter, J. Samways	Neutron Spectrum Measurements with Proton Recoil Counters in the Blanket and Reflector of Zebra Core 12 (MZB/2)	MTN78
J. Marshall	The Data and Model for the PNC Mixed 80 Per Cent and 90 Per Cent B4C Absorber	MTN79
D. Jowitt, Miss P. Smart, G. Ingram	Reaction Rate Scans in MZB/3 using Fission Chambers	MTN80
J. L. Rowlands, C. J. Dean, M. F. James, J. D. Macdougall, R. W. Smith	The FGL5 and FD5 Cross-section Set	MTN81
M. J. Grimstone	The Application of the Standard Build-Up Factor and Removal-Diffusion Methods to the Kochel Gamma Ray Experiments in MZB	MTN82
M. J. Grimstone, P. C. Miller, Y. Sekiguchi	The Application of the Standard 1D Removal-Diffusion (Comprash) Method to the Kochel Neutron Experiments on MZB	MTN83
M. J. Grimstone, A. D. Knipe	Monte Carlo Analysis of the Kochel Gamma-Ray Experiments in MZB: The Radial Calculations	MTN84
A. Sugawara	Analysis of the MZC Control Rod Experiments using Transport Theory Methods	MTN85
J. Marshall, J. Samways	Calculated Reactivities for MZC Configurations using the Standard Method	MTN86
D. W. Sweet	Further Data on Central Reaction Rate Measurements in MZA and MZB	MTN87
P. C. Miller	The Application of the Standard 2D Removal -Diffusion (Comprash) Method to the Kochel Neutron Experiments on MZB	MTN88

D. Jowitt, Miss P. A. Smart, G. Ingram, B. L. H. Burbidge	Reaction Rate Scans in MZC using Fission Chambers	MTN89
A. D. Knipe	Corrections to Gamma Dose-Rate Measurements made in the Kochel Experiments in Core MZB Part 1 : Ionisation Chamber Measurements	MTN90
M. J. Grimstone, A. D. Knipe	Monte Carlo Analysis of the Kochel Gamma-Ray Experiments in MZB: Axial Calculations	MTN91
A. M. Broomfield, M. D. Carter	The MZC Control Rod Worth Experiments and their Analysis using the Standard Calculation Method	MTN92
J. Marshall, J. Samways	A Comparison Between Measured and Calculated Reaction Rate Distributions in MZC	MTN93
G. Ingram, D. Jowitt, Miss P. A. Smart, B. L. H. Burbidge, M. Smith	Reanalysis of Measured U238 Fission Rate Scans in MZA, MZB/1 and MZB/2	MTN94
P. C. Miller	Transport Analysis of Neutron Penetrations in the MZB/2 Radial Shield	MTN95
J. M. Stevenson, S. F. Swoboda	A Summary of Calculations of the Central and Distributed Perturbations in Assemblies MZA and MZB	MTN96
B. L. H. Burbidge, G. Ingram, Miss M. P. Smith	Reaction Rate Scans using Foils in the PNC Control Rod Version of Zebra Core 12/4	MTN97
P. J. Collins	Fine Structure Studies of the PNC Mocked-Up Control Rods using the PIJ Code	MTN98
R. W. Smith	A Reassessment of the Comparison between Measured and Calculated Reaction Rate Distributions in MZA	MTN99
P. J. Collins	Analysis of Axial Fission Chamber Scans near Control Rods in MZC	MTN100
J. M. Stevenson, S. F. Swoboda	Further Calculations of Reaction Rate Distributions in MZB with FGL5 Data and Comparison with Experimental Results	MTN101
A. F. Avery, A. D. Knipe	Calculations of Gamma-Ray Dose Rates in the Control Rod Experiments of MZC	MTN102
J. P. Hardiman	Analysis of Sodium Removal Experiments in MZB/2 Part 2	MTN103
R. W. Smith	The Reactivity Calibration of Specified Control Rods in MZA and MZB (Versions 1,2,3 and 4) on an Absolute Scale based on Measured Periods and the Inhour Equation.	MTN104
J. D. Macdougall	Corrections to the Standard Method of Calculating Reaction Rate Scans in Zebra with Results for MZB	MTN105

Additional References

The MONK-7 Nuclear Criticality Monte Carlo code
(The Answers Service, SercoAssurance Winfrith, UK)

APPENDIX A. EXAMPLE CALCULATIONAL MODELS. (Only one configuration is given here)

MONK-JEF-2.2 Models for the central BN rod. Three calculations are involved: the assembly with the added edge elements, the assembly with the central group of 2x2 elements replaced by follower and the assembly with the follower replaced by the absorber rod.

```
* MONK8B Input Listing for MZB/3 Model B, 8 extra edge elements
* Assembly 12 is MZB the second core in the MOZART Programme.
* Version 3 has the approximately uniform radial blanket
* containing the natural uranium metal plates
* Reactor structure: elements arranged on a square grid
* The Core Elements contain Core Cells and an Axial Blanket Cell,
* enclosed in a stainless steel sheath.
* The standard plates have a width of 5.067 cm.
* The Element sheath has an inner width 5.102 cm, outer width 5.2544 cm.
* The elements occupy a lattice area of 5.3721 cm square.
* Groups of 5x5 elements form the superlattice
*       There is a gap between these groups of elements of 0.2667 cm
* There are 408 Radial Blanket Elements
* The radial shielding elements consist of the Steel bar MST9F10
* which is about 300 cm high.
* These are represented explicitly within an outer radius and also
* homogenised (over the overall average lattice area) to fill the
* remaining space in the outer cylinder (pitch 5.4254 cm)
* The outer radius of the shielding region has been taken to be 95.91 cm
*       the enveloping circumference, rather than the value corresponding
*       to the area of shielding material
* Core Element structure (PART 26):
*       The element consists of combinations of the following cells:
*       Core Cell PART 19, Axial Blanket Cell PART 20 ,
*       Plenum Cell PART 21, element reflected in the mid-plane.
* Structure of the Radial Blanket element PART 28.
*       Central region PART 22, Upper region Cell PART 23 ,
*       Plenum Cell PART 21, element reflected in the mid-plane.
* Special Element in core centre region
*       (for reaction rate calculations) (PART 30):
*       This element contains the special cell PART 24
* All Enclosed in the stainless steel sheaths.
**********************************************************************
* material 1 - U/Pu oxide plate core
* material 2 - U/Pu plate clad
* material 3 - PUIX8 Plutonium metal plate core
* material 4 - PUIX8 Plutonium metal clad
* material 5 - PUVI8 Plutonium metal plate core
* material 6 - PUVI8 Plutonium metal clad
* material 7 - UO2 plate  core UO23R4
* material 8 - UO2 plate clad UO23R4
* material 9 - UO2 plate  core UO24R4
* material 10 - UO2 plate clad UO24R4
* material 11 - U8 natural uranium region
* material 12 - U2 natural uranium region
* material 13 - Sodium plate core NASTDL4
* material 14 - Sodium plate clad NASTDL4
* material 15 - Sodium plate core NASTBR4
* material 16 - Sodium plate clad NASTBR4
* material 17 - Steel STSTBR8
* material 18 - Steel STSTDL8
* material 19 - MST1
* material 20 - MST2
* material 21 - MST3 Steel block
* material 22 - MST8
* material 23 - Steel bar MST9F10 at actual density (width 5.08 cm)
* material 24 - Steel bar averaged over the mean spacing of 5.4254 cm
* material 25 - GI8
* material 26 - GII8
* material 27 - GIII8
* material 28 - Smeared stainless steel sheath - average lattice pitch
* material 29 - Smeared mild steel sheath - average lattice pitch
* material 30 - ALSC3
* material 31 - ALG8
* material 32 - AL2O34
```

```
* material 33 - U/Pu oxide plate core at reactor core centre
* material 34 - PUIX8 plate core at reactor core centre
* material 35 - UO23R4 plate core at reactor core centre
* material 36 - PUX8 Plutonium metal plate core
* material 37 - PUX8 Plutonium metal clad
* material 38 - PUXI8 Plutonium metal plate core
* material 39 - PUXI8 Plutonium metal clad
* material 40 - Sodium plate core NASTDM4
* material 41 - Sodium plate can NASTDM4
* material 42 - PUV8 Plutonium metal plate core
* material 43 - PUV8 Plutonium metal clad
* material 44 - PUVII8 Plutonium metal plate core
* material 45 - PUVII8 Plutonium metal clad
* material 46 - PUVIII8 Plutonium metal plate core
* material 47 - PUVIII8 Plutonium metal clad
* material 48 - PUXII8 Plutonium metal plate core
* material 49 - PUXII8 Plutonium metal clad
*
**************************************************************************
COLUMNS 1 132
BEGIN MATERIAL SPECIFICATION
NUMBER DENSITY
MATERIAL 1
 C   6.2771E-05  O16 4.2860E-02  AL  2.7943E-05  SI  2.6845E-05
 FE  1.3500E-05 NI  1.2846E-05
 U234  7.4340E-07  U235  1.1548E-04  U238  1.5938E-02
 NP237  2.4466E-07  PU239  4.7730E-03 PU240  5.3344E-04
 PU241  5.0303E-05  PU242  4.7919E-06 AM241  2.6204E-05
MATERIAL 2
 H1  2.0111E-05  C   1.6876E-04  SI  5.9180E-04  P   2.6177E-05
 S   2.5282E-05  CR  1.3956E-02  MN  1.0995E-03  FE  5.0428E-02
 NI  6.9005E-03  NB  2.8363E-04
MATERIAL 3
 H1  1.5145E-04 C   2.8155E-04 N   9.2216E-06 O16  5.7245E-05
 AL  2.3065E-05 SI  2.8430E-05 CR  6.0974E-06 MN  1.7099E-06
 FE  1.3036E-05 NI  2.6810E-05 GA  2.1190E-03
U238    5.2779E-06  PU238  3.5515E-05  PU239  2.8995E-02
PU240  6.9474E-03  PU241  1.1413E-03  PU242  1.8046E-04
AM241  5.9252E-05
MATERIAL 4
 H1  1.3771E-05  C   1.1312E-04  SI  3.6529E-04  P  1.3425E-05
 CR  9.3855E-03  MN  8.5801E-04  FE  3.5483E-02 NI  4.1575E-03
 CU  1.6626E-02
MATERIAL 5
 H1  1.0485E-04  C   2.2876E-04  N   2.4312E-05 O16  3.5962E-05
 AL  1.7408E-05  CR  3.1616E-06  MN  1.0687E-06  FE  1.9344E-05
 NI  6.8024E-06  GA  2.2555E-03
 U238      2.4663E-07  PU238   3.6995E-05  PU239   2.8972E-02
 PU240  7.3421E-03  PU241   1.1537E-03  PU242   2.0132E-04
 AM241   8.6769E-05
MATERIAL 6
 H1   1.3955E-05  C    1.1413E-04  SI   3.6853E-04  P    1.3545E-05
 CR   9.4688E-03  MN   8.6563E-04  FE   3.5798E-02  NI   4.1944E-03
 CU   1.6626E-02
MATERIAL 7
H1 3.0915E-05  C  1.1933E-05  O16 4.6151E-02  AL 3.4645E-06
SI 2.3076E-05  MN 1.1343E-07  FE 1.3390E-06  NI 1.2742E-06
MO 3.2478E-07
U235 1.6595E-04  U238 2.2908E-02
MATERIAL 8
H1 1.9528E-05  C  1.2651E-04  SI 6.3619E-04  P  3.4607E-04
S  3.5596E-05  CR 1.3636E-02  MN 8.4422E-04  FE 4.7664E-02
NI 8.3138E-03
MATERIAL 9
H1  2.4503E-05  C   3.0842E-05  O16 4.5733E-02  SI  1.3190E-05
FE  6.6332E-06
U234 1.1871E-06  U235 1.6462E-04  U238 2.2694E-02
MATERIAL 10
 H1  1.7335E-05  C    1.4546E-04  SI   6.0964E-04  P    2.2563E-05
 S   2.1792E-05  CR   1.2365E-02  MN   9.7951E-04  FE   4.3411E-02
 NI   6.0134E-03  CU   8.1603E-04  AG   1.2368E-03
MATERIAL 11
H1  4.4048E-05  C   4.9283E-04  SI  2.1076E-04  FE  1.0599E-04
U235 3.3369E-04  U238 4.6021E-02
MATERIAL 12
```

```
H1  4.3899E-05  C   4.6047E-04  SI  1.9692E-04  FE  9.9032E-05
U235 3.3962E-04  U238 4.6785E-02
MATERIAL 13
H1  1.3418E-05  O16 5.6353E-06  NA  2.3168E-02  CA  3.5994E-06
FE  1.6144E-07
MATERIAL 14
H1 2.4319E-05  C  2.8978E-04  SI 6.0218E-04  P  3.2445E-05
S  3.2865E-05  CR 1.4602E-02  MN 1.3425E-03  FE 5.4467E-02
NI 7.0225E-03  NB 3.0815E-04
MATERIAL 15
 H1  2.1098E-06 LI  3.8296E-07 B   1.4752E-07 O16  1.9937E-06
 NA  2.3119E-02 K   4.6230E-07 CA  1.7244E-06 FE   3.8077E-08
MATERIAL 16
 H1  2.1496E-05  C   2.1646E-04  SI  6.0171E-04  P   2.7979E-05
 S   2.7023E-05  CR  1.5000E-02  MN  1.0806E-03  FE  5.4056E-02
 NI  7.2502E-03  NB  3.0316E-04
MATERIAL 17
H1 2.3265E-05  C  7.8091E-04  AL 1.7381E-04  SI 1.3358E-03
TI 2.9384E-04  CR 1.6325E-02  MN 9.3901E-04  FE 5.8278E-02
NI 7.7510E-03  CU 7.3801E-05  MO 9.7764E-05
MATERIAL 18
H1 2.3115E-05  C  7.7587E-04  AL 1.7269E-04  SI 1.3272E-03
TI 2.9195E-04  CR 1.6220E-02  MN 9.3295E-04  FE 5.7902E-02
NI 7.7009E-03  CU 7.3324E-05  MO 9.7133E-05
MATERIAL 19
 H1  2.8122E-05  C   5.1129E-04  AL  1.4007E-04  TI  3.9465E-05
 CR  2.7256E-05  MN  3.2675E-04  FE  8.3911E-02  NI  4.8294E-05
 CU  4.4603E-05  MO  9.8477E-06
MATERIAL 20
 H1   2.7967E-05  C    5.0847E-04  AL   1.3930E-04 TI   3.9247E-05
 CR   2.7106E-05  MN   3.2495E-04  FE   8.3448E-02 NI   4.8028E-05
 CU   4.4357E-05  MO   9.7934E-06
MATERIAL 21
 H1  2.8087E-05  C   5.1066E-04  AL  1.3989E-04  TI  3.9416E-05
 CR  2.7222E-05  MN  3.2634E-04  FE  8.3806E-02  NI  4.8234E-05
 CU  4.4548E-05  MO  9.8355E-06
MATERIAL 22
 H1   2.7730E-05  C    5.0417E-04  AL   1.3812E-04  TI   3.8915E-05
 CR   2.6876E-05  MN   3.2220E-04  FE   8.2742E-02  NI   4.7622E-05
 CU   4.3982E-05  MO   9.7106E-06
MATERIAL 23
H1  4.6306E-05 C   6.8972E-04 SI  3.1158E-04 P   4.2944E-05
S   3.7110E-05 MN  7.1275E-04 FE  8.1432E-02
MATERIAL 24
H1  4.0597E-05 C   6.0468E-04 SI  2.7317E-04 P   3.7649E-05
S   3.2535E-05 MN  6.2488E-04 FE  7.1392E-02
MATERIAL 25
 H1  4.8551E-05  C   8.1417E-02  S   1.2207E-05  FE  6.1336E-06
MATERIAL 26
 H1  2.0286E-05  C   8.5101E-02  S   1.2751E-06  FE  1.8306E-06
MATERIAL 27
 H1  1.9906E-05  C   8.3507E-02  FE  2.3351E-06
MATERIAL 28
 H1  9.7398E-06  C   3.2692E-04  AL  1.4553E-04  SI  4.1943E-04
 TI  1.2302E-04  V   3.8541E-05  CR  6.7589E-03  MN  5.0032E-04
 FE  2.3765E-02  NI  3.7801E-03  CU  3.0896E-05  MO  6.1393E-05
MATERIAL 29
 H1  1.0937E-04  C   1.3002E-04  SI  1.9624E-05  P   5.9314E-06
 S   1.9478E-05  MN  1.1537E-04  FE  3.2730E-02
MATERIAL 30
 AL   4.7590E-02 SI   4.5790E-06 MN   9.3634E-07 FE   2.9936E-05
 CU   1.8214E-06
MATERIAL 31
 AL   2.6704E-02  SI   1.0296E-05  MN   6.5793E-07  FE   3.6374E-05
 CU   4.5505E-07
MATERIAL 32
 H1   5.1483E-05  B10  4.5063E-06  B11  1.6599E-05  O16  6.6386E-02
 AL   4.4240E-02
MATERIAL 33
 C   6.2771E-05  O16 4.2860E-02  AL  2.7943E-05  SI  2.6845E-05
 FE  1.3500E-05 NI  1.2846E-05
 U234  7.4340E-07  U235  1.1548E-04  U238  1.5938E-02
 NP237  2.4466E-07  PU239  4.7730E-03 PU240  5.3344E-04
 PU241  5.0303E-05  PU242  4.7919E-06 AM241  2.6204E-05
MATERIAL 34
```

```
 H1  1.5145E-04 C   2.8155E-04 N   9.2216E-06 O16  5.7245E-05
 AL  2.3065E-05 SI  2.8430E-05 CR  6.0974E-06 MN  1.7099E-06
 FE  1.3036E-05 NI  2.6810E-05 GA  2.1190E-03
U238    5.2779E-06  PU238  3.5515E-05  PU239  2.8995E-02
PU240  6.9474E-03  PU241  1.1413E-03  PU242  1.8046E-04
AM241  5.9252E-05
MATERIAL 35
H1 3.0915E-05  C  1.1933E-05  O16 4.6151E-02  AL 3.4645E-06
SI 2.3076E-05  MN 1.1343E-07  FE 1.3390E-06  NI 1.2742E-06
MO 3.2478E-07
U235 1.6595E-04  U238 2.2908E-02
MATERIAL 36
 H1  1.0485E-04 C   2.9524E-04 N   1.0060E-05 O16 4.5503E-05
 AL  2.1760E-05 SI  1.5887E-05 CR  4.2908E-06 MN  1.0687E-06
 FE  1.4928E-05 NI  1.6206E-05 GA  2.2417E-03
U238       1.4305E-06  PU238  3.4035E-05  PU239  2.9107E-02
PU240  6.9117E-03  PU241  1.1359E-03  PU242  1.8531E-04
AM241  3.3658E-05
MATERIAL 37
 H1 1.3587E-05 C  1.2050E-04 SI 5.2025E-04 P  2.6701E-05
 S  1.5471E-05 TI 5.7590E-06 CR 9.9679E-03 MN 8.5308E-04
 FE 3.3844E-02 NI 4.8383E-03 CU 1.6868E-02
MATERIAL 38
 H1  1.7475E-04 C   2.2876E-04 N   1.1737E-05 O16 4.1833E-05
 AL  1.8713E-05 SI  1.8396E-05 CR  6.0974E-06 MN  1.0687E-06
 FE  2.2287E-05 NI  1.7606E-05 GA  2.2490E-03
U238     6.9057E-07  PU238 3.7488E-05  PU239 2.8990E-02
PU240 6.9709E-03  PU241 1.1546E-03  PU242 1.8482E-04
AM241 3.0855E-05
MATERIAL 39
 H1 1.3404E-05 C  1.1825E-04 SI 5.1057E-04 P  2.6205E-05
 S  1.5188E-05 TI 5.6508E-06 CR 9.7825E-03 MN 8.3722E-04
 FE 3.3215E-02 NI 4.7483E-03 CU 1.6868E-02
MATERIAL 40
H1 1.3418E-05  O16 5.6353E-06  NA 2.3168E-02  CA 3.5994E-06
FE 1.6144E-07
MATERIAL 41
H1 2.1522E-05  C  2.1672E-04  SI 7.8781E-04  P  3.2216E-05
S  1.6234E-05  CR 1.5953E-02  MN 1.2635E-03  FE 5.2254E-02
NI 7.8948E-03  NB 3.4089E-04
MATERIAL 42
 H1   1.7475E-04 C    2.5027E-04 N    1.3413E-05 O16  5.0640E-05
 AL   2.1760E-05 SI   2.3831E-05 CR   5.1941E-06 MN   1.0687E-06
 FE   1.6610E-05 NI   1.1804E-05 GA   2.2424E-03 MO   1.9583E-06
 U238   1.3318E-06  PU238   2.9103E-05  PU239   2.9328E-02
 PU240   6.7928E-03  PU241   9.8832E-04  PU242   1.6639E-04
 AM241   1.1785E-04
MATERIAL 43
 H1   1.3404E-05 C    9.2801E-05 SI   4.1625E-04 P    1.8432E-05
 S    9.3252E-06 CR   9.2549E-03 MN   7.5220E-04 FE   3.4310E-02
 NI   4.5397E-03 CU   1.6626E-02
MATERIAL 44
 H1  1.3980E-04  C   2.0335E-04  N   6.7066E-06  O16 5.4310E-05
 AL  1.6973E-05  SI  1.0870E-05  CR  4.0649E-06  MN  8.5494E-07
 FE  1.0513E-05  NI  9.0032E-06  GA  2.0492E-03
U238   9.3720E-07  PU238  3.1569E-05  PU239  2.9028E-02
PU240  6.9606E-03  PU241  1.1208E-03  PU242  1.8725E-04
AM241  8.0243E-05
MATERIAL 45
 H1   1.3771E-05  C    1.1357E-04  SI   3.6675E-04  P    1.3479E-05
 CR   9.4231E-03  MN   8.6145E-04  FE   3.5625E-02  NI   4.1742E-03
 CU  1.6626E-02
MATERIAL 46
 H1   1.2815E-04  C    4.2429E-04  N    2.4312E-05  O16  8.8804E-05
 AL   2.3065E-05  SI   1.4215E-05  CR   3.6133E-06  MN   1.4962E-06
 FE   1.6400E-05  NI   8.6031E-06  GA   2.0247E-03
U238  6.9057E-07  PU238 3.0583E-05  PU239 2.9035E-02
PU240 6.9371E-03  PU241 1.1304E-03  PU242 1.8773E-04
AM241 7.1186E-05
MATERIAL 47
 H1   1.3771E-05 C    1.1340E-04 SI   3.6619E-04 P    1.3461E-05
 CR   9.4087E-03 MN   8.6013E-04 FE   3.5570E-02 NI   4.1678E-03
 CU  1.6626E-02
MATERIAL 48
 H1  1.7475E-04 C   2.6298E-04 N   6.7066E-06 O16 4.1833E-05
```

```
 AL  1.7408E-05 SI  2.2159E-05 CR  9.2590E-06 MN  8.5494E-07
 FE  1.4928E-05 NI  2.3809E-05 GA  2.3032E-03
U238      1.6771E-06   PU238 3.6995E-05  PU239 2.9064E-02
PU240 6.8990E-03  PU241 1.1606E-03  PU242 1.7997E-04
AM241 2.7359E-05
MATERIAL 49
 H1 1.3220E-05 C  1.1685E-04 SI 5.0450E-04 P  2.5895E-05
 S  1.5004E-05 TI 5.5851E-06 CR 9.6661E-03 MN 8.2726E-04
 FE 3.2820E-02 NI 4.6918E-03 CU 1.6868E-02
END
*
*********************************************************************
BEGIN MATERIAL GEOMETRY
*
*                                                       PLATES
*
*********************************************************************
* Plate 1, the Pu metal plate UPUO24
PART 1 NEST
BOX     M1  -2.4765  -2.4765  0.03734  4.953          4.953   0.55312
BOX     M2  -2.5335  -2.5335  0.0      5.067   5.067   0.6278
BOX     M28  -2.7127 -2.7127   0.0     5.4254  5.4254   0.6278
*
* Plate 2, the Pu metal plate PUIX8
PART 2 NEST
BOX     M3  -2.3355  -2.3355  0.04572  4.671   4.671   0.23506
BOX     M4  -2.5335  -2.5335  0.0      5.067   5.067   0.3265
BOX     M28  -2.7127 -2.7127   0.0     5.4254  5.4254   0.3265
*
* Plate 3, the Pu metal plate PUVI8
PART 3 NEST
BOX     M5  -2.3355  -2.3355  0.04572  4.671   4.671   0.23506
BOX     M6  -2.5335  -2.5335  0.0      5.067   5.067   0.3265
BOX     M28  -2.7127 -2.7127   0.0     5.4254  5.4254   0.3265
*
* Plate 4, the UO2 plate UO23R4
PART 4 NEST
BOX     M7  -2.4255  -2.4255  0.03683 4.851   4.851   0.55424
BOX     M8  -2.5335  -2.5335  0.0     5.067   5.067   0.6279
BOX     M28  -2.7127 -2.7127   0.0     5.4254  5.4254  0.6279
*
* Plate 5, the UO2 plate UO24R4
PART 5 NEST
BOX     M9  -2.4255  -2.4255  0.03683 4.851   4.851   0.55424
BOX     M10  -2.5335  -2.5335 0.0     5.067   5.067   0.6279
BOX     M28  -2.7127 -2.7127   0.0     5.4254  5.4254  0.6279
*
* Central region cells for calculating reaction rate ratios
* Plate 6, the special Pu metal plate UPUO24
PART 6 NEST
BOX     M33  -2.4765  -2.4765 0.03734  4.953          4.953   0.55312
BOX     M2  -2.5335  -2.5335  0.0      5.067   5.067   0.6278
BOX     M28  -2.7127 -2.7127   0.0     5.4254  5.4254   0.6278
*
* Plate 7, the special Pu metal plate PUIX8
PART 7 NEST
BOX     M34  -2.3355  -2.3355 0.04572  4.671   4.671   0.23506
BOX     M4  -2.5335  -2.5335  0.0      5.067   5.067   0.3265
BOX     M28  -2.7127 -2.7127   0.0     5.4254  5.4254   0.3265
*
* Plate 8, the special UO2 plate UO23R4
PART 8 NEST
BOX     M35  -2.4255  -2.4255 0.03683 4.851   4.851   0.55424
BOX     M8  -2.5335  -2.5335  0.0     5.067   5.067   0.6279
BOX     M28  -2.7127 -2.7127   0.0     5.4254  5.4254  0.6279
*
* Plate 9, the sodium plate NASTDL4
PART 9 NEST
BOX     M13  -2.4815  -2.4815 0.03683 4.963  4.963   0.54234
BOX     M14 -2.5335  -2.5335  0.0     5.067   5.067   0.616
BOX     M28  -2.7127 -2.7127   0.0     5.4254  5.4254  0.616
*
* Plate 10, the sodium plate NASTBR4
PART 10 NEST
BOX     M15  -2.4815  -2.4815 0.03683 4.963  4.963   0.54234
```

```
BOX     M16 -2.5335  -2.5335  0.0     5.067   5.067   0.616
BOX     M28  -2.7127 -2.7127   0.0     5.4254  5.4254  0.616
*
* Plate 11, the graphite plate GII8 (modified from GIII8)
PART 11 NEST
BOX     M26  -2.5335  -2.5335 0.0     5.067   5.067   0.31775
BOX     M28  -2.7127 -2.7127   0.0     5.4254  5.4254  0.31775
*
* Axial blanket U8 plate
PART 12 NEST
BOX     M11     -2.5335 -2.5335 0.0     5.067   5.067   0.3175
BOX     M28  -2.7127 -2.7127   0.0     5.4254  5.4254  0.3175
*
* Plate 13, the steel plate STSTBR8
PART 13 NEST
BOX     M17  -2.5335  -2.5335 0.0     5.067   5.067   0.3172
BOX     M28  -2.7127 -2.7127   0.0     5.4254  5.4254  0.3172
*
* Plate 14, the graphite plate GI8
PART 14 NEST
BOX     M25  -2.5335  -2.5335 0.0     5.067   5.067   0.3180
BOX     M28  -2.7127 -2.7127   0.0     5.4254  5.4254  0.3180
*
* Plenum aluminium cylinder ALSC3
PART 15 NEST
BOX     M29     -2.5335 -2.5335 0.0     5.067   5.067   7.62
BOX     M28  -2.7127 -2.7127   0.0     5.4254  5.4254  7.62
*
* Plenum plate MST1
PART 16 NEST
BOX     M19     -2.5335 -2.5335 0.0     5.067   5.067   2.5385
BOX     M28  -2.7127 -2.7127   0.0     5.4254  5.4254  2.5385
*
* Plenum plate MST3
PART 17 NEST
BOX     M21     -2.5335 -2.5335 0.0     5.067   5.067   7.6063
BOX     M28  -2.7127 -2.7127   0.0     5.4254  5.4254  7.6063
*
*
************************************************************************
*
*                                       Radial blanket components
*
************************************************************************
* Uranium metal U2
PART 18 NEST
BOX     M12     -2.5335 -2.5335 0.0     5.067   5.067   1.2723
BOX     M28      -2.7127 -2.7127        0.0     5.4254  5.4254  1.2723
*
* Graphite GII8
PART 19 NEST
BOX     M26     -2.5335 -2.5335 0.0     5.067   5.067   0.31775
BOX     M28  -2.7127 -2.7127   0.0     5.4254  5.4254  0.31775
*
* Mild steel MST8
PART 20 NEST
BOX     M22     -2.5335 -2.5335 0.0     5.067   5.067   0.3147
BOX     M28  -2.7127 -2.7127   0.0     5.4254  5.4254  0.3147
*
* Stainless steel STSTDL8
PART 21 NEST
BOX     M18     -2.5335 -2.5335 0.0     5.067   5.067   0.3236
BOX     M28  -2.7127 -2.7127   0.0     5.4254  5.4254  0.3236
*
* ALUMINIUM ALG8
PART 22 NEST
BOX     M31     -2.5335 -2.5335 0.0     5.067   5.067   0.3170
BOX     M28  -2.7127 -2.7127   0.0     5.4254  5.4254  0.3170
*
* Aluminium oxide AL2O34
PART 23 NEST
BOX     M32     -2.5335 -2.5335 0.0     5.067   5.067   0.6317
BOX     M28  -2.7127 -2.7127   0.0     5.4254  5.4254  0.6317
*
*
```

```
* Mild steel MST2
PART 24 NEST
BOX     M20     -2.5335 -2.5335 0.0     5.067   5.067   1.2718
BOX     M28   -2.7127 -2.7127   0.0     5.4254  5.4254  1.2718
*
**********************************************************************
*
*                                                          CELLS
*
**********************************************************************
*
* Inner Core Cell
PART 25 ARRAY
1  1  14  9  4  9  2  9  4  9  13  4  9  1  9  4  9
*
* Outer Core Cell 1B
PART 26 ARRAY
1  1  14  9  5  9  3  13  5  9  9  5  14  3  9  5  9
*
* Axial blanket Cell 1A
PART 27 ARRAY
1  1  20  9  12  14  9  13  12  9  14  9  13
12  9  14  9  12  13  9  14  12  9
*
* Upper Axial Plenum Cell
PART 28 ARRAY
1  1  5  15  17  15  16  15
*
* Lower Axial Plenum Cell
PART 29 ARRAY
1  1  5  15  16  15  17  15
*
* Radial blanket central region cell
PART 30 ARRAY
1  1  10  19  10  19  21  18  11  10  20  19  10
*
* Radial blanket outer region Cell
PART 31 ARRAY
1  1  20  22  22  23  14  22  18  22  14  23  24
22  14  22  22  18  23  22  14  20  22
*
* Core Cell in the central region,
PART 32 ARRAY
1  1  14  9  8  9  7  9  8  9  13  8  9  6  9  8  9
*
* Steel packing pieces to line up the elements
*
*
* Inner core packing
PART 33 NEST
BOX     M17  -2.7127 -2.7127   0.0     5.4254  5.4254  2.51575
*
* Outer core packing
PART 34 NEST
BOX     M17  -2.7127 -2.7127   0.0     5.4254  5.4254  2.064
*
* radial blanket element packing (reduced by 0.003)
PART 35 NEST
BOX     M17  -2.7127 -2.7127   0.0     5.4254  5.4254  1.2456
*
**********************************************************************
*
*                                                        ELEMENTS
*
**********************************************************************
*
* The Inner Core Element
* height = 89.0461 + 2*(34.9564 + 33.0048) =224.9685
* 2.51575 cm Smeared steel region above and below (height = 230.0 cm)
*
PART 36 ARRAY
1  1  23  33  29  (27)*4  (25)*11  (27)*4  28  33
*
* The Outer Core Element
* height = 2*(44.9748 +34.9564 + 33.0048) = 2* 112.936 =225.872
```

```
* 2.064 cm Smeared steel region above and below (height = 115.0 cm)
*
PART 37 ARRAY
1  1  24  34  29  (27)*4  (26)*12  (27)*4  28  34
*
*The Radial Blanket element 1B
* height = 2*(50.296 + 30.4506 + 33.0048) = 2*113.7514 = 227.5028
* (1.2486 cm Smeared steel region above and below)
*
PART 38 ARRAY
1  1   30  35  29  (31)*3  (30)*20  (31)*3   28  35
*
* The Special Inner Core Element
*
PART 39 ARRAY
1  1  23  33  29  (27)*4  (25)*3   (32)*5  (25)*3  (27)*4  28  33
*
*
* steel bar
PART 40 NEST
BOX     M23  -2.54   -2.54     0.0     5.08    5.08    230.0
BOX     M0  -2.7127 -2.7127    0.0     5.4254  5.4254  230.0
*
**************************************************************************
*
*                        ALTERNATIVE INNER CORE CELLS AND ELEMENTS
*
*
**************************************************************************
*
* Plate 41, the Pu metal plate PUX8
PART 41 NEST
BOX     M36  -2.3355  -2.3355 0.04572  4.671   4.671   0.23506
BOX     M37  -2.5335  -2.5335 0.0      5.067   5.067   0.3265
BOX     M28  -2.7127 -2.7127   0.0     5.4254  5.4254   0.3265
*
* Plate 42, the Pu metal plate PUXI8
PART 42 NEST
BOX     M38  -2.3355  -2.3355 0.04572  4.671   4.671   0.23506
BOX     M39  -2.5335  -2.5335 0.0      5.067   5.067   0.3265
BOX     M28  -2.7127 -2.7127   0.0     5.4254  5.4254   0.3265
*
* Plate 43, the sodium plate NASTDM4
PART 43 NEST
BOX     M40  -2.4815  -2.4815 0.03683 4.963  4.963   0.54234
BOX     M41 -2.5335  -2.5335  0.0     5.067  5.067   0.616
BOX     M28  -2.7127 -2.7127   0.0     5.4254  5.4254  0.616
*
*
**************************************************************************
*
* Alternative Inner Core Cells
* Cell 30B
PART 44 ARRAY
1  1  14  9  4  9  41  9  4  9  13  4  9  1  9  4  9
*
* Cell 30BG
PART 45 ARRAY
1  1  14  43  4  43  41  43  4  43  13  4  43  1  43  4  43
*
* Cell 30D
PART 46 ARRAY
1  1  14  43  4  43  42  43  4  43  13  4  43  1  43  4  43
*
* Alternative Axial blanket Cell 30G
PART 47 ARRAY
1  1  20  43  12  14  43  13  12  43  14  43  13
12  43  14  43  12  13  43  14  12  43
*
* Alternative inner core elements
*
* Element C12-30B
PART 48 ARRAY
1  1  23  33  29  (27)*4  (44)*11  (27)*4  28  33
*
```

```
* Element C12-30BG
PART 49 ARRAY
1  1  23  33  29  (47)*4  (45)*11  (47)*4  28  33
*
* Element C12-30D
PART 50 ARRAY
1  1  23  33  29  (47)*4  (46)*11  (47)*4  28  33
*
*
************************************************************************
*
*                        ALTERNATIVE OUTER CORE CELLS AND ELEMENTS
*
*
************************************************************************
*
*
* Plate 51, the Pu metal plate PUV8
PART 51 NEST
BOX     M42  -2.3355  -2.3355 0.04572  4.671   4.671   0.23506
BOX     M43  -2.5335  -2.5335 0.0      5.067   5.067   0.3265
BOX     M28  -2.7127 -2.7127   0.0     5.4254  5.4254   0.3265
*
* Plate 52, the Pu metal plate PUVII8
PART 52 NEST
BOX     M44  -2.3355  -2.3355 0.04572  4.671   4.671   0.23506
BOX     M45  -2.5335  -2.5335 0.0      5.067   5.067   0.3265
BOX     M28  -2.7127 -2.7127   0.0     5.4254  5.4254   0.3265
*
* Plate 53, the Pu metal plate PUVIII8
PART 53 NEST
BOX     M46  -2.3355  -2.3355 0.04572  4.671   4.671   0.23506
BOX     M47  -2.5335  -2.5335 0.0      5.067   5.067   0.3265
BOX     M28  -2.7127 -2.7127   0.0     5.4254  5.4254   0.3265
*
* Plate 54, the Pu metal plate PUVIII8
PART 54 NEST
BOX     M48  -2.3355  -2.3355 0.04572  4.671   4.671   0.23506
BOX     M49  -2.5335  -2.5335 0.0      5.067   5.067   0.3265
BOX     M28  -2.7127 -2.7127   0.0     5.4254  5.4254   0.3265
*
*
* Outer Core Cell 1A
PART 55 ARRAY
1  1  14  10  5  10  51  13  5  10  10  5  14  51  10  5  10
*
*
* Outer Core Cell 1BG
PART 56 ARRAY
1  1  14  43  5  43  3  13  5  43  43  5  14  3  43  5  43
*
*
* Outer Core Cell 1C
PART 57 ARRAY
1  1  14  9  5  9  52  13  5  9  9  5  14  52  9  5  9
*
* Outer Core Cell 1D
PART 58 ARRAY
1  1  14  9  5  9  53  13  5  9  9  5  14  53  9  5  9
*
*
* Outer Core Cell 1DG
PART 59 ARRAY
1  1  14  43  5  43  53  13  5  43  43  5  14  53  43  5  43
*
*
* Outer Core Cell 1G
PART 60 ARRAY
1  1  14  43  5  43  54  13  5  43  43  5  14  54  43  5  43
*
*
* Axial blanket Cell 1
PART 61 ARRAY
1  1  20  10  12  14  10  13  12  10  14  10  13
12  10  14  10  12  13  10  14  12  10
```

```
*
*
* Axial blanket Cell 1AG
PART 62 ARRAY
1  1  20  43  12  14  43  13  12  43  14  43  13
12  43  14  43  12  13  43  14  12  43
*
* The Outer Core Element 1A
*
PART 63 ARRAY
1  1  24  34  29  (61)*4  (55)*12  (61)*4  28  34
*
*
* The Outer Core Element 1BG
*
PART 64 ARRAY
1  1  24  34  29  (62)*4  (56)*12  (62)*4  28  34
*
*
* The Outer Core Element 1C
*
PART 65 ARRAY
1  1  24  34  29  (27)*4  (57)*12  (27)*4  28  34
*
*
* The Outer Core Element 1D
*
PART 66 ARRAY
1  1  24  34  29  (27)*4  (58)*12  (27)*4  28  34
*
*
* The Outer Core Element 1DG
*
PART 67 ARRAY
1  1  24  34  29  (62)*4  (59)*12  (62)*4  28  34
*
*
* The Outer Core Element 1G
*
PART 68 ARRAY
1  1  24  34  29  (62)*4  (60)*12  (62)*4  28  34
*
*
************************************************************************
*
*                                                  ARRAYS OF ELEMENTS
* Uniform group of 5x5 elements
*
************************************************************************
* Inner Core array
*
* 5x5 Special core centre region for reaction rate data.
PART 69 ARRAY
5  5  1  (39)*25
*
*
*
************************************************************************
*                                                            ROW 1
************************************************************************
*                                                            ROW 1
************************************************************************
*
* Row 1, the bottom set of groups of size 3x4 and 5x4 (5 along x axis)
* 5 arrays
*
* Left side
PART 70 ARRAY
3  4  1  (40)*9  40 (38)*2
*
* Left centre
PART 71 ARRAY
5  4  1  (40)*5  (40)*4  38  (38)*10
*
* Centre
```

```
PART 72 ARRAY
5  4  1  (40)*5  (38)*15
*
* Right centre
PART 73 ARRAY
5  4  1  (40)*5  38  (40)*4  (38)*10
*
* Right side
PART 74 ARRAY
3  4  1  (40)*9  (38)*2  40
*
* combine these arrays to form the row 1 array
PART 75 ARRAY
5  1  1  70  71  72  73  74
*
*
************************************************************************
*                                                              ROW 2
************************************************************************
* 7 arrays of elements
*
* Bottom left outer group
PART 76 ARRAY
5  5  1  (40)*10  (40)*4  38  (40)*3  (38)*2  (40)*2  (38)*3
*
* Bottom left second group
PART 77 ARRAY
5  5  1  40  (38)*4  (38)*20
*
* Bottom left centre group
PART 78 ARRAY
5  5  1  (38)*15  (38)*3  68  67  68  67  (66)*2  65
*
* Central group
PART 79 ARRAY
5  5  1  (38)*15  (66)*5  (65)*5
*
* Bottom right centre group
PART 80 ARRAY
5  5  1  (38)*15  67  68  68 (38)*2  65  (66)*3   68
*
* Bottom next right group
PART 81 ARRAY
5  5  1  (38)*4  40  (38)*20
*
* Bottom right outer group
PART 82 ARRAY
5  5  1  (40)*10  38  (40)*4  (38)*2  (40)*3  (38)*3  (40)*2
*
* combine these 7 arrays to form the row 2 array
PART 83 ARRAY
7  1  1  76  77  78  79  80  81  82
*
************************************************************************
*                                                              ROW 3
************************************************************************
* 9 arrays of elements, the left and right hand ones being 4x5 arrays
*
* Left side
PART 84 ARRAY
4  5  1  (40)*12  (40)*3  38  (40)*3  38
*
* Outer left
PART 85 ARRAY
5  5  1  40 (38)*4 (38)*20
*
* Left Centre
PART 86 ARRAY
5  5  1   (38)*4  67  (38)*3  (66)*2  (38)*2  66  65  37
38  66  65  37  63  68  65  37  63  50
*
* Core left
PART 87 ARRAY
5  5  1   66  (65)*2  (37)*2  65  37  (63)*2  50  37  63  (50)*3
63  (50)*4  (50)*2  (49)*2  48
```

```
*
*  Core centre
PART 88 ARRAY
5  5  1  37  (63)*3  37  (50)*10  (49)*5  (48)*5
*
* Core right
PART 89 ARRAY
5  5  1   (37)*2  (65)*2  66  50  (63)*2  37  65  (50)*3  63  37
(50)*4  63  48  49  (50)*3
*
* Right Centre
PART 90 ARRAY
5  5  1     68  (38)*4  65  66  (38)*3  64  65  66  (38)*2
63  37  65  66  38  50  63  65  66  67
*
* Outer right
PART 91 ARRAY
5  5  1  (38)*4  40  (38)*20
*
* Right side
PART 92 ARRAY
4  5  1  (40)*12  38  (40)*3  38  (40)*3
*
* combine these arrays to form the row 3 array
PART 93 ARRAY
9  1  1  84  85  86  87  88  89  90  91  92
*
*
************************************************************************
*                                                              ROW 4
************************************************************************
* 9 arrays of elements, the left and right hand ones being 4x5 arrays
*
* Left side
PART 94 ARRAY
4  5  1  (40)*2  (38)*2  (40)*2  (38)*2  (40)*2  (38)*2
(40)*2  (38)*2  40  (38)*3
*
* Outer left
PART 95 ARRAY
5  5  1  (38)*4  68  (38)*4  66  (38)*3  68  66   (38)*3  68  66
(38)*3  67  65
*
* Left Core
PART 96 ARRAY
5  5  1   66  65  37  63  50  65  37  63  (50)*2  65  63  (50)*3
37  63  (50)*3  37  (50)*3  48
*
* Centre Left
PART 97 ARRAY
5  5  1   50  49  (48)*3  49  (48)*4  (48)*3  (36)*2 (48)*2  (36)*3
48  (36)*4
*
* Centre
PART 98 ARRAY
5  5  1   (48)*5  (36)*20
*
* Centre right
PART 99 ARRAY
5  5  1  (48)*3  49  50  36  (48)*3  49  (36)*2 (48)*3  (36)*3 (48)*2
(36)*3 (48)*2
*
* Right Core
PART 100 ARRAY
5  5  1   50  63  37  65  66  (50)*2  63  37  65  (50)*3  63  65
(50)*3  63  37  48  (50)*3  37
*
* Outer right
PART 101 ARRAY
5  5  1  68  (38)*4  67  (38)*4  66  (38)*4  66  68  (38)*3
65  67  (38)*3
*
* Right side
PART 102 ARRAY
4  5  1  (38)*2 (40)*2  (38)*2 (40)*2  (38)*2  (40)*2  (38)*2 (40)*2
```

```
(38)*3  40
*
* combine these arrays to form the row 3 array
PART 103 ARRAY
9  1  1  94  95  96  97  98  99  100  101  102
*
*
************************************************************************
*  The middle row                                                ROW 5
************************************************************************
* 9 arrays of elements, the left and right hand ones being 4x5 arrays
*
* Left side
PART 104 ARRAY
4  5  1  40  (38)*3  40  (38)*3  40  (38)*3  40  (38)*3  40  (38)*3
*
* Outer left
PART 105 ARRAY
5  5  1  (38)*3  66  65  (38)*3  66  65  (38)*3  66  65
(38)*3  66  65  (38)*3  66  65
*
* Left Core
PART 106 ARRAY
5  5  1   63  (50)*2  49  48  63  (50)*2  49  48  63  (50)*2  49  48
63  (50)*2  49  48  63  (50)*2  49  48
*
*  Centre Left
PART 107 ARRAY
5  5  1   48  (36)*4  48  (36)*4  48  (36)*4  48  (36)*4  48  (36)*4
*
* Centre right
PART 108 ARRAY
5  5  1   (36)*4  48  (36)*4  48  (36)*4  48  (36)*4  48  (36)*4  48
*
* Right Core
PART 109 ARRAY
5  5  1   48  49  (50)*2  37  48  49  (50)*2  63  48  49  (50)*2  63
48  49  (50)*2  63  48  49  (50)*2  37
*
* Outer right
PART 110 ARRAY
5  5  1  65  66  (38)*3  65  66  (38)*3  65  66  (38)*3  65  66  (38)*3
65  66   (38)*3
*
* Right side
PART 111 ARRAY
4  5  1  (38)*3  40  (38)*3  40  (38)*3  40  (38)*3  40  (38)*3  40
*
* combine these arrays to form the row 3 array
PART 112 ARRAY
9  1  1  104  105  106  107  69  108  109  110  111
*
*
************************************************************************
*                                                             ROW 6
************************************************************************
* 9 arrays of elements, the left and right hand ones being 4x5 arrays
*
* Left side
PART 113 ARRAY
4  5  1   40  (38)*3  (40)*2  (38)*2  (40)*2  (38)*2  (40)*2  (38)*2
(40)*2  (38)*2
*
* Outer left
PART 114 ARRAY
5  5  1   (38)*3  67  65  (38)*3  68  66  (38)*4  66  (38)*4  67
(38)*4  68
*
*
* Left Core
PART 115 ARRAY
5  5  1   37  (50)*3  48 37  63  (50)*3   65  63  (50)*3
65  37  63  (50)*2  66  65  37  63  50
*
* Centre Left
```

```
PART 116 ARRAY
5  5  1   (48)*2  (36)*3  (48)*2  (36)*3  (48)*3  (36)*2
49  (48)*3  36   50  49  (48)*3
*
* Centre
PART 117 ARRAY
5  5  1   (36)*20  (48)*5
*
* Centre right
PART 118 ARRAY
5  5  1  (36)*4  48  (36)*3  (48)*2  (36)*2 (48)*3   (48)*4  49
(48)*3  49  50
*
* Right Core
PART 119 ARRAY
5  5  1   48  (50)*3  37  (50)*3  63  37  (50)*3  63  65
(50)*2  63  37  65  50  63  37  65  66
*
* Outer right
PART 120 ARRAY
5  5  1   65  67  (38)*3  66  68  (38)*3  66  68  (38)*3  66  (38)*4
68  (38)*4
*
* Right side
PART 121 ARRAY
4  5  1   (38)*3  40  (38)*2 (40)*2  (38)*2 (40)*2  (38)*2 (40)*2
(38)*2 (40)*2
*
* combine these arrays to form the row 3 array
PART 122 ARRAY
9  1  1  113  114  115  116  117  118  119  120  121
*
*
************************************************************************
*                                                          ROW 7
************************************************************************
*
* 9 arrays of elements, the left and right hand ones being 4x5 arrays
*
* Left side
PART 123 ARRAY
4  5  1   (40)*3  38  (40)*3  38  (40)*12
*
* Outer left
PART 124 ARRAY
5  5  1   (38)*20   40 (38)*4
*
* Left Centre
PART 125 ARRAY
5  5  1   67  66  65  63  50  38  66  65  37  63  (38)*2  66  65  64
(38)*3  66  65  (38)*4  68
*
* Core left
PART 126 ARRAY
5  5  1  (50)*3  49  48  63  (50)*4  37  63  (50)*3  65  37  (63)*2  50
66  (65)*2  (37)*2
*
*  Core centre
PART 127 ARRAY
5  5  1    (48)*5  (49)*5  (50)*10  37  (63)*3  37
*
* Core right
PART 128 ARRAY
5  5  1  48  (49)*2  (50)*2  (50)*4  63  (50)*3  63  37
50  (63)*2  37  65  (37)*2  (65)*2  66
*
* Right centre
PART 129 ARRAY
5  5  1  50  63  37  66  68  63  37  65  66  38  37  65  66  (38)*2
(66)*2  (38)*3  67  (38)*4
*
* Outer right
PART 130 ARRAY
5  5  1   (38)*20  (38)*4  40
*
```

```
* Right side
PART 131 ARRAY
4  5  1   38  (40)*3  38  (40)*3  (40)*12
*
* combine these arrays to form the row 7 array
PART 132 ARRAY
9  1  1  123  124  125  126  127  128  129  130  131
*
*
************************************************************************
*                                                          ROW 8
************************************************************************
* 7 arrays of elements
*
* left outer group
PART 133 ARRAY
5  5  1   (40)*2  (38)*3 (40)*3  (38)*2  (40)*4  38  (40)*10
*
* left second group
PART 134 ARRAY
5  5  1  (38)*20  40  (38)*4
*
*  left centre group
PART 135 ARRAY
5  5  1  68  (66)*3  65  (38)*2  68  68  67  (38)*15
*
* Central group
PART 136 ARRAY
5  5  1  (65)*5  (66)*5  (38)*15
*
*  right centre group
PART 137 ARRAY
5  5  1    65  (66)*2  67  68  67  68  (38)*3  (38)*15
*
*  next right group
PART 138 ARRAY
5  5  1  (38)*20   (38)*4  40
*
*  right outer group
PART 139 ARRAY
5  5  1   (38)*3  (40)*2 (38)*2  (40)*3  38  (40)*4   (40)*10
*
* combine these 7 arrays to form the row 2 array
PART 140 ARRAY
7  1  1  133  134  135  136  137  138  139
*
*
************************************************************************
*                                                          ROW 9
************************************************************************
*
* Row 9, the top set of groups of size 3x4 and 5x4 (5 along the x axis)
* 5 arrays
*
* Left side
PART 141 ARRAY
3  4  1  40 (38)*2  (40)*9
*
* Left centre
PART 142 ARRAY
5  4  1  (38)*10  (40)*4  38  (40)*5
*
* Centre
PART 143 ARRAY
5  4  1  (38)*15  (40)*5
*
* Right centre
PART 144 ARRAY
5  4  1  (38)*10  38  (40)*4  (40)*5
*
* Right side
PART 145 ARRAY
3  4  1  (38)*2  40  (40)*9
*
* combine these arrays to form the row 9 array
```

```
PART 146 ARRAY
5  1  1  141  142  143  144  145
*
*
************************************************************************
*
*         Cluster of superlattice groups in a circle of shield material
*
************************************************************************
* Cluster of superlattice groups in a circle of shield material
PART 147   CLUSTER
BOX  P146   -56.9667   94.9445   -115.0  113.9334  21.7016 230.0
BOX  P140   -94.9445   67.8175   -115.0  189.889   27.127  230.0
BOX  P132   -116.6461  40.6905   -115.0  233.2922  27.127  230.0
BOX  P122   -116.6461  13.5635   -115.0  233.2922  27.127  230.0
BOX  P112    -116.6461 -13.5635   -115.0  233.2922  27.127  230.0
BOX  P103    -116.6461 -40.6905   -115.0  233.2922  27.127  230.0
BOX  P93    -116.6461 -67.8175   -115.0  233.2922  27.127  230.0
BOX  P83    -94.9445  -94.9445   -115.0  189.889   27.127  230.0
BOX  P75    -56.9667  -116.6461  -115.0  113.9334  21.7016 230.0
ZROD  M24     0.0     0.0     -116.0       135.0    232.0
*
************************************************************************
* Albedo for free boundaries at side and top and reflection at bottom
*
ALBEDO 0.0  0.0  0.0
END
*
************************************************************************
*
BEGIN CONTROL DATA
STAGES -10  2400  5000  STDV 0.0001
END
*
************************************************************************
*
BEGIN SOURCE GEOMETRY
ZONEMAT
ALL / MATERIAL 1
END
*
************************************************************************
*
BEGIN ACTION TALLIES
     NONORM
     NO ACTION TALLIES
     NOPRINT FLUXES  SCEDST  BNDXNG MATACT REGACT  NPARAM  SYSCAT
     SGUIDE HOLACT
END
*
************************************************************************
```

```
* MONK8B Input Listing for MZB/3 Model B, Na Follower at centre
* and 8 extra outer core elements.
************************************************************************
* material 1 - U/Pu oxide plate core
* material 2 - U/Pu plate clad
* material 3 - PUIX8 Plutonium metal plate core
* material 4 - PUIX8 Plutonium metal clad
* material 5 - PUVI8 Plutonium metal plate core
* material 6 - PUVI8 Plutonium metal clad
* material 7 - UO2 plate  core UO23R4
* material 8 - UO2 plate clad UO23R4
* material 9 - UO2 plate  core UO24R4
* material 10 - UO2 plate clad UO24R4
* material 11 - U8 natural uranium region
* material 12 - U2 natural uranium region
* material 13 - Sodium plate core NASTDL4
* material 14 - Sodium plate clad NASTDL4
* material 15 - Sodium plate core NASTBR4
* material 16 - Sodium plate clad NASTBR4
* material 17 - Steel STSTBR8
* material 18 - Steel STSTDL8
* material 19 - MST1
* material 20 - MST2
* material 21 - MST3 Steel block
* material 22 - MST8
* material 23 - Steel bar MST9F10 at actual density (width 5.08 cm)
* material 24 - Steel bar averaged over the mean spacing of 5.4254 cm
* material 25 - GI8
* material 26 - GII8
* material 27 - GIII8
* material 28 - Smeared stainless steel sheath - average lattice pitch
* material 29 - Smeared mild steel sheath - average lattice pitch
* material 30 - ALSC3
* material 31 - ALG8
* material 32 - AL2O34
* material 33 - U/Pu oxide plate core at reactor core centre
* material 34 - PUIX8 plate core at reactor core centre
* material 35 - UO23R4 plate core at reactor core centre
* material 36 - PUX8 Plutonium metal plate core
* material 37 - PUX8 Plutonium metal clad
* material 38 - PUXI8 Plutonium metal plate core
* material 39 - PUXI8 Plutonium metal clad
* material 40 - Sodium plate core NASTDM4
* material 41 - Sodium plate can NASTDM4
* material 42 - PUV8 Plutonium metal plate core
* material 43 - PUV8 Plutonium metal clad
* material 44 - PUVII8 Plutonium metal plate core
* material 45 - PUVII8 Plutonium metal clad
* material 46 - PUVIII8 Plutonium metal plate core
* material 47 - PUVIII8 Plutonium metal clad
* material 48 - PUXII8 Plutonium metal plate core
* material 49 - PUXII8 Plutonium metal clad
* materials 50 to 58 are the follower materials
*
************************************************************************
COLUMNS 1 132
BEGIN MATERIAL SPECIFICATION
NUMBER DENSITY
MATERIAL 1
 C   6.2771E-05  O16 4.2860E-02  AL  2.7943E-05  SI  2.6845E-05
 FE  1.3500E-05 NI  1.2846E-05
 U234  7.4340E-07  U235  1.1548E-04  U238  1.5938E-02
 NP237  2.4466E-07  PU239  4.7730E-03 PU240  5.3344E-04
 PU241  5.0303E-05  PU242  4.7919E-06 AM241  2.6204E-05
MATERIAL 2
 H1  2.0111E-05  C   1.6876E-04  SI  5.9180E-04  P   2.6177E-05
 S   2.5282E-05  CR  1.3956E-02  MN  1.0995E-03  FE  5.0428E-02
 NI  6.9005E-03  NB  2.8363E-04
MATERIAL 3
 H1  1.5145E-04 C   2.8155E-04 N   9.2216E-06 O16  5.7245E-05
 AL  2.3065E-05 SI  2.8430E-05 CR  6.0974E-06 MN  1.7099E-06
 FE  1.3036E-05 NI  2.6810E-05 GA  2.1190E-03
U238    5.2779E-06  PU238  3.5515E-05  PU239  2.8995E-02
PU240  6.9474E-03  PU241  1.1413E-03  PU242  1.8046E-04
AM241  5.9252E-05
```

```
MATERIAL 4
 H1  1.3771E-05  C   1.1312E-04  SI  3.6529E-04  P  1.3425E-05
 CR  9.3855E-03  MN  8.5801E-04  FE  3.5483E-02 NI  4.1575E-03
 CU  1.6626E-02
MATERIAL 5
 H1  1.0485E-04  C   2.2876E-04  N   2.4312E-05 O16  3.5962E-05
 AL  1.7408E-05  CR  3.1616E-06  MN  1.0687E-06  FE  1.9344E-05
 NI  6.8024E-06  GA  2.2555E-03
 U238      2.4663E-07  PU238   3.6995E-05  PU239   2.8972E-02
 PU240  7.3421E-03  PU241   1.1537E-03  PU242   2.0132E-04
 AM241   8.6769E-05
MATERIAL 6
 H1   1.3955E-05  C    1.1413E-04  SI   3.6853E-04  P    1.3545E-05
 CR   9.4688E-03  MN   8.6563E-04  FE   3.5798E-02  NI   4.1944E-03
 CU   1.6626E-02
MATERIAL 7
H1 3.0915E-05  C  1.1933E-05  O16 4.6151E-02  AL 3.4645E-06
SI 2.3076E-05  MN 1.1343E-07  FE 1.3390E-06  NI 1.2742E-06
MO 3.2478E-07
U235 1.6595E-04  U238 2.2908E-02
MATERIAL 8
H1 1.9528E-05  C  1.2651E-04  SI 6.3619E-04  P  3.4607E-04
S  3.5596E-05  CR 1.3636E-02  MN 8.4422E-04  FE 4.7664E-02
NI 8.3138E-03
MATERIAL 9
H1  2.4503E-05  C   3.0842E-05  O16 4.5733E-02  SI  1.3190E-05
FE  6.6332E-06
U234 1.1871E-06  U235 1.6462E-04  U238 2.2694E-02
MATERIAL 10
 H1  1.7335E-05  C    1.4546E-04  SI   6.0964E-04  P    2.2563E-05
 S   2.1792E-05  CR   1.2365E-02  MN   9.7951E-04  FE   4.3411E-02
 NI   6.0134E-03  CU   8.1603E-04  AG   1.2368E-03
MATERIAL 11
H1  4.4048E-05  C   4.9283E-04  SI  2.1076E-04  FE  1.0599E-04
U235 3.3369E-04  U238 4.6021E-02
MATERIAL 12
H1  4.3899E-05  C   4.6047E-04  SI  1.9692E-04  FE  9.9032E-05
U235 3.3962E-04  U238 4.6785E-02
MATERIAL 13
H1  1.3418E-05  O16 5.6353E-06  NA  2.3168E-02  CA  3.5994E-06
FE  1.6144E-07
MATERIAL 14
H1 2.4319E-05  C  2.8978E-04  SI 6.0218E-04  P  3.2445E-05
S  3.2865E-05  CR 1.4602E-02  MN 1.3425E-03  FE 5.4467E-02
NI 7.0225E-03  NB 3.0815E-04
MATERIAL 15
 H1  2.1098E-06 LI  3.8296E-07 B   1.4752E-07 O16  1.9937E-06
 NA  2.3119E-02 K   4.6230E-07 CA  1.7244E-06 FE   3.8077E-08
MATERIAL 16
 H1  2.1496E-05  C   2.1646E-04  SI  6.0171E-04  P   2.7979E-05
 S   2.7023E-05  CR  1.5000E-02  MN  1.0806E-03  FE  5.4056E-02
 NI  7.2502E-03  NB  3.0316E-04
MATERIAL 17
H1 2.3265E-05  C  7.8091E-04  AL 1.7381E-04  SI 1.3358E-03
TI 2.9384E-04  CR 1.6325E-02  MN 9.3901E-04  FE 5.8278E-02
NI 7.7510E-03  CU 7.3801E-05  MO 9.7764E-05
MATERIAL 18
H1 2.3115E-05  C  7.7587E-04  AL 1.7269E-04  SI 1.3272E-03
TI 2.9195E-04  CR 1.6220E-02  MN 9.3295E-04  FE 5.7902E-02
NI 7.7009E-03  CU 7.3324E-05  MO 9.7133E-05
MATERIAL 19
 H1  2.8122E-05  C   5.1129E-04  AL  1.4007E-04  TI  3.9465E-05
 CR  2.7256E-05  MN  3.2675E-04  FE  8.3911E-02  NI  4.8294E-05
 CU  4.4603E-05  MO  9.8477E-06
MATERIAL 20
 H1   2.7967E-05  C    5.0847E-04  AL   1.3930E-04 TI   3.9247E-05
 CR   2.7106E-05  MN   3.2495E-04  FE   8.3448E-02 NI   4.8028E-05
 CU   4.4357E-05  MO   9.7934E-06
MATERIAL 21
 H1  2.8087E-05  C   5.1066E-04  AL  1.3989E-04  TI  3.9416E-05
 CR  2.7222E-05  MN  3.2634E-04  FE  8.3806E-02  NI  4.8234E-05
 CU  4.4548E-05  MO  9.8355E-06
MATERIAL 22
 H1   2.7730E-05  C    5.0417E-04  AL   1.3812E-04  TI   3.8915E-05
 CR   2.6876E-05  MN   3.2220E-04  FE   8.2742E-02  NI   4.7622E-05
```

```
 CU   4.3982E-05  MO   9.7106E-06
MATERIAL 23
H1  4.6306E-05 C   6.8972E-04 SI  3.1158E-04 P   4.2944E-05
S   3.7110E-05 MN  7.1275E-04 FE  8.1432E-02
MATERIAL 24
H1  4.0597E-05 C   6.0468E-04 SI  2.7317E-04 P   3.7649E-05
S   3.2535E-05 MN  6.2488E-04 FE  7.1392E-02
MATERIAL 25
 H1  4.8551E-05  C   8.1417E-02  S   1.2207E-05  FE  6.1336E-06
MATERIAL 26
 H1  2.0286E-05  C   8.5101E-02  S   1.2751E-06  FE  1.8306E-06
MATERIAL 27
 H1  1.9906E-05  C   8.3507E-02  FE  2.3351E-06
MATERIAL 28
 H1  9.7398E-06  C   3.2692E-04  AL  1.4553E-04  SI  4.1943E-04
 TI  1.2302E-04  V   3.8541E-05  CR  6.7589E-03  MN  5.0032E-04
 FE  2.3765E-02  NI  3.7801E-03  CU  3.0896E-05  MO  6.1393E-05
MATERIAL 29
 H1  1.0937E-04  C   1.3002E-04  SI  1.9624E-05  P   5.9314E-06
 S   1.9478E-05  MN  1.1537E-04  FE  3.2730E-02
MATERIAL 30
 AL   4.7590E-02 SI   4.5790E-06 MN   9.3634E-07 FE   2.9936E-05
 CU   1.8214E-06
MATERIAL 31
 AL   2.6704E-02  SI   1.0296E-05  MN   6.5793E-07  FE   3.6374E-05
 CU   4.5505E-07
MATERIAL 32
 H1   5.1483E-05  B10  4.5063E-06  B11  1.6599E-05  O16  6.6386E-02
 AL   4.4240E-02
MATERIAL 33
 C   6.2771E-05  O16 4.2860E-02  AL  2.7943E-05  SI  2.6845E-05
 FE  1.3500E-05 NI  1.2846E-05
 U234  7.4340E-07  U235  1.1548E-04  U238  1.5938E-02
 NP237  2.4466E-07  PU239  4.7730E-03 PU240  5.3344E-04
 PU241  5.0303E-05  PU242  4.7919E-06 AM241  2.6204E-05
MATERIAL 34
 H1  1.5145E-04 C   2.8155E-04 N   9.2216E-06 O16  5.7245E-05
 AL  2.3065E-05 SI  2.8430E-05 CR  6.0974E-06 MN  1.7099E-06
 FE  1.3036E-05 NI  2.6810E-05 GA  2.1190E-03
U238    5.2779E-06  PU238  3.5515E-05  PU239  2.8995E-02
PU240  6.9474E-03  PU241  1.1413E-03  PU242  1.8046E-04
AM241  5.9252E-05
MATERIAL 35
H1 3.0915E-05  C  1.1933E-05  O16 4.6151E-02  AL 3.4645E-06
SI 2.3076E-05  MN 1.1343E-07  FE 1.3390E-06  NI 1.2742E-06
MO 3.2478E-07
U235 1.6595E-04  U238 2.2908E-02
MATERIAL 36
 H1  1.0485E-04 C   2.9524E-04 N   1.0060E-05 O16 4.5503E-05
 AL  2.1760E-05 SI  1.5887E-05 CR  4.2908E-06 MN  1.0687E-06
 FE  1.4928E-05 NI  1.6206E-05 GA  2.2417E-03
U238       1.4305E-06  PU238  3.4035E-05  PU239  2.9107E-02
PU240  6.9117E-03  PU241  1.1359E-03  PU242  1.8531E-04
AM241  3.3658E-05
MATERIAL 37
 H1 1.3587E-05 C  1.2050E-04 SI 5.2025E-04 P  2.6701E-05
 S  1.5471E-05 TI 5.7590E-06 CR 9.9679E-03 MN 8.5308E-04
 FE 3.3844E-02 NI 4.8383E-03 CU 1.6868E-02
MATERIAL 38
 H1  1.7475E-04 C   2.2876E-04 N   1.1737E-05 O16 4.1833E-05
 AL  1.8713E-05 SI  1.8396E-05 CR  6.0974E-06 MN  1.0687E-06
 FE  2.2287E-05 NI  1.7606E-05 GA  2.2490E-03
U238     6.9057E-07  PU238 3.7488E-05  PU239 2.8990E-02
PU240 6.9709E-03  PU241 1.1546E-03  PU242 1.8482E-04
AM241 3.0855E-05
MATERIAL 39
 H1 1.3404E-05 C  1.1825E-04 SI 5.1057E-04 P  2.6205E-05
 S  1.5188E-05 TI 5.6508E-06 CR 9.7825E-03 MN 8.3722E-04
 FE 3.3215E-02 NI 4.7483E-03 CU 1.6868E-02
MATERIAL 40
H1 1.3418E-05  O16 5.6353E-06  NA 2.3168E-02  CA 3.5994E-06
FE 1.6144E-07
MATERIAL 41
H1 2.1522E-05  C  2.1672E-04  SI 7.8781E-04  P  3.2216E-05
S  1.6234E-05  CR 1.5953E-02  MN 1.2635E-03  FE 5.2254E-02
```

```
NI 7.8948E-03  NB 3.4089E-04
MATERIAL 42
 H1   1.7475E-04 C    2.5027E-04 N    1.3413E-05 O16  5.0640E-05
 AL   2.1760E-05 SI   2.3831E-05 CR   5.1941E-06 MN   1.0687E-06
 FE   1.6610E-05 NI   1.1804E-05 GA   2.2424E-03 MO   1.9583E-06
 U238   1.3318E-06  PU238   2.9103E-05  PU239   2.9328E-02
 PU240   6.7928E-03  PU241   9.8832E-04  PU242   1.6639E-04
 AM241   1.1785E-04
MATERIAL 43
 H1   1.3404E-05 C    9.2801E-05 SI   4.1625E-04 P    1.8432E-05
 S    9.3252E-06 CR   9.2549E-03 MN   7.5220E-04 FE   3.4310E-02
 NI   4.5397E-03 CU   1.6626E-02
MATERIAL 44
 H1  1.3980E-04  C   2.0335E-04  N   6.7066E-06  O16 5.4310E-05
 AL  1.6973E-05  SI  1.0870E-05  CR  4.0649E-06  MN  8.5494E-07
 FE  1.0513E-05  NI  9.0032E-06  GA  2.0492E-03
U238   9.3720E-07  PU238  3.1569E-05  PU239  2.9028E-02
PU240  6.9606E-03  PU241  1.1208E-03  PU242  1.8725E-04
AM241  8.0243E-05
MATERIAL 45
 H1   1.3771E-05  C    1.1357E-04  SI   3.6675E-04  P    1.3479E-05
 CR   9.4231E-03  MN   8.6145E-04  FE   3.5625E-02  NI   4.1742E-03
 CU  1.6626E-02
MATERIAL 46
 H1   1.2815E-04  C    4.2429E-04  N    2.4312E-05  O16  8.8804E-05
 AL   2.3065E-05  SI   1.4215E-05  CR   3.6133E-06  MN   1.4962E-06
 FE   1.6400E-05  NI   8.6031E-06  GA   2.0247E-03
U238  6.9057E-07  PU238 3.0583E-05  PU239 2.9035E-02
PU240 6.9371E-03  PU241 1.1304E-03  PU242 1.8773E-04
AM241 7.1186E-05
MATERIAL 47
 H1   1.3771E-05 C    1.1340E-04 SI   3.6619E-04 P    1.3461E-05
 CR   9.4087E-03 MN   8.6013E-04 FE   3.5570E-02 NI   4.1678E-03
 CU  1.6626E-02
MATERIAL 48
 H1  1.7475E-04 C   2.6298E-04 N   6.7066E-06 O16 4.1833E-05
 AL  1.7408E-05 SI  2.2159E-05 CR  9.2590E-06 MN  8.5494E-07
 FE  1.4928E-05 NI  2.3809E-05 GA  2.3032E-03
U238      1.6771E-06   PU238 3.6995E-05  PU239 2.9064E-02
PU240 6.8990E-03  PU241 1.1606E-03  PU242 1.7997E-04
AM241 2.7359E-05
MATERIAL 49
 H1 1.3220E-05 C  1.1685E-04 SI 5.0450E-04 P  2.5895E-05
 S  1.5004E-05 TI 5.5851E-06 CR 9.6661E-03 MN 8.2726E-04
 FE 3.2820E-02 NI 4.6918E-03 CU 1.6868E-02
MATERIAL 50
* B90 pins, Cylindrical Region 1, Radius 3.19 cm
B10     5.5640E-02     B11     6.0727E-03     C       1.4161E-02
Al27    1.4871E-05     Si      1.5172E-04     P31     5.2419E-06
S       2.0300E-06     Cr      1.8345E-03     Mn55    1.7292E-04
Fe      6.6141E-03     Ni      1.0676E-03     Nb      4.2072E-05
MATERIAL 51
* B80 pins, Cylindrical Region 2, Radius 4.5 cm
B10     4.6103E-02     B11     1.1587E-02     C       1.3900E-02
Si      1.8202E-04     P       7.0733E-06     S       4.8797E-06
Cr      3.8605E-03     Mn      3.3044E-04     Fe      1.2689E-02
Ni      1.8843E-03
MATERIAL 52
* Aluminium Outer Region. Outer square boundary 10.2 cm x 10.2 cm.
* Inner circular boundary, radius 4.5 cm.
AL      6.0181E-02     SI      5.7905E-06     MN      1.1841E-06
FE      3.7856E-05     CU      2.3033E-06
MATERIAL 53
* Aluminium Follower. Outer square boundary 10.2 cm x 10.2 cm
AL      5.9628E-02     SI      5.7373E-06     MN      1.1732E-06
FE      3.7509E-05     CU      2.2821E-06
MATERIAL 54
* Outer Square Region. The sheath of the B80/B90 Element, 10.7442 cm width
C       3.0522E-05     Si      2.1320E-04     P       8.2850E-06
S       5.7156E-06     Cr      4.5217E-03     Mn      3.8703E-04
Fe      1.4849E-02     Ni      2.2070E-03
MATERIAL 55
* Outer Square Region, Follower
C       5.9184E-05     Si      4.1341E-04     P       1.6065E-05
S       1.1083E-05     Cr      8.7679E-03     Mn      7.5048E-04
```

```
Fe      2.8794E-02      Ni      4.2796E-03
MATERIAL 56
* Cylinder, Follower
C       1.2275E-04      Si      8.5740E-04      P       3.3319E-05
S       2.2986E-05      Cr      1.8185E-02      Mn      1.5565E-03
Fe      5.9718E-02      Ni      8.8758E-03
MATERIAL 57
* Sodium
O       6.7640E-06      Na23    2.3890E-02      Fe      1.9673E-07
MATERIAL 58
* EndPlate Regions, BN B30, B80
C       7.6919E-05      Si      5.3728E-04      P       2.0879E-05
S       1.4404E-05      Cr      1.1395E-02      Mn      9.7536E-04
Fe      3.7422E-02      Ni      7.6919E-05
END
*
**************************************************************************
BEGIN MATERIAL GEOMETRY
*
*                                                          PLATES
*
**************************************************************************
* Plate 1, the Pu metal plate UPUO24
PART 1 NEST
BOX     M1  -2.4765  -2.4765  0.03734  4.953          4.953   0.55312
BOX     M2  -2.5335  -2.5335  0.0      5.067   5.067   0.6278
BOX     M28  -2.7127 -2.7127   0.0     5.4254  5.4254   0.6278
*
* Plate 2, the Pu metal plate PUIX8
PART 2 NEST
BOX     M3  -2.3355  -2.3355  0.04572  4.671   4.671   0.23506
BOX     M4  -2.5335  -2.5335  0.0      5.067   5.067   0.3265
BOX     M28  -2.7127 -2.7127   0.0     5.4254  5.4254   0.3265
*
* Plate 3, the Pu metal plate PUVI8
PART 3 NEST
BOX     M5  -2.3355  -2.3355  0.04572  4.671   4.671   0.23506
BOX     M6  -2.5335  -2.5335  0.0      5.067   5.067   0.3265
BOX     M28  -2.7127 -2.7127   0.0     5.4254  5.4254   0.3265
*
* Plate 4, the UO2 plate UO23R4
PART 4 NEST
BOX     M7  -2.4255  -2.4255  0.03683 4.851   4.851   0.55424
BOX     M8  -2.5335  -2.5335  0.0     5.067   5.067   0.6279
BOX     M28  -2.7127 -2.7127   0.0     5.4254  5.4254  0.6279
*
* Plate 5, the UO2 plate UO24R4
PART 5 NEST
BOX     M9  -2.4255  -2.4255  0.03683 4.851   4.851   0.55424
BOX     M10  -2.5335  -2.5335 0.0     5.067   5.067   0.6279
BOX     M28  -2.7127 -2.7127   0.0     5.4254  5.4254  0.6279
*
* Control Rod Regions
*
* Part 6, the Na Follower, Length 91.44 cm, inside 90.5
PART 6 NEST
ZROD M57  0.0  0.0  0.47             4.5125         90.5
* the steel of the Cylinder, a slightly different composition
* cf Absorber
ZROD M56  0.0  0.0  0.47             4.9225         90.5
* The sodium between the cylinder and the calandria walls
BOX M57        -4.93   -4.93   0.47  9.86     9.86    90.5
* The side walls of the calandria
BOX M55     -5.3721  -5.3721    0.47         10.7442 10.7442 90.5
* The end plates of the Calandria
BOX M58     -5.3721   -5.3721   0.0     10.7442        10.7442   91.44
BOX   M0   -5.4254    -5.4254   0.0     10.8508   10.8508   91.44
*
* Part 7, the follower in the axial blanket region
PART 7 NEST
* The sodium within the Cylinder
ZROD M57  0.0  0.0  0.47             4.5125         34.62
* the steel of the Cylinder, a slightly different composition
* cf Absorber
ZROD M56  0.0  0.0  0.47             4.9225         34.62
```

```
* The sodium between the cylinder and the calandria walls
BOX M57        -4.93   -4.93   0.47  9.86     9.86    34.62
* The side walls of the calandria
BOX M55     -5.3721  -5.3721    0.47         10.7442 10.7442 34.62
* The end plates of the Calandria
BOX M58     -5.3721   -5.3721   0.0     10.7442       10.7442   35.56
BOX   M0   -5.4254    -5.4254   0.0     10.8508   10.8508   35.56
*
* Top and bottom packing for the Control rod
PART 8 NEST
BOX   M17  5.4254    -5.4254   0.0     10.8508   10.8508   0.7152
*
* Plate 9, the sodium plate NASTDL4
PART 9 NEST
BOX     M13  -2.4815  -2.4815 0.03683 4.963  4.963   0.54234
BOX     M14 -2.5335  -2.5335  0.0     5.067   5.067   0.616
BOX     M28  -2.7127 -2.7127   0.0     5.4254  5.4254  0.616
*
* Plate 10, the sodium plate NASTBR4
PART 10 NEST
BOX     M15  -2.4815  -2.4815 0.03683 4.963  4.963   0.54234
BOX     M16 -2.5335  -2.5335  0.0     5.067   5.067   0.616
BOX     M28  -2.7127 -2.7127   0.0     5.4254  5.4254  0.616
*
* Plate 11, the graphite plate GII8 (modified from GIII8)
PART 11 NEST
BOX     M26  -2.5335  -2.5335 0.0     5.067   5.067   0.31775
BOX     M28  -2.7127 -2.7127   0.0     5.4254  5.4254  0.31775
*
* Axial blanket U8 plate
PART 12 NEST
BOX     M11     -2.5335 -2.5335 0.0     5.067   5.067   0.3175
BOX     M28  -2.7127 -2.7127   0.0     5.4254  5.4254  0.3175
*
* Plate 13, the steel plate STSTBR8
PART 13 NEST
BOX     M17  -2.5335  -2.5335 0.0     5.067   5.067   0.3172
BOX     M28  -2.7127 -2.7127   0.0     5.4254  5.4254  0.3172
*
* Plate 14, the graphite plate GI8
PART 14 NEST
BOX     M25  -2.5335  -2.5335 0.0     5.067   5.067   0.3180
BOX     M28  -2.7127 -2.7127   0.0     5.4254  5.4254  0.3180
*
* Plenum aluminium cylinder ALSC3
PART 15 NEST
BOX     M29     -2.5335 -2.5335 0.0     5.067   5.067   7.62
BOX     M28  -2.7127 -2.7127   0.0     5.4254  5.4254  7.62
*
* Plenum plate MST1
PART 16 NEST
BOX     M19     -2.5335 -2.5335 0.0     5.067   5.067   2.5385
BOX     M28  -2.7127 -2.7127   0.0     5.4254  5.4254  2.5385
*
* Plenum plate MST3
PART 17 NEST
BOX     M21     -2.5335 -2.5335 0.0     5.067   5.067   7.6063
BOX     M28  -2.7127 -2.7127   0.0     5.4254  5.4254  7.6063
*
*
************************************************************************
*
*                                       Radial blanket components
*
************************************************************************
* Uranium metal U2
PART 18 NEST
BOX     M12     -2.5335 -2.5335 0.0     5.067   5.067   1.2723
BOX     M28      -2.7127 -2.7127        0.0     5.4254  5.4254  1.2723
*
* Graphite GII8
PART 19 NEST
BOX     M26     -2.5335 -2.5335 0.0     5.067   5.067   0.31775
BOX     M28  -2.7127 -2.7127   0.0     5.4254  5.4254  0.31775
*
```

```
* Mild steel MST8
PART 20 NEST
BOX     M22     -2.5335 -2.5335 0.0     5.067   5.067   0.3147
BOX     M28   -2.7127 -2.7127   0.0     5.4254  5.4254  0.3147
*
* Stainless steel STSTDL8
PART 21 NEST
BOX     M18     -2.5335 -2.5335 0.0     5.067   5.067   0.3236
BOX     M28   -2.7127 -2.7127   0.0     5.4254  5.4254  0.3236
*
* ALUMINIUM ALG8
PART 22 NEST
BOX     M31     -2.5335 -2.5335 0.0     5.067   5.067   0.3170
BOX     M28   -2.7127 -2.7127   0.0     5.4254  5.4254  0.3170
*
* Aluminium oxide AL2O34
PART 23 NEST
BOX     M32     -2.5335 -2.5335 0.0     5.067   5.067   0.6317
BOX     M28   -2.7127 -2.7127   0.0     5.4254  5.4254  0.6317
*
*
* Mild steel MST2
PART 24 NEST
BOX     M20     -2.5335 -2.5335 0.0     5.067   5.067   1.2718
BOX     M28   -2.7127 -2.7127   0.0     5.4254  5.4254  1.2718
*
************************************************************************
*
*                                                              CELLS
*
************************************************************************
*
* Inner Core Cell
PART 25 ARRAY
1  1  14  9  4  9  2  9  4  9  13  4  9  1  9  4  9
*
* Outer Core Cell 1B
PART 26 ARRAY
1  1  14  9  5  9  3  13  5  9  9  5  14  3  9  5  9
*
* Axial blanket Cell 1A
PART 27 ARRAY
1  1  20  9  12  14  9  13  12  9  14  9  13
12  9  14  9  12  13  9  14  12  9
*
* Upper Axial Plenum Cell
PART 28 ARRAY
1  1  5  15  17  15  16  15
*
* Lower Axial Plenum Cell
PART 29 ARRAY
1  1  5  15  16  15  17  15
*
* Radial blanket central region cell
PART 30 ARRAY
1  1  10  19  10  19  21  18  11  10  20  19  10
*
* Radial blanket outer region Cell
PART 31 ARRAY
1  1  20  22  22  23  14  22  18  22  14  23  24
22  14  22  22  18  23  22  14  20  22
*
*  Forming the Control Element. Grouping the plenum cells
PART 32 ARRAY
2  2  1   28  28  28  28
*  1  1  7  8  32  7  6  7  32  8
*
* Steel packing pieces to line up the elements
*
*
* Inner core packing
PART 33 NEST
BOX     M17   -2.7127 -2.7127   0.0     5.4254  5.4254  2.51575
*
* Outer core packing
```

```
PART 34 NEST
BOX     M17  -2.7127 -2.7127   0.0     5.4254  5.4254  2.064
*
* radial blanket element packing (reduced by 0.003)
PART 35 NEST
BOX     M17  -2.7127 -2.7127   0.0     5.4254  5.4254  1.2456
*
************************************************************************
*
*                                                          ELEMENTS
*
************************************************************************
*
* The Inner Core Element
* height = 89.0461 + 2*(34.9564 + 33.0048) =224.9685
* 2.51575 cm Smeared steel region above and below (height = 230.0 cm)
*
PART 36 ARRAY
1  1  23  33  29  (27)*4  (25)*11  (27)*4  28  33
*
* The Outer Core Element
* height = 2*(44.9748 +34.9564 + 33.0048) = 2* 112.936 =225.872
* 2.064 cm Smeared steel region above and below (height = 115.0 cm)
*
PART 37 ARRAY
1  1  24  34  29  (27)*4  (26)*12  (27)*4  28  34
*
*The Radial Blanket element 1B
* height = 2*(50.296 + 30.4506 + 33.0048) = 2*113.7514 = 227.5028
* (1.2486 cm Smeared steel region above and below)
*
PART 38 ARRAY
1  1   30  35  29  (31)*3  (30)*20  (31)*3   28  35
*
* The Special Inner Core Element
* replaced by the Control Element
*
PART 39 ARRAY
1  1  7  8  32  7  6  7  32  8
*
* steel bar
PART 40 NEST
BOX     M23  -2.54   -2.54     0.0     5.08    5.08    230.0
BOX     M0  -2.7127 -2.7127    0.0     5.4254  5.4254  230.0
*
************************************************************************
*
*                        ALTERNATIVE INNER CORE CELLS AND ELEMENTS
*
*
************************************************************************
*
* Plate 41, the Pu metal plate PUX8
PART 41 NEST
BOX     M36  -2.3355  -2.3355 0.04572  4.671   4.671   0.23506
BOX     M37  -2.5335  -2.5335 0.0      5.067   5.067   0.3265
BOX     M28  -2.7127 -2.7127   0.0     5.4254  5.4254   0.3265
*
* Plate 42, the Pu metal plate PUXI8
PART 42 NEST
BOX     M38  -2.3355  -2.3355 0.04572  4.671   4.671   0.23506
BOX     M39  -2.5335  -2.5335 0.0      5.067   5.067   0.3265
BOX     M28  -2.7127 -2.7127   0.0     5.4254  5.4254   0.3265
*
* Plate 43, the sodium plate NASTDM4
PART 43 NEST
BOX     M40  -2.4815  -2.4815 0.03683 4.963   4.963   0.54234
BOX     M41 -2.5335  -2.5335  0.0     5.067   5.067   0.616
BOX     M28  -2.7127 -2.7127   0.0     5.4254  5.4254  0.616
*
*
************************************************************************
*
* Alternative Inner Core Cells
* Cell 30B
```

```
PART 44 ARRAY
1  1  14  9  4  9  41  9  4  9  13  4  9  1  9  4  9
*
* Cell 30BG
PART 45 ARRAY
1  1  14  43  4  43  41  43  4  43  13  4  43  1  43  4  43
*
* Cell 30D
PART 46 ARRAY
1  1  14  43  4  43  42  43  4  43  13  4  43  1  43  4  43
*
* Alternative Axial blanket Cell 30G
PART 47 ARRAY
1  1  20  43  12  14  43  13  12  43  14  43  13
12  43  14  43  12  13  43  14  12  43
*
* Alternative inner core elements
*
* Element C12-30B
PART 48 ARRAY
1  1  23  33  29  (27)*4  (44)*11  (27)*4  28  33
*
* Element C12-30BG
PART 49 ARRAY
1  1  23  33  29  (47)*4  (45)*11  (47)*4  28  33
*
* Element C12-30D
PART 50 ARRAY
1  1  23  33  29  (47)*4  (46)*11  (47)*4  28  33
*
*
************************************************************************
*
*                        ALTERNATIVE OUTER CORE CELLS AND ELEMENTS
*
*
************************************************************************
*
*
* Plate 51, the Pu metal plate PUV8
PART 51 NEST
BOX     M42  -2.3355  -2.3355 0.04572  4.671   4.671   0.23506
BOX     M43  -2.5335  -2.5335 0.0      5.067   5.067   0.3265
BOX     M28  -2.7127 -2.7127   0.0     5.4254  5.4254   0.3265
*
* Plate 52, the Pu metal plate PUVII8
PART 52 NEST
BOX     M44  -2.3355  -2.3355 0.04572  4.671   4.671   0.23506
BOX     M45  -2.5335  -2.5335 0.0      5.067   5.067   0.3265
BOX     M28  -2.7127 -2.7127   0.0     5.4254  5.4254   0.3265
*
* Plate 53, the Pu metal plate PUVIII8
PART 53 NEST
BOX     M46  -2.3355  -2.3355 0.04572  4.671   4.671   0.23506
BOX     M47  -2.5335  -2.5335 0.0      5.067   5.067   0.3265
BOX     M28  -2.7127 -2.7127   0.0     5.4254  5.4254   0.3265
*
* Plate 54, the Pu metal plate PUVIII8
PART 54 NEST
BOX     M48  -2.3355  -2.3355 0.04572  4.671   4.671   0.23506
BOX     M49  -2.5335  -2.5335 0.0      5.067   5.067   0.3265
BOX     M28  -2.7127 -2.7127   0.0     5.4254  5.4254   0.3265
*
*
* Outer Core Cell 1A
PART 55 ARRAY
1  1  14  10  5  10  51  13  5  10  10  5  14  51  10  5  10
*
*
* Outer Core Cell 1BG
PART 56 ARRAY
1  1  14  43  5  43  3  13  5  43  43  5  14  3  43  5  43
*
*
* Outer Core Cell 1C
```

```
PART 57 ARRAY
1  1  14  9  5  9  52  13  5  9  9  5  14  52  9  5  9
*
* Outer Core Cell 1D
PART 58 ARRAY
1  1  14  9  5  9  53  13  5  9  9  5  14  53  9  5  9
*
*
* Outer Core Cell 1DG
PART 59 ARRAY
1  1  14  43  5  43  53  13  5  43  43  5  14  53  43  5  43
*
*
* Outer Core Cell 1G
PART 60 ARRAY
1  1  14  43  5  43  54  13  5  43  43  5  14  54  43  5  43
*
*
* Axial blanket Cell 1
PART 61 ARRAY
1  1  20  10  12  14  10  13  12  10  14  10  13
12  10  14  10  12  13  10  14  12  10
*
*
* Axial blanket Cell 1AG
PART 62 ARRAY
1  1  20  43  12  14  43  13  12  43  14  43  13
12  43  14  43  12  13  43  14  12  43
*
* The Outer Core Element 1A
*
PART 63 ARRAY
1  1  24  34  29  (61)*4  (55)*12  (61)*4  28  34
*
*
* The Outer Core Element 1BG
*
PART 64 ARRAY
1  1  24  34  29  (62)*4  (56)*12  (62)*4  28  34
*
*
* The Outer Core Element 1C
*
PART 65 ARRAY
1  1  24  34  29  (27)*4  (57)*12  (27)*4  28  34
*
*
* The Outer Core Element 1D
*
PART 66 ARRAY
1  1  24  34  29  (27)*4  (58)*12  (27)*4  28  34
*
*
* The Outer Core Element 1DG
*
PART 67 ARRAY
1  1  24  34  29  (62)*4  (59)*12  (62)*4  28  34
*
*
* The Outer Core Element 1G
*
PART 68 ARRAY
1  1  24  34  29  (62)*4  (60)*12  (62)*4  28  34
*
*
************************************************************************
*
*                                                ARRAYS OF ELEMENTS
* Uniform group of 5x5 elements
*
************************************************************************
* Inner Core array
*
* 5x5 Special core centre region containing the control rod.
* -2.7127 -2.7127     0.0     5.4254  5.4254  230.0
```

```
* Overall width 27.127, half widths 13.5635,
PART 69 CLUSTER
BOX  P36   -13.5635   -13.5635   0.0  5.4254 5.4254  230.0
BOX  P36    -8.1381   -13.5635   0.0  5.4254 5.4254  230.0
BOX  P36    -2.7127   -13.5635   0.0  5.4254 5.4254  230.0
BOX  P36     2.7127   -13.5635   0.0  5.4254 5.4254  230.0
BOX  P36     8.1381   -13.5635   0.0  5.4254 5.4254  230.0
BOX  P36   -13.5635    -8.1381   0.0  5.4254 5.4254  230.0
BOX  P36    -8.1381    -8.1381   0.0  5.4254 5.4254  230.0
BOX  P36    -2.7127    -8.1381   0.0  5.4254 5.4254  230.0
BOX  P36     2.7127    -8.1381   0.0  5.4254 5.4254  230.0
BOX  P36     8.1381    -8.1381   0.0  5.4254 5.4254  230.0
BOX  P36   -13.5635    -2.7127   0.0  5.4254 5.4254  230.0
BOX  P36    -8.1381    -2.7127   0.0  5.4254 5.4254  230.0
BOX  P39    -2.7127    -2.7127   0.0  10.8508   10.8508 230.0
BOX  P36     8.1381    -2.7127   0.0  5.4254 5.4254  230.0
BOX  P36   -13.5635     2.7127   0.0  5.4254 5.4254  230.0
BOX  P36    -8.1381     2.7127   0.0  5.4254 5.4254  230.0
BOX  P36     8.1381     2.7127   0.0  5.4254 5.4254  230.0
BOX  P36   -13.5635     8.1381   0.0  5.4254 5.4254  230.0
BOX  P36    -8.1381     8.1381   0.0  5.4254 5.4254  230.0
BOX  P36    -2.7127     8.1381   0.0  5.4254 5.4254  230.0
BOX  P36     2.7127     8.1381   0.0  5.4254 5.4254  230.0
BOX  P36     8.1381     8.1381   0.0  5.4254 5.4254  230.0
BOX  M0    -13.5635   -13.5635   0.0  27.127 27.127  230.0
*
************************************************************************
*                                                              ROW 1
************************************************************************
*
* Row 1, the bottom set of groups of size 3x4 and 5x4 (5 along x axis)
* 5 arrays
*
* Left side
PART 70 ARRAY
3  4  1  (40)*9  40 (38)*2
*
* Left centre
PART 71 ARRAY
5  4  1  (40)*5  (40)*4  38  (38)*10
*
* Centre
PART 72 ARRAY
5  4  1  (40)*5  (38)*15
*
* Right centre
PART 73 ARRAY
5  4  1  (40)*5  38  (40)*4  (38)*10
*
* Right side
PART 74 ARRAY
3  4  1  (40)*9  (38)*2  40
*
* combine these arrays to form the row 1 array
PART 75 ARRAY
5  1  1  70  71  72  73  74
*
*
************************************************************************
*                                                              ROW 2
************************************************************************
* 7 arrays of elements
*
* Bottom left outer group
PART 76 ARRAY
5  5  1  (40)*10  (40)*4  38  (40)*3  (38)*2  (40)*2  (38)*3
*
* Bottom left second group
PART 77 ARRAY
5  5  1  40  (38)*4  (38)*20
*
* Bottom left centre group
PART 78 ARRAY
5  5  1  (38)*15  (38)*3  68  67  68  67  (66)*2  65
*
```

```
* Central group
PART 79 ARRAY
5  5  1  (38)*15  (66)*5  (65)*5
*
* Bottom right centre group
PART 80 ARRAY
5  5  1  (38)*15  67  68  68 (38)*2  65  (66)*3   68
*
* Bottom next right group
PART 81 ARRAY
5  5  1  (38)*4  40  (38)*20
*
* Bottom right outer group
PART 82 ARRAY
5  5  1  (40)*10  38  (40)*4  (38)*2  (40)*3  (38)*3  (40)*2
*
* combine these 7 arrays to form the row 2 array
PART 83 ARRAY
7  1  1  76  77  78  79  80  81  82
*
************************************************************************
*                                                              ROW 3
************************************************************************
* 9 arrays of elements, the left and right hand ones being 4x5 arrays
*
* Left side
PART 84 ARRAY
4  5  1  (40)*12  (40)*3  38  (40)*3  38
*
* Outer left
PART 85 ARRAY
5  5  1  40 (38)*4 (38)*20
*
* Left Centre
PART 86 ARRAY
5  5  1   (38)*4  67  (38)*3  (66)*2  (38)*2  66  65  37
38  66  65  37  63  68  65  37  63  50
*
* Core left
PART 87 ARRAY
5  5  1   66  (65)*2  (37)*2  65  37  (63)*2  50  37  63  (50)*3
63  (50)*4  (50)*2  (49)*2  48
*
*  Core centre
PART 88 ARRAY
5  5  1  37  (63)*3  37  (50)*10  (49)*5  (48)*5
*
* Core right
PART 89 ARRAY
5  5  1   (37)*2  (65)*2  66  50  (63)*2  37  65  (50)*3  63  37
(50)*4  63  48  49  (50)*3
*
* Right Centre
PART 90 ARRAY
5  5  1     68  (38)*4  65  66  (38)*3  64  65  66  (38)*2
63  37  65  66  38  50  63  65  66  67
*
* Outer right
PART 91 ARRAY
5  5  1  (38)*4  40  (38)*20
*
* Right side
PART 92 ARRAY
4  5  1  (40)*12  38  (40)*3  38  (40)*3
*
* combine these arrays to form the row 3 array
PART 93 ARRAY
9  1  1  84  85  86  87  88  89  90  91  92
*
*
************************************************************************
*                                                              ROW 4
************************************************************************
* 9 arrays of elements, the left and right hand ones being 4x5 arrays
*
```

```
* Left side
PART 94 ARRAY
4  5  1  (40)*2  (38)*2  (40)*2  (38)*2  (40)*2  (38)*2
(40)*2  (38)*2  40  (38)*3
*
* Outer left
PART 95 ARRAY
5  5  1  (38)*4  68  (38)*4  66  (38)*3  68  66   (38)*3  68  66
(38)*3  67  65
*
* Left Core
PART 96 ARRAY
5  5  1   66  65  37  63  50  65  37  63  (50)*2  65  63  (50)*3
37  63  (50)*3  37  (50)*3  48
*
* Centre Left
PART 97 ARRAY
5  5  1   50  49  (48)*3  49  (48)*4  (48)*3  (36)*2 (48)*2  (36)*3
48  (36)*4
*
* Centre
PART 98 ARRAY
5  5  1   (48)*5  (36)*20
*
* Centre right
PART 99 ARRAY
5  5  1  (48)*3  49  50  36  (48)*3  49  (36)*2 (48)*3  (36)*3 (48)*2
(36)*3 (48)*2
*
* Right Core
PART 100 ARRAY
5  5  1   50  63  37  65  66  (50)*2  63  37  65  (50)*3  63  65
(50)*3  63  37  48  (50)*3  37
*
* Outer right
PART 101 ARRAY
5  5  1  68  (38)*4  67  (38)*4  66  (38)*4  66  68  (38)*3
65  67  (38)*3
*
* Right side
PART 102 ARRAY
4  5  1  (38)*2 (40)*2  (38)*2 (40)*2  (38)*2  (40)*2  (38)*2 (40)*2
(38)*3  40
*
* combine these arrays to form the row 3 array
PART 103 ARRAY
9  1  1  94  95  96  97  98  99  100  101  102
*
*
************************************************************************
*  The middle row                                              ROW 5
************************************************************************
* 9 arrays of elements, the left and right hand ones being 4x5 arrays
*
* Left side
PART 104 ARRAY
4  5  1  40  (38)*3  40  (38)*3  40  (38)*3  40  (38)*3  40  (38)*3
*
* Outer left
PART 105 ARRAY
5  5  1  (38)*3  66  65  (38)*3  66  65  (38)*3  66  65
(38)*3  66  65  (38)*3  66  65
*
* Left Core
PART 106 ARRAY
5  5  1   63  (50)*2  49  48  63  (50)*2  49  48  63  (50)*2  49  48
63  (50)*2  49  48  63  (50)*2  49  48
*
*  Centre Left
PART 107 ARRAY
5  5  1   48  (36)*4  48  (36)*4  48  (36)*4  48  (36)*4  48  (36)*4
*
* Centre right
PART 108 ARRAY
5  5  1   (36)*4  48  (36)*4  48  (36)*4  48  (36)*4  48  (36)*4  48
```

```
*
* Right Core
PART 109 ARRAY
5  5  1   48  49  (50)*2  37  48  49  (50)*2  63  48  49  (50)*2  63
48  49  (50)*2  63  48  49  (50)*2  37
*
* Outer right
PART 110 ARRAY
5  5  1  65  66  (38)*3  65  66  (38)*3  65  66  (38)*3  65  66  (38)*3
65  66   (38)*3
*
* Right side
PART 111 ARRAY
4  5  1  (38)*3  40  (38)*3  40  (38)*3  40  (38)*3  40  (38)*3  40
*
* combine these arrays to form the row 3 array
PART 112 ARRAY
9  1  1  104  105  106  107  69  108  109  110  111
*
*
************************************************************************
*                                                          ROW 6
************************************************************************
* 9 arrays of elements, the left and right hand ones being 4x5 arrays
*
* Left side
PART 113 ARRAY
4  5  1   40  (38)*3  (40)*2  (38)*2  (40)*2  (38)*2  (40)*2  (38)*2
(40)*2  (38)*2
*
* Outer left
PART 114 ARRAY
5  5  1   (38)*3  67  65  (38)*3  68  66  (38)*4  66  (38)*4  67
(38)*4  68
*
*
* Left Core
PART 115 ARRAY
5  5  1   37  (50)*3  48 37  63  (50)*3   65  63  (50)*3
65  37  63  (50)*2  66  65  37  63  50
*
* Centre Left
PART 116 ARRAY
5  5  1   (48)*2  (36)*3  (48)*2  (36)*3  (48)*3  (36)*2
49  (48)*3  36   50  49  (48)*3
*
* Centre
PART 117 ARRAY
5  5  1   (36)*20  (48)*5
*
* Centre right
PART 118 ARRAY
5  5  1  (36)*4  48  (36)*3  (48)*2  (36)*2 (48)*3   (48)*4  49
(48)*3  49  50
*
* Right Core
PART 119 ARRAY
5  5  1   48  (50)*3  37  (50)*3  63  37  (50)*3  63  65
(50)*2  63  37  65  50  63  37  65  66
*
* Outer right
PART 120 ARRAY
5  5  1   65  67  (38)*3  66  68  (38)*3  66  68  (38)*3  66  (38)*4
68  (38)*4
*
* Right side
PART 121 ARRAY
4  5  1   (38)*3  40  (38)*2 (40)*2  (38)*2 (40)*2  (38)*2 (40)*2
(38)*2 (40)*2
*
* combine these arrays to form the row 3 array
PART 122 ARRAY
9  1  1  113  114  115  116  117  118  119  120  121
*
*
```

```
************************************************************************
*                                                            ROW 7
************************************************************************
*
* 9 arrays of elements, the left and right hand ones being 4x5 arrays
*
* Left side
PART 123 ARRAY
4  5  1   (40)*3  38  (40)*3  38  (40)*12
*
* Outer left
PART 124 ARRAY
5  5  1   (38)*20   40 (38)*4
*
* Left Centre
PART 125 ARRAY
5  5  1   67  66  65  63  50  38  66  65  37  63  (38)*2  66  65  64
(38)*3  66  65  (38)*4  68
*
* Core left
PART 126 ARRAY
5  5  1  (50)*3  49  48  63  (50)*4  37  63  (50)*3  65  37  (63)*2  50
66  (65)*2  (37)*2
*
*  Core centre
PART 127 ARRAY
5  5  1    (48)*5  (49)*5  (50)*10  37  (63)*3  37
*
* Core right
PART 128 ARRAY
5  5  1  48  (49)*2  (50)*2  (50)*4  63  (50)*3  63  37
50  (63)*2  37  65  (37)*2  (65)*2  66
*
* Right centre
PART 129 ARRAY
5  5  1  50  63  37  66  68  63  37  65  66  38  37  65  66  (38)*2
(66)*2  (38)*3  67  (38)*4
*
* Outer right
PART 130 ARRAY
5  5  1   (38)*20  (38)*4  40
*
* Right side
PART 131 ARRAY
4  5  1   38  (40)*3  38  (40)*3  (40)*12
*
* combine these arrays to form the row 7 array
PART 132 ARRAY
9  1  1  123  124  125  126  127  128  129  130  131
*
*
************************************************************************
*                                                            ROW 8
************************************************************************
* 7 arrays of elements
*
* left outer group
PART 133 ARRAY
5  5  1   (40)*2  (38)*3 (40)*3  (38)*2  (40)*4  38  (40)*10
*
* left second group
PART 134 ARRAY
5  5  1  (38)*20  40  (38)*4
*
*  left centre group
PART 135 ARRAY
5  5  1  68  (66)*3  65  (38)*2  68  68  67  (38)*15
*
* Central group
PART 136 ARRAY
5  5  1  (65)*5  (66)*5  (38)*15
*
*  right centre group
PART 137 ARRAY
5  5  1    65  (66)*2  67  68  67  68  (38)*3  (38)*15
```

```
*
*  next right group
PART 138 ARRAY
5  5  1  (38)*20   (38)*4  40
*
*  right outer group
PART 139 ARRAY
5  5  1   (38)*3  (40)*2 (38)*2  (40)*3  38  (40)*4   (40)*10
*
* combine these 7 arrays to form the row 2 array
PART 140 ARRAY
7  1  1  133  134  135  136  137  138  139
*
*
*********************************************************************
*                                                            ROW 9
*********************************************************************
*
* Row 9, the top set of groups of size 3x4 and 5x4 (5 along the x axis)
* 5 arrays
*
* Left side
PART 141 ARRAY
3  4  1  40 (38)*2  (40)*9
*
* Left centre
PART 142 ARRAY
5  4  1  (38)*10  (40)*4  38  (40)*5
*
* Centre
PART 143 ARRAY
5  4  1  (38)*15  (40)*5
*
* Right centre
PART 144 ARRAY
5  4  1  (38)*10  38  (40)*4  (40)*5
*
* Right side
PART 145 ARRAY
3  4  1  (38)*2  40  (40)*9
*
* combine these arrays to form the row 9 array
PART 146 ARRAY
5  1  1  141  142  143  144  145
*
*
*********************************************************************
*
*         Cluster of superlattice groups in a circle of shield material
*
*********************************************************************
* Cluster of superlattice groups in a circle of shield material
PART 147   CLUSTER
BOX  P146   -56.9667   94.9445   -115.0  113.9334  21.7016 230.0
BOX  P140   -94.9445   67.8175   -115.0  189.889   27.127  230.0
BOX  P132   -116.6461  40.6905   -115.0  233.2922  27.127  230.0
BOX  P122   -116.6461  13.5635   -115.0  233.2922  27.127  230.0
BOX  P112    -116.6461 -13.5635   -115.0  233.2922  27.127  230.0
BOX  P103    -116.6461 -40.6905   -115.0  233.2922  27.127  230.0
BOX  P93    -116.6461 -67.8175   -115.0  233.2922  27.127  230.0
BOX  P83    -94.9445  -94.9445   -115.0  189.889   27.127  230.0
BOX  P75    -56.9667  -116.6461  -115.0  113.9334  21.7016 230.0
ZROD  M24     0.0     0.0     -116.0       135.0    232.0
*
*********************************************************************
* Albedo for free boundaries at side and top and reflection at bottom
*
ALBEDO 0.0  0.0  0.0
END
*
*********************************************************************
*
BEGIN CONTROL DATA
STAGES -10  2400  5000  STDV 0.0001
END
```

```
*
**********************************************************************
*
BEGIN SOURCE GEOMETRY
ZONEMAT
ALL / MATERIAL 1
END
*
**********************************************************************
*
BEGIN ACTION TALLIES
     NONORM
     NO ACTION TALLIES
     NOPRINT FLUXES  SCEDST  BNDXNG MATACT REGACT  NPARAM  SYSCAT
     SGUIDE HOLACT
END
*
**********************************************************************
```

```
* MONK8B Input Listing for MZB/3 Model B,
* 8 added edge elements and a central BN rod
************************************************************************
* material 1 - U/Pu oxide plate core
* material 2 - U/Pu plate clad
* material 3 - PUIX8 Plutonium metal plate core
* material 4 - PUIX8 Plutonium metal clad
* material 5 - PUVI8 Plutonium metal plate core
* material 6 - PUVI8 Plutonium metal clad
* material 7 - UO2 plate  core UO23R4
* material 8 - UO2 plate clad UO23R4
* material 9 - UO2 plate  core UO24R4
* material 10 - UO2 plate clad UO24R4
* material 11 - U8 natural uranium region
* material 12 - U2 natural uranium region
* material 13 - Sodium plate core NASTDL4
* material 14 - Sodium plate clad NASTDL4
* material 15 - Sodium plate core NASTBR4
* material 16 - Sodium plate clad NASTBR4
* material 17 - Steel STSTBR8
* material 18 - Steel STSTDL8
* material 19 - MST1
* material 20 - MST2
* material 21 - MST3 Steel block
* material 22 - MST8
* material 23 - Steel bar MST9F10 at actual density (width 5.08 cm)
* material 24 - Steel bar averaged over the mean spacing of 5.4254 cm
* material 25 - GI8
* material 26 - GII8
* material 27 - GIII8
* material 28 - Smeared stainless steel sheath - average lattice pitch
* material 29 - Smeared mild steel sheath - average lattice pitch
* material 30 - ALSC3
* material 31 - ALG8
* material 32 - AL2O34
* material 33 - U/Pu oxide plate core at reactor core centre
* material 34 - PUIX8 plate core at reactor core centre
* material 35 - UO23R4 plate core at reactor core centre
* material 36 - PUX8 Plutonium metal plate core
* material 37 - PUX8 Plutonium metal clad
* material 38 - PUXI8 Plutonium metal plate core
* material 39 - PUXI8 Plutonium metal clad
* material 40 - Sodium plate core NASTDM4
* material 41 - Sodium plate can NASTDM4
* material 42 - PUV8 Plutonium metal plate core
* material 43 - PUV8 Plutonium metal clad
* material 44 - PUVII8 Plutonium metal plate core
* material 45 - PUVII8 Plutonium metal clad
* material 46 - PUVIII8 Plutonium metal plate core
* material 47 - PUVIII8 Plutonium metal clad
* material 48 - PUXII8 Plutonium metal plate core
* material 49 - PUXII8 Plutonium metal clad
* materials 50 to 58 are the control rod regions
*
************************************************************************
COLUMNS 1 132
BEGIN MATERIAL SPECIFICATION
NUMBER DENSITY
MATERIAL 1
 C   6.2771E-05  O16 4.2860E-02  AL  2.7943E-05  SI  2.6845E-05
 FE  1.3500E-05 NI  1.2846E-05
 U234  7.4340E-07  U235  1.1548E-04  U238  1.5938E-02
 NP237  2.4466E-07  PU239  4.7730E-03 PU240  5.3344E-04
 PU241  5.0303E-05  PU242  4.7919E-06 AM241  2.6204E-05
MATERIAL 2
 H1  2.0111E-05  C   1.6876E-04  SI  5.9180E-04  P   2.6177E-05
 S   2.5282E-05  CR  1.3956E-02  MN  1.0995E-03  FE  5.0428E-02
 NI  6.9005E-03  NB  2.8363E-04
MATERIAL 3
 H1  1.5145E-04 C   2.8155E-04 N   9.2216E-06 O16  5.7245E-05
 AL  2.3065E-05 SI  2.8430E-05 CR  6.0974E-06 MN  1.7099E-06
 FE  1.3036E-05 NI  2.6810E-05 GA  2.1190E-03
U238    5.2779E-06  PU238  3.5515E-05  PU239  2.8995E-02
PU240  6.9474E-03  PU241  1.1413E-03  PU242  1.8046E-04
AM241  5.9252E-05
```

```
MATERIAL 4
 H1  1.3771E-05  C   1.1312E-04  SI  3.6529E-04  P  1.3425E-05
 CR  9.3855E-03  MN  8.5801E-04  FE  3.5483E-02 NI  4.1575E-03
 CU  1.6626E-02
MATERIAL 5
 H1  1.0485E-04  C   2.2876E-04  N   2.4312E-05 O16  3.5962E-05
 AL  1.7408E-05  CR  3.1616E-06  MN  1.0687E-06  FE  1.9344E-05
 NI  6.8024E-06  GA  2.2555E-03
 U238      2.4663E-07  PU238   3.6995E-05  PU239   2.8972E-02
 PU240  7.3421E-03  PU241   1.1537E-03  PU242   2.0132E-04
 AM241   8.6769E-05
MATERIAL 6
 H1   1.3955E-05  C    1.1413E-04  SI   3.6853E-04  P    1.3545E-05
 CR   9.4688E-03  MN   8.6563E-04  FE   3.5798E-02  NI   4.1944E-03
 CU   1.6626E-02
MATERIAL 7
H1 3.0915E-05  C  1.1933E-05  O16 4.6151E-02  AL 3.4645E-06
SI 2.3076E-05  MN 1.1343E-07  FE 1.3390E-06  NI 1.2742E-06
MO 3.2478E-07
U235 1.6595E-04  U238 2.2908E-02
MATERIAL 8
H1 1.9528E-05  C  1.2651E-04  SI 6.3619E-04  P  3.4607E-04
S  3.5596E-05  CR 1.3636E-02  MN 8.4422E-04  FE 4.7664E-02
NI 8.3138E-03
MATERIAL 9
H1  2.4503E-05  C   3.0842E-05  O16 4.5733E-02  SI  1.3190E-05
FE  6.6332E-06
U234 1.1871E-06  U235 1.6462E-04  U238 2.2694E-02
MATERIAL 10
 H1  1.7335E-05  C    1.4546E-04  SI   6.0964E-04  P    2.2563E-05
 S   2.1792E-05  CR   1.2365E-02  MN   9.7951E-04  FE   4.3411E-02
 NI   6.0134E-03  CU   8.1603E-04  AG   1.2368E-03
MATERIAL 11
H1  4.4048E-05  C   4.9283E-04  SI  2.1076E-04  FE  1.0599E-04
U235 3.3369E-04  U238 4.6021E-02
MATERIAL 12
H1  4.3899E-05  C   4.6047E-04  SI  1.9692E-04  FE  9.9032E-05
U235 3.3962E-04  U238 4.6785E-02
MATERIAL 13
H1  1.3418E-05  O16 5.6353E-06  NA  2.3168E-02  CA  3.5994E-06
FE  1.6144E-07
MATERIAL 14
H1 2.4319E-05  C  2.8978E-04  SI 6.0218E-04  P  3.2445E-05
S  3.2865E-05  CR 1.4602E-02  MN 1.3425E-03  FE 5.4467E-02
NI 7.0225E-03  NB 3.0815E-04
MATERIAL 15
 H1  2.1098E-06 LI  3.8296E-07 B   1.4752E-07 O16  1.9937E-06
 NA  2.3119E-02 K   4.6230E-07 CA  1.7244E-06 FE   3.8077E-08
MATERIAL 16
 H1  2.1496E-05  C   2.1646E-04  SI  6.0171E-04  P   2.7979E-05
 S   2.7023E-05  CR  1.5000E-02  MN  1.0806E-03  FE  5.4056E-02
 NI  7.2502E-03  NB  3.0316E-04
MATERIAL 17
H1 2.3265E-05  C  7.8091E-04  AL 1.7381E-04  SI 1.3358E-03
TI 2.9384E-04  CR 1.6325E-02  MN 9.3901E-04  FE 5.8278E-02
NI 7.7510E-03  CU 7.3801E-05  MO 9.7764E-05
MATERIAL 18
H1 2.3115E-05  C  7.7587E-04  AL 1.7269E-04  SI 1.3272E-03
TI 2.9195E-04  CR 1.6220E-02  MN 9.3295E-04  FE 5.7902E-02
NI 7.7009E-03  CU 7.3324E-05  MO 9.7133E-05
MATERIAL 19
 H1  2.8122E-05  C   5.1129E-04  AL  1.4007E-04  TI  3.9465E-05
 CR  2.7256E-05  MN  3.2675E-04  FE  8.3911E-02  NI  4.8294E-05
 CU  4.4603E-05  MO  9.8477E-06
MATERIAL 20
 H1   2.7967E-05  C    5.0847E-04  AL   1.3930E-04 TI   3.9247E-05
 CR   2.7106E-05  MN   3.2495E-04  FE   8.3448E-02 NI   4.8028E-05
 CU   4.4357E-05  MO   9.7934E-06
MATERIAL 21
 H1  2.8087E-05  C   5.1066E-04  AL  1.3989E-04  TI  3.9416E-05
 CR  2.7222E-05  MN  3.2634E-04  FE  8.3806E-02  NI  4.8234E-05
 CU  4.4548E-05  MO  9.8355E-06
MATERIAL 22
 H1   2.7730E-05  C    5.0417E-04  AL   1.3812E-04  TI   3.8915E-05
 CR   2.6876E-05  MN   3.2220E-04  FE   8.2742E-02  NI   4.7622E-05
```

```
 CU   4.3982E-05  MO   9.7106E-06
MATERIAL 23
H1  4.6306E-05 C   6.8972E-04 SI  3.1158E-04 P   4.2944E-05
S   3.7110E-05 MN  7.1275E-04 FE  8.1432E-02
MATERIAL 24
H1  4.0597E-05 C   6.0468E-04 SI  2.7317E-04 P   3.7649E-05
S   3.2535E-05 MN  6.2488E-04 FE  7.1392E-02
MATERIAL 25
 H1  4.8551E-05  C   8.1417E-02  S   1.2207E-05  FE  6.1336E-06
MATERIAL 26
 H1  2.0286E-05  C   8.5101E-02  S   1.2751E-06  FE  1.8306E-06
MATERIAL 27
 H1  1.9906E-05  C   8.3507E-02  FE  2.3351E-06
MATERIAL 28
 H1  9.7398E-06  C   3.2692E-04  AL  1.4553E-04  SI  4.1943E-04
 TI  1.2302E-04  V   3.8541E-05  CR  6.7589E-03  MN  5.0032E-04
 FE  2.3765E-02  NI  3.7801E-03  CU  3.0896E-05  MO  6.1393E-05
MATERIAL 29
 H1  1.0937E-04  C   1.3002E-04  SI  1.9624E-05  P   5.9314E-06
 S   1.9478E-05  MN  1.1537E-04  FE  3.2730E-02
MATERIAL 30
 AL   4.7590E-02 SI   4.5790E-06 MN   9.3634E-07 FE   2.9936E-05
 CU   1.8214E-06
MATERIAL 31
 AL   2.6704E-02  SI   1.0296E-05  MN   6.5793E-07  FE   3.6374E-05
 CU   4.5505E-07
MATERIAL 32
 H1   5.1483E-05  B10  4.5063E-06  B11  1.6599E-05  O16  6.6386E-02
 AL   4.4240E-02
MATERIAL 33
 C   6.2771E-05  O16 4.2860E-02  AL  2.7943E-05  SI  2.6845E-05
 FE  1.3500E-05 NI  1.2846E-05
 U234  7.4340E-07  U235  1.1548E-04  U238  1.5938E-02
 NP237  2.4466E-07  PU239  4.7730E-03 PU240  5.3344E-04
 PU241  5.0303E-05  PU242  4.7919E-06 AM241  2.6204E-05
MATERIAL 34
 H1  1.5145E-04 C   2.8155E-04 N   9.2216E-06 O16  5.7245E-05
 AL  2.3065E-05 SI  2.8430E-05 CR  6.0974E-06 MN  1.7099E-06
 FE  1.3036E-05 NI  2.6810E-05 GA  2.1190E-03
U238    5.2779E-06  PU238  3.5515E-05  PU239  2.8995E-02
PU240  6.9474E-03  PU241  1.1413E-03  PU242  1.8046E-04
AM241  5.9252E-05
MATERIAL 35
H1 3.0915E-05  C  1.1933E-05  O16 4.6151E-02  AL 3.4645E-06
SI 2.3076E-05  MN 1.1343E-07  FE 1.3390E-06  NI 1.2742E-06
MO 3.2478E-07
U235 1.6595E-04  U238 2.2908E-02
MATERIAL 36
 H1  1.0485E-04 C   2.9524E-04 N   1.0060E-05 O16 4.5503E-05
 AL  2.1760E-05 SI  1.5887E-05 CR  4.2908E-06 MN  1.0687E-06
 FE  1.4928E-05 NI  1.6206E-05 GA  2.2417E-03
U238       1.4305E-06  PU238  3.4035E-05  PU239  2.9107E-02
PU240  6.9117E-03  PU241  1.1359E-03  PU242  1.8531E-04
AM241  3.3658E-05
MATERIAL 37
 H1 1.3587E-05 C  1.2050E-04 SI 5.2025E-04 P  2.6701E-05
 S  1.5471E-05 TI 5.7590E-06 CR 9.9679E-03 MN 8.5308E-04
 FE 3.3844E-02 NI 4.8383E-03 CU 1.6868E-02
MATERIAL 38
 H1  1.7475E-04 C   2.2876E-04 N   1.1737E-05 O16 4.1833E-05
 AL  1.8713E-05 SI  1.8396E-05 CR  6.0974E-06 MN  1.0687E-06
 FE  2.2287E-05 NI  1.7606E-05 GA  2.2490E-03
U238     6.9057E-07  PU238 3.7488E-05  PU239 2.8990E-02
PU240 6.9709E-03  PU241 1.1546E-03  PU242 1.8482E-04
AM241 3.0855E-05
MATERIAL 39
 H1 1.3404E-05 C  1.1825E-04 SI 5.1057E-04 P  2.6205E-05
 S  1.5188E-05 TI 5.6508E-06 CR 9.7825E-03 MN 8.3722E-04
 FE 3.3215E-02 NI 4.7483E-03 CU 1.6868E-02
MATERIAL 40
H1 1.3418E-05  O16 5.6353E-06  NA 2.3168E-02  CA 3.5994E-06
FE 1.6144E-07
MATERIAL 41
H1 2.1522E-05  C  2.1672E-04  SI 7.8781E-04  P  3.2216E-05
S  1.6234E-05  CR 1.5953E-02  MN 1.2635E-03  FE 5.2254E-02
```

```
NI 7.8948E-03  NB 3.4089E-04
MATERIAL 42
 H1   1.7475E-04 C    2.5027E-04 N    1.3413E-05 O16  5.0640E-05
 AL   2.1760E-05 SI   2.3831E-05 CR   5.1941E-06 MN   1.0687E-06
 FE   1.6610E-05 NI   1.1804E-05 GA   2.2424E-03 MO   1.9583E-06
 U238   1.3318E-06  PU238   2.9103E-05  PU239   2.9328E-02
 PU240   6.7928E-03  PU241   9.8832E-04  PU242   1.6639E-04
 AM241   1.1785E-04
MATERIAL 43
 H1   1.3404E-05 C    9.2801E-05 SI   4.1625E-04 P    1.8432E-05
 S    9.3252E-06 CR   9.2549E-03 MN   7.5220E-04 FE   3.4310E-02
 NI   4.5397E-03 CU   1.6626E-02
MATERIAL 44
 H1  1.3980E-04  C   2.0335E-04  N   6.7066E-06  O16 5.4310E-05
 AL  1.6973E-05  SI  1.0870E-05  CR  4.0649E-06  MN  8.5494E-07
 FE  1.0513E-05  NI  9.0032E-06  GA  2.0492E-03
U238   9.3720E-07  PU238  3.1569E-05  PU239  2.9028E-02
PU240  6.9606E-03  PU241  1.1208E-03  PU242  1.8725E-04
AM241  8.0243E-05
MATERIAL 45
 H1   1.3771E-05  C    1.1357E-04  SI   3.6675E-04  P    1.3479E-05
 CR   9.4231E-03  MN   8.6145E-04  FE   3.5625E-02  NI   4.1742E-03
 CU  1.6626E-02
MATERIAL 46
 H1   1.2815E-04  C    4.2429E-04  N    2.4312E-05  O16  8.8804E-05
 AL   2.3065E-05  SI   1.4215E-05  CR   3.6133E-06  MN   1.4962E-06
 FE   1.6400E-05  NI   8.6031E-06  GA   2.0247E-03
U238  6.9057E-07  PU238 3.0583E-05  PU239 2.9035E-02
PU240 6.9371E-03  PU241 1.1304E-03  PU242 1.8773E-04
AM241 7.1186E-05
MATERIAL 47
 H1   1.3771E-05 C    1.1340E-04 SI   3.6619E-04 P    1.3461E-05
 CR   9.4087E-03 MN   8.6013E-04 FE   3.5570E-02 NI   4.1678E-03
 CU  1.6626E-02
MATERIAL 48
 H1  1.7475E-04 C   2.6298E-04 N   6.7066E-06 O16 4.1833E-05
 AL  1.7408E-05 SI  2.2159E-05 CR  9.2590E-06 MN  8.5494E-07
 FE  1.4928E-05 NI  2.3809E-05 GA  2.3032E-03
U238      1.6771E-06   PU238 3.6995E-05  PU239 2.9064E-02
PU240 6.8990E-03  PU241 1.1606E-03  PU242 1.7997E-04
AM241 2.7359E-05
MATERIAL 49
 H1 1.3220E-05 C  1.1685E-04 SI 5.0450E-04 P  2.5895E-05
 S  1.5004E-05 TI 5.5851E-06 CR 9.6661E-03 MN 8.2726E-04
 FE 3.2820E-02 NI 4.6918E-03 CU 1.6868E-02
MATERIAL 50
*  Outer Square Region, Absorber
C       5.8633E-05     Si      4.0956E-04     P31     1.5916E-05
S       1.0980E-05     Cr      8.6863E-03     Mn55    7.4349E-04
Fe      2.8526E-02     Ni      4.2398E-03
*  Cylinder, Absorber
MATERIAL 51
C       1.2133E-04     Si      8.4752E-04     P31     3.2935E-05
S       2.2721E-05     Cr      1.7975E-02     Mn55    1.5386E-03
Fe      5.9031E-02     Ni      8.7736E-03
*  Tube+Cans, BN, B30, B80
MATERIAL 52
C       1.0721E-04     Si      7.4886E-04     P31     2.9101E-05
S       2.0076E-05     Cr      1.5883E-02     Mn55    1.3595E-03
Fe      5.2159E-02     Ni      7.7523E-03
*  Absorber Region, BN
MATERIAL 53
B10     2.0915E-02     B11     8.4684E-02     C       2.6745E-02
Fe      2.0962E-05
MATERIAL 54
* Outer Square Region. The sheath of the B80/B90 Element, 10.7442 cm width
C       3.0522E-05     Si      2.1320E-04     P       8.2850E-06
S       5.7156E-06     Cr      4.5217E-03     Mn      3.8703E-04
Fe      1.4849E-02     Ni      2.2070E-03
MATERIAL 55
* Outer Square Region, Follower
C       5.9184E-05     Si      4.1341E-04     P       1.6065E-05
S       1.1083E-05     Cr      8.7679E-03     Mn      7.5048E-04
Fe      2.8794E-02     Ni      4.2796E-03
MATERIAL 56
```

```
* Cylinder, Follower
C       1.2275E-04     Si      8.5740E-04     P       3.3319E-05
S       2.2986E-05     Cr      1.8185E-02     Mn      1.5565E-03
Fe      5.9718E-02     Ni      8.8758E-03
MATERIAL 57
* Sodium
O       6.7640E-06     Na23    2.3890E-02     Fe      1.9673E-07
MATERIAL 58
* EndPlate Regions, BN B30, B80
C       7.6919E-05     Si      5.3728E-04     P       2.0879E-05
S       1.4404E-05     Cr      1.1395E-02     Mn      9.7536E-04
Fe      3.7422E-02     Ni      7.6919E-05
END
*
************************************************************************
BEGIN MATERIAL GEOMETRY
*
*                                                        PLATES
*
************************************************************************
* Plate 1, the Pu metal plate UPUO24
PART 1 NEST
BOX     M1  -2.4765  -2.4765  0.03734  4.953          4.953   0.55312
BOX     M2  -2.5335  -2.5335  0.0      5.067   5.067  0.6278
BOX     M28  -2.7127 -2.7127  0.0     5.4254  5.4254  0.6278
*
* Plate 2, the Pu metal plate PUIX8
PART 2 NEST
BOX     M3  -2.3355  -2.3355  0.04572  4.671   4.671  0.23506
BOX     M4  -2.5335  -2.5335  0.0      5.067   5.067  0.3265
BOX     M28  -2.7127 -2.7127  0.0     5.4254  5.4254  0.3265
*
* Plate 3, the Pu metal plate PUVI8
PART 3 NEST
BOX     M5  -2.3355  -2.3355  0.04572  4.671   4.671  0.23506
BOX     M6  -2.5335  -2.5335  0.0      5.067   5.067  0.3265
BOX     M28  -2.7127 -2.7127  0.0     5.4254  5.4254  0.3265
*
* Plate 4, the UO2 plate UO23R4
PART 4 NEST
BOX     M7  -2.4255  -2.4255  0.03683 4.851   4.851  0.55424
BOX     M8  -2.5335  -2.5335  0.0     5.067   5.067  0.6279
BOX     M28  -2.7127 -2.7127  0.0     5.4254  5.4254 0.6279
*
* Plate 5, the UO2 plate UO24R4
PART 5 NEST
BOX     M9  -2.4255  -2.4255  0.03683 4.851   4.851  0.55424
BOX     M10  -2.5335  -2.5335 0.0     5.067   5.067  0.6279
BOX     M28  -2.7127 -2.7127  0.0     5.4254  5.4254 0.6279
*
* Control Rod Regions
*
* Part 6, the BN Absorber, Length 91.44 cm, inside 90.5
PART 6 NEST
ZROD BH1  0.0  0.0  0.47             4.9225         90.5
* The sodium between the cylinder and the calandria walls
BOX M57        -4.93   -4.93   0.47  9.86     9.86    90.5
* The side walls of the calandria
BOX M50     -5.3721  -5.3721    0.47         10.7442 10.7442 90.5
* The end plates of the Calandria
BOX M58     -5.3721   -5.3721   0.0     10.7442        10.7442   91.44
BOX   M0   -5.4254    -5.4254   0.0     10.8508   10.8508   91.44
*
* Part 7, the follower in the axial blanket region
PART 7 NEST
* The sodium within the Cylinder
ZROD M57  0.0  0.0  0.47             4.5125         34.62
* the steel of the Cylinder, a slightly different composition
* cf Absorber
ZROD M56  0.0  0.0  0.47             4.9225         34.62
* The sodium between the cylinder and the calandria walls
BOX M57        -4.93   -4.93   0.47  9.86     9.86    34.62
* The side walls of the calandria
BOX M55     -5.3721  -5.3721    0.47         10.7442 10.7442 34.62
* The end plates of the Calandria
```

```
BOX M58     -5.3721   -5.3721   0.0     10.7442       10.7442   35.56
BOX   M0   -5.4254    -5.4254   0.0     10.8508   10.8508   35.56
*
* Top and bottom packing for the Control rod
PART 8 NEST
BOX   M17  5.4254    -5.4254   0.0     10.8508   10.8508   0.7152
*
* Plate 9, the sodium plate NASTDL4
PART 9 NEST
BOX     M13  -2.4815  -2.4815 0.03683 4.963  4.963   0.54234
BOX     M14 -2.5335  -2.5335  0.0     5.067   5.067   0.616
BOX     M28  -2.7127 -2.7127   0.0     5.4254  5.4254  0.616
*
* Plate 10, the sodium plate NASTBR4
PART 10 NEST
BOX     M15  -2.4815  -2.4815 0.03683 4.963  4.963   0.54234
BOX     M16 -2.5335  -2.5335  0.0     5.067   5.067   0.616
BOX     M28  -2.7127 -2.7127   0.0     5.4254  5.4254  0.616
*
* Plate 11, the graphite plate GII8 (modified from GIII8)
PART 11 NEST
BOX     M26  -2.5335  -2.5335 0.0     5.067   5.067   0.31775
BOX     M28  -2.7127 -2.7127   0.0     5.4254  5.4254  0.31775
*
* Axial blanket U8 plate
PART 12 NEST
BOX     M11     -2.5335 -2.5335 0.0     5.067   5.067   0.3175
BOX     M28  -2.7127 -2.7127   0.0     5.4254  5.4254  0.3175
*
* Plate 13, the steel plate STSTBR8
PART 13 NEST
BOX     M17  -2.5335  -2.5335 0.0     5.067   5.067   0.3172
BOX     M28  -2.7127 -2.7127   0.0     5.4254  5.4254  0.3172
*
* Plate 14, the graphite plate GI8
PART 14 NEST
BOX     M25  -2.5335  -2.5335 0.0     5.067   5.067   0.3180
BOX     M28  -2.7127 -2.7127   0.0     5.4254  5.4254  0.3180
*
* Plenum aluminium cylinder ALSC3
PART 15 NEST
BOX     M29     -2.5335 -2.5335 0.0     5.067   5.067   7.62
BOX     M28  -2.7127 -2.7127   0.0     5.4254  5.4254  7.62
*
* Plenum plate MST1
PART 16 NEST
BOX     M19     -2.5335 -2.5335 0.0     5.067   5.067   2.5385
BOX     M28  -2.7127 -2.7127   0.0     5.4254  5.4254  2.5385
*
* Plenum plate MST3
PART 17 NEST
BOX     M21     -2.5335 -2.5335 0.0     5.067   5.067   7.6063
BOX     M28  -2.7127 -2.7127   0.0     5.4254  5.4254  7.6063
*
*
************************************************************************
*
*                                       Radial blanket components
*
************************************************************************
* Uranium metal U2
PART 18 NEST
BOX     M12     -2.5335 -2.5335 0.0     5.067   5.067   1.2723
BOX     M28      -2.7127 -2.7127       0.0     5.4254  5.4254  1.2723
*
* Graphite GII8
PART 19 NEST
BOX     M26     -2.5335 -2.5335 0.0     5.067   5.067   0.31775
BOX     M28  -2.7127 -2.7127   0.0     5.4254  5.4254  0.31775
*
* Mild steel MST8
PART 20 NEST
BOX     M22     -2.5335 -2.5335 0.0     5.067   5.067   0.3147
BOX     M28  -2.7127 -2.7127   0.0     5.4254  5.4254  0.3147
*
```

```
* Stainless steel STSTDL8
PART 21 NEST
BOX     M18     -2.5335 -2.5335 0.0     5.067   5.067   0.3236
BOX     M28   -2.7127 -2.7127   0.0     5.4254  5.4254  0.3236
*
* ALUMINIUM ALG8
PART 22 NEST
BOX     M31     -2.5335 -2.5335 0.0     5.067   5.067   0.3170
BOX     M28   -2.7127 -2.7127   0.0     5.4254  5.4254  0.3170
*
* Aluminium oxide AL2O34
PART 23 NEST
BOX     M32     -2.5335 -2.5335 0.0     5.067   5.067   0.6317
BOX     M28   -2.7127 -2.7127   0.0     5.4254  5.4254  0.6317
*
*
* Mild steel MST2
PART 24 NEST
BOX     M20     -2.5335 -2.5335 0.0     5.067   5.067   1.2718
BOX     M28   -2.7127 -2.7127   0.0     5.4254  5.4254  1.2718
*

************************************************************************
*
*                                                          CELLS
*
************************************************************************
*
* Inner Core Cell
PART 25 ARRAY
1  1  14  9  4  9  2  9  4  9  13  4  9  1  9  4  9
*
* Outer Core Cell 1B
PART 26 ARRAY
1  1  14  9  5  9  3  13  5  9  9  5  14  3  9  5  9
*
* Axial blanket Cell 1A
PART 27 ARRAY
1  1  20  9  12  14  9  13  12  9  14  9  13
12  9  14  9  12  13  9  14  12  9
*
* Upper Axial Plenum Cell
PART 28 ARRAY
1  1  5  15  17  15  16  15
*
* Lower Axial Plenum Cell
PART 29 ARRAY
1  1  5  15  16  15  17  15
*
* Radial blanket central region cell
PART 30 ARRAY
1  1  10  19  10  19  21  18  11  10  20  19  10
*
* Radial blanket outer region Cell
PART 31 ARRAY
1  1  20  22  22  23  14  22  18  22  14  23  24
22  14  22  22  18  23  22  14  20  22
*
*  Forming the Control Element. Grouping the plenum cells
PART 32 ARRAY
2  2  1   28  28  28  28
*  1  1  7  8  32  7  6  7  32  8
*
* Steel packing pieces to line up the elements
*
*
* Inner core packing
PART 33 NEST
BOX     M17   -2.7127 -2.7127   0.0     5.4254  5.4254  2.51575
*
* Outer core packing
PART 34 NEST
BOX     M17   -2.7127 -2.7127   0.0     5.4254  5.4254  2.064
*
* radial blanket element packing (reduced by 0.003)
```

```
PART 35 NEST
BOX     M17  -2.7127 -2.7127   0.0     5.4254  5.4254  1.2456
*
*********************************************************************
*
*                                                          ELEMENTS
*
*********************************************************************
*
* The Inner Core Element
* height = 89.0461 + 2*(34.9564 + 33.0048) =224.9685
* 2.51575 cm Smeared steel region above and below (height = 230.0 cm)
*
PART 36 ARRAY
1  1  23  33  29  (27)*4  (25)*11  (27)*4  28  33
*
* The Outer Core Element
* height = 2*(44.9748 +34.9564 + 33.0048) = 2* 112.936 =225.872
* 2.064 cm Smeared steel region above and below (height = 115.0 cm)
*
PART 37 ARRAY
1  1  24  34  29  (27)*4  (26)*12  (27)*4  28  34
*
*The Radial Blanket element 1B
* height = 2*(50.296 + 30.4506 + 33.0048) = 2*113.7514 = 227.5028
* (1.2486 cm Smeared steel region above and below)
*
PART 38 ARRAY
1  1   30  35  29  (31)*3  (30)*20  (31)*3   28  35
*
* The Special Inner Core Element
* replaced by the Control Element
*
PART 39 ARRAY
1  1  7  8  32  7  6  7  32  8
*
* steel bar
PART 40 NEST
BOX     M23  -2.54   -2.54     0.0     5.08    5.08    230.0
BOX     M0  -2.7127 -2.7127    0.0     5.4254  5.4254  230.0
*
*********************************************************************
*
*                       ALTERNATIVE INNER CORE CELLS AND ELEMENTS
*
*
*********************************************************************
*
* Plate 41, the Pu metal plate PUX8
PART 41 NEST
BOX     M36  -2.3355  -2.3355 0.04572  4.671   4.671   0.23506
BOX     M37  -2.5335  -2.5335 0.0      5.067   5.067   0.3265
BOX     M28  -2.7127 -2.7127   0.0     5.4254  5.4254   0.3265
*
* Plate 42, the Pu metal plate PUXI8
PART 42 NEST
BOX     M38  -2.3355  -2.3355 0.04572  4.671   4.671   0.23506
BOX     M39  -2.5335  -2.5335 0.0      5.067   5.067   0.3265
BOX     M28  -2.7127 -2.7127   0.0     5.4254  5.4254   0.3265
*
* Plate 43, the sodium plate NASTDM4
PART 43 NEST
BOX     M40  -2.4815  -2.4815 0.03683 4.963   4.963   0.54234
BOX     M41 -2.5335  -2.5335  0.0     5.067   5.067   0.616
BOX     M28  -2.7127 -2.7127   0.0     5.4254  5.4254  0.616
*
*
*********************************************************************
*
* Alternative Inner Core Cells
* Cell 30B
PART 44 ARRAY
1  1  14  9  4  9  41  9  4  9  13  4  9  1  9  4  9
*
* Cell 30BG
```

```
PART 45 ARRAY
1  1  14  43  4  43  41  43  4  43  13  4  43  1  43  4  43
*
* Cell 30D
PART 46 ARRAY
1  1  14  43  4  43  42  43  4  43  13  4  43  1  43  4  43
*
* Alternative Axial blanket Cell 30G
PART 47 ARRAY
1  1  20  43  12  14  43  13  12  43  14  43  13
12  43  14  43  12  13  43  14  12  43
*
* Alternative inner core elements
*
* Element C12-30B
PART 48 ARRAY
1  1  23  33  29  (27)*4  (44)*11  (27)*4  28  33
*
* Element C12-30BG
PART 49 ARRAY
1  1  23  33  29  (47)*4  (45)*11  (47)*4  28  33
*
* Element C12-30D
PART 50 ARRAY
1  1  23  33  29  (47)*4  (46)*11  (47)*4  28  33
*
*
************************************************************************
*
*                        ALTERNATIVE OUTER CORE CELLS AND ELEMENTS
*
*
************************************************************************
*
*
* Plate 51, the Pu metal plate PUV8
PART 51 NEST
BOX     M42  -2.3355  -2.3355 0.04572  4.671   4.671   0.23506
BOX     M43  -2.5335  -2.5335 0.0      5.067   5.067   0.3265
BOX     M28  -2.7127 -2.7127   0.0     5.4254  5.4254   0.3265
*
* Plate 52, the Pu metal plate PUVII8
PART 52 NEST
BOX     M44  -2.3355  -2.3355 0.04572  4.671   4.671   0.23506
BOX     M45  -2.5335  -2.5335 0.0      5.067   5.067   0.3265
BOX     M28  -2.7127 -2.7127   0.0     5.4254  5.4254   0.3265
*
* Plate 53, the Pu metal plate PUVIII8
PART 53 NEST
BOX     M46  -2.3355  -2.3355 0.04572  4.671   4.671   0.23506
BOX     M47  -2.5335  -2.5335 0.0      5.067   5.067   0.3265
BOX     M28  -2.7127 -2.7127   0.0     5.4254  5.4254   0.3265
*
* Plate 54, the Pu metal plate PUVIII8
PART 54 NEST
BOX     M48  -2.3355  -2.3355 0.04572  4.671   4.671   0.23506
BOX     M49  -2.5335  -2.5335 0.0      5.067   5.067   0.3265
BOX     M28  -2.7127 -2.7127   0.0     5.4254  5.4254   0.3265
*
*
* Outer Core Cell 1A
PART 55 ARRAY
1  1  14  10  5  10  51  13  5  10  10  5  14  51  10  5  10
*
*
* Outer Core Cell 1BG
PART 56 ARRAY
1  1  14  43  5  43  3  13  5  43  43  5  14  3  43  5  43
*
*
* Outer Core Cell 1C
PART 57 ARRAY
1  1  14  9  5  9  52  13  5  9  9  5  14  52  9  5  9
*
* Outer Core Cell 1D
```

```
PART 58 ARRAY
1  1  14  9  5  9  53  13  5  9  9  5  14  53  9  5  9
*
*
* Outer Core Cell 1DG
PART 59 ARRAY
1  1  14  43  5  43  53  13  5  43  43  5  14  53  43  5  43
*
*
* Outer Core Cell 1G
PART 60 ARRAY
1  1  14  43  5  43  54  13  5  43  43  5  14  54  43  5  43
*
*
* Axial blanket Cell 1
PART 61 ARRAY
1  1  20  10  12  14  10  13  12  10  14  10  13
12  10  14  10  12  13  10  14  12  10
*
*
* Axial blanket Cell 1AG
PART 62 ARRAY
1  1  20  43  12  14  43  13  12  43  14  43  13
12  43  14  43  12  13  43  14  12  43
*
* The Outer Core Element 1A
*
PART 63 ARRAY
1  1  24  34  29  (61)*4  (55)*12  (61)*4  28  34
*
*
* The Outer Core Element 1BG
*
PART 64 ARRAY
1  1  24  34  29  (62)*4  (56)*12  (62)*4  28  34
*
*
* The Outer Core Element 1C
*
PART 65 ARRAY
1  1  24  34  29  (27)*4  (57)*12  (27)*4  28  34
*
*
* The Outer Core Element 1D
*
PART 66 ARRAY
1  1  24  34  29  (27)*4  (58)*12  (27)*4  28  34
*
*
* The Outer Core Element 1DG
*
PART 67 ARRAY
1  1  24  34  29  (62)*4  (59)*12  (62)*4  28  34
*
*
* The Outer Core Element 1G
*
PART 68 ARRAY
1  1  24  34  29  (62)*4  (60)*12  (62)*4  28  34
*
*
************************************************************************
*
*                                                    ARRAYS OF ELEMENTS
* Uniform group of 5x5 elements
*
************************************************************************
* Inner Core array
*
* 5x5 Special core centre region containing the control rod.
* -2.7127 -2.7127     0.0     5.4254  5.4254  230.0
* Overall width 27.127, half widths 13.5635,
PART 69 CLUSTER
BOX  P36   -13.5635   -13.5635   0.0  5.4254 5.4254  230.0
BOX  P36    -8.1381   -13.5635   0.0  5.4254 5.4254  230.0
```

```
BOX  P36    -2.7127   -13.5635   0.0  5.4254 5.4254  230.0
BOX  P36     2.7127   -13.5635   0.0  5.4254 5.4254  230.0
BOX  P36     8.1381   -13.5635   0.0  5.4254 5.4254  230.0
BOX  P36   -13.5635    -8.1381   0.0  5.4254 5.4254  230.0
BOX  P36    -8.1381    -8.1381   0.0  5.4254 5.4254  230.0
BOX  P36    -2.7127    -8.1381   0.0  5.4254 5.4254  230.0
BOX  P36     2.7127    -8.1381   0.0  5.4254 5.4254  230.0
BOX  P36     8.1381    -8.1381   0.0  5.4254 5.4254  230.0
BOX  P36   -13.5635    -2.7127   0.0  5.4254 5.4254  230.0
BOX  P36    -8.1381    -2.7127   0.0  5.4254 5.4254  230.0
BOX  P39    -2.7127    -2.7127   0.0  10.8508   10.8508 230.0
BOX  P36     8.1381    -2.7127   0.0  5.4254 5.4254  230.0
BOX  P36   -13.5635     2.7127   0.0  5.4254 5.4254  230.0
BOX  P36    -8.1381     2.7127   0.0  5.4254 5.4254  230.0
BOX  P36     8.1381     2.7127   0.0  5.4254 5.4254  230.0
BOX  P36   -13.5635     8.1381   0.0  5.4254 5.4254  230.0
BOX  P36    -8.1381     8.1381   0.0  5.4254 5.4254  230.0
BOX  P36    -2.7127     8.1381   0.0  5.4254 5.4254  230.0
BOX  P36     2.7127     8.1381   0.0  5.4254 5.4254  230.0
BOX  P36     8.1381     8.1381   0.0  5.4254 5.4254  230.0
BOX  M0    -13.5635   -13.5635   0.0  27.127 27.127  230.0
*
************************************************************************
*                                                              ROW 1
************************************************************************
*
* Row 1, the bottom set of groups of size 3x4 and 5x4 (5 along x axis)
* 5 arrays
*
* Left side
PART 70 ARRAY
3  4  1  (40)*9  40 (38)*2
*
* Left centre
PART 71 ARRAY
5  4  1  (40)*5  (40)*4  38  (38)*10
*
* Centre
PART 72 ARRAY
5  4  1  (40)*5  (38)*15
*
* Right centre
PART 73 ARRAY
5  4  1  (40)*5  38  (40)*4  (38)*10
*
* Right side
PART 74 ARRAY
3  4  1  (40)*9  (38)*2  40
*
* combine these arrays to form the row 1 array
PART 75 ARRAY
5  1  1  70  71  72  73  74
*
*
************************************************************************
*                                                              ROW 2
************************************************************************
* 7 arrays of elements
*
* Bottom left outer group
PART 76 ARRAY
5  5  1  (40)*10  (40)*4  38  (40)*3  (38)*2  (40)*2  (38)*3
*
* Bottom left second group
PART 77 ARRAY
5  5  1  40  (38)*4  (38)*20
*
* Bottom left centre group
PART 78 ARRAY
5  5  1  (38)*15  (38)*3  68  67  68  67  (66)*2  65
*
* Central group
PART 79 ARRAY
5  5  1  (38)*15  (66)*5  (65)*5
*
```

```
* Bottom right centre group
PART 80 ARRAY
5  5  1  (38)*15  67  68  68 (38)*2  65  (66)*3   68
*
* Bottom next right group
PART 81 ARRAY
5  5  1  (38)*4  40  (38)*20
*
* Bottom right outer group
PART 82 ARRAY
5  5  1  (40)*10  38  (40)*4  (38)*2  (40)*3  (38)*3  (40)*2
*
* combine these 7 arrays to form the row 2 array
PART 83 ARRAY
7  1  1  76  77  78  79  80  81  82
*
************************************************************************
*                                                          ROW 3
************************************************************************
* 9 arrays of elements, the left and right hand ones being 4x5 arrays
*
* Left side
PART 84 ARRAY
4  5  1  (40)*12  (40)*3  38  (40)*3  38
*
* Outer left
PART 85 ARRAY
5  5  1  40 (38)*4 (38)*20
*
* Left Centre
PART 86 ARRAY
5  5  1   (38)*4  67  (38)*3  (66)*2  (38)*2  66  65  37
38  66  65  37  63  68  65  37  63  50
*
* Core left
PART 87 ARRAY
5  5  1   66  (65)*2  (37)*2  65  37  (63)*2  50  37  63  (50)*3
63  (50)*4  (50)*2  (49)*2  48
*
*  Core centre
PART 88 ARRAY
5  5  1  37  (63)*3  37  (50)*10  (49)*5  (48)*5
*
* Core right
PART 89 ARRAY
5  5  1   (37)*2  (65)*2  66  50  (63)*2  37  65  (50)*3  63  37
(50)*4  63  48  49  (50)*3
*
* Right Centre
PART 90 ARRAY
5  5  1     68  (38)*4  65  66  (38)*3  64  65  66  (38)*2
63  37  65  66  38  50  63  65  66  67
*
* Outer right
PART 91 ARRAY
5  5  1  (38)*4  40  (38)*20
*
* Right side
PART 92 ARRAY
4  5  1  (40)*12  38  (40)*3  38  (40)*3
*
* combine these arrays to form the row 3 array
PART 93 ARRAY
9  1  1  84  85  86  87  88  89  90  91  92
*
*
************************************************************************
*                                                          ROW 4
************************************************************************
* 9 arrays of elements, the left and right hand ones being 4x5 arrays
*
* Left side
PART 94 ARRAY
4  5  1  (40)*2  (38)*2  (40)*2  (38)*2  (40)*2  (38)*2
(40)*2  (38)*2  40  (38)*3
```

```
*
* Outer left
PART 95 ARRAY
5  5  1  (38)*4  68  (38)*4  66  (38)*3  68  66   (38)*3  68  66
(38)*3  67  65
*
* Left Core
PART 96 ARRAY
5  5  1   66  65  37  63  50  65  37  63  (50)*2  65  63  (50)*3
37  63  (50)*3  37  (50)*3  48
*
* Centre Left
PART 97 ARRAY
5  5  1   50  49  (48)*3  49  (48)*4  (48)*3  (36)*2 (48)*2  (36)*3
48  (36)*4
*
* Centre
PART 98 ARRAY
5  5  1   (48)*5  (36)*20
*
* Centre right
PART 99 ARRAY
5  5  1  (48)*3  49  50  36  (48)*3  49  (36)*2 (48)*3  (36)*3 (48)*2
(36)*3 (48)*2
*
* Right Core
PART 100 ARRAY
5  5  1   50  63  37  65  66  (50)*2  63  37  65  (50)*3  63  65
(50)*3  63  37  48  (50)*3  37
*
* Outer right
PART 101 ARRAY
5  5  1  68  (38)*4  67  (38)*4  66  (38)*4  66  68  (38)*3
65  67  (38)*3
*
* Right side
PART 102 ARRAY
4  5  1  (38)*2 (40)*2  (38)*2 (40)*2  (38)*2  (40)*2  (38)*2 (40)*2
(38)*3  40
*
* combine these arrays to form the row 3 array
PART 103 ARRAY
9  1  1  94  95  96  97  98  99  100  101  102
*
*
**********************************************************************
*  The middle row                                          ROW 5
**********************************************************************
* 9 arrays of elements, the left and right hand ones being 4x5 arrays
*
* Left side
PART 104 ARRAY
4  5  1  40  (38)*3  40  (38)*3  40  (38)*3  40  (38)*3  40  (38)*3
*
* Outer left
PART 105 ARRAY
5  5  1  (38)*3  66  65  (38)*3  66  65  (38)*3  66  65
(38)*3  66  65  (38)*3  66  65
*
* Left Core
PART 106 ARRAY
5  5  1   63  (50)*2  49  48  63  (50)*2  49  48  63  (50)*2  49  48
63  (50)*2  49  48  63  (50)*2  49  48
*
*  Centre Left
PART 107 ARRAY
5  5  1   48  (36)*4  48  (36)*4  48  (36)*4  48  (36)*4  48  (36)*4
*
* Centre right
PART 108 ARRAY
5  5  1   (36)*4  48  (36)*4  48  (36)*4  48  (36)*4  48  (36)*4  48
*
* Right Core
PART 109 ARRAY
5  5  1   48  49  (50)*2  37  48  49  (50)*2  63  48  49  (50)*2  63
```

```
48  49  (50)*2  63  48  49  (50)*2  37
*
* Outer right
PART 110 ARRAY
5  5  1  65  66  (38)*3  65  66  (38)*3  65  66  (38)*3  65  66  (38)*3
65  66   (38)*3
*
* Right side
PART 111 ARRAY
4  5  1  (38)*3  40  (38)*3  40  (38)*3  40  (38)*3  40  (38)*3  40
*
* combine these arrays to form the row 3 array
PART 112 ARRAY
9  1  1  104  105  106  107  69  108  109  110  111
*
*
*********************************************************************
*                                                          ROW 6
*********************************************************************
* 9 arrays of elements, the left and right hand ones being 4x5 arrays
*
* Left side
PART 113 ARRAY
4  5  1   40  (38)*3  (40)*2  (38)*2  (40)*2  (38)*2  (40)*2  (38)*2
(40)*2  (38)*2
*
* Outer left
PART 114 ARRAY
5  5  1   (38)*3  67  65  (38)*3  68  66  (38)*4  66  (38)*4  67
(38)*4  68
*
*
* Left Core
PART 115 ARRAY
5  5  1   37  (50)*3  48 37  63  (50)*3   65  63  (50)*3
65  37  63  (50)*2  66  65  37  63  50
*
* Centre Left
PART 116 ARRAY
5  5  1   (48)*2  (36)*3  (48)*2  (36)*3  (48)*3  (36)*2
49  (48)*3  36   50  49  (48)*3
*
* Centre
PART 117 ARRAY
5  5  1   (36)*20  (48)*5
*
* Centre right
PART 118 ARRAY
5  5  1  (36)*4  48  (36)*3  (48)*2  (36)*2 (48)*3   (48)*4  49
(48)*3  49  50
*
* Right Core
PART 119 ARRAY
5  5  1   48  (50)*3  37  (50)*3  63  37  (50)*3  63  65
(50)*2  63  37  65  50  63  37  65  66
*
* Outer right
PART 120 ARRAY
5  5  1   65  67  (38)*3  66  68  (38)*3  66  68  (38)*3  66  (38)*4
68  (38)*4
*
* Right side
PART 121 ARRAY
4  5  1   (38)*3  40  (38)*2 (40)*2  (38)*2 (40)*2  (38)*2 (40)*2
(38)*2 (40)*2
*
* combine these arrays to form the row 3 array
PART 122 ARRAY
9  1  1  113  114  115  116  117  118  119  120  121
*
*
*********************************************************************
*                                                          ROW 7
*********************************************************************
*
```

```
* 9 arrays of elements, the left and right hand ones being 4x5 arrays
*
* Left side
PART 123 ARRAY
4  5  1   (40)*3  38  (40)*3  38  (40)*12
*
* Outer left
PART 124 ARRAY
5  5  1   (38)*20   40 (38)*4
*
* Left Centre
PART 125 ARRAY
5  5  1   67  66  65  63  50  38  66  65  37  63  (38)*2  66  65  64
(38)*3  66  65  (38)*4  68
*
* Core left
PART 126 ARRAY
5  5  1  (50)*3  49  48  63  (50)*4  37  63  (50)*3  65  37  (63)*2  50
66  (65)*2  (37)*2
*
*  Core centre
PART 127 ARRAY
5  5  1    (48)*5  (49)*5  (50)*10  37  (63)*3  37
*
* Core right
PART 128 ARRAY
5  5  1  48  (49)*2  (50)*2  (50)*4  63  (50)*3  63  37
50  (63)*2  37  65  (37)*2  (65)*2  66
*
* Right centre
PART 129 ARRAY
5  5  1  50  63  37  66  68  63  37  65  66  38  37  65  66  (38)*2
(66)*2  (38)*3  67  (38)*4
*
* Outer right
PART 130 ARRAY
5  5  1   (38)*20  (38)*4  40
*
* Right side
PART 131 ARRAY
4  5  1   38  (40)*3  38  (40)*3  (40)*12
*
* combine these arrays to form the row 7 array
PART 132 ARRAY
9  1  1  123  124  125  126  127  128  129  130  131
*
*
************************************************************************
*                                                          ROW 8
************************************************************************
* 7 arrays of elements
*
* left outer group
PART 133 ARRAY
5  5  1   (40)*2  (38)*3 (40)*3  (38)*2  (40)*4  38  (40)*10
*
* left second group
PART 134 ARRAY
5  5  1  (38)*20  40  (38)*4
*
*  left centre group
PART 135 ARRAY
5  5  1  68  (66)*3  65  (38)*2  68  68  67  (38)*15
*
* Central group
PART 136 ARRAY
5  5  1  (65)*5  (66)*5  (38)*15
*
*  right centre group
PART 137 ARRAY
5  5  1    65  (66)*2  67  68  67  68  (38)*3  (38)*15
*
*  next right group
PART 138 ARRAY
5  5  1  (38)*20   (38)*4  40
```

```
*
*  right outer group
PART 139 ARRAY
5  5  1   (38)*3  (40)*2 (38)*2  (40)*3  38  (40)*4   (40)*10
*
* combine these 7 arrays to form the row 2 array
PART 140 ARRAY
7  1  1  133  134  135  136  137  138  139
*
*
************************************************************************
*                                                              ROW 9
************************************************************************
*
* Row 9, the top set of groups of size 3x4 and 5x4 (5 along the x axis)
* 5 arrays
*
* Left side
PART 141 ARRAY
3  4  1  40 (38)*2  (40)*9
*
* Left centre
PART 142 ARRAY
5  4  1  (38)*10  (40)*4  38  (40)*5
*
* Centre
PART 143 ARRAY
5  4  1  (38)*15  (40)*5
*
* Right centre
PART 144 ARRAY
5  4  1  (38)*10  38  (40)*4  (40)*5
*
* Right side
PART 145 ARRAY
3  4  1  (38)*2  40  (40)*9
*
* combine these arrays to form the row 9 array
PART 146 ARRAY
5  1  1  141  142  143  144  145
*
*
************************************************************************
*
*         Cluster of superlattice groups in a circle of shield material
*
************************************************************************
* Cluster of superlattice groups in a circle of shield material
PART 147   CLUSTER
BOX  P146   -56.9667   94.9445   -115.0  113.9334  21.7016 230.0
BOX  P140   -94.9445   67.8175   -115.0  189.889   27.127  230.0
BOX  P132   -116.6461  40.6905   -115.0  233.2922  27.127  230.0
BOX  P122   -116.6461  13.5635   -115.0  233.2922  27.127  230.0
BOX  P112    -116.6461 -13.5635   -115.0  233.2922  27.127  230.0
BOX  P103    -116.6461 -40.6905   -115.0  233.2922  27.127  230.0
BOX  P93    -116.6461 -67.8175   -115.0  233.2922  27.127  230.0
BOX  P83    -94.9445  -94.9445   -115.0  189.889   27.127  230.0
BOX  P75    -56.9667  -116.6461  -115.0  113.9334  21.7016 230.0
ZROD  M24     0.0     0.0     -116.0       135.0    232.0
*
************************************************************************
* Albedo for free boundaries at side and top and reflection at bottom
*
ALBEDO 0.0  0.0  0.0
END
*
************************************************************************
*
BEGIN HOLE DATA
* Array of absorber pins in a stainless steel cylinder
GLOBE
* number of cylindrical regions
6
* outer radius of cylinder and Material number of Cylinder
4.9225  51
```

```
* inner radius of cylinder . Array of subunits is to follow
4.5125  SUB
* 12 equally spaced pins
       12
* no angular offset
       1
* radius of circle location of the centres of the pins
       3.46
* material numbers of the pin constituents, tube+can and boron
       52  52  53
* outer radius of pin tube and radius of boron absorber
       0.775  0.655  0.55
* Note, the radius of the Ta absorber pin is 0.655 cm
* radius separating the ring of 12 and ring of 6
2.625   SUB
       6
* angular offset of 45o
       1.5
       1.79
       52  52  53
       0.775   0.655   0.55
* outer radius pin tube+can and MatNo and radius of absorber + MatNo
0.775  52
0.655  52
0.55   53
* the sodium filling the calandria
7
*
************************************************************************
*
BEGIN CONTROL DATA
STAGES -5  2400  5000  STDV 0.0002
END
*
************************************************************************
*
BEGIN SOURCE GEOMETRY
ZONEMAT
ALL / MATERIAL 1
END
*
************************************************************************
*
BEGIN ACTION TALLIES
     NONORM
     NO ACTION TALLIES
     NOPRINT FLUXES  SCEDST  BNDXNG MATACT REGACT  NPARAM  SYSCAT
     SGUIDE HOLACT
END
*
************************************************************************
```

LIST OF TABLES

LIST OF FIGURES